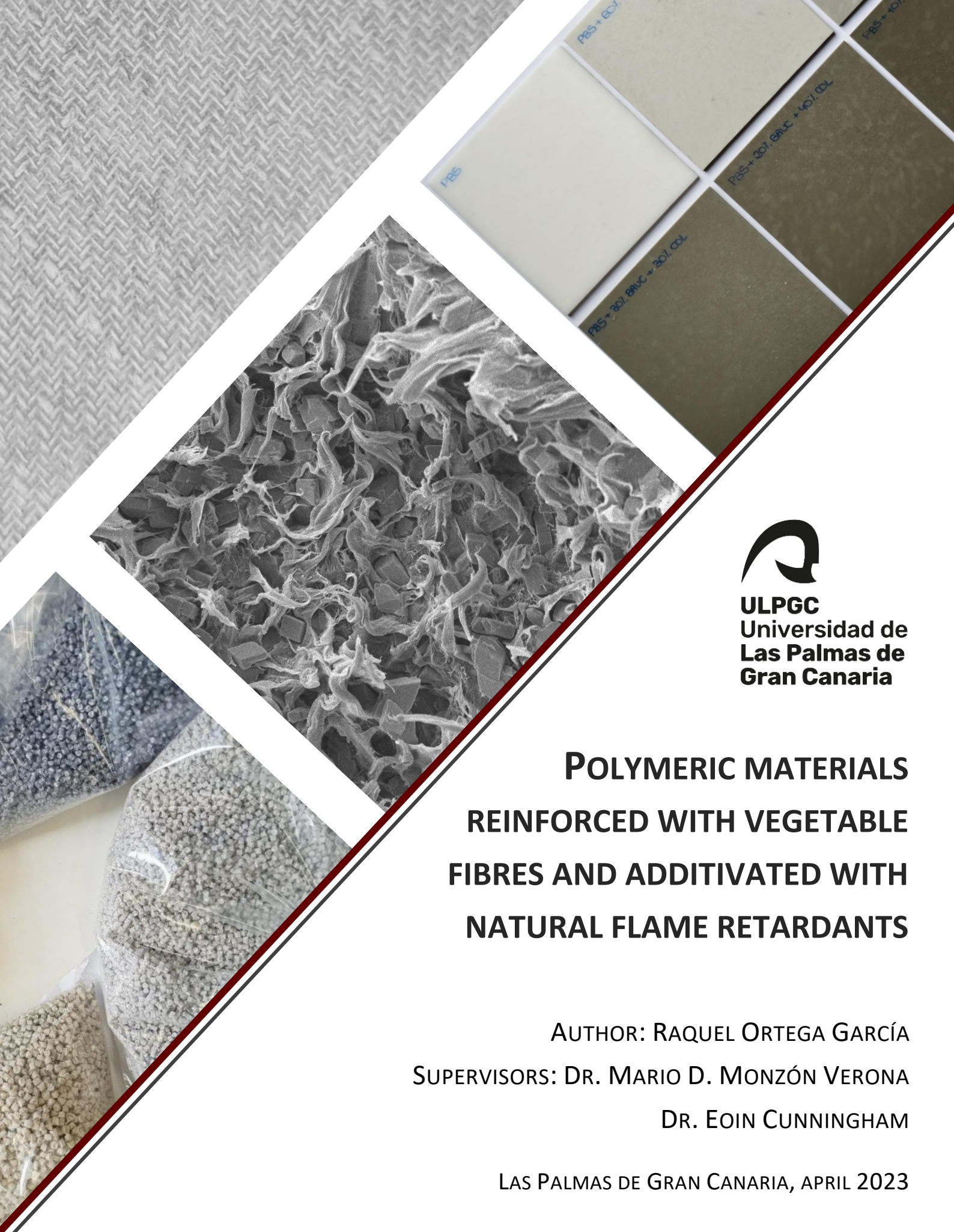

ULPGC
Universidad de
Las Palmas de
Gran Canaria

POLYMERIC MATERIALS REINFORCED WITH VEGETABLE FIBRES AND ADDITIVATED WITH NATURAL FLAME RETARDANTS

AUTHOR: RAQUEL ORTEGA GARCÍA

SUPERVISORS: DR. MARIO D. MONZÓN VERONA

DR. EOIN CUNNINGHAM

LAS PALMAS DE GRAN CANARIA, APRIL 2023

PHD PROGRAM: CHEMICAL, MECHANICAL AND MANUFACTURING ENGINEERING

ULPGC
Universidad de
Las Palmas de
Gran Canaria

PHD PROGRAM IN CHEMICAL, MECHANICAL AND MANUFACTURING ENGINEERING

PHD THESIS

POLYMERIC MATERIALS REINFORCED WITH VEGETABLE FIBRES AND ADDITIVATED WITH NATURAL FLAME RETARDANTS

AUTHOR: RAQUEL ORTEGA GARCÍA

SUPERVISORS: DR. MARIO D. MONZÓN VERONA

DR. EOIN GUNNINGHAM

INTEGRATED AND ADVANCED MANUFACTURING RESEARCH GROUP OF UNIVERSITY OF LAS PALMAS DE GRAN CANARIA

LAS PALMAS DE GRAN CANARIA, APRIL 2023

D Jose Miguel Doña Rodríguez COORDINADOR DEL PROGRAMA DE DOCTORADO Ingenierías Química, Mecánica y de Fabricación DE LA UNIVERSIDAD DE LAS PALMAS DE GRAN CANARIA

INFORMA,

De que la Comisión Académica del Programa de Doctorado, en su sesión de fecha ..... tomó el acuerdo de dar el consentimiento para su tramitación, a la tesis doctoral titulada "Materiales poliméricos reforzados con fibras vegetales y aditivados con retardantes de llama de origen natural" presentada por el/la doctorando/a D/Dª Raquel Ortega García y dirigida por el Doctor Mario Domingo Monzón Verona y el Doctor Eoin Cunningham

Y para que así conste, y a efectos de lo previsto en el Artº 11 del Reglamento de Estudios de Doctorado (BOULPGC 04/03/2019) de la Universidad de Las Palmas de Gran Canaria, firmo la presente en Las Palmas de Gran Canaria, a.....de.....de dos mil veintitrés.

UNIVERSIDAD DE LAS PALMAS DE GRAN CANARIA
ESCUELA DE DOCTORADO

Programa de doctorado Ingenierías Química, Mecánica y de Fabricación

Título de la Tesis: Materiales poliméricos reforzados con fibras vegetales y aditivados con retardantes de llama de origen natural

Tesis Doctoral presentada por D/Dª Raquel Ortega García

Dirigida por el Dr. D. Mario Domingo Monzón Verona

Codirigida por el Dr. D. Eoin Cunningham

Las Palmas de Gran Canaria, a 20 de Abril de 2023

El/la Director/a, El/la Codirector/a El/la Doctorando/a,

ACKNOWLEDGMENTS

En primer lugar, quiero expresar mi agradecimiento a mis directores de tesis. A Mario por darme la posibilidad de trabajar en este tema y por la confianza depositada en mi para el desarrollo de esta tesis.

I would like to thank Dr. Eoin Cunningham who agreed to be my co-director from the beginning and gave me the opportunity to do research stays at Queen's University of Belfast. This work would not have been possible without these research stays and the collaboration with the Polymer Processing Research Centre. Thanks to all the members who helped me in the completion of my tasks and who patiently taught me everything I needed to know in order to carry out this work. Special thanks to Paula Douglas, for all that you taught me about characterisation and for our conversations in the lab, you taught me a lot not only about research but also on a personal level. Thanks also to all the students I met during my research stays who welcomed me from day one, helped me with everything I needed and made Belfast my home.

Gracias también a todos mis compañeros del grupo de investigación Fabricación Integrada y Avanzada que han hecho que el día a día fuera más llevadero con sus risas, con los desayunos y que en los malos momentos me han escuchado y me han brindado ayuda siempre que lo he necesitado. Sin ustedes la última etapa de esta tesis no habría sido posible.

Por último, quiero dedicar este trabajo a mi familia por todo lo que han hecho por mí y porque sin ellos no habría podido conseguirlo, no existen palabras suficientes para agradeceros. A mi madre por apoyarme siempre, por esforzarte tanto por mi hermana y por mí, por enseñarme y por brindarme todo su cariño y apoyo en el transcurso de este largo y duro camino. A mi hermana Laura, gracias por preocuparte tanto por mí, por tus palabras de aliento, por creer en mí desde siempre, por celebrar mis logros, sabes que eres muy importante para mí. A mi pareja Clifi, gracias por estar a mi lado día tras día mientras me pasaba horas y horas en el ordenador, por ayudarme tanto, por apoyarme, sé que ha sido difícil, pero sin ti esto no habría salido adelante. A mi padre, te lo prometí y aquí está, gracias por guiarme siempre.

Esta tesis doctoral ha sido cofinanciada por la Agencia Canaria de Investigación, Innovación y Sociedad de la Información de la Consejería de Economía, Industria, Comercio y Conocimiento y por el Fondo Social Europeo (FSE) Programa Operativo Integrado de Canarias 2014-2020, Eje 3 Tema Prioritario 74 (85%)

ABSTRACT

The rapid increase in the use of polymers and their impact on the current lifestyle is almost incalculable. Nowadays, it is difficult to find objects that do not contain plastic materials due to their price, lightness, insulation, and resistance characteristics, among others. Plastics are used in a wide variety of applications because they can be individually adapted to the requirements and needs of a certain product. In Europe, by sector, packaging is the largest field of application followed by construction and automotive industry, and in these last two sectors fire resistance of materials is key.

The knowledge of the fire properties allows to predict how materials behave in case of fire, how combustion starts, evolves, and spreads, and enables us to find solutions to improve their behaviour. To minimize fire hazard and accomplish fire safety requirements, different solutions have been developed to prevent ignition or reduce the heat released during combustion of materials. For polymers, these methods include engineering approach, less flammable polymers, and flame retardant (FR) additives. The use of FR additives is the most common method because it is well-accepted, cost effective and relatively easy to incorporate. The term flame retardant is defined by ISO 13943 as "substance added, or a treatment applied, to a material in order to suppress or delay the appearance of a flame and/or reduce the flame spread rate". Therefore, the term "flame retardant" refers to a function, not a family of chemicals. Classifying flame retardants by their nature, they can be separated into halogenated, phosphorous, nitrogenous, silicon compounds, carbonaceous, metal oxides and hydroxides, borates, nanoclays and natural flame retardants. Those based on halogenated compounds have been the most used ones due to their effectiveness, cost, availability, and the industry's extensive experience with this class of additives. However, these compounds are harmful to health and the environment, thus, new environmental regulations have entered into force that limit and even prevent their use. Finding alternatives is a great challenge for the industry of flame retardants because the other types of flame retardant are usually polymer specific, so one additive may work for a particular polymer while it may have no effect on another.

The increasing concern in the environment has promoted several studies focused on the improvement of the sustainability of materials, industrial processes, and the management of the huge amount of polymeric waste produced in the world. For this reason, flame retardants based on natural sources are attracting a great deal of interest. Natural flame retardants are additives that can be obtained by simple isolation from natural or biological sources, therefore, they have high availability and enable industrial processes to be almost CO_2 neutral. Additionally, the

development of natural flame retardants from renewable resources also promotes the use of bio-based polymers in many technical fields, thus maintaining the sustainability of the composite as a whole and preserving its good environmental impact. However, research on natural flame retardants in biopolymers is still scarce and more research is needed in this field.

In addition to the natural flame retardants and biopolymers, another option to improve the sustainability is the use natural fibres as reinforcement. The use of natural fibres is attractive because they are a renewable and biodegradable resource. Nevertheless, there are some disadvantages, such as quality variability, low impact resistance, limited processing temperatures and high combustibility. To improve the fire performance of composites, different strategies can be used, such as reducing the flammability of the matrix, the reinforcement or the whole composite. Regarding to the reinforcement, synthetic and natural chemical treatments can be applied to improve the fire resistance properties of natural fibres. Therefore, this thesis presents two main challenges, to improve the fire performance of plastic by using natural flame retardants, and to reduce the high combustibility of plant fibres.

In summary, the main objective of this thesis is to develop polymeric composites reinforced with vegetable fibres and additivated with natural flame retardants, and then evaluate their fire resistance to determine their capacity to replace conventional reinforcement materials.

This general objective is achieved through the following specific objectives:

1. **Evaluation of natural flame retardants applicable to the composite under study**

A proper evaluation of the natural flame retardants would yield a material with optimal fire properties using the least amount of additive possible. Therefore, the polymeric matrix, origin, availability, and price are considered when choosing them.

2. **Treatment of natural fibres**

The use of natural fibres as reinforcement in composites is a topic of great interest, but they present some disadvantages such as poor compatibility with polymer matrix and high combustibility due to their origin. Considering the drawbacks, it is concluded that some modifications are necessary to reduce their burning nature and to achieve a good coupling between the matrix and the fibre.

3. **Formulation of the composites**

Once the flame retardants and the chemical treatments to be used have been determined, it is necessary to study the process conditions to manufacture the composites. This is because the additives influence the pressure, temperature, and process time parameters. Then, the parts are manufactured by compression moulding, varying the type of additive, the reinforcement, and their percentage.

4. **Characterization of the materials**

Due to natural flame retardants are often used in high percentages, the properties of the materials, especially the mechanical ones, are affected. To understand how these properties are influenced, thermal, mechanical, optical, and rheological tests are conducted on polymers, fibres, and composites.

5. **Fire tests**

Finally, fire test of polymers, fibres, and composites such as UL94 and cone calorimeter, are performed to ascertain the effect of the flame retardants and treatments used.

With the results obtained from the mechanical and fire tests, an optimisation is carried out to determine the best additives and treatments, and a feedback process is carried out until the optimal solution is determined. A summary of the experimental tests carried out is presented below, together with the results and conclusions.

SELECTION OF THE NATURAL FLAME RETARDANTS

n the evaluation of natural flame retardants applicable to the composite under study, it has been observed that some of the most commonly used flame retardants have their alternative of natural origin, but that these have not yet been studied in depth. Since the aim of this thesis is to maintain as far as possible the natural character of the additive because the reinforcement is a natural fibre fabric, it is proposed to use additives that come directly from the source or that do not require many synthesis or refinement processes. One of the additives that meets these requirements is brucite, which, although it requires high loadings, has proven to be effective. On the other hand, the use of boehmite was considered because, although it requires separation from the main mineral and its efficiency is not as good as that of brucite, it is an additive that has not been studied in detail and could be an interesting alternative to aluminium hydroxide. Finally, of the flame retardants of biological origin, lignin was selected because it is a residue obtained in the paper industry and its use gives it additional value.

FLAME RETARDANCY OF POLYMERS

Since the selected additives have not been studied in detail, it is necessary to perform several cycles to obtain the optimum additive percentage for the plastic matrix. For this reason, three stages have been carried out in this study.

In **Stage 1**, boehmite, brucite and lignin were used as retardant additives and the matrix used was polypropylene (PP) in two viscosities. According to the literature, minerals should be used up to 60-70% to obtain a flame retardant material, for this reason, boehmite and brucite were used

at 45 and 60% to study their effect and tendency. On the other hand, some authors have shown that 20% lignin improves the flame retardant properties of polypropylene, so it was decided to study the effect of lignin at 10 and 20%. In the DSC (Differential Scanning Calorimetry) test, it was observed that boehmite and brucite act as a nucleant of PP because they increase the percentage of crystallinity, favour the formation of crystals and improve the homogeneity of the crystal structure. In addition, samples with mineral additives have a higher storage modulus than virgin PP in the temperature range tested in the DMA (Dynamic Mechanical Analysis) test, thus improving thermo-mechanical stability. However, the mechanical properties were negatively affected. The additives increase the elastic and flexural modulus up to 4430 and 4330 MPa, respectively, for the samples with 60% additive, compared to 1700 and 1500 MPa obtained for the unfilled PP. In terms of strength, the maximum tensile stress and impact strength were reduced by up to 42% and 82%, respectively. Therefore, the additives used stiffen, but also reduce the strength of the composite materials. The fire test results were also unsatisfactory. Brucite and boehmite improved the fire resistance, but not sufficiently, and lignin worsened it. For this reason, it was decided to discard lignin for later stages, and the samples with boehmite and brucite were optimised.

To overcome the problem of poor mechanical properties and fire resistance, synergistic admixtures of additives can be used. A synergistic mixture consists of using a combination of additives in which the retarding effect is greater than the sum of the effect of the individual components. For this reason, it was decided to study the possibility of developing synergistic mixtures using a second additive to improve the effect of the main additive or additive 1, boehmite or brucite, or to complement it by making up for some of its deficiencies. The search for this second additive could lead to better flame retardant properties with a lower total additive percentage and with a lower effect on the mechanical properties. For this purpose, the optimal percentage of boehmite or brucite in the synergistic mixture is first calculated. Since both the maximum tensile and impact strength are significantly reduced, in order to obtain a balance between mechanical and fire properties, an optimisation of the results was carried out by restricting the maximum tensile strength to a minimum while minimising the propagation velocity. The result obtained for boehmite was 30.89%, approximating 30%, and for brucite, the optimum additive percentage was 40.29%, approximating 40%. Before proceeding to the second stage, a verification of the calculated optimum percentages was carried out. Since the value obtained for the maximum strength of the boehmite samples was higher than expected, the optimum percentage of boehmite was increased to 35% in the verification. In the case of brucite, there was no change.

In **Stage 2**, for the choice of the second additive, the main component of boehmite and brucite, AlO(OH) and Mg(OH)2 respectively, was considered because there are few articles on synergistic blends with these minerals. Following these criteria, it was determined that colemanite and expandable graphite (EG) could be candidates for synergistic additives. It was stipulated that the total additive content should be less than 60% to see if it is possible to achieve improved fire properties with a lower additive content and less impairment of mechanical properties. Therefore, considering that the additive percentage of boehmite and brucite were 35 and 40% respectively and that the total additive content should be less than 60%, 10 and 15% were set for colemanite and 10% for expandable graphite. At this stage it was concluded that expandable graphite also acts as a nucleant in polypropylene and in the case of colemanite contradictory conclusions were obtained between the results of the melting and crystallisation curves, so it cannot be confirmed that it acts as a nucleant. In terms of mechanical properties, similar trends were obtained, with the additives adding stiffness and decreasing the strength of the material. However, the mixture of brucite and colemanite shows promising mechanical results, as the mechanical properties were better compared to other samples with the same or even higher percentage of additive. In the fire tests, it was observed that the boehmite samples do not have a synergistic effect with colemanite and expandable graphite. As the results obtained in this stage and in stage 1 were not satisfactory, the use of boehmite was discarded. In the case of brucite, both colemanite and expandable graphite seem to have a synergistic effect. As in both the MCC (microscale combustion calorimetry) and CC (cone calorimeter) tests, the brucite/colemanite mixture performed best and the brucite/EG mixture presented manufacturing problems, it was decided to use the brucite/colemanite mixture in the next stage. Finally, since the mixture of brucite and colemanite seems to have a synergistic effect but the total percentage used is not sufficient to meet the requirements of the UL94 test, it was decided to use this mixture at 60% in total in the next stage and compare it with the PP+60%Bruc mixture, in order to confirm whether they have a synergistic effect.

To confirm that the brucite/colemanite mixture acts as a synergistic mixture, in **Stage 3** it was decided to study its effect in different proportions and thus determine the optimum percentages of each component. For this purpose, a total additive percentage of 60% was established and a level every 10% was set for each of the additives. In addition, to confirm that these additives act effectively as retardants, a 60% calcium carbonate mixture was added. Finally, as the additives used are of natural origin, but the matrix is of synthetic origin, it was decided to add a bioplastic to the study. In this case, it was decided to use PBS (polybutylene succinate) because it has similar properties to isotactic polypropylene, and has not been investigated in depth in terms of fire resistance. In summary, for the two polymeric matrices, it was decided to study the brucite/colemanite mixture at 60% total additive by varying the proportion of each component to determine which mixture is optimal. The mechanical test showed that the additive has a

significant influence on the mechanical properties by increasing the elastic modulus and flexural modulus and decreasing the ultimate tensile and impact strength. In the PP mixtures, it was observed that the substitution of part of the brucite by colemanite improves the mechanical properties, while no improvement was observed in the PBS matrix. In the UL94 test, it was confirmed that brucite and colemanite act as synergistic additives as the results obtained in their blends are better than when used separately. Furthermore, in the PP matrix better results were obtained with higher proportions of brucite, while in the PBS matrix better results were obtained with higher percentages of colemanite. The cone calorimeter test confirmed the conclusions of the UL94 test. Analysing the results of both tests together, it was obtained that the optimum samples in the PP matrix are PP+40%Bruc+20%Col and PP+30%Bruc+30%Col, and in the PBS matrix PBS+20%Bruc+40%Col and PP+10%Bruc+50%Col. Therefore, these mixtures are the ones that were used as matrices in the manufacture of the composites reinforced with natural fibres.

CHEMICAL TREATMENTS APPLIED TO NATURAL FIBRES

At the same time as improving the fire properties of the plastic matrix, the study of chemical treatments applicable to the linen fibre fabric was carried out. The reinforcing material used in the composites was a technical linen fabric FlaxDry BL with a density of 200g/m^2 and 2x2 twill structure.

In the review of the state of the art about chemical treatments applicable to fibres, it was observed that natural treatments can be applied to improve their fire resistance properties. For this reason, a synthetic and a natural treatment were selected taking into account their effect and availability. Of the synthetic options, silane treatment (3-Aminopropyltriethoxysilane 0.6%) was selected because it has been shown to improve mechanical and fire properties. On the other hand, from the natural treatments, banana pseudostem sap (BPS) was selected due to its high availability in the Canary Islands and the effect observed on different natural fibres. In this case, the influence of the concentration and addition of boric acid on linen fabric was studied. The concentrations studied were pure BPS (1:1), half concentrate (2:1) and quarter concentrate (4:1) and 3% boric acid (BA) was added. On the one hand, the silane treatment slightly improves the flame retardant properties. It delays the propagation speed, increasing the flame time by 7 seconds, but not enough to be used as a composite reinforcement. On the other hand, the BPS treatment significantly improved the thermal stability by completely inhibiting ignition. In conclusion, the mixed formulation of BPS 4:1 and 3%BA proved to be the most suitable for improving the fire resistance of the linen fabric.

COMPOSITES REINFORCED WITH NATURAL FIBRES

Throughout this thesis, the properties of the polymeric matrices on the one hand and the fabric on the other hand have been improved, so this chapter unifies the conclusions obtained, the mixtures and the treatment determined as optimal. For this purpose, the polymeric matrices without additive, with the optimal mixtures and with calcium carbonate, were reinforced with the treated and untreated linen fabric to determine which formulation is best for each matrix and whether fibre treatment is necessary.

During manufacturing, the composites obtained showed good visual characteristics because the mixture of the polymer with the additives was able to penetrate the fabric, thus achieving good adhesion between the matrix and the reinforcement. However, when the fabric is treated with the BPS adhesion worsens. In the study of the mechanical properties, both additives and treatment have a significant effect. The additives at 60% considerably decrease the mechanical properties of the composite and the treatment enhances this effect because it hinders the adhesion of the fibre to the plastic matrix. In the tensile test, additives increase the elastic modulus because they increase the stiffness of the material, but they also make it less strong by decreasing the ultimate tensile strength. The key variable in the elastic modulus is the hardness of the particles, since the harder they are, the higher the modulus. The same conclusions are drawn in bending and impact tests. The flexural modulus increases as the hardness of the additives increases and the impact strength decreases due to the density of the particles because they reduce the effective cross-section. In the UL94 test of PP composites, a significant effect of additives and treatment is obtained. Blends with brucite and colemanite inhibit horizontal flame spread and decrease vertical flame speed, but not enough to meet the test criteria. However, the treatment improves the flame retardant properties by preventing vertical flame propagation and significantly reducing the flame time thus obtaining a V-1 classification for the PP+40-20/LN-T composite. Therefore, the treatment of linen with BPS is key in PP composites. In the UL94 test of PBS composites, a significant effect of additives and treatment is also obtained. Blends of brucite and colemanite succeed in inhibiting flame both vertically and horizontally and the flame is extinguished in less than 10s, therefore all composites with these blends are classified as V-0. The treatment reduces the propagation speed, but it is not necessary to apply it as flame retardants allow the composites to pass the test and has the disadvantage of reducing the mechanical properties.

In summary, during the development of this thesis, two main problems have been addressed: halogenated flame retardants and the high combustibility of natural fibres Through the methodology carried out to improve the polymer and fibre properties separately, it has been determined that the best mixture for PP composite is 40% brucite plus 20% colemanite with linen

fabric treated with BPS 4:1+3%BA and for PBS composite is 10% brucite plus 50% colemanite with untreated linen fabric. In addition, between the two polymeric matrices, PBS is selected for its better fire properties and its more sustainable character.

RESUMEN

El rápido aumento del uso de polímeros y su impacto en el estilo de vida actual es casi incalculable. Hoy en día, es difícil encontrar objetos que no contengan materiales plásticos debido a sus características de precio, ligereza, aislamiento y resistencia, entre otras. Los plásticos se utilizan en una gran variedad de aplicaciones porque pueden adaptarse individualmente a los requisitos y necesidades de un determinado producto. En Europa, por sectores, el envasado es el mayor campo de aplicación, seguido de la construcción y la industria del automóvil, y en estos dos últimos sectores la resistencia al fuego de los materiales es clave.

El conocimiento de las propiedades del fuego permite predecir cómo se comportan los materiales en caso de incendio, cómo se inicia, evoluciona y propaga la combustión, y permite encontrar soluciones para mejorar su comportamiento. Para minimizar el riesgo de incendio y cumplir los requisitos de seguridad, se han desarrollado diferentes soluciones para evitar la ignición o reducir el calor liberado durante la combustión de los materiales. En el caso de los polímeros, estos métodos incluyen un enfoque de ingeniería, polímeros menos inflamables y aditivos ignífugos (FR). El uso de aditivos ignífugos es el método más común porque está bien aceptado, es rentable y relativamente fácil de incorporar. El término retardante de llama se define en la norma ISO 13943 como "sustancia añadida, o un tratamiento aplicado, a un material con el fin de suprimir o retrasar la aparición de una llama y/o reducir la velocidad de propagación de la llama". Por tanto, el término "retardante de llama" se refiere a una función, no a una familia de sustancias químicas. Clasificando los retardantes de llama por su naturaleza, pueden separarse en halogenados, fosforados, nitrogenados, compuestos de silicio, carbonosos, óxidos e hidróxidos metálicos, boratos, nanoarcillas y retardantes de llama naturales. Los basados en compuestos halogenados han sido los más utilizados debido a su eficacia, coste, disponibilidad y por la amplia experiencia de la industria con esta clase de aditivos. Sin embargo, estos compuestos son perjudiciales para la salud y el medio ambiente, por lo que han entrado en vigor nuevas normativas medioambientales que limitan e incluso impiden su uso. Encontrar alternativas es un gran reto para la industria de los retardantes de llama, ya que los otros tipos de retardantes de llama suelen ser específicos de cada polímero, por lo que un aditivo puede funcionar para un polímero concreto mientras que puede no tener ningún efecto en otro.

La creciente preocupación por el medio ambiente ha promovido varios estudios centrados en la mejora de la sostenibilidad de los materiales, los procesos industriales y la gestión de la enorme cantidad de residuos poliméricos que se producen en el mundo. Por este motivo, los retardantes de llama basados en fuentes naturales están despertando un gran interés. Los retardantes de llama

naturales son aditivos que pueden obtenerse por simple aislamiento a partir de fuentes naturales o biológicas, por lo que tienen una alta disponibilidad y permiten que los procesos industriales sean casi neutros en CO_2. Además, el desarrollo de retardantes de llama naturales a partir de recursos renovables también promueve el uso de polímeros de base biológica en muchos campos técnicos, manteniendo así la sostenibilidad del composite en su conjunto y preservando su buen impacto medioambiental. Sin embargo, la investigación sobre retardantes de llama naturales en biopolímeros sigue siendo escasa y es necesario seguir investigando en este campo.

Además de los retardantes de llama naturales y los biopolímeros, otra opción para mejorar la sostenibilidad es el uso de fibras naturales como refuerzo. El uso de fibras naturales es atractivo porque son un recurso renovable y biodegradable. Sin embargo, presentan algunas desventajas, como la variabilidad de la calidad, la baja resistencia al impacto, las temperaturas de procesamiento limitadas y la alta combustibilidad. Para mejorar el comportamiento al fuego de los composites, se pueden utilizar diferentes estrategias como reducir la inflamabilidad de la matriz, del refuerzo o de todo el compuesto. En cuanto al refuerzo, para mejorar las propiedades de resistencia al fuego de las fibras naturales, se pueden aplicar tratamientos químicos sintéticos y naturales. Por lo tanto, esta tesis presenta dos retos principales, mejorar el comportamiento al fuego de la matriz plástica mediante el uso de retardantes de llama naturales, y reducir la alta combustibilidad de las fibras vegetales.

En resumen, el objetivo principal de esta tesis es desarrollar composites poliméricos reforzados con fibras vegetales y aditivados con retardantes de llama naturales, y posteriormente evaluar su resistencia al fuego para determinar su capacidad para sustituir a los materiales de refuerzo convencionales.

Este objetivo general se alcanza a través de los siguientes objetivos específicos:

1. Evaluación de los retardantes de llama naturales aplicables al composite objeto de estudio.

Una correcta evaluación de los retardantes de llama naturales permite obtener un material con propiedades ignífugas óptimas utilizando la menor cantidad de aditivo posible. Por lo tanto, a la hora de elegirlos se tiene en cuenta la matriz polimérica, el origen, la disponibilidad y el precio.

2. Tratamiento de las fibras naturales

El uso de fibras naturales como refuerzo en materiales compuestos es un tema de gran interés, pero presentan algunos inconvenientes como su escasa compatibilidad con la matriz polimérica y su alta combustibilidad debido a su origen. Teniendo en cuenta estos inconvenientes, se concluye

que son necesarias algunas modificaciones para reducir su combustibilidad y conseguir un buen acoplamiento entre la matriz y la fibra.

3. **Formulación de los composites**

Una vez determinados los retardantes de llama y los tratamientos químicos que utilizar, es necesario estudiar las condiciones del proceso de fabricación de los composites. Esto es debido a que los aditivos influyen en los parámetros de presión, temperatura y tiempo de proceso. A continuación, se fabrican las piezas mediante moldeo por compresión, variando el tipo de aditivo, el refuerzo y su porcentaje.

4. **Caracterización de los materiales**

Debido a que los retardantes de llama naturales se utilizan a menudo en porcentajes elevados, las propiedades de los materiales, especialmente las mecánicas, se ven afectadas. Para comprender cómo se ven influidas estas propiedades, se realizan ensayos térmicos, mecánicos, ópticos y reológicos en polímeros, fibras y materiales compuestos.

5. **Ensayos de fuego**

Por último, se realizan ensayos de fuego de polímeros, fibras y materiales compuestos, como UL94 y calorímetro de cono, para determinar el efecto de los retardantes de llama y los tratamientos utilizados.

Con los resultados obtenidos en los ensayos mecánicos y de fuego, se lleva a cabo una optimización para determinar los mejores aditivos y tratamientos, y se realiza un proceso de retroalimentación hasta determinar la solución óptima. A continuación, se presenta un resumen de las pruebas experimentales realizadas, junto con los resultados y las conclusiones.

SELECCIÓN DE LOS RETARDANTES DE LLAMA NATURALES

En la evaluación de los retardantes de llama naturales aplicables al composite objeto de estudio, se ha observado que algunos de los retardantes de llama más utilizados tienen su alternativa de origen natural, pero que éstas aún no han sido estudiadas en profundidad. Dado que el objetivo de esta tesis es mantener en la medida de lo posible el carácter natural del aditivo porque el refuerzo es un tejido de fibras natural, se propone utilizar aditivos que procedan directamente de la fuente o que no requieran muchos procesos de síntesis o refinamiento. Uno de los aditivos que cumple estos requisitos es la brucita, que, aunque requiere altas cargas, ha demostrado ser eficaz. Por otro lado, se consideró el uso de boehmita porque, aunque requiere separación del mineral principal y su eficacia no es tan buena como la de la brucita, es un aditivo que no se ha estudiado en detalle y podría ser una alternativa interesante al hidróxido de aluminio. Por último, de los retardantes de llama de origen biológico, se seleccionó la lignina porque es un residuo que se obtiene en la industria papelera y su uso le confiere un valor adicional.

Dado que los aditivos seleccionados no han sido estudiados en detalle, es necesario realizar varios ciclos hasta obtener el porcentaje de aditivo óptimo para la matriz plástica. Por este motivo, en este estudio se han llevado a cabo tres etapas.

En la **Etapa 1**, se utilizaron boehmita, brucita y lignina como aditivos retardantes y la matriz utilizada fue polipropileno (PP) en dos viscosidades. Según la bibliografía, los minerales deben utilizarse hasta un 60-70% para obtener un material ignífugo, por esta razón, la boehmita y la brucita se utilizaron al 45 y al 60% para estudiar su efecto y tendencia. Por otro lado, algunos autores han demostrado que un 20% de lignina mejora las propiedades ignífugas del polipropileno, por lo que se decidió estudiar el efecto de la lignina al 10 y al 20%. En el ensayo de DSC (Calorimetría Diferencial de Barrido), se observó que la boehmita y la brucita actúan como nucleante del PP porque aumentan el porcentaje de cristalinidad, favorecen la formación de cristales y mejoran la homogeneidad de la estructura de los cristales. Además, las muestras con aditivos minerales tienen un módulo de almacenamiento superior al del PP virgen en el intervalo de temperaturas ensayado en la prueba DMA (Análisis Mecánico Dinámico), por lo que mejoran la estabilidad termo-mecánica. Sin embargo, las propiedades mecánicas se vieron afectadas negativamente. Los aditivos aumentan el módulo elástico y de flexión hasta 4430 y 4330 MPa, respectivamente, para las muestras con un 60% de aditivo, en comparación con los 1700 y 1500 MPa obtenidos para el PP sin relleno. En cuanto a la resistencia, la tensión máxima a tracción y la resistencia al impacto se redujeron hasta un 42% y un 82%, respectivamente. Por lo tanto, los aditivos utilizados rigidizan, pero también reducen la resistencia de los materiales compuestos. Los resultados del ensayo de fuego tampoco fueron satisfactorios. La brucita y la boehmita mejoraron la resistencia al fuego, pero no lo suficiente, y la lignina la empeoró. Por este motivo, se decidió descartar la lignina para etapas posteriores y se optimizaron las muestras con boehmita y brucita.

Para solventar el problema de bajas propiedades mecánicas y resistencia al fuego, se pueden utilizar mezclas sinérgicas de aditivos. Una mezcla sinérgica consiste en utilizar una combinación de aditivos en la que el efecto retardante es mayor que la suma del efecto de los componentes individuales. Por esta razón, se decidió estudiar la posibilidad de desarrollar mezclas sinérgicas utilizando un segundo aditivo para mejorar el efecto del aditivo principal o aditivo 1, boehmita o brucita, o para complementarlo supliendo algunas de sus deficiencias. La búsqueda de este segundo aditivo podría conducir a mejores propiedades ignífugas con un menor porcentaje de aditivo total y con un menor efecto sobre las propiedades mecánicas. Para ello, se calcula primero el porcentaje óptimo de boehmita o brucita en la mezcla sinérgica. Dado que tanto la tensión

máxima como la resistencia al impacto se reducen significativamente, para obtener un equilibrio entre las propiedades mecánicas y las propiedades frente al fuego, se llevó a cabo una optimización de los resultados restringiendo un mínimo de la resistencia máxima a la tracción y minimizando al mismo tiempo la velocidad de propagación. El resultado obtenido para la boehmita fue del 30,89%, aproximado al 30%, y para la brucita, el porcentaje óptimo de aditivo fue del 40,29%, aproximado al 40%. Antes de pasar a la segunda etapa, se llevó a cabo una verificación de los porcentajes óptimos calculados. Dado que el valor obtenido para la resistencia máxima de las muestras de boehmita fue superior al esperado, en la verificación se aumentó el porcentaje óptimo de boehmita al 35%. En el caso de la brucita no hubo cambios.

En la **Etapa 2**, para la elección del segundo aditivo, se consideró el componente principal de la boehmita y la brucita, AlO(OH) y $Mg(OH)_2$ respectivamente, porque hay pocos artículos sobre mezclas sinérgicas con estos minerales. Siguiendo estos criterios, se determinó que la colemanita y el grafito expandible (EG) podían ser candidatos a aditivos sinérgicos. Se estipuló que el contenido total de aditivo debía ser inferior al 60% para ver si es posible conseguir una mejora de las propiedades frente al fuego con un menor contenido de aditivo y una menor afectación de las propiedades mecánicas. Por lo tanto, considerando que el porcentaje de aditivo de la boehmita y la brucita eran 35 y 40% respectivamente y que el contenido total de aditivo debía ser inferior al 60%, se fijaron 10 y 15% para la colemanita y 10% para el grafito expandible. En esta etapa se concluyó que el grafito expandible también actúa como nucleante en el polipropileno y en el caso de la colemanita se obtuvieron conclusiones contradictorias entre los resultados de las curvas de fusión y cristalización, por lo que no se puede confirmar que actúe como nucleante. En cuanto a las propiedades mecánicas se obtuvieron tendencias similares, los aditivos aportan rigidez y disminuyen la resistencia del material. Sin embargo, la mezcla de brucita y colemanita muestra resultados mecánicos prometedores, ya que las propiedades mecánicas fueron mejores en comparación a otras muestras con el mismo porcentaje de aditivo o incluso superior. En los ensayos de fuego, se observó que las muestras de boehmita no tienen un efecto sinérgico con la colemanita y el grafito expandible. Como los resultados obtenidos en esta etapa y en la etapa 1 no fueron satisfactorios, se descartó el uso de boehmita. En el caso de la brucita, tanto la colemanita como el grafito expandible parecen tener un efecto sinérgico. Como tanto en la prueba MCC (calorimetría de combustión a microescala) como en la prueba CC (calorímetro de cono), la mezcla de brucita/colemanita obtuvo los mejores resultados y la mezcla de brucita/EG presentó problemas de fabricación, se decidió utilizar la mezcla de brucita/colemanita en la siguiente etapa. Por último, dado que la mezcla de brucita y colemanita parece tener un efecto sinérgico pero el porcentaje total utilizado no es suficiente para cumplir los requisitos de la prueba UL94, se decidió utilizar esta mezcla al 60% en total en la siguiente fase y compararla con la mezcla PP+60%Bruc, a fin de confirmar si tienen un efecto sinérgico.

Para confirmar que la mezcla de brucita/colemanita actúa como una mezcla sinérgica, en la **Etapa 3** se decidió estudiar su efecto en diferentes proporciones y así determinar los porcentajes óptimos de cada componente. Para ello, se estableció un porcentaje total de aditivo del 60% y se fijó un nivel cada 10% para cada uno de los aditivos. Además, para confirmar que estos aditivos actúan eficazmente como retardantes, se añadió una mezcla de carbonato cálcico al 60%. Por último, como los aditivos utilizados son de origen natural, pero la matriz es de origen sintético, se optó por añadir un bioplástico al estudio. En este caso, se decidió utilizar PBS (succinato de polibutileno) porque tiene propiedades similares al polipropileno isotáctico, y no se ha investigado en profundidad en términos de resistencia al fuego. En resumen, para las dos matrices poliméricas, se decidió estudiar la mezcla brucita/colemanita al 60% de aditivo total variando la proporción de cada componente para determinar qué mezcla es la óptima. En el ensayo mecánico se obtuvo que el aditivo tiene una influencia significativa en las propiedades mecánicas ya que aumentan el módulo elástico y de flexión y disminuyen la resistencia última a la tracción y al impacto. En las mezclas de PP se observó que la sustitución de parte de la brucita por colemanita mejora las propiedades mecánicas, mientras que en la matriz de PBS no se observó ninguna mejora. En el ensayo UL94 se confirmó que la brucita y la colemanita actúan como aditivos sinérgicos ya que los resultados obtenidos en sus mezclas son mejores que cuando se utilizan por separado. Además, en la matriz de PP se obtuvieron mejores resultados con mayores proporciones de brucita, mientras que en la matriz de PBS se obtuvieron mejores resultados con mayores porcentajes de colemanita. La prueba del calorímetro de cono confirmó las conclusiones de la prueba UL94. Analizando conjuntamente los resultados de ambos ensayos, se obtuvo que las muestras óptimas en la matriz PP son PP+40%Bruc+20%Col y PP+30%Bruc+30%Col, y en la matriz PBS PBS+20%Bruc+40%Col y PP+10%Bruc+50%Col. Por tanto, estas mezclas son las que se emplearon como matrices en la fabricación de los composites reforzados con fibras naturales.

TRATAMIENTOS QUÍMICOS APLICADOS A LAS FIBRAS NATURALES

Paralelamente a la mejora de las propiedades frente al fuego de la matriz plástica, se llevó a cabo el estudio de tratamientos químicos aplicables al tejido de lino. El material de refuerzo utilizado en los composites fue un tejido de lino técnico FlaxDry BL con una densidad de 200g/m^2 y estructura de sarga 2x2.

En la revisión del estado del arte sobre tratamiento químicos aplicables a las fibras se observó que se pueden aplicar tratamientos naturales para mejorar sus propiedades de resistencia al fuego. Por este motivo se seleccionó un tratamiento sintético y otro natural teniendo en cuenta su efecto y disponibilidad. De las opciones sintéticas, se seleccionó el tratamiento con silano (3-

Aminopropiltrietoxisilano al 0,6%) porque se ha demostrado que mejora las propiedades mecánicas y frente al fuego. Por otro lado, de los tratamientos naturales, se seleccionó la savia de pseudotallo de platanera (BPS) debido a su alta disponibilidad en las Islas Canarias y al efecto observado en diferentes fibras naturales. En este caso, se estudió la influencia de la concentración y la adición de ácido bórico en tejido de lino. Las concentraciones estudiadas fueron BPS puro (1:1), concentrado a la mitad (2:1) y concentrado a la cuarta parte (4:1) y se añadió ácido bórico (BA) al 3%. Por un lado, el tratamiento con silano mejora ligeramente las propiedades ignífugas. Retrasa la velocidad de propagación, aumentando el tiempo de llama en 7 segundos, pero no lo suficiente como para ser utilizado como refuerzo de un composite. Por otro lado, el tratamiento con BPS mejoró significativamente la estabilidad térmica inhibiendo completamente la ignición. En conclusión, la formulación mixta de BPS 4:1 y 3%BA resultó ser la más adecuada para mejorar la resistencia al fuego del tejido de lino.

COMPOSITES REFORZADOS CON FIBRAS NATURALES

A lo largo de esta tesis se han ido mejorando las propiedades de las matrices poliméricas por un lado y del tejido por otro, por lo que en este capítulo se unifican las conclusiones obtenidas, las mezclas y el tratamiento determinado como óptimo. Para ello, las matrices poliméricas sin aditivo, con las mezclas óptimas y con carbonato cálcico, se reforzaron con el tejido de lino tratado y sin tratar para determinar qué formulación es la mejor para cada matriz y si es necesario el tratamiento de la fibra.

Durante la fabricación, los composites obtenidos mostraron buenas características visuales debido a que la mezcla del polímero con los aditivos fue capaz de penetrar en el tejido, consiguiendo así una buena adhesión entre la matriz y el refuerzo. Sin embargo, cuando el tejido se trata con el BPS la adhesión empeora. En el estudio de las propiedades mecánicas, tanto los aditivos como el tratamiento tienen un efecto significativo. Los aditivos al estar al 60% disminuyen considerablemente las propiedades mecánicas del composite y el tratamiento potencia este efecto porque dificulta la adhesión de la fibra a la matriz plástica. En el ensayo de tracción, los aditivos aumentan el módulo elástico porque incrementan la rigidez del material, pero también lo hacen menos resistente al disminuir la resistencia máxima a la tracción. La variable clave en el módulo elástico es la dureza de las partículas, ya que cuanto más duras sean, mayor será el módulo. En los ensayos de flexión y de impacto se obtienen las mismas conclusiones. El módulo de flexión aumenta a medida que aumenta la dureza de los aditivos y la resistencia al impacto disminuye debido a la densidad de las partículas porque reducen la sección transversal efectiva. En el ensayo UL94 de composites de PP, se obtiene un efecto significativo de los aditivos y del tratamiento. Las mezclas con brucita y colemanita inhiben la propagación horizontal de la llama

y disminuyen la velocidad vertical de la llama, pero no lo suficiente como para cumplir los criterios del ensayo. Sin embargo, el tratamiento mejora las propiedades ignífugas impidiendo la propagación vertical de la llama y reduciendo significativamente el tiempo de la llama obteniendo así una clasificación V-1 para el composite PP+40-20/LN-T. Por lo tanto, el tratamiento del lino con BPS es clave en los composites de PP. En el ensayo UL94 de composites de PBS, también se obtiene un efecto significativo de los aditivos y el tratamiento. Las mezclas de brucita y colemanita consiguen inhibir la llama tanto vertical como horizontalmente y la llama se extingue en menos de 10s, por lo tanto, todos los composites con estas mezclas se clasifican como V-0. El tratamiento reduce la velocidad de propagación, pero no es necesario aplicarlo ya que los retardantes de llama permiten a los composites superar el ensayo y tiene el inconveniente de reducir las propiedades mecánicas.

En resumen, durante el desarrollo de esta tesis se han abordado dos problemas principales: los retardantes de llama halogenados y la alta combustibilidad de las fibras naturales. Mediante la metodología llevada a cabo para mejorar las propiedades del polímero y de la fibra por separado, se ha determinado que la mejor mezcla para el composite PP es 40% brucita más 20% colemanita con tejido de lino tratado con BPS 4:1+3%BA y para el composite PBS es 10% brucita más 50% colemanita con tejido de lino sin tratar. Además, entre las dos matrices poliméricas, se selecciona el PBS por sus mejores propiedades ignífugas y su carácter más sostenible.

CONTENTS

CHAPTER 1

INTRODUCTION

TABLE OF CONTENTS

This introductory chapter contains the justification of the thesis topic, the objectives to achieve it and the relationship between them. Finally, the structure of the manuscript and the contents of each chapter are shown.

1. JUSTIFICATION

The rapid increase in the use of polymers and their impact on the current lifestyle is almost incalculable. Nowadays, it is difficult to find objects that do not contain plastic materials due to their price, lightness, insulation, and resistance characteristics, among others. In addition, plastics have brought numerous benefits to society, improving sustainability and food safety, contributing to a more energy-efficient world, and even saving our lives. However, due to the large amount of plastic waste generated each year, the environmental regulations are becoming increasingly stringent, requiring "clean" processes and raw materials. The use of natural fibres that can replace conventional fibres is becoming a promising avenue for improved sustainability.

The use of natural fibres is attractive because they are a renewable and biodegradable resource, and thermal recycling of the composite is possible. Nevertheless, there are some disadvantages, such as quality variability, low impact resistance and limited processing temperatures, which often limit the polymers used as matrix. It should be noted that natural fibre reinforced polymers have their main applications in the transport industry, where fire behaviour is a key requirement. The knowledge of the fire properties of materials allows us to predict how materials behave in case of fire, how combustion starts, evolves, and spreads, and enables us to find solutions to improve their behaviour.

To improve the fire behaviour of these materials, different strategies can be used to reduce the flammability of the matrix, the reinforcement, or the entire composite. Flame retardants based on halogenated compounds have been the most widely used until new environmental regulations came into force restricting their use due to the toxic gases they emit to the environment. These substances have been the most effective solutions to improve the fire performance of plastic materials. Finding alternatives is an important challenge for the flame-retardant industry. In fact, these products remain important in the market because there are no alternatives to replace them with similar effectiveness. Nowadays, regulations in this field address not only fire protection aspects, but also other issues such as recyclability, environmental impact, and toxicity of the compounds released. Such regulations mean that when designing fire protection strategies, the market has to adapt and consider multiple factors. Consequently, it is not possible to make decisions based only on the most effective solution to protect materials from fire.

The increasing concern to reduce the ecological footprint of materials has stimulated the development of new plastics and additives from renewable resources. As already mentioned, the use of natural fibres as reinforcement for composites is a topic of great current interest because it reduces the negative effects that non-renewable sources have on the environment. For this reason, the industry is also exploring the use of natural flame retardants, which would provide additional environmental value to the composite. The drawback is that the availability of natural flame retardants on the market is limited, and the study of their use is quite recent. Compounds such as minerals, chitosan, lignin, etc. are found in the literature, but the flame retardancy results are still not comparable to those of halogenated compounds.

In summary, the composites studied present two main challenges, improve the fire behaviour of the plastic using natural flame retardants, and reduce the high combustibility of vegetable fibres.

2. OBJECTIVES

The main objective of this thesis is to develop polymeric composites reinforced with vegetable fibres and additivated with natural flame retardants, and then evaluate their fire resistance to determine their capacity to replace conventional reinforcement materials.

This general objective is achieved through the following specific objectives:

- **Evaluation of natural flame retardants applicable to the composite under study**

  A proper evaluation of the natural flame retardants would yield a material with optimal fire properties using the least amount of additive possible. The term “flame retardant” refers to a function, not a family of chemicals, whereby a variety of chemical compositions with different properties and molecular structures function as flame retardants. Moreover, they do not all have the same effect on different polymers. Therefore, the polymeric matrix, origin, availability, and price are considered when choosing them.

- **Treatment of natural fibres**

  The use of natural fibres as reinforcement in composites is a topic of great interest, but they present some disadvantages such as poor compatibility with polymer matrix and high combustibility due to their origin. Considering the drawbacks, it is concluded that some modifications are necessary to reduce their burning nature and to achieve a good coupling between the matrix and the fibre.

- **Formulation of the composites**

  Once the flame retardants and the chemical treatments to be used have been determined, it is necessary to study the process conditions to manufacture the composites. This is

because the additives influence the pressure, temperature, and process time parameters. Then, the parts are manufactured by compression moulding, varying the type of additive, the reinforcement, and their percentage.

- **Characterization of the materials**

  Due to natural flame retardants are often used in high percentages, the properties of the materials, especially the mechanical ones, are affected. To understand how these properties are influenced, thermal, mechanical, optical, and rheological tests are conducted on polymers, fibres, and composites.

- **Fire tests**

  Finally, fire test of polymers, fibres, and composites such as UL94 and cone calorimeter, are performed to ascertain the effect of the flame retardants and treatments used.

With the results obtained in the mechanical and fire tests, an optimisation is carried out to determine the best additives and treatments, and thus execute a feedback process as shown in the following diagram.

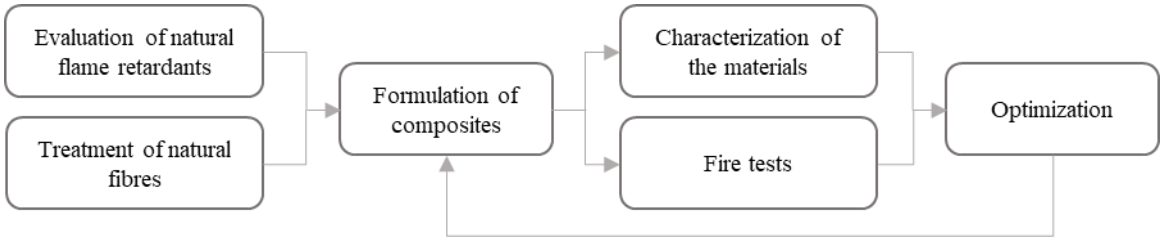

FIGURE 1: THESIS ORGANIZATION AND INTERRELATION BETWEEN OBJECTIVES

3. STRUCTURE OF THE DOCUMENT

The document is divided into seven chapters, as described below:

- **Chapter 1: Introduction.** This chapter describes the reasons and objectives that have led to the development of this thesis and explains the structure of the document.
- **Chapter 2: State of the art.** This chapter contains an introduction to flame retardants, then focuses on those of natural origin, and reviews the state of the art of their use in thermoplastic polymers. Subsequently, the flammability of natural fibres and the chemical treatments applied to improve their fire resistance are studied. Finally, fire tests and the basic concepts necessary to understand them are described.
- **Chapter 3: Materials and methods.** During the development of this thesis, three feedback cycles have been carried out to improve the properties of the polymeric matrix with the same characterization tests performed at each stage. This chapter summarises the materials used, composite production and subsequent characterisation and evaluation.

- **Chapter 4: Flame retardancy of polymers.** Three stages have been carried out to improve the fire resistance properties of polymer matrices. In the first stage, boehmite, brucite and lignin were used as fire retardant additives and the matrix used was polypropylene in two viscosities. In the second stage, the additives were boehmite, brucite, colemanite and expandable graphite in polypropylene. In the last stage, brucite and colemanite were used in both polypropylene and polybutylene succinate. This chapter summarises the different mixtures studied, the characterization results, the optimization and the conclusions of each stage. Finally, the mixtures selected for the manufacture of the composites are defined.
- **Chapter 5: Chemical treatments applied to natural fibres**. The first section describes the different treatments selected to improve the fire properties of the natural fibres. Then, the materials and methods used in each treatment, as well as the tests carried out for their characterization. Finally, the results obtained, and the optimum treatment selected for the next stage are shown.
- **Chapter 6: Composites reinforced with natural fibres.** This chapter describes the methodology used for the manufacture of the composites reinforced with natural fibres and proceeds with their characterization. The results obtained in the tests, discussion and conclusions are shown.
- **Chapter 7: Conclusions and future lines.** This chapter summarizes the main conclusions drawn from this research and the potential research lines that emerged from the development of this doctoral thesis.
- **Annex:** This document contains all the characterization results not included in the memory.

CHAPTER 2

STATE OF THE ART

TABLE OF CONTENTS

This chapter first introduces the importance of studying fire properties, how the combustion process works and how the fire resistance properties of materials can be improved. Then, provides an overview of flame retardants in polymers, their mechanism of action, types and then goes into more detail on those of natural origin reviewing their use in thermoplastics. The next section studies the characteristics of natural fibres and the chemical treatments applicable to improve their fire resistance. Finally, the last section summarizes the fire tests carried out and the basic concepts necessary for their understanding.

1. INTRODUCTION

The rapid increase in the use of polymers and their impact on the present way of life is almost incalculable. Plastics have brought numerous benefits to society, improving food sustainability and safety, contributing to a more energy-efficient world, and even saving our lives. Nowadays polymers are used in our daily life in different dominions of sciences, technologies, and industry; from polymers used for packaging to biopolymers in medical applications. In fact, the global production of plastics increased more than 390 million tonnes in 2021 [1] and it is estimated that by 2050 world production will be almost 590 MMT and one fifth of global oil consumption [2]. Due to it is an essential material for our society, our sector must focus on sustainability and positive impact of plastics on people and the planet. For example, in Europe in 2020 only 29.5 Mt of the 55 produced were collected, of which 34.6% was sent to recycling centres, 42% to energy recovery and 23.4% to landfill [1]. The data has been improving over the years, but the increase in post-consumer plastic waste remains a serious concern for environmental conservation.

As mentioned before, plastics are used in a wide variety of applications because they can be individually adapted to the requirements and needs of a certain product. In Europe, by sector, packaging is the largest field of application followed by construction and automotive industry (Figure 1). In addition to the mechanical, health and insulation requirements, among others, that plastic materials must accomplish, there are certain applications where fire resistance is key. In relation to the sectors represented in Figure 1, fire is a very important factor in transport, construction, as well as electronics, which represent 33% of European demand. Despite improvements in systems to prevent or stop fires, fire costs approximately 1% of global gross domestic product (GDP) per year and causes several thousand deaths in Europe [3]. Global statistics on fires in 2019 showed that 31.6% were structural fires (residentials and others), causing almost 14000 deaths and 30000 injuries. Furthermore, transport accounted 13.4% of fires

and 862 deaths and 2821 injuries [4]. Consequently, improving the fire resistance of plastics is an important research topic because fire is a constant risk.

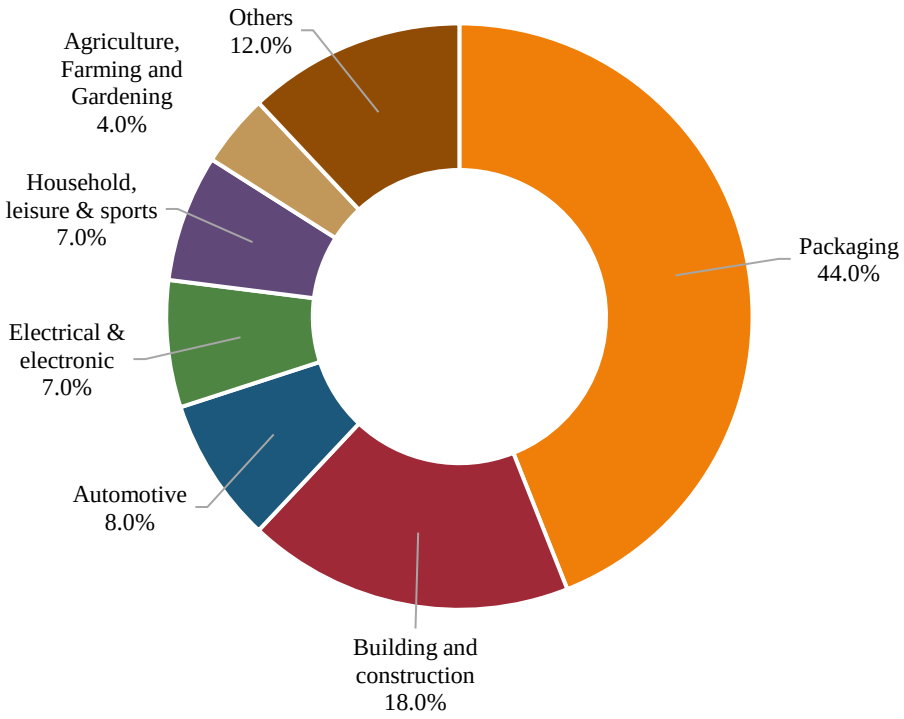

FIGURE 1: PLASTIC DEMAND BY SEGMENT IN EUROPE IN 2021 [1]

Another clear example of the importance of fire is the aircraft sector, which is the most regulated. According to the Federal Aviation Administration (FAA), in case of an-inflight fire, "Delaying the aircraft's descent by only two minutes is likely to make the difference between a successful landing and evacuation, and a complete loss of the aircraft and its occupants." [5]. In fact, in-flight fires were the cause with the fourth highest number of on-board fatalities and the seventh most frequent cause of accidents in 2005 [6]. There are several possible causes in the production of an accidental fire, but experience and real cases of fire accidents show how it can become a real safety hazard and risk. Indeed, F. Uddin summarized aircraft accidents in which fire caused serious harm to lives and valuables and described the types of aircraft fires and their effects [7].

There are currently two fundamental strategies for fighting fires: the eradication of fires once they have broken out and prevention through the protection of materials, and in this case, we focus on the latter. To minimize fire hazard and accomplish fire safety requirements, different solutions have been developed to prevent ignition or reduce the heat released during combustion of materials. For polymers, these methods include engineering approach, less flammable polymers,

and flame retardant (FR) additives [8]. Engineering approach is an economical but unsafe method. It involves finding a way to remove the polymer from the fire risk scenario, for example by means of a fire shield or by modifying the construction where the material is used. The drawback occurs when the barrier is damaged, fractured, loses adhesion, or falls down due to impact or time, leaving the flammable material exposed to fire. On the other hand, low flammable polymers are a durable and robust solution as, whatever the fire risk scenario, the material presents a minimal fire risk. Nevertheless, they are expensive, so their use is limited by economic conditions, and many of them are difficult to recycle. Finally, FR additives are the most common because it is a well-accepted method, cost effective and relatively easy to incorporate and for this reason they are the strategy that will be pursued. However, in order to understand how flame retardants work, it is first necessary to understand the combustion process of the materials.

2. COMBUSTION OF POLYMERS

Polymers are compounds that in general terms are highly flammable due to their chemical structure, which is mainly composed of carbon and hydrogen [9]. Furthermore, the polymers most commonly used in the plastics sector are composed of a series of organic monomers and are therefore susceptible to combustion. When a plastic burns, a thermo-oxidative reaction takes place which reduces the carbonaceous chains of the polymer to low molecular weight monomers or groups of monomers and these in turn to carbon dioxide, water, and other combustion products of lower molecular weight than the original polymer. For this reaction to take place there must be three components, a heat source, a fuel (polymer), and a combustive (oxygen from the air) [10] and if any of these components is removed combustion stops. It is therefore necessary to understand how this cycle occurs in order to know how it can be avoided. The combustion process includes several stages, ignition, fire growth, fully developed fire and finally fire decay [11]. In the first stage, ignition is defined as the start of flaming combustion, usually due to an ignition source such as a flame, a cigarette, a glowing wire, etc [12]. Later in the fire growth phase there is an increase in the heat release rate and temperature of the fire which contributes to its growth [13]. During this phase, the fire spreads rapidly and within a few minutes the heat and smoke generated produce a so-called "flashover", at which point it is difficult to control the fire [14], thus producing the fully developed fire phase. Finally, the fire decays because all combustible material has been consumed or because the source of heat or the combustive has been eliminated.

When we focus on the material, combustion takes place by two mechanisms, gas and condensed phase. Figure 2 shows how the combustion cycle of the material occurs. When polymers are subjected to a given amount of heat, the weakest bonds are broken first and degradation of the material occurs. Due to this process, the material releases a layer of carbon and

flammable volatiles from the pyrolysis of the polymer. These volatiles mix with atmospheric oxygen and at some point, the lower ignition limit is reached. At this point, if a flame is present, ignition occurs and if there is no flame, auto-ignition may occur if a sufficiently high temperature is reached. As the reaction of the combustible gases is exothermic, heat is released which feeds the flame. If the energy generated is greater than that absorbed by the endothermic pyrolysis reactions, the flame spreads, thus generating more heat to fuel the process. Consequently, further degradation of the material occurs, thus promoting a self-sustaining combustion cycle that continues until one or more of the factors limit the continuation of the cycle [15].

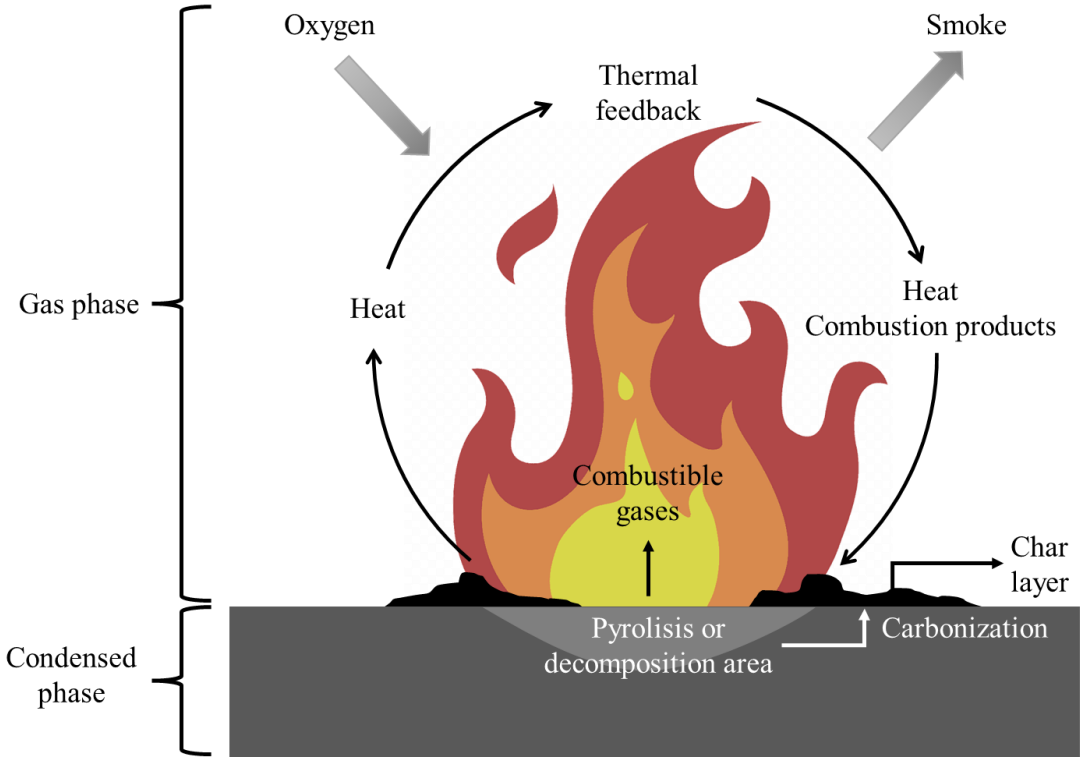

FIGURE 2: COMBUSTION CYCLE BASED ON [13,16]

Considering all the processes that occur during this cycle, flame retardants can prevent fire by physical or chemical action in solid or gas phase. The following section reviews flame retardants, types and finally focuses on those of natural origin.

3. FLAME RETARDANTS IN POLYMERS

Flame retardant is defined by ISO 13943 as “substance added, or a treatment applied, to a material in order to suppress or delay the appearance of a flame and/or reduce the flame spread rate” [17]. Therefore, the term “flame retardant” refers to a function, not a family of chemicals. Flame retardants can be separated into several classes according to their place of action, gas or

condensed phase; mode of action, physical or chemical; chemical nature, halogenated, phosphorus, nitrogen, etc; and incorporation type, additive or reactive [18].

To understand how flame retardants improve the fire behaviour of materials, it is necessary to consider all the stages involved on the combustion cycle. Once the polymer has been subjected to an ignition source and the combustion has started, the accumulation of heat on the material causes its thermal degradation and the emission of combustible gases. The physical action of the flame retardants involves the absorption of combustion energy due to the endothermic process of FR decomposition, the dilution of volatiles by the release of non-combustible gases, and the formation of a protective layer which isolates the material from heat and oxygen. Regarding to the chemical action, in gas phase, the release of substances that inhibit the flame or reduce its intensity, and in condensed phase, the formation of non-combustible carbonous chains as well as the decrease of the molecular weight of the polymer [15]. Lastly, emphasise the difference between a reactive and an additive FR. The first type modifies the polymer molecule by binding onto the polymer chain, thus, one of the main advantages is that it avoids alterations in the physical and mechanical properties of the functionalised polymer. On the other hand, the second type act as a charge, so present several advantages such as easy handling and processing, lower cost and no additional chemicals need. However, it is necessary to use higher loadings, so the rheological and mechanical properties are compromised.

3.1 TYPES OF FLAME RETARDANTS

According to the chemical nature classification, flame retardants can be separated into halogenated, phosphorus, nitrogen, silicon, carbon, metallic oxides and hydroxides, borate, nano-clays, and natural flame retardants [19]. Those based on halogenated compounds have been the most used ones due to their effectiveness, cost, availability, and extensive industry experience with this class of additives [20]. However, these compounds are harmful to health and the environment, thus, new environmental regulations have entered into force that limit and even prevent their use. These restrictions are caused by the improvement of analytical techniques that allow the detection of small amounts of compounds in animals and plants far away from areas where these additives are produced, distributed, and consumed, and by the ecological pressure for the use of chemicals, especially the halogen group [15]. Furthermore, these halogenated retardants have been found at increasing levels in household dust, human blood, breast milk, and wild animals [21,22]. Unfortunately, many of these chemicals are now recognized as global contaminants and are associated with adverse health effects in animals and humans, including endocrine and thyroid disruption, immunotoxicity, reproductive toxicity, cancer, and adverse effects on foetal and child development and neurologic function [23–27]. For this reason, the

scientific community has been heavily focused on finding alternatives, recognizing the necessity of a change, in the face of the increasing pressure from environmental concerns. Alternatives include metal hydroxides [28,29], phosphorus compounds [30,31], carbon nanotubes [32], expandable graphite [33], clays [34], and nanoparticles [13], among others, but they have the disadvantage that they are usually polymer-specific, so one additive may work for a particular polymer while it may have no effect on another. In addition, they are often less effective than halogenated retardants and require higher loadings to meet flammability criteria, therefore, find alternatives is a great challenge for the industry of flame retardants.

Humanity's recent evolution towards a more sustainable society has motivated all segments of society to critically evaluate our use of natural resources (energy, water, etc.), toxicity issues and environmental impact. The increasing concern in the environment has promoted several studies focused on the improvement of the sustainability of materials, industrial processes, and the management of the huge amount of polymer waste produced in the world. Nowadays, new solutions of flame retardants based on natural sources are attracting great interest. Natural flame retardants are additives that can be obtained by simple isolation from natural or biological sources [35]. In addition, they have high availability and enable industrial processes to be nearly CO_2 neutral since bio-based products release no more CO_2 at the end of their life than was originally metabolized in the biological production of the raw material [36]. Additionally, the development of natural flame retardants from renewable resources also promotes the use of bio-based polymers in many technical fields, thus maintaining the sustainability of the composite as a whole and preserving its good environmental impact. However, research on natural flame retardants in biopolymers is still scarce and there is a need to further promote this field.

For this reason, this thesis focuses on the use of flame retardants of natural origin. As the composite under study in this thesis is based on a thermoplastic matrix, a review of the state of the art of these additives in both non-biodegradable and biodegradable/bio-based thermoplastic polymers is carried out.

3.2 NATURAL FLAME RETARDANTS IN NON-BIODEGRADABLE THERMOPLASTIC POLYMERS

As mentioned above, natural flame retardants are additives that can be obtained by simple isolation from natural or biological sources and their types include mainly mineral additives and bio-based compounds. The following is an overview of both types, including the most important or representative ones.

3.2.1 MINERAL ADDITIVES

Mineral by definition is “inorganic substance found on the surface or in the various layers of the earth's crust” [37]. These substances have been widely used as retardants because in addition to being non-combustible, they are functional fillers. The incorporation of any non-combustible filler such as minerals reduces the flammability of a polymer because it reduces the total amount of fuel, the diffusion rate of oxygen and fuel in the polymer, as well as increases the heat capacity, thermal conductivity, reflectivity, and emissivity [38]. In addition to these effects, some mineral flame retardants decompose endothermically, generate inert gases that dilute the combustible gases and form protective layers, thus enhancing the retardant effect. Due to their effect, low price compared to other additives, low toxicity and low corrosion, this group of additives has the highest market share [39]. However, they have the disadvantage that high addition levels are necessary, at least 40 wt% and sometimes even up to 80 wt% depending on the polymer matrix or the standard to be met [40], so the mechanical and rheological properties are significantly affected.

Although almost all mineral FR are based on mineral ores, there are natural and synthetic. Natural minerals are those that are produced by mechanical separation of the mineral ore and then subjected to mechanical disintegration processes, while the synthetic ones are always obtained by chemical processes [40]. Between the two types, the volume of those of synthetic origin is much higher compared to those of natural origin mainly because the compounds of interest are not directly available in the ore minerals or because their purity is insufficient. The following is a review of the main mineral retardants, specifying their type, origin, mechanism of action and examples of use in thermoplastic matrices. Within this type of retardants, the most commonly used are metal hydroxides, zinc carbonates and borates, being metallic hydroxides the most important ones [10]. Metal hydroxides are additives that act in three parts of the combustion cycle through physical and chemical processes [40]. First, their decomposition reactions are endothermic and therefore absorb heat from the ignition source. At the same time, due to this reaction they generate water which dilutes the combustible gases and cools the surface of the polymer. Finally, they generate the corresponding oxide, which acts as a barrier layer that prevents the release of low molecular weight decomposition products and thermally insulates the polymer, thus protecting it against further decomposition.

Among the metal hydroxides are aluminium hydroxide, magnesium hydroxide, calcium hydroxide and aluminium oxide-hydroxide. Of these, aluminium hydroxide (ATH), also called alumina ($Al(OH)_3$), is the most important and has the largest share of the world market [39]. The use of this additive goes back a century, but it was not until the mid-1960s that it had its first significant commercial use as a flame retardant in unsaturated polyester [41]. Aluminium hydroxide is mainly found in the form of gibbsite, a mineral that is the main component of bauxite.

However, it is not pure enough for direct use, so it has to undergo a chemical process called the Bayer process, therefore, it is considered a synthetic mineral. The uses of ATH include precursor for aluminium compounds, flame retardant, medicine, vaccine component, feedstocks to ceramics and water purifier [40,42–44]. As for its use as a flame retardant, its effect is due to its decomposition reaction is endothermic and generates alumina (Al_2O_3) and water. This reaction takes place at about 180-200°C [38], so it cannot be used in plastics that require higher process temperatures.

$$2Al(OH)_3 \rightarrow Al_2O_3 + 3H_2O$$

Today, ATH is used in many types of polymers and there are a large number of commercially available grades that vary in purity, particle size distribution and shape [41]. In addition, because it is the most demanded flame retardant nowadays, there are numerous studies on its application, so some of the published articles are summarised below. One of the important applications of ATH is wire and cable insulation, for this reason, Farzad et al. studied the effect of this additive on the electrical and fire properties of the polypropylene (PP)/ethylene propylene diene monomer (EPDM) blend [45]. The polymeric matrix had a 60:40 PP/EPDM ratio and the additive was added at different contents, 25, 50, 70 and 100 phr. The test performed to study the effect of the additive on flammability was the LOI, which determines the minimum oxygen concentration necessary to sustain a stable flaming combustion of a material under certain conditions. Materials with values below 21 are referred to as combustible, while higher values are referred to as self-extinguishing. As for the results, it was observed that the blend with no additive presented a 20.6%, therefore it is considered as combustible, however an addition of 25 phr increased the LOI to 25%. When increasing the ATH content, the LOI continued to increase but from 75 phr to 100 phr there was no significant effect on the LOI. Therefore, it is not necessary to use ATH contents at 100 phr because the improvement of the fire properties does not justify the loss of mechanical properties.

Another example of the use of ATH in polypropylene is the study carried out by Parida et al [46]. In this study, nano and micro ATH were used to determine the effect of particle size and 2% maleic anhydride (MAPP) was used to improve the compatibility of the polymer with the additive. The additive percentages used for nano ATH were 1, 2 and 3% while for micro ATH 5, 10 and 20%. The characterisation tests performed for the evaluation of the fire properties were vertical burning test (UL94), LOI, smoke density, spread of flame and cone calorimetry. UL-94, LOI and cone calorimetry are explained in detail in Section 5. In addition, thermal, mechanical, and morphological tests were performed. In cone calorimetry it was observed that both micro and nano ATH substantially improved the time to ignition (TTI) and that the addition of the compatibilizer MAPP showed more TTI which confirmed the improvement in the interfacial

adhesion between the two components. As for the peak of heat release rate (pHRR), an improvement of 35.42% was obtained in the 20% micro ATH sample, confirming that the presence of ATH improved the fire properties. Regarding the particle size, the larger particle size of the charges results in a denser network that prevents early ignition of the sample and improves heat dissipation.

ATH has also been applied to both synthetic fibre and natural fibre composites. To improve the flame retardant properties of a composite, a retardant can be added to the matrix, the fibre or the composite as a whole. For the matrix, it should be noted that the FR content must be minimal so that there is enough polymer to bind the fibre, but sufficient to achieve a UL94 V-0 rating. El-Sabbagh et al. for example applied ATH in a PP/Flax composite and studied the effect of different grades of ATH, varied percentages and used other synergistic additives in order to achieve an optimal retardation system with the least possible impact on the mechanical properties of the composite [47] The percentage of reinforcement was 30 and 50% and MAPP was used as a coupling agent. As for the additives, the three ATH grades, Apyral 32, 40 CD and 60CD were added at percentages ranging from 30 to 60% and with regard to the synergistic additives, zinc borate (ZB) at 2% and Exolit AP-422 at 1.56 and 6.06%. The conclusions obtained were firstly that it is possible to obtain a natural fibre composite with a V-0 level, which means that they self-extinguish the flame in less than 10 seconds, and with a minimum loss in mechanical properties. It was observed that natural fibre improves both fire and mechanical properties and that the higher the percentage the better the effect. Furthermore, the recommended ATH percentage of 67% to obtain the V-0 rating can be reduced to 40% in flax/PP composites. As for the different grades of ATH, although all grades achieved V-0 classification, it was observed in the cone calorimetry that the use of fine particles delays the onset of combustion, reduces the heat release rate (HRR), and shortens flame-out times. On the other hand, ATH shows a greater increase in flame retardancy after 40% ATH, so this ATH content acts as a threshold value. Finally, in the study of synergistic additives, it was found that both ZB and AP-422 enhance flame retardancy by improving UL94 classification and decreasing heat release rate (HRR).

In summary, ATH has been used in a multitude of articles, for example in different thermoplastic polymeric matrices such as ethylene vinyl acetate copolymer (EVA) [48,49], high density polyethylene (HDPE) [50–52], thermoplastic polyurethane (TPU) [53] and PP [54–56]. It has also been used with other additives to enhance its retarding effect such as clays [48], melamine compounds [49], expandable graphite (EG) [50], red phosphorus (RP) [50], zinc borate (ZB) [50,55], fullerene (C_{60}) [51] and mica [53]. In addition, surface treatments have also been applied to improve its adhesion to the polymer matrix and reduce the percentage of additive used, such as magnesium strearate [52], maleic anhydride [54–56] and 3-Aminopropyltriethoxysilane

(APS) [56]. Table 1 below summarises these articles, specifying the matrix, the percentages of additives used, and the conclusions obtained.

TABLE 1: EXAMPLES OF ATH APPLICATION IN NON-BIODEGRADABLE PETROLEUM-BASED THERMOPLASTICS

Matrix	FR systems	Conclusions	Ref
EVA	68% ATH 63%ATH/ 5%Nano clay (NC)	The addition of the nanoclay to the ATH is a clear benefit as a further reduction of the pHRR is achieved. In the TGA test, an increase in thermal stability was also observed and it was concluded that the nanoclay acts as a barrier, reducing the flow of volatiles, oxygen and heat into the sample.	[48]
EVA	ATH 130 phr 108 ATH/ 22 melamine 108 ATH/22 melamine phosphate (MP) 108 ATH/22 melamine borate (MB)	In all the samples studied, the materials are classified as V-0 in the UL94 test. In the calorimetric cone test, a reduction in pHRR of between 71 and 77 is obtained with respect to the EVA reference sample, with the lowest value corresponding to EVA-ATH. Therefore, the ATH/MB combination improved the flame retardant properties and reduced the smoke production.	[49]
HDPE	40% ATH 35%ATH/5%EG 35%ATH/5%RP 30%ATH/5%EG/5%RP 30%ATH/5%EG/5%ZB	The addition of 40%ATH reduced the pHRR by 59.56% and the addition of the halogen-free flame retardant increased this reduction, reaching a decrease of 79.16% in the sample 30%ATH/5%EG/5%RP. ATH showed synergistic effects with EG and RP separately, but the effect is better with the combination of the three additives.	[50]
HDPE	37-160 ATH 0-3 fullerene (C_{60})	There was a synergistic effect between ATH and C_{60}. C_{60} improved flame resistance and thermal or thermo-oxidative stability by absorption of carbon-centred free radicals to form a cross-linked network. The flame resistance improved significantly with the addition of very low C_{60} content because it slowed down the degradation rate at the beginning and prolonged the ignition time even at very low concentrations. In addition, the ATH content could be reduced from 160 to 120 phr, and the mechanical properties of the composite showed some degree of improvement.	[51]
HDPE	ATH 10-60 phr + RP + Magnesium strearate	The three compounds used can play a synergistic effect but have adverse effects of other material properties. From a content of 50phr ATH, an improvement of the flame properties is obtained and when the content is increased to 60 phr, the composite can reach UL94 V0 level, and the flexural strength and hardness will also be improved, but the impact resistance and melt flow index decreased.	[52]
TPU	ATH 70-80 phr 70 ATH/20 mica 80 ATH/20 mica	UL94 and LOI test results indicate that composites with 70 and 80 phr ATH exhibit fire retardancy (UL94 V2). The use of mica has no effect on the performance of the ATH composites, but its inclusion facilitates processing and reduces the price of the composites. ATH surface treatment with 1% isostearic acid resulted in a small increase in the fire resistance of the composites, but not enough to improve the classification.	[53]
PP	4% wt nanofiller ATH + 0-5% MAPP	Improvements in the tensile and impact properties of the PP/ATH samples were observed after loading with MAPP and a loading of 1 wt.% was determined to be the optimum coupling agent addition content because it gave the best performance in tensile and impact tests. On the other hand, higher loadings of MAPP decreased the mechanical performance of the nanocomposites due to the excessive amount of grafted maleic anhydride which does not support a higher adhesion between the PP matrix and the ATH nanoparticle.	[54]

TABLE 1: CONTINUED

Matrix	FR systems	Conclusions	Ref
PP/PE copolymer	ATH ATH+ZB ATH+ZB+MAPP	The addition of MAPP in the composites with ATH has had almost no effect, whereas in composites containing ZnB, it has increased tensile modulus. The addition of ATH has improved the flame retardancy of the polymer and the addition of ZnB has further increased the LOI. However, the addition of MAPP decreased the LOI.	[55]
PP	ATH 5-40% + APS/MAPP	The incorporation of ATH nanoparticles increased the LOI values, and these values increased with increasing ATH loadings. Comparing the untreated, MAPP-treated and APS-treated samples, the LOI values are higher with treatment, being more significant in the MAPP-treated samples. In the UL94 HB combustion test, the differences in propagation velocity in the untreated and APS-treated samples were not significant. In contrast, the MAPP-treated samples showed significant differences, especially at high ATH.	[56]

In summary, ATH can be applied in a multitude of matrices, but it is necessary to consider that the processing temperature of the polymer should not be higher than the decomposition temperature of the ATH. The minimum percentages needed to obtain an improvement in flame retardancy is 40%, but it is possible to use ATH nano filler and reduce the percentage of additive significantly. It should also be noted that the application of surface treatments to the ATH and the use of synergistic additives can improve the properties of the material.

One of the peculiarities of ATH is that if thermal decomposition takes place under certain conditions, it occurs in two stages with the formation of an intermediate, the aluminium oxide-hydroxide AlO(OH), also called boehmite. This compound is also a component of bauxite ore and present the advantage that it decomposes at 340°C, so it can be used with polymers with higher process temperatures. The drawback compared to ATH is that the enthalpy of decomposition and the release of volatiles are significantly lower, 560 kJ/g compared to 1300 kJ/g for $Al(OH)_3$ [38], so its effect on flame retardancy may be lower.

$$2AlOOH \rightarrow Al_2O_3 + H_2O$$

In addition to its use as a low-cost flame retardant additive, boehmite is used as a raw material for the production of alpha and gamma alumina, cosmetic product, membrane, coating, adsorbent, catalytic support, vaccine adjuvant, optical material, corrosion inhibitor and composite reinforcement in ceramics [57].

The following is a review of its use in different polymers, including synergies with other additives and its use as a nanoparticle. For example, El Hage R et al. compared the effect of ATH and boehmite on the flame retardancy of EVA [58]. Three new synthesised additives, ATH-2 and two pseudoboehmites (Pseudo-1 and Pseudo-2) and two commercial minerals, ATH-1 (Martinal

ON313) and Boehm-1 (Apyral AOH20) were used as additives. The loading level of the fillers was 25% by weight for all samples. In the cone calorimetric test, it was observed that the highest peak HRR (pHRR) of the samples with additives were obtained with the two ATH. However, in all the samples with boehmite, a significant reduction of the pHRR was obtained, not only with respect to the unfilled EVA but also with respect to the samples with ATH. In fact, the best pHRR value was obtained in the EVA/Pseudo-1 mixture and the reduction with respect to EVA and EVA/ATH was 66 and 45% respectively. As for the mass loss curves, the same trend was obtained, therefore, Pseudo-1 and Pseudo-2 were more efficient in improving flame retardancy. This difference in behaviour was justified because the residues of these two samples showed a slight swelling and were highly cohesive with traces of char, while in the other samples practically no cohesion or char was observed. Therefore, the effect of Pseudo-1 and Pseudo-2 is strongly related to the barrier effect. In fact, these observations were confirmed by PCFC results and by SEM and EDX analysis of the residues because a rapid formation of a cohesive and homogeneous insulating layer on the surface of the composites was observed.

On the other hand, Xiang L. and Songgang F. studied the effect of boehmite in polyethylene terephthalate (PET) and its combination with vermiculite (VMT) [59]. The percentages of boehmite used ranged from 8 to 12% and vermiculite from 1 to 4%. To study the effect of the retardants, LOI, UL94, cone calorimeter test (CC) and thermogravimetry analysis (TGA) were performed. The results showed that 12% boehmite can effectively improve the flame resistance since a LOI of 32.4% and a V0 rating (3.2 mm) were obtained. Next, with the addition of vermiculite, the flame retardancy, thermal stability and combustion behaviour of the composite were improved, indicating that 2.5% VMT and 9.5% boehmite contents in PET had synergistic flame retardant effects. Furthermore, by replacing part of the boehmite with vermiculite, the flexural and tensile strengths of the composites were also improved. The result could be attributed to the fact that vermiculite is a mica-type silicate and has a layered structure with blocking effects, so that by covering the surface of the material it can insulate oxygen, increasing the density of the carbon layer and thus improving the condensed phase flame retardant effect.

Another example of a synergistic effect is the mixture of melamine cyanurate (MCA) and boehmite in polyamide-6 (PA6) [60]. The total additive content used was 15% for all mixtures and in this case the main additive was melamine cyanurate with percentages of 9, 11, 13 and 15% and boehmite with 2, 4 and 6%. As in the previous article, the behaviour of the composites was analysed by LOI, UL94, cone calorimeter and TGA. The results showed that MCA can effectively retard the flame of PA6 and that by replacing part of MCA with boehmite, the flame retardancy of the composite improves at first, but as the percentage of boehmite increases, it then worsens. The flame retardancy, thermal stability and combustion behaviour data of the

4%Boeh/11%MCA/PA6 composite were better than those of the 15%MCA/PA6 composite, so the appropriate amounts of MCA and boehmite in PA6 have synergistic effects. The authors attribute these results to the fact that when part of the MCA is replaced by boehmite in a small amount, the improvement of the flame retardant effect in the condensed phase is greater due to the effect of boehmite than the weakening of the flame retardant effect in the gas phase due to the reduction of the amount of MCA. However, when the boehmite content increases, the decrease of the effect in the gas phase is more significant than the increase in the condensed phase, so the overall performance decreases.

Another interesting study is the one carried out by Camino et al., in which they compared the retarding effect of various mineral additives in EVA, aluminium hydroxide, magnesium hydroxide, boehmite and hydrotalcite [61]. Specifically, the crystalline phases of aluminium hydroxide and magnesium hydroxide were gibbsite and brucite, respectively, and 50wt% additive was used in all samples. The LOI, UL94 and mass loss calorimeter tests were used to determine the fire behaviour. In this study it was found that a minimum of 50% additive is required for appreciable fire retardant behaviour. Firstly, in the UL-94 test, only the mixture corresponding to aluminium hydroxide (Apyral 40D) was able to classify as level V-2 and the rest classified as HB. In the case of LOI, although all the samples presented a LOI greater than 21% and the improvement with respect to the unfilled EVA is significant, the sample corresponding to boehmite obtained the lowest value. In the mass loss calorimeter, the same trend was obtained with respect to boehmite, but the most interesting result was the one corresponding to the sample with hydrotalcite. The sample with hydrotalcite had the longest ignition time, the lowest gas temperature, and the longest time to reach the maximum heat release rate. This difference in behaviour was mainly associated with two effects. On the one hand, the heat absorption related to water loss over a wide temperature range (from 200 to 500 °C), in particular the interlayer water loss and on the other hand, the formation of a charring layer with a rather compact intumescent surface even until the end of the test. In the case of boehmite, due to the lower water yield and the lower heat absorbed by the decomposition reaction compared to the other additives used, poor flame retardant properties were obtained.

Another important field of application for boehmite is its use as a nanoparticle. There are numerous articles about nanocomposites with boehmite because like many other nanofillers, it improves mechanical properties, thermal degradation, barrier properties, as well as fire resistance [62]. It has been applied in different polymeric matrices such as low density polyethylene (LDPE) [63], polyamide-6 (PA6) [63], polyethersulfone (PES) [64], poly(ethylene terephthalate) (PET) [65], poly(methyl methacrylate) (PMMA) [66] and poly(vinyl alcohol) (PVA) [67], among others. In general, the percentages used vary from 2% to 50% depending on the polymer matrix [62],

particle size and geometry, etc., although in general terms percentages lower than 30% are used. In terms of results, all the articles agree that nano-boehmite is an effective flame retardant and represents an interesting alternative because it allows to obtain better results with lower percentages of additive. However, it is necessary to consider that in order to obtain nanoparticles, additional synthesis processes are required, which increases the cost and consumption of reagents, as well as complicating the compounding production process by requiring additional protective measures to avoid the risks involved in handling nanoparticles [68].

Another important mineral additive is magnesium hydroxide (MH). MH is an additive that behaves similarly to ATH and is in fact the second most widely used additive. One of the main advantages of MH over ATH is that it has a higher thermal stability because its decomposition starts at 300°C, which makes it feasible for use in polymers with higher processing temperatures. Another advantage is that there are natural sources of magnesium hydroxide, called brucite, which are of sufficiently high purity to be used only with drying and milling. It is true that there are deposits where brucite is mixed with significant amounts of calcium carbonate, but it is also possible to mine it. Its use as a flame retardant represents its most important application [40], but it is also found in animal nutrition, antibacterial agent, pharmaceuticals, fertiliser, water treatment, cement and pulp and paper industries and for obtaining magnesium oxide [40,69,70].

Like the previous additives, MH decomposes endothermically, generating water that dilutes the combustible gases and the corresponding oxide that forms a protective layer. Compared to ATH, the enthalpy of decomposition is higher, 1450 kJ/g versus 1300 kJ/g, so it has a higher endothermic effect [38].

$$Mg(OH)_2 \rightarrow MgO + H_2O$$

Due to the low toxicity of magnesium hydroxide and its higher thermal stability, its use has been studied in a multitude of polymeric matrices, both as a synthetic and natural additive, and it has also been used with other additives and with surface treatments to improve adhesion. Regarding to polymeric matrices, studies have been carried out on LDPE [71,72], LDPE/EVA [73], HDPE/EVA blend [74], EVA [75–77], PP [78,79], PET [80], EPDM [81], among others. Among these examples are studies on their use as nanoparticles and although they have better results, they present the problem that the cost of the additives is higher and that additional precautions have to be taken in manufacturing [71,76,77,80].

Table 2 summarises some of these referenced articles, specifying the matrix, the percentages of additives used, and the conclusions obtained.

TABLE 2: EXAMPLES OF MH APPLICATION IN NON-BIODEGRADABLE PETROLEUM-BASED THERMOPLASTICS

Matrix	FR systems	Conclusions	Ref
LDPE	Brucite 40-65 phr Maleic anhydride 8 phr Oleic acid (OA) 2-9.75 phr	The addition of OA caused a decrease in particle size and surface polarity of the brucite, which favours a better dispersion of the brucite in the matrix and consequently a better flame resistance. The best blend was obtained when the OA/brucite ratio was 3:20 and the brucite content in the LDPE compound was 55 phr, because the LOI was 29%, the UL94 V-0 classification, as well as good mechanical properties.	[72]
LDPE/EVA	50, 55 and 60 wt% of three synthetic (K, KM and KM-P) and two natural (M3-C2 and M16) MH Synergistic additives, red phosphorus, phosphite ester and Si-compound at 10 wt%	The purity of natural retardants is lower than that of synthetic retardants and therefore they have lower LOI values. In comparison, the natural MH (M3) at 60% has a LOI of 30.9% while the synthetic (KM), which shows the best results, has a LOI of 37.7%. However, both synthetic and natural obtained a V-0 rating when used at 60%. Because KM (synthetic MH) had the best LOI results, it was selected for blending with the synergistic additives. It was observed that both red phosphorus and Si-compound had a synergistic effect with the MH allowing the reduction of the total additive content to 50%.	[73]
HDPE/EVA blend	30-60% MH	The results obtained in both LOI, UL-94 and CC showed that MH improved flame retardancy. For an additive content of 50 wt%, the UL-94 V-0 rating and the highest LOI value were obtained, suggesting that the formation of intact, consolidated, and coarse residue structures prevented the underlying polymeric materials from burning.	[74]
EVA	Brucite + Aluminum phosphate (AIP) 50 wt% APTES coupling agent	The addition of aluminium phosphate improves mechanical properties as well as flame retardant and smoke suppressant properties. These improvements were attributed to the AIP creating a firm and porous protective carbon layer on the EVA composite. In addition, the spongy surface of Bruc/AlP/APTES has good compatibility with EVA and entangles more polymer chains, thus improving mechanical properties.	[75]
PP	MH 100 phr Surface treatment with titanate and zinc stearate	The treatments improve the particle distribution, mechanical properties and LOI values of the composites. In the case of titanate stearate, a more significant improvement is obtained and the maximum LOI value of 30.2% is obtained with the 2 phr treatment.	[78]
PP	10 and 30%MH 1% MAPP	The best results were obtained for the samples with 30%MH. The addition of maleic anhydride as a compatibilizer had a positive effect on both mechanical properties and thermal resistance, as well as reducing particle agglomeration during extrusion. In fact, with 30%MH a reduction of the linear rate of combustion of 28% was obtained with respect to unfilled PP and with the compatibilizer it increased up to 42%.	[79]
PET	Carbon microspheres (CMS) and MH at proportions 1:9, 3:7, 5:5, 7:3 and 9:1 and the dosage was 1wt% of PET	The optimal addition ratio of CMSs/MH was 5:5 because the LOI increased by 28.6% compared to pure PET. In addition, the combination of CMSs and MH can effectively improve smoke suppression. This effectiveness was mainly attributed to the condensed phase mechanism. The CMSs/MH increased the activation energy of thermal degradation and thus improved the thermal stability of the composites. Furthermore, they promoted the cross-linking of the pyrolysis products and improved the continuity and density of the carbon layer, thus obtaining a dense and continuous carbon layer at the end of combustion, which effectively blocked the heat transfer.	[80]

Finally, it is worth mentioning that the group of hydroxides includes calcium hydroxide. Calcium hydroxide is one of the most widely available and cheapest metal hydroxides, however, although the decomposition occurs at around 430℃ and the enthalpy is 1150 kJ/g [38], it does not seem to have a sufficient retarding effect for its application in polymers [41].

Next in the group of minerals are the carbonates, namely hydromagnesite (HM) and huntite (HU). These are two compounds that occur naturally together in different proportions, are not easy to separate and have flame-retardant properties [38]. This mixture is presented as an alternative to the commonly used aluminium hydroxide and magnesium hydroxide because it is considered a more environmentally friendly alternative [82]. Hydromagnesite is a hydrate magnesium carbonate that releases water and carbon dioxide, and its decomposition temperature is around 220℃. On the other hand, huntite is an anhydrous calcium magnesium carbonate that releases carbon dioxide, and its decomposition temperature is around 400℃ [38,83].

$$Hydromagnesite: Mg_5(CO_3)_4(OH)_2 \cdot 4H_2O \rightarrow 5MgO + 4CO_2 + 5H_2O$$
$$Huntite: Mg_3Ca(CO_3)_4 \rightarrow 3MgO + CaO + 4CO_2$$

The authors Hollingbery L.A. and Hull T.R. have studied this mixture at different ratios in EVA polymer [82]. The proportions of hydromagnesite and huntite studied were 100/0, 67/24, 57/41, 50/43 and 5/93, and they were compared with MDH, ATH and calcium carbonate. The conclusions drawn from the study were that the endothermic decomposition of hydromagnesite coincides with the temperature range at which polymers such as ethylene vinyl acetate and polyethylene thermally decompose, so it may work well as a fire retardant. On the other hand, huntite decomposes between 450℃ and 750℃ suggesting that most of the polymer has completely volatilised and that the mechanism of action of huntite is not simply the endothermic release of vapour from inert diluent. In the cone calorimetric test, it was shown that mixtures of huntite and hydromagnesite behave similarly to aluminium hydroxide, so it was concluded that huntite has a much greater effect than an inert diluent filler. Additionally, SEM observation of the ashes showed that the endothermic release of water and carbon dioxide from the hydromagnesite helps to reduce the initial peak heat release and increase the time to ignition and that the huntite also reduces the heat transferred to the underlying polymer and further dilutes the gas phase with non-combustible carbon dioxide. In summary, the retarding effect of the huntite and hydromagnesite mixtures is due to the combined actions of the two minerals.

The following is a summary of a study on the use of other minerals carried out by Terzi E. et al. in which they compared the effect of raw boron minerals and commercial flame retardants on wood plastic composites [84]. The minerals used were colemanite, tincalconite and ulexite,

and the commercial flame retardants were borax, magnesium hydroxide and zinc borate. For the composites, the plastic matrix used was HDPE with 50% wood flour and additives in percentages of 5, 10 and 15%. In the cone calorimeter, it was observed that the highest TTI value was recorded for the sample with 15%MH followed by ulexite at the same loading level. Next in the pHRR a decrease was obtained with respect to the percentage used for all the additives and the best result was for the 15%MH sample with a reduction of 42.6% compared to the control sample. Following this composite is 15% colemanite, 15% ulexite and 15% tincalconite with a reduction of 42.6%, 40% and 35.6%, respectively. Therefore, the minerals show better results in pHRR than the commercial additives borax and zinc borate. In conclusion, colemanite presented the best behaviour in cone calorimetry according to the pHRR value without decreasing the flexural properties compared to the other minerals. In terms of its behaviour, it was observed that when subjected to heat it acts in a similar way to magnesium hydroxide. Therefore, colemanite is presented as a good option due to its effect, low cost and considerably low environmental concerns. In addition, it does not contain heavy metals in its composition and is five times cheaper than ZB and three times cheaper than MH [84].

Considering the results obtained in the previous study, colemanite is another mineral that can be used as a natural flame retardant. Colemanite (COL) is a hydrated calcium borate with the formula $Ca_2B_6O_{11} \cdot 5H_2O$ and its main deposits are in Turkey [85]. This mineral is promising for use as a natural flame retardant additive due to its relatively high dehydration temperature above 300℃ and its water release. Furthermore, colemamite acts as a smoke suppressor [86]. The decomposition mechanism of colemanite mainly involves the release of water, and this occurs in two stages [87]. In the former, the structural OH groups form water and in the latter the hydrogen bonds formed between water and boron chains are broken. The second step is accompanied by the release of water vapour, appropriately termed explosive dehydration, which is typically observed during thermal decomposition of hydrated crystalline solid [88]. The water molecules formed are trapped tightly within the crystal structure as internal water which upon heating causes the crystal to explode under internal vapour pressure [85].

$$Ca_2B_6O_{11} \cdot 5H_2O \rightarrow 2CaO \cdot B_2O_3 + 5H_2O$$

An example of improved fire properties is the research carried out by Bilici I. in which the effect of colemanite on recycled polyethylene was studied [89]. In this case colemanite was used at very high percentages, from 50 to 80% (w/w), with satisfactory results in the manufacture in spite of the high loading. In the DSC, it was observed that the addition of colemanite increased the softening temperature by about 10℃, thus improving the working temperature of PE. As for the fire properties, a satisfactory effect was also obtained because all the mixtures obtained a LOI

higher than 21, therefore they are classified as self-extinguishing, and as the percentage of colemanite increased, the LOI value increased, reaching 31 in the 80% mixture.

Among the boron-based additives, zinc borates have been widely used in combination with aluminium and magnesium hydroxides [81,90,91], and colemanite, being a natural hydrated calcium borate, could be a promising alternative. An example is the research conducted by Isitman N and Kaynak C. [92]. In this study they partially replaced aluminium hydroxide with colemanite in order to improve fire retardancy and decrease the total percentage of additive. As polymeric matrix they used LDPE and with respect to the additives they established three levels of total percentage 55, 60 and 65% and in each of them they used colemanite at 5, 10 and 20%. Firstly, it was observed that in order to classify the material as V-0 in the UL94 test, the aluminium hydroxide (ATH) load must be 65%. However, when colemanite is added, it is possible to decrease the additive percentage. It was observed that when ATH is partially replaces by colemanite, even at 5%, the samples with 60% total additive satisfies the V-0 criteria and the LOI values are above 28%. In the cone calorimetric test, it was also observed that by comparing the reference sample with composites containing colemanite, similar flame retardancy behaviour could be obtained with a total additive percentage of 60%, therefore both additives perform better when combined. This improved fire retardant effect was attributed to a better protective character of the fire residues and a more effective trapping of the fuel in the condensed phase.

Another example of the study of synergistic mixtures with colemanite is the research carried out by Cavodeau et al. [86]. In this study, colemanite is used with aluminium hydroxide (ATH) and magnesium hydroxide (MH) in EVA and EMA. Ethylene-vinyl acetate (EVA) and ethylene-methyl acrylate (EMA) are copolymers commonly used in the cable industry; therefore, they must meet fire resistance criteria. As high additive loadings are necessary to achieve a resistance material, a total additive content of 60% was established and the proportions of the additive mixtures 50/10 and 30/30 hydroxide/colemanite. In the EVA mixtures with ATH and COL it was found that the two additives were not synergistic because the increased amount of colemanite used alone improves the fire resistance of the materials more strongly. In the case of MH and COL, MH showed worse results with respect to ATH, and it was observed that they did not show synergy either because the combination of both additives 30ATH/30COL decreased the TTI and increased the pHRR and total heat released (THR). On the other hand, in the EMA matrix, it was observed that the substitution of half of ATH with COL slightly improved pHRR and THR, but the improvement was not as significant as with EVA. Regarding to MH, it improved the flame retardancy of EMA and the residue was more cohesive. In addition, when COL replaced part of the MH, pHRR, THR, mass loss and TSR (Total Smoke Released) decreased, so the addition of colemanite improved the properties. Finally, for all samples it was observed that colemanite acts

as a smoke suppressant because it decreases the TSR, and this reduction increases as the amount of colemanite increases.

In the case of brucite, studies on mixtures with cobalt zeolite in polypropylene [93], nanocarbon black in ethylene-vinyl acetate [94] and dimethyl methylphosphonate (DMMP) in polyurethane foams [95] are found, but it is not investigated in detail and most of them are not natural additives. However, in the case of magnesium hydroxide, its combination with colemanite has been studied and good results have been obtained, making colemanite a promising additive for use as a synergist with brucite.

Another example of additives with a synergistic effect with magnesium hydroxide is expandable graphite. Expandable graphite (EG) is a partially oxidized form of graphite which contains intercalated species such as sulfuric acid anions in between the stacked graphene layers [96]. Expandable graphite is prepared from natural graphite by chemical treatment and has been widely used as a flame retardant in a variety of polymers [97]. At industrial scale, the synthesis of expandable graphite can be performed by liquid-phase graphite-sulfuric acid reactions in the presence of strong chemical oxidants such as potassium permanganate, nitric acid, and hydrogen peroxide [98]. The expansion of the EG with temperature occur due to the vaporization of the intercalated guest ions which form a gas that can cause the rapid expansion of the flakes in a worm-like manner [99]. This implies that the gases that cause the expansion mainly contain carbon dioxide and sulphur dioxide [96]. This additive has been used for various polymeric matrices obtaining a substantial improvement in mechanical properties, electrical conductivity, and fire resistance [96,100–104]. Although EG is a cheap and abundant flame retardant additive, it has the same disadvantage as minerals because a high percentage is necessary to obtain a satisfactory flame retardant effect, which negatively affects the mechanical properties [97]. Therefore, EG needs to be combined with other flame retardants to achieve a high flame retardancy efficiency.

For example, Chen X. et al. studied the flammability and synergistic effect of expandable graphite with magnesium hydroxide in polypropylene [105]. Two particle sizes for the expandable graphite were used, 50 and 80 mesh, and magnesium hydroxide surface was treated with stearate. The proportions were 50 matrix/50 additive and for the mixtures of additives 100/0, 95/5, 90/10, 85/15 and 80/20. In the UL94 test, it was observed that the PP composites with MH alone did not pass the UL94 rating, but with the addition of EG it was significantly improved. The particle size of EG has a large effect on flammability, as a smaller particle size and a loading of 10 phr achieved the most stringent classification, while a larger particle size required a loading of 20 phr to achieve the V-0 classification. Therefore, EG with smaller size has much better

synergistic effect with MH for polypropylene composites. Regarding LOI test, it increased linearly with increasing amount of EG, and better results were obtained with the smaller particle size. In conclusion, EG had a good synergistic effect with MH in PP composites.

Subsequently, these authors carried out the cone calorimeter test and XPS analysis of the ash in order to obtain more information about the synergy observed in the previous study [106]. PP in the CC test burned very fast after ignition with a sharp peak in the HRR curve. With the addition of MH, the pHRR was reduced by 62.5% and the burn time was prolonged from 300 to about 470 seconds. Then with the substitution of part of the MH by EG, the intensity of the peaks decreased further and as in the previous study the best result was obtained for the smaller particle size EG. The main parameter responsible for this decrease in HRR is the MLR (Mass loss rate) during combustion which was significantly reduced compared to the values observed for PP. Therefore, the consistency between the HRR and MLR results confirms that the flame retardant mechanism of EG with MH is in the condensed phase. As for the TTI, an increase was obtained with the addition of MH from 21 to 26 s and with EG up to 32-33 s. Finally, the peak EHC values of the composites were much lower than for the unfilled PP, obtaining the lowest value for the composite with the smallest particle size EG. In conclusion, MH and EG present a synergistic effect because they can efficiently prevent heat and gas transfer between the flame zone and the burning substrate and thus delay the pyrolysis of PP.

Another example of this synergy is the study carried out by Li Z. and Qu B. in which they applied MH and EG synergy in EVA blends [107]. In this case they studied the effect of the particle size and expansion ratio of EG. As in previous cases, the MH composites did not meet the UL94 test criteria, with the exception of the sample with a 200phr content which, due to its high percentage, obtained the V-0 classification. With the addition of EG, it was observed that the particle size and expansion ratio have a great effect on the flammability because when comparing the 4 types, it was observed that those with the largest particle size and highest expansion ratio achieved the V-O with a 10phr content, while the other two failed. Then, once it was determined which of the four types was the best, the percentages of MH were varied while maintaining a total amount of 130phr. The LOI results showed that the value increased with the amount of EG and that all samples achieved the V-0 classification in the UL-94 test. Therefore, in the next test the amount of MH was varied while maintaining the EG at 10phr. With this last test, it was found that with the total amount of 100phr, 90 phr of MH and 10 phr of EG, the material achieved the V-0 classification with a LOI of 38, so it is possible to reduce the total amount of additive while maintaining the same properties. In the cone calorimetric test, it was found that the EG prolonged the burning time by up to 190 s and the pHRR decreased with increasing the EG particle size and expansion ratio as in UL94 test. The same occur for EHC and

MLR, so it is concluded that expandable graphite has a synergistic effect with magnesium hydroxide and the effect is better at higher particle sizes and expansion ratios.

In summary, to select a mineral additive it is important to take into account first of all its decomposition temperature because it must be higher than the process temperature of the polymer, the enthalpy of decomposition because the higher it is the greater the endothermic effect and the amount of water released because although it is beneficial for flame retardancy, it could break the protective layer formed by the oxide generated in the decomposition [38]. In addition, consider that it is possible to use synergistic mixtures that allow to obtain improved properties with a minor effect on the mechanical properties.

3.2.2 BIO-BASED FLAME RETARDANTS

This section reviews the state of the art of bio-based flame retardants. Bio-based flame retardants are biomolecules obtained from nature, so they are considered more renewable and sustainable additives because they are not obtained from sources such as petroleum [108]. There are many flame retardants of biological origin, and they are mainly divided into biomolecules from plants and from a living organism.

Starting with plant-based compounds we find cellulose, hemicellulose, and lignin, which are the three main components of natural fibres. Cellulose is one of the most abundant biopolymers in nature and accounts for approximately half of the atmospheric CO_2 fixed by photosynthesis [109]. It is a fibrous component found mainly in the cell wall of plants as well as in bacteria, fungi and algae and consists of chains of glucose units [36]. Cellulose has attractive and excellent properties and for this reason is used in various industries such as paper, fibres, cosmetics, clothing, and veterinary foods [108]. Cellulose can be extracted from biomass by different methods, but the most widely used is based on the paper production process. The decomposition of cellulose is produced in various steps between 260 to 350°C and the mechanism of action is based on the production of char, but this production depends on several factors such as thermal degradation conditions, surrounding compounds, degree of cellulose polymerisation, crystallinity and even particle size [36]. Due to the effect of cellulose is only in char formation, it is almost impossible to achieve satisfactory flame retardancy using cellulose alone [108], so it has to be used with other additives, or modified with other compounds that complement its effect. The application of cellulose has been more focused on poly(lactic acid) (PLA), but some examples of its use in polyolefins are shown in Table 3.

On the other hand, hemicellulose is the second most abundant component of lignocellulosic biomass and is composed of highly branched low molecular weight chains of different sugars

[36]. Its main function is to reinforce the cell wall by interacting with cellulose and lignin. The methods of extraction of hemicellulose from biomass are mainly based on treatments with aqueous alkaline solutions. Hemicellulose has been used in several industrial applications, such as in thermoplastics and as additives in cosmetics and pharmaceuticals, because of its reproducibility, low cost, and biodegradability. However, due to the low molecular weight of hemicellulose, its thermal decomposition is rapid, it starts at around 180ºC and reaches the maximum weight loss between 250 and 350°C [110], so its use as a FR in polymeric materials is limited.

Finally, lignin is the third main component of biomass, and its function is to fill the gap between cellulose and hemicellulose in plants, thus providing cell wall strength and rigidity [108]. Lignin has a complex structure composed of a 3D cross-linked network whose base unit is the phenylpropanoid and contains a wide variety of functional groups such as methoxyl and hydroxyl phenol and many different bonds, for this reason its structure is still unclear due to its complexity and variability [111]. The extraction of lignin from the other components is possible using the same pre-treatments used for cellulose isolation developed for the paper industry and biorefineries. The extraction processes are divided into two categories: sulphur and non-sulphur processes [36]. The sulphur processes include Kraft lignin and lignosulphonate lignin, and the non-sulphur processes include organosolv lignin and soda lignin. It must be considered that the performance of lignin depends on its origin, degree of polymerisation, impurities, so the process used for its extraction influences its behaviour as a retardant. Lignin starts to decompose at 160°C, so the onset degradation temperature is lower than for cellulose and hemicellulose because it is produced the breakage of the relatively weak bonds. However, the cleavage of stronger bonds in the aromatic rings occur at higher temperatures and hinder fibre oxidation [112]. In fact, the degradation continues up to 700°C and forms a carbonised residue of 30 to 50 % by weight when decomposition takes place in an inert atmosphere [113]. As with cellulose and hemicellulose, this carbonisation ability gives it the potential to act as a flame retardant additive in polymeric materials. Table 3 shows several examples of their use in polymeric matrices.

On the other hand, phytic acid and tannic acid are compounds also found in plants. Phytic acid is the main form of phosphorus storage in seeds and can constitute up to 6% of the dry weight of cereals and oilseeds [114]. For this reason, phytic acid has attracted interest because of its renewable aspect and its high phosphorus content, although it has been mainly applied to improve tissue properties. Tannic acid is a natural phenolic compound commonly found in the peels of fruits, vegetables, cocoa, and nuts. It contains five gallol groups and five catechol groups, so it can form non-covalent bonds such as hydrogen bonds and hydrophobic interactions with various

molecules, making it suitable for use with other retardants.[108]. However, there is currently not much research on its use as flame retardant.

TABLE 3: EXAMPLES OF BIOBASED FR IN PETROLEUM-BASED THERMOPLASTICS

Matrix	FR systems	Conclusions	Ref
PP	Hydroxyethyl cellulose, melamine, melamine phosphate, expandable graphite and HEC modified with phosphoric acid and melamine	A halogen-free intumescent flame retardant (HECPM) was successfully prepared by introducing phosphoric acid and melamine into the cellulose structure. TGA curves showed that the char obtained from HECPM is higher than 43% at 600 °C, indicating the higher carbonisation capacity of HECPM. When PP was mixed with 30% HECPM, the LOI value is 29.5% and the samples can exceed UL-94 V-0 classification. In addition, the synergistic effect between HECPM and EG in PP was found to be associated with a possible mechanism in condensed phase.	[115]
HDPE	0.4 to 1%Cellulose nanocrystals (CNC) coated with zinc oxide nanoparticles (ZnO)	The addition of ZnO-coated CNCs to HDPE decreases the average mass loss, peak heat release rate and total smoke release compared to pure polymer and increases the ignition time. The observed effect is due to the additive create a layer of char around the outer surface of the polymer, which helps to reduce polymer mass loss rates and results in slower combustion, especially near the peak combustion.	[116]
PP	Lignin and PN functionalized lignin (PN-lignin) at 20 and 30%	Compared to pure lignin, the thermal stability with P-NT lignin is further increased at the same loading level. In addition, the amount of char residue also increases significantly by about 50% at 600 °C. PN-lignin shows a much higher flame retardancy because the carbon layer is much more compact which improves the flame resistance.	[117]
PP	Lignin (5-20%), ATH, MP, poly(vinyl alcohol) (PVA), monoammonium phosphate (AHP) and ammonium polyphosphate (APP)	The TGA and CC results confirm the retarding effect of LIG as FR for PP, both alone and in synergy with phosphate composites and ATH. Composites with lignin alone and with ATH and PVA give very low smoke opacity and low CO yield during combustion, but with lower average HRR and shorter overall burn times compared to those obtained using phosphates. On the other hand, lignin and phosphate compounds give longer combustion times.	[118]
ABS*	5-20% Lignin, 5-15% maleic anhydride	A 32% reduction in pHRR is observed with a lignin loading of 20% by weight. Total heat release (THR) and mass loss rate also decrease with increasing lignin loading. Compatibilization with maleic anhydride further reduces the flammability of ABS due to the enhancement of the carbonisation layer. When the amount used is 10% by weight, the reduction of PHRR reaches 44% compared to pure ABS. The carbon layer is mainly responsible for the improvement of flame retardancy, in addition to the lignin capturing free radicals thus contributing to the reduction of the flammability of ABS.	[119]
EVA	40-50% MH, 10-60% Kraft lignin and 10-20% P-lignin	The results showed that, thanks to their carbonisation effect, both untreated and phosphorylated lignins allow a significant reduction of the pHRR. However, due to the lower thermal stability of lignins, their presence reduces the time to ignition (TTI). The combination of the carbonisation effect of lignin and the endothermic effect of magnesium hydroxide allows a further reduction of the pHRR and a certain improvement of the ignition resistance of the composite.	[120]

* ABS (Acrylonitrile butadiene styrene)

TABLE 3: CONTINUED

Matrix	FR systems	Conclusions	Ref
PP	Polyethyleneimine (PEI), phytic acid, sodium hydroxide and hydrogen chloride	A new polyelectrolyte complex (PEC) that effectively combines the carbon and nitrogen elements of PEI and the carbon and phosphorus elements of PA, and exhibits intumescent behaviour, was manufactured. The introduction of PEC effectively reduces the pHRR and THR values of PP/PEC systems during the MCC* test, which implies a strong barrier effect on the transfer of volatile pyrolysis products into the combustion chamber.	[121]

* MCC (Micro-scale combustion calorimetry)

Finally, there is a bio-based retardant from living organisms, the DNA. Deoxyribonucleic acid (DNA) is a molecule found in all living organisms and represents potential as an intumescent flame retardant system for polymeric materials because it contains the three typical components of these systems [36]. When DNA is degraded, the phosphate groups produce phosphoric acid, which is the acid source; the deoxyribose units act as the carbonising agent as they decompose leading to the formation of aromatic structures, and the nitrogen-containing bases act as the blowing agent releasing ammonia. An example of the application of DNA in polymers is the study carried out by Alongi J et al. about the use of DNA as an additive and as a coating in EVA copolymer [122]. Both bulk and surface, DNA was applied at 15 % by weight. The composites were analysed by cone calorimetry and combustion tests, and it was shown that the application of DNA as a DNA coating is more effective than its bulk addition. This is because the coating is able to block the ignition of the copolymer at a flux of 35 kW/m^2, as well as postpone and greatly reduce the combustion kinetics under a heat flux of 50 kW/m^2. Finally, the coating is also able to protect the underlying material from the butane/propane flame applied three consecutive times to the sample for 5s. However, in both cases, DNA has been shown to be an effective carbon former that exerts a heat shielding effect on the EVA copolymer.

3.3 NATURAL FLAME RETARDANTS IN BIODEGRADABLE/BIOBASED THERMOPLASTIC POLYMERS

Before reviewing the use of natural flame retardants in biodegradable and/or polymer-based polymers, it is necessary to emphasise the difference between the two types. Bioplastics are defined as plastic materials that are bio-based, biodegradable or have both properties [123]. Therefore, it is necessary to distinguish the term biodegradable from the term bio-based because the term bio-based is related to the origin of the product, while biodegradable is related to the end of life of the product. So far, a limited number of articles have been published on the flame retardancy of bioplastics and most of them are dedicated to poly(lactic acid) (PLA). The flame retardant possibilities of green composites based on polybutylene succinate (PBS) and thermoplastic starch (TPS) have also been investigated, but to a lesser extent and are still a field

of research to be explored. The following is a review of the use of natural retardants in bioplastics, especially those discussed in the previous section.

Regarding the types of additives mentioned in the previous section, it should be noted that most of the articles focus on the use of bio-based additives and that the use of minerals is quite rare. However, there are some examples of the use of ATH and MH in PLA. For example, Zhao P. et al. studied the effect of phosphorus-modified magnesium hydroxide on the mechanical and fire properties of composites. It was observed that with an additive percentage of 30% the LOI increases from 21.2 to 24.3. At the same time, the pHRR and THR values decrease significantly from 323 W/g to 155 W/g and from 17.6 kJ/g to 11.0 kJ/g, respectively. Regarding the modification of the additive, it does not seem to have a clear effect on the flammability because pHRR increases and THR decreases, so it is not possible to draw conclusions. However, in the mechanical properties the additive modification improved the behaviour, so it is a promising method that could be used in other polymeric systems to improve the interaction with the polymer.

Another example of the application of MH in PLA is the study developed by Kongkraeireug N. on poly(Lactic Acid)/High Impact Polystyrene/Wood Flour Composites [124]. The 80/20/20 PLA/HIPS/WF composite was mixed with different proportion of MH (20, 30 and 40 phr). It was observed that the addition of HIPS to the composite increases the impact strength and elongation at break, but decreases the tensile strength, Young's Modulus, and flame resistance. On the other hand, the addition of 20% wood flour improved the mechanical properties but deteriorated the flame resistance. However, MH significantly improved the composite strength, but at the expense of mechanical properties. It is therefore necessary to find a middle ground where the flame resistance is improved but the strength of the composite is not significantly impaired.

Yanagisawa et al. investigated the flame resistance of PLA using ATH with a high loading of 50 wt% and combined with phenolic resins [125]. The application was electronic product housings where a high level of flame resistance is required. The authors concluded that the mechanism of action was mainly the formation of homogeneous char layers due to the phenolic resins on the surface of the composite upon heating. In fact, this char formed allowed to decrease ATH loading. The phenolic resin provides a high yield in the production of the protective layer which could be enhanced by the formation of aluminium oxide by the decomposition of ATH and this formed char would be sufficiently protective to achieve good FR performance.

Another example of the use of ATH is that carried out by Cao et al.[126]. In this case the ATH was applied as a nanorod-shaped hybrid flame retardant (NRH-FR) that was synthesized by the reaction of benzenephosphinic acid (BPA) with powdery aluminium hydroxide. The

additive was applied at 10-40% by weight and the flame retardancy was analysed by UL-94 and LOI test. In the LOI results, it was observed that with an addition of 10%, a LOI of 21.5 was achieved, which makes the composite self-extinguishing. As the additive percentage increased, the LOI increased further to 25.5 for a content of 40%. In the UL-94 test, 10% gave a V-1 rating and increasing to 20% gave a V-0 rating, so a 20% loading is sufficient to give a significant improvement in flame retardancy. Observation of the ash indicated the formation of a dense and coherent carbon layer that protects the underlying polymers from attack by oxygen and radiant heat during the combustion process. In terms of mechanism, the authors conclude that the benzenephosphinic acid units release $PO2^{\cdot}$ radicals that can inhibit free radical reactions in the gas phase and form polyphosphates in the condensed phase, which reduce heat transfer. On the other hand, ATH generates water vapour during combustion which reduces the temperature of the condensed phase and dilutes the concentration of the combustible gases. In addition, ATH decomposes into Al2O3 and cross-links with the polyphosphates from the decomposition of BPA to form a coherent carbonisation layer in the condensed phase.

Finally, a study on the application of hydromagnesite/huntite (HH) on PLA [127]. Three different grades of HH were applied where one was surface treated with stearic acid. In addition, three different silane coupling agents were used. To study the effect of additive percentage on the thermal, flammability and mechanical properties of PLA composites, weight percentages of 40, 50 and 60 wt% were used. Subsequently, to examine the effect of surface treatment and particle size, a fixed percentage of 50% was set. The composites were characterised by LOI, UL-94, mass loss calorimeter, TGA, tensile, impact and dynamic mechanical analysis (DMA) tests. The addition of HH improves the flame retardant properties of the composites because it reduces the TTI, pHRR, HRR, MLR and total heat evolved (THE) values as the amount added increases. However, the addition of HH deteriorates the initial thermal stability and the tensile and impact strengths of the composites as the amount of HH added increases. The surface modifications had no significant effect on the fire performance of the composites, but the mechanical properties increase, including tensile strength, impact strength and elastic modulus. Finally, it was observed that the use of larger particle size deteriorates tensile strength and flammability properties and improves impact strength and elastic modulus.

As for bio-based flame retardants, there are several examples of the application of cellulose, lignin, starch, phytic acid, among others. Costes et al. in their study about cellulose/phosphorus combinations for PLA composites [128]. They combined microcrystalline cellulose (MCC) or nanocrystalline cellulose (NCC) with phosphorus to improve thermal stability and flame retardant properties. Phosphorus was introduced by chemical grafting into the cellulose or by melt blending using a phosphorus agent of biological origin, in this case aluminium phytate. The percentage of

additive used in all samples was 20% and the composites were characterised by TGA, cone calorimeter and UL-94 tests. Regarding to the conclusions, the phosphorylation process allowed the grafting of 16.5% by weight of P, but this process led to the generation of water-soluble cellulose and the loss of the nanometric shape of the particles, so the phosphorylation was performed only on microcrystalline cellulose. It was observed that 20% by weight of MCC-P allowed to reach the UL94 V-0 level but had a significant effect on pHRR. The only mixture in which a significant reduction in pHRR was obtained was when aluminium phytate was combined with P-MCC. As for NCC, the combination of aluminium phytate and NCC allowed a significant decrease in pHRR to be achieved, in fact to the level of that obtained for MCC-P + Al-Phy. Therefore, the high specific surface area of NCC proved to be very useful to promote the formation of a more insulating carbonised layer.

In another study, cellulose nanofiber was applied in PLA combined with ammonium polyphosphate (APP) [129]. Mixtures of both additives were applied at 5, 10 and 20%, while APP and CNF were applied individually at 20 and 5% respectively. It was concluded that the flame retardant system by braiding APP with CNF is highly effective because with the addition of only 5% additive the composite was classified as UL-94 V-0. This behaviour is mainly due to the catalytic carbon-forming ability of APP and the synergistic effect of CNF in reinforcing the carbon layer. In addition, the addition of 5% allows the PLA composite to maintain a high tensile strength of 50.3 MPa and the impact strength is increased by 54% compared to PA. Therefore, the developed blend can contribute to the application of PLA in new fields such as automotive, packaging, electrical and electronics.

The following are examples of applications of lignin in both PLA and PBS and it can be seen that, as with cellulose, that lignin must be modified or combined with other additives to have an efficient flame retardant effect. With PLA, we found it modified with urea, phosphoric acid and ammonium phosphate, and combined with ammonium polyphosphate (APP) [130,131] and with the PBS matrix modified with phosphorus compounds [132]. Zhang R. et al. used alkaline lignin modified with urea by the Mannich reaction[130]. The modified lignin (UM-Lig) was applied in combination with APP and the total percentage of additive in all samples was 23%. In addition, in order to identify the best APP/UM-Lig mixture, different proportions of both components were studied. It was observed that the developed retardant system had a high efficiency in improving the flame retardancy of PLA and the optimum ratio between APP and UM-Lig is 4:1. When the retardant content is 23% by weight, the LOI value increases to 34.5%, the V-0 classification is obtained and the pHRR and THR values are significantly reduced compared to blends in which APP alone or APP with unmodified lignin is applied. Furthermore, in the TGA test, the APP/UM-Lig blend was found to improve the thermal stability of PLA and promote PLA to form more

carbon. The carbon residue of PLA/APP/UM-Lig can reach 9% by weight at 800°C, while only 6% by weight remains in the PLA/APP/lignin sample.

On the other hand, Costes L. et al. in their article compared the effect of two types of lignins, kraft and organosolv, on PLA [131]. The lignins were chemically modified using a two-step method that allowed the grafting of phosphorus and nitrogen in order to improve their flame retardant action on PLA. The reagents used for grafting were phosphoric acid and ammonium phosphate. The percentage of additive used was 20% for both treated and untreated lignins and the composites were characterised by cone calorimetry, UL-94 and TGA. This study highlighted the importance of the origin and method of lignin extraction because differences in behaviour were obtained. Organosolv lignin compared to kraft lignin was less thermally stable and contained more carboxylic acid and phenolic OH functions, which are responsible for increased degradation of PLA during melt processing. The use of these lignins reduced the heat released during combustion due to the formation of an insulating carbon layer, decreased the pHRR and THR, but also drastically reduced the TTI and thermal stability of PLA. To overcome this, the lignins were chemically modified with phosphorus and nitrogen compounds. The modified lignins were found to be very effective in reducing the flammability of PLA composites. The modified PLA/lignin composites obtained a V0 rating at UL-94 and maintained the TTI and thermal stability of PLA. Once modified, the effect of both lignins became similar and neither the plant origin nor the extraction process of the lignins affected the properties of the composites.

Finally, of the examples with lignin, the research carried out by Zhang R. et al. on its application in PBS [132]. In this study they first compared the performance between alkali lignin and organosolv lignin unmodified and secondly modified with various phosphorus compounds. The percentage of additive used in the two stages was 20%.First, a TGA test of the two types of lignin was performed and it was observed that they degrade in the same temperature range and have a high residue. However, in the MCC test the alkaline lignin showed a lower effective heat of combustion than organosolv lignin, and it was attributed to the release of sulphur dioxide. The incorporation of unmodified lignin in PBS resulted in a reduction of the TTI but, on the other hand, the heat release rate decreased due to the thick carbonisation layer formed. Subsequently, alkaline lignin was modified with various phosphorus compounds and the modification with dihydrogen ammonium phosphate (DHAP) resulted in a higher decrease in peak heat release. In summary, the modified lignin further enhances the barrier effect, and this fact was confirmed by microscopic observations revealing that the barrier effect was further enhanced by the improved cohesion of the charcoal.

Another bio-based additive applied in PLA is tannic acid (TA). In the study developed by Laoutid F. et al. [133], tannic acid (TA) was investigated as a flame retardant for PLA and different strategies were explored in order to improve its charring effect. The first one consisted in combining TA with organomodified montmorillonite (oMMT). This additive limit the thermo-oxidative degradation of the AT and promotes the formation of an effective carbonisation layer. The second strategy was to combine tannic acid with a phosphorus-based compound of biological origin, i.e., a metal phytate salt. The third and last strategy explored was to chemically modify the TA by phosphoric acid. Firstly, it was confirmed that tannic acid alone has no flame retardant effect and must be combined with other compounds. When combined with oMMT, the thermal degradation pathway of TA shifts towards thermal decomposition, the amount of carbon formed during combustion increases and a further reduction of pHRR (around -50%) is achieved. On the other hand, the combination of tannic acid with metal phytate salts, by the additive route required at least 30 wt.% of additive to achieve a significant reduction of the pHRR. However, the reactive route proved to be more effective, because only 20 wt.% allows a strong reduction of the pHRR (-58%) without affecting the ignition time. Finally, the use of phosphorylated TA favours thermal degradation of PLA due to the hydrolysis of tannic acid produced during its phosphorylation, so it is necessary to optimise the phosphorylation process to avoid it.

Another example of a bio-based FR in PBS is phytic acid [134]. Chen s. et al. applied a novel fully bio-based intumescent system composed by phytic acid (PA) and guasine (GU). First, PA-GU was synthesized by convenient ionic reaction, and it was added to PBS at 0, 10, 20 and 30%. The additive synthesized was characterized by XRD and SEM, and composites by TGA, cone calorimeter, LOI and vertical burning test. It was found that PA-GU can improve the performance of PBS because it promotes the formation of a continuous and stable protective layer during combustion. When the percentage of additive is 10%, a significant difference is obtained with respect to unfilled PBS. The composite achieves V-2 classification, the LOI increases by 10%, the pHRR of the sample is reduced by 59.2% and the THR is reduced by 38.6%. Subsequently, as the percentage of additive increases, its effect increases, although not enough to achieve V-0 classification. The flame retardant effect will be better as the amount of flame retardant increases. The successful of this fully sustainable bio-based, fully sustainable bio-based, fully sustainable bio-based flame retardant PBS compound not only means the expansion of the application of PBS such as in electrical appliances and construction, but also provides a new idea for the preparation of fully bio-based flame retardant materials. bio-based flame retardant materials. The authors justified the effect of this retardant to the fact that as phytic acid is rich in phosphate groups it provides a source of acid, and guanosine containing nitrogen and carbon as a source of gas and carbon constitute a fully biological based intumescent flame retardant system. In the combustion process, the phytic acid decomposes into polyphosphoric acid, which is rapidly esterified with the

guanosine-containing carbon ring to form a cross-linked carbon layer. The carbon layer then expands under the action of gas to form an expanded carbon layer. Due to the stability of the expanded carbon layer, it effectively prevents the transfer of flammable substances between the composite and the external environment and thus prevents further burning of the substrate.

3.4 CONCLUSIONS

In this section of the state of the art, a review of flame retardants in general has been carried out and then focused on the application of flame retardants of natural origin. It has been seen that some of the most widely used flame retardants currently available have their alternative of natural origin, but they have not yet been studied in depth, as is the case of brucite. Firstly, mineral retardants have a good flame retardant effectiveness, but high additive loads are necessary, which means an important detriment in the mechanical and rheological properties. There are alternatives such as surface treatments, the combination with other additives or the use of these compounds as nanoparticles, but this increases the cost, increases the number of processes necessary to obtain the composite and reduces to some extent the natural character of the additive in question. One possibility would be to use combinations of additives in which all the components are natural, but this has not been studied much so far. The same applies to bio-based retardants. As the main mechanism of action is the generation of the carbonaceous layer, they require other compounds to favour this effect or to supplement other gas or condensed phase mechanisms.

Since the objective of this thesis is to maintain the natural character of the additive as much as possible because the reinforcement to be used for the composite is a natural fibre fabric, it is proposed to use additives that come directly from the source or that do not require many synthesis or refinement processes. For this reason, the use of surface treatments on the additives or the use of nanoparticles is not considered. One of the additives that meets these criteria is brucite, which, although it requires high loadings, it has been found to be very effective. On the other hand, the use of boehmite is considered because although it requires separation from the main mineral and its effectiveness is not as good as that of brucite, it is an additive that has not been studied in detail and could be an interesting alternative to aluminium hydroxide. Finally, of the bio-based flame retardants, lignin is selected because it is a waste product obtained in the paper industry and its use gives it additional value.

4. NATURAL FIBRES

Natural fibres are those obtained from natural sources such as animals, plants, or minerals, in this case we focused on vegetable fibres. Vegetable fibres are those derived from plants and can be separated into fibres extracted from stems, leaves, or fruits, among others. Normally, the fibres from stem present better properties, lower cost and for this reason have undergone further development. These fibres are mainly composed of three structural polymers, cellulose, hemicellulose, and lignin, and to a lesser extent protein, starch, and inorganics [135]. These polymers differ in composition and structure and their content varies according to the species, type, variety and even the age of the plant, resulting in different physical properties. Table 4summarizes some vegetal fibres with their chemical composition and physical-mechanical properties.

TABLE 4: CHEMICAL COMPOSITION AND PHYSICAL-MECHANICAL PROPERTIES OF SOME VEGETABLE FIBRES [135]

Fibre	Cellulose (%)	Hemicellulose (%)	Lignin (%)	Tensile strength (MPa)	Young's modulus (GPa)	Density (g/cm^3)
Abaca	56-63	20-25	7-9	400	12	1.5
Bagasse	55.2	16.8	25.3	290	17	1.25
Bamboo	26-43	30	21-31	140-230	11-17	0.6-1.1
Flax	71	18.6-20.6	2.2	345-1035	27.6	1.5
Jute	61-71	14-20	12-13	393-773	26.5	1.3
Hemp	68	15	10	690	70	1.48
Sisal	65	12	9.9	511-635	9.4-22	1.5
Pineapple	81	-	12.7	400-627	1.44	0.8-1.6

One of the important applications of natural fibres is their use as reinforcement in polymeric composites. The main advantages over synthetic fibres are that they have low weight, low cost, less damage to processing equipment, good relative mechanical properties, biodegradability, and they are a renewable resource, among others [136]. In addition, in recent years regulations have come into force that seek renewable, recyclable, biodegradable and environmentally friendly raw material, and consequently the market of natural fibres has increased considerably. In fact, the natural fibres market was valued in 2021 at 4460 million USD and is expected to increase to 68447 million USD by 2029 [137].

On the other hand, natural fibres present some disadvantages as quality variability, lower impact resistance, poor compatibility with polymer matrix, restricted processing temperatures and high combustibility. Therefore, it is necessary to study the interaction of these materials with fire.

For this reason, the next sections give a review of fire properties of natural fibres as well as the chemical treatments that can be applied to improve their resistance.

4.1 FIRE PROPERTIES

Natural fibres are complex organic materials, which when subjected to high temperatures result in changes in their physical and chemical structure. Their fire behaviour depends on their constituents, percentage, and morphology [138]. Of the above-mentioned constituents of vegetable fibres, cellulose and lignin have the greatest influence on flammability [47]. The decomposition of cellulose is produced in various steps between 260 to 350°C and supports the flammability process because it generates flammable volatiles and gases, but also non-combustible gases, tars, and some char [139]. Oppositely, lignin decomposes from 160°C to 400°C approximately. Firstly, it is produced the breakage of the relatively weak bonds, so the degradation temperature is lower, but the cleavage of stronger bonds in the aromatic rings occur at higher temperatures and hinder fibre oxidation [112], Lastly, hemicellulose decomposes between 200 and 260°C and release incombustible gases, such as CO_2, and less tar than cellulose [140]. Besides to the composition, fibre orientation also plays an important role due to it results in less oxygen permeability through fibres and, consequently, flammability resistance is improved [138].

There are other factors that influences the flammability. For example, Galaska et al. studied the heat release rate and mass loss rates of some plant fibres, cotton, kapok, flax, hemp, jute, ramie, sisal, and bamboo using microscale combustion calorimetry [141]. The conclusions extracted indicate that in this case the effect of impurity salt levels due to the fibre extraction process are more important than the difference in lignin content.

TABLE 5: HRR DATA FOR PLANT FIBRES [141]

Sample	Chard yield (%)	HRR peak (W/g)	HRR peak temp (°C)
Bamboo	8.73 ± 0.27	266.33 ± 11.37	363.33 ± 0.58
Cotton	20.53 ± 0.07	173.67 ± 13.65	358.33 ± 2.52
Flax	18.48 ± 0.38	214 ± 1	378.67 ± 0.58
Hemp	22.14 ± 0.15	189.33 ± 6.66	353.33 ± 3.06
Jute	14 ± 0.05	236.33 ± 5.69	383.33 ± 2.08
Kapok	14.77 ± 0.62	174.67 ± 14.05	362.33 ± 2.52
Ramie	10.50 ± 0.10	330.33 ± 3.21	390.33 ± 2.08
Sisal	15.56 ± 0.06	208.33 ± 3.21	378.33 ± 1.53

Other example is that Kozlowski [142] compared leaf fibres (cabuya and abaca) with bast fibres (flax and hemp) and obtained a considerably lower heat release rate in the bast fibre despite its lower lignin content. In summary, although a higher cellulose content promotes flammability due to flammable volatiles and an increase in lignin promotes the formation of an insulating char, it is necessary to study each type of fibre in detail.

When natural fibres are used as reinforcement in plastic composites, burning rates decrease [143], but there is still a need to improve their resistance. The options available are to reduce the flammability of the matrix, the fibre reinforcement and/or the composite as a whole, so the following section focuses on the chemical treatments, synthetic and natural that can be used to reduce the flammability of natural fibres.

4.2 TREATMENTS TO IMPROVE FIRE PROPERTIES

Chemical treatments applied to natural fibres are generally focused on reduce their hydrophilic nature and the absorption of moisture to improve the adhesion fibre-matrix. Nevertheless, when a composite is subjected to heating, softening and creep behaviour of the fibre and matrix occur, resulting in buckling or failure of the load-bearing composite structures, which carries an elevated risk [144]. For this reason, it is important to meet the objective of reducing the flammable nature of natural fibres.

Some studies have concluded that the incorporation of flame retardants or flame retarded fibres can enhance fire properties, but with the drawback of the reduction of mechanical properties [145]. There are two types of techniques to improve the fire behaviour of natural fibres and textiles, non-durable and durable, depending on their final use, as textiles can be subjected to cleaning under various conditions. However, due to in this case the natural fibres are inside the composite, it is not necessary to consider the permanence of the FR treatment due to washing.

The common flame retardants for cellulosic fibres are inorganic salts, borax and boric acid, ammonium and phosphorus compounds, and sulphates [146]. As in polymeric matrices, halogenates have shown good flame-retardant effect, durability, and comfort, but during combustion the smoke presents carcinogenic, toxic, and corrosive compounds, so they were banned by USA and EU communities [147]. For this reason, the research has focused on halogen-free FR. For example, two commercial phosphorus compounds have been widely used for cellulosic substrates, Pyrovatex® and Proban®, however, the former can release formaldehyde during textile service and the latter loses 50% of the unreacted flame retardant in the first wash cycle [148]. Therefore, one problem that is currently receiving a lot of attention is the emission

of toxic products from thermal decomposition and combustion of materials as well as the release of smoke [149].

Other treatments that are getting attention are those based on natural resources. In fact, different plant extracts and protein-based products have been explored for use in textiles and/or polymeric materials. The main challenges to be overcome are the development of more cost-effective, environmentally friendly, and sustainable chemicals, as well as reduce the quantity of formaldehyde released during FR application or during service.

4.2.1 Synthetic treatments

Different chemicals are available in the market that catalyse the pyrolysis of cellulose and restrict the release of flammable gases. Generally, these chemicals work by the condensed phase mechanism, but there are other examples such as the combination of antimony with halogen, which works in the vapor phase and is also very popular in this field [150]. However, as mentioned above, the use of halogen in natural fibres is not well accepted due to the negative environmental impact. Despite everything, they still dominate the textile flame retardant market, with 61% of the revenue share in 2021 [151]. As mentioned above, there are durable and non-durable treatments, some involve a complex synthesis or application process, while others only require dipping followed by curing and/or drying. In addition, the number of existing synthetic treatments is numerous, therefore, some non-halogenated treatments are summarised below.

Fire retardants have been used for lignocellulosic materials over 350 years [149]. In the early stages of the study of how to improve the flame properties of fabric, it was discovered that the application of ammoniums, phosphates, metallic salts, borates, among others, were quite effective in improving the flame retardancy of fibres such as cotton, linen and jute, and Perkin studied that each of these compounds required a minimum amount to make the material non-flammable [152]. However, the problem with these treatments was that they involved the addition of metallic salts, which are non-durable, so replenishment was necessary. For this reason, durable flame retardant treatments based on organophosphorus FR were later developed, leading to those used today.

One of the halogen-free flame retardant methods used since then is the synergism between phosphorus and nitrogen, which has a good effect in some specific cases, but cannot be considered universal. In some cases, the effect due to phosphorus FR is clearly observed, but its occurrence depends on the nitrogen compound used, probably due to the formation of reactive P-N. On the other hand, nitrogen compounds can trigger the action of phosphorus, due to the neutralisation or buffering of phosphorus acids [149]. One study of the use of P-N compounds is the application of the ammonium salt of triethalamine phosphoric ester acid (ATEPEA), which is considered a

reactive flame retardant due to it is grafted onto the cotton fabric through P-O-C covalent bonds [153]. The treatment was applied at concentrations of 100, 150, 200 and 250 g/L in a fibre/solution ratio 1:20 at 75°C for 30 min, followed by curing at 170°C for 5 min, rinsing and drying. The ATEPEA-treated cotton fabric showed excellent flame resistance and durability. In the cone calorimeter test, the treated cotton fabric could not be ignited and the pHRR was 8.28 kW/m^2 compared to 195.1 kW/m^2 for the control cotton. These significant changes indicate that the treatment considerably improves the fire properties because it induces the formation of carbon to protect from combustion, in fact the residue weight was 36.1%. The same conclusions were extracted in LOI, vertical flammability and TGA test, therefore, ATEPEA has a wide potential for application in the textile industry, but with the disadvantage of the synthesis process which involves several stages.

Another case of a phosphorus synthesised flame retardant is the two-component formaldehyde-free and halogen-free Neo-FR, developed by Yang et al. [154]. The performance of the flame retardant was evaluated by LOI and vertical flammability and the results were compared with the commercial flame retardant Pyrovatex CP New. The LOI test results were plotted against weight gain for both flame retardants and the values are significantly higher than the untreated sample, increasing from 17.8 (control cotton) to 33.8 for Neo-FR when the weight gain is 25.8%. When comparing both FRs, the data showed that both have similar performance at the same level of weight gain, but Neo-FR was slight lower than Pyrovatex. In vertical flammability test, the same conclusions were extracted, the after flame and afterglow time were zero despite the wash cycles for both FRs, but the char lengths of Pyrovatex were slightly shorter. In the analysis of the char morphology, swollen membranes and inflated balloon-like substances were observed between and on the fibres. This is explained by the release of non-flammable nitrogen gas which forms swollen layers on the surface of the fibres. Furthermore, a dense char was observed on the surface which prevents the combustion of the fibre, and which is verified by TGA with 36.5% ash remaining at 500°C of treated fabric. Therefore, this morphology supports that the mechanism of action of Neo-FR is intumescent, as well as explaining its high efficiency.

Other example of treatment using phosphoric compounds is the study of Szolnoki et al. [155]. The method implemented was an immersion of preheated hemp fabric into cold phosphoric acid (PA) solution followed by a neutralisation with ammonium hydroxide solution, called termotex treatment, a sol-gel treatment using aminosilane, and a combination of both methods. The fabrics were characterized with thermogravimetric analysis (TGA) and mass loss type cone calorimeter test. TGA curves shows that the sol-gel method does not influence the degradation temperature compared to the untreated fabric, while the thermotex treatment decreases that temperature more than 60°C, demonstrating its catalytic effect on cellulose dehydration. Then, the combination of

both methods showed an intermediate range of decomposition, which can be attributed to the protective effect of the sol-gel method by avoiding acid hydrolysis of the cellulose. In cone calorimetric, the best results were obtained with the combination of treatments, which increased the time to ignition (TTI) from 3-6 s to 15 s and reduced the peak of heat release rate (pHRR) by 87.5%. As well as in TGA, the sol-gel method alone does not influence the fire behaviour.

The use of phosphoric acid with bio-based retardants is also possible. Maksym et al. prepared a low cost bio-flame-retardant liquid (BFL) with bio-waste chitosan and phosphoric acid (PA) for application to kenaf, animal and cocoon fibres [156]. The preparation of the solution consisted in mix a 5% of chitosan solution using 2% acetic acid until the solution became yellow and then add 5% of PA. The treated fibres showed excellent self-extinguishing behaviour and achieved the V-0 level in the UL-94 test. The effect is justified because PA promotes the formation of a char layer, which inhibits the passage of heat and oxygen, and the nitrogen in the chitosan molecule dilutes the combustible gases and decreases the influence of fire. In addition to its retarding effect, the main advantages of this treatment are that it is a simple process, and the reagents are cheaper.

Because there are numerous phosphorus-based retardants as well as combinations with nitrogen, Table 6 summarises some examples and their results, ranging from simple to complex compounds and processes.

TABLE 6: FR SYSTEMS BASED ON PHOSPHORUS AND NITROGEN COMPOUNDS FOR VEGETABLE FIBRES

FR system	Fibre type	Results	Ref
N-hydroxymethyl-3-dimethylphosphonopropionamide (HDPP), triallyl phosphate (TAP) and triallyl phosphoramide	Cotton	The increment in phosphorus content improves the LOI values and HDPP proved to be more efficient	[157]
Pyrovatex CP (PCP), diammonium phosphate (DAP), phosphoric acid (PA), tributyl phosphate (TBP), triallyl phosphate (TAP) and triallyl phosphoric triamide (TPT)	Cotton	PCP, PA and DAP have better flame retardant behaviour that the other compounds at the same level of phosphorus content due to their higher activation energy of decomposition, higher char content and lower heat of combustion	[158]
Urea, guanidine carbonate and melamine formaldehyde with tributhyl phosphate (TBP)	Cotton	An increased LOI values of treated cotton fabric with N additives indicated P-N synergism behaviour	[159]
Ammonium salt of arginine hexamethylenephosphonic acid (AAHMPA)	Cotton	AAHMPA treated cotton showed excellent flame retardancy and high durability with a LOI of 45.1% when treated with 35 wt% AAHMPA and 28.6% after 50 laundering cycles	[160]

TABLA 6: CONTINUED

FR system	Fibre type	Results	Ref
N,N,N′,N′-tetra (2-hydroxypropyl) ethylenediamine (EDTP) with phosphoric acid (PA) and urea	Cotton	The synthesized FR-EDPT increased the LOI value in a 130% and reduced the pHRR in a 74% of the cotton fabric	[161]
Ammonium salt of melamine hexa(methylphosphonic acid) (AMHMPA)	Cotton	Treated cotton fabric showed no cytotoxicity to the environment and humans and exhibited outstanding durability and excellent flame retardancy, reaching a LOI value of 43 for the 90 g/L AMHMPA treatment	[162]
Monoammonium phosphate, urea, melamine	Cotton	The cotton fabric showed outstanding fire resistance and durability, with a high LOI of 51.1 and a pHRR reduction of 70.11%. In addition, it is possible to restore the reduced flame-retardant properties by washing with an acetic acid solution	[163]
Ammonium salt of chloramine (methylenephosphonic acid) ethylene-organic phosphate acid	Cotton	The flame retardant not only reacted with cellulose, also polymerized at some degree improving the weight gain, durability and stiffness of the fabric. In fact, the after flame and afterglow time remained zero after 50 laundry cycles. In addition, the pHRR was reduced by 93.1%	[164]

As shown in the table, there are treatments with complex compounds whose synthesis or application processes involve many steps, making them difficult to obtain and apply, while in others no synthesis process is necessary. In summary, the application of phosphorus compounds and their synergy with nitrogen has been shown to considerably improve the fire properties of cellulosic fibres.

On the other hand, the use of boron compounds dates to at least 1735 where borax, vitreol and other mineral substances were patented for canvas and linen [165]. Since then, borax and boric acid are applied in cellulosic fibres and are still often used as a non-durable flame retardant. They have been applied on materials such as bamboo, coir fibre and different types of wood, and with other compounds such as phosphates and formaldehydes. In the study of Levan and Tran, borax-boric acid solutions at different concentrations, from 0.9 to 17%, were applied to southern pine [166]. In fire tube tests it was observed that after removal of the Bunsen burner at 4 min, the samples with add-on levels between 0 to 5 continued to burn, while those with higher retention levels stopped burning. Comparing the weight loss data with addition levels, it was observed that up to 5 add-on% the weight loss gradually decreased to about 60%, but in the region between 5

and 7.5% addition, there is a sharp reduction up to 20% weight loss. The results obtained in heat release rate apparatus were consistent with fire tube test, ignition times increased with increasing levels of add-on% and heat released decreased, reaching a reduction of 40%. In conclusion, loading levels of at least 7.5% are necessary to obtain a significant improvement.

Other examples of applications in wood materials are basswood [167], beech [168], saw dust [169] and white birch [170]. Basswood blocks were treated with aqueous solutions of boric acid (BA), guanylurea phosphate (GUP) and a mixture of them (70% GUP and 30% BA). The treatment conditions were the same for all groups and the final chemical retentions were 3.49%, 7.77% and 7.48%, respectively. The treatment of the wood in all three cases increased weight loss at lower temperatures, decreased weight loss at higher temperatures and promote charring. In boric acid treated wood, it lost considerably more weight at a lower temperature because BA catalyses the dehydration of the wood. However, the GUP-treated wood showed a similar behaviour to the untreated wood at this temperature, but at higher temperature its activation is observed, and it generates more char. Subsequently, the effect of the combination of both compounds was observed in the cone calorimeter test. The fire retardant efficiency of the mixture of BA and GUP was much better than separately, demonstrating that they have a synergistic effect on wood. This synergistic effect arises from the differing fire retardant mechanism and activation temperatures, so the two compounds complement each other.

Beech was transformed into laminated veneer lumber (LVL) using melamine formaldehyde (MF) and phenol formaldehyde (PF) adhesives. Then, the wood specimens were impregnated with aqueous solutions of boric acid, borax and diammonium phosphate at 5% [168]. The boric acid and borax mixtures showed some efficacy in retarding flame spread due to their char-forming effect, their rather low melting point and their formation of glassy films when exposed to high temperatures in fires. However, the treatment with DAP and BA-BX mixture at 50/25/25 ratio showed higher fire resistance and the lowest mass losses with the LVL glued with MF. In fact, this treatment showed the lowest heat release in combustion with and without flame stage and glowing stage. This effect is justified by the fact that borax tends to reduce flame spread but can favour smouldering or glowing, so boric acid helps to suppress smouldering and DPA enhances this effect by increasing fire resistance and decreasing mass loss.

Nagieb et al. also used an adhesive, urea formaldehyde (UF), mixed with BA and BX for saw dust composite [169]. BA and BX were added to the UF at concentrations of 0.5, 1 and 5% (w/v) in a relation 5:1 BA:BX (w/w). In addition, the glue was catalysed with ammonium chloride and paraffin wax was added as a hydrophobic substance. The addition of paraffin wax reduced the glowing time from 90 to 68s, but the treatment with 0.5% BA+BX had a more noticeable

effect since it increases the reduction by half. In the case of 5% BA+BX, the glowing time was reduced to 17s and the char length decreased to the minimum length of 2mm, therefore, its addition improves flame retardation. In conclusion, the ideal concentration of fire-retardant needed to obtain a flame proofing material was 5%.

Subsequently, Pendieu et al. applied boric acid in wood particleboards made of white birch with urea formaldehyde as adhesive and ammonium chloride as a catalyst [170]. The treatment was applied at three percentages, 8, 12 and 16% before adding the adhesive and catalyst, unlike the previous case where everything was applied together. The results of the study showed that boric acid can be used as a fire retardant in wood particleboards and that at higher concentrations a significant improvement was obtained. Comparing the control sample with the 16% boric acid treatment, the afterflame time was reduced from 20 to 0 s and the flame spread speed from 6.6 to 2.4 mm/s, which is a significant reduction. In addition, it was observed that it contributes to decreasing the swelling of the thickness, so it is interesting to study this effect as it could reduce the amount of adhesive needed and consequently the production costs.

Finally, the application of boric acid and borax on coir fibre and bamboo fibre is studied. The coir fibre is a natural fibre extracted from the husk of coconut and can be used to manufacture medium-density panel boards [171]. One of the advantages of this panel boards is that without treatment they have a LOI value of 28, which corresponds to the group of limited fire resistance, and their properties in the flammability test according to IS5509:2000 are promising. However, the treatment with boric acid and borax allows a considerable improvement in the flammability, flame penetration and burning rate, with values relatively higher than the prescribed minimum requirements for all the three tests. Therefore, these results allow the application of these panels in more varied applications involving strict fire safety standards. In the case of bamboo, the effect of boric acid, borax and their mixtures at different proportions has been studied [172]. All treatments were applied at 20% for 2 h at 100°C and cone calorimeter and TGA tests were carried out to study their effect. The order of the pHRR and THR values was: Control > Boric Acid:Borax 7:3 Boric Acid > Boric Acid:Borax 3:7 > Borax > Boric Acid:Borax 1:1. These results demonstrated that borax presents a better performance restricting the heat release than boric acid and an excellent synergistic effect could be obtained by a mixture with 1:1 proportion. In addition, the minimum value of total amount of smoke release per unit (TSP) was obtained in 1:1 boric acid:borax treatment and compared to the untreated sample the value could be reduced by 91.81%. Therefore, borax restricts the heat release, reduces flame spread and boric acid suppresses glowing and exhibits better smoke suspension. Therefore, the combination of both compounds is promising for improving the fire properties of cellulosic fibres and the application process is simpler as it does not require synthesis processes.

The treatments listed above were focused on improving the fire properties, but there are other treatments whose main objective is to improve adhesion with the plastic matrix, but which have also been shown to improve the fire properties, such as treatments with silane. The effect of silanes on fibre-matrix adhesion is because the molecule has bifunctional groups where one reacts with the fibre while the other reacts with the plastic matrix, thus creating a bridge between them. There are different silanes applicable to fibres in general, but for coupling natural fibres they are relatively limited, usually trialkoxysilanes [173]. The following is a summary of some treatments with silanes that have been shown to improve fire properties.

The first is the application of γ-aminopropyltriethoxysilane (APS) to banana fibres [174]. Silanes find it more difficult to react directly with the hydroxyl groups of cellulosic fibres, so it is necessary to activate the alkoxysilane by hydrolysis to form more reactive silanol groups. For this reason, to get an alkoxy functional silane into the fibre, it is necessary to dissolve the silane in the appropriate alcohol, and then hydrolysis can be achieved by treatment with water. In this research, the banana fibres are immersed for 1 hour in a 0.6% APTES solution with a mixture of ethanol/water in a 6:4 ratio. After the treatment, the fibres were chopped and used to reinforce a PLA composite. Comparing the composites with untreated (UTB) and treated fibres (SiB), it was observed that in UL94 test, the samples had less dripping, were not able to ignite the cotton, and burnt slowly compared to PLA/UTB. Furthermore, in the cone calorimeter, the addition of SiB reduced the pHRR value from 397.8 to 339.5 kW/m^2 and the THR and MLR decreased by 34% and 23% respectively compared with PLA/UTB. These results indicate that silane treatment increases the resistivity toward the flame and suggest that it may lead to the generation of higher amount of char residue.

Samyn et al. applied 3-aminopropyltriethoxysilane (APTES) to flax fabric with a previous alkaline treatment [175]. The objective of this pre-treatment is to remove impurities from the fibres and to promote the formation of hydroxyl groups on the surface. Silane binds to the hydroxyl groups present in the fibre, so this pre-treatment enhances the reaction. The alkaline treatment was carried with a 5 wt% NaOH for 1 hour under stirring, followed by a neutralization with tap water and drying. Then, the fabric was immersed in APTES at 10 wt% in an ethanol/water solution (ratio 70/30 v/v) for 1 hour. The treatments improved the adhesion with the resins, but more defects were observed, and regarding to fire behaviour no differences were observed between treated and untreated materials. Since the fabric was not analysed independently, it is not possible to determine why no differences were observed, but it should be noted that in this case the concentration is much higher compared to the previous study and may have a counterproductive effect.

Another silane applied to natural fibres is the triphenylsilane. Czlonka et al. studied the effects of alkaline, maleic and silane chemical treatments on eucalyptus fibres for use in polyurethane composites foams [176]. Alkaline treatment was applied with 5% sodium hydroxide solution for 30 min, 10% maleic anhydride at 60°C for 3 hours and silane at 5% triphenylsilanol in ethanol with ultrasounds for 3 hours. Comparing the treatments, silane treatment displayed the highest mechanical and fire properties. In cone calorimeter tests of the foams, it was observed that silane decreased the pHRR by approx. 60% compared to the untreated fibre and decreased the total heat release (THR) and total smoke release (TSR), despite using only 2% fibres. The reduction could be attributed to the formation of a stable char layer on the polymer surface and the release of non-combustible gases, in fact the carbonized residue increased by up to 37%.

Finally, it is worth to mentioning the study by Basak and Samanta in which they studied the effect of pH on the treatment of jute fabric [177]. The treatment was applied under different pH, 4.5, 7, 10 and 12 using acetic acid and soda ash to adjust it. The effect of the pH was measured by LOI, vertical flammability, temperature profile of burning zone and cone calorimeter tests. The LOI values of the control and acidic pH were 22 and 21, respectively, whereas the alkaline showed 32 and 37 for pH 10 and 12, showing that the alkaline pH improves the flame properties of the fabric. This fact is confirmed in the vertical flammability test, where it was observed that with increasing the pH the sample does not catch and sustain the flame and burns completely with afterglow, while the acidic shows no difference compared to the control sample. Furthermore, in the cone calorimeter test, the time to ignition (TTI) and flame-out time increased from 7 to 14 and from 47 to 93, for the pH 10 sample and the heat release rate decreased by 25.4%. This fact is justified because the alkaline pH blocks the reactive hydroxyl group of cellulose forming soda-cellulose and a strong, deep black, foamy char is formed due to the intumescent mechanism. In addition, it releases water which blocks the air in the vicinity of the burning sample and restricts the formation of flammable gases. In conclusion, alkaline pH improves the thermal stability of the lignocellulosic jute fabric.

4.2.2 TREATMENTS BASED ON BIOMOLECULES

Treatments based on biomolecules have received a great deal of interest, scientific and industrial, due to their low environmental impact, as well as the fact that some are derived from by-products of the agro-food industry. Plant extracts are interesting as flame retardants due to their content of different oxides, minerals salts, tannins, organic acids, etc. and protein-based products due to the natural nitrogen, phosphorous and sulphur chains [150]. The different biomolecule-based treatment, their origin, composition, mechanism of action and examples of their effect on different natural fibres are reviewed below. Plant-based treatments include banana

pseudostem sap (BPS), pomegranate rind extract (PRE), green coconut shell extract (GCSE), spinach juice (SJ) and phytic acid (PA).

Banana pseudostem sap (BPS) is the solution extracted from the pseudostem of the banana plant. Banana plants only bear fruit once in their life cycle, so once the fruit is harvested, the pseudostem is cut and often left on the plantation producing an accumulation of residues. The pseudostem contains 90% water, 0.6% of fibre and 9.4% of pulp [178] and one of the options for its revalorization is the mechanical extraction of the fibre. The water obtained from the pseudostem is normally used as a fertilizer in the agricultural field due to its high amount of metallic content. When it is extracted, the BPS is colourless but with time the solution changes to a light khaki-brown colour because of the oxidation of antharaquinonoid groups [179].

The composition of the BPS has been determined by energy dispersive X-ray (EDX), secondary ion mass spectroscopy (ToF-SIMS) and X-ray fluorescence (XRF) in different articles, showing the presence of metallic elements like potassium, silicious, magnesium, phosphorus, sodium, calcium, and chlorine [180–182]. These elements are present in BPS in the form of inorganic salts, metal oxides, phosphates and phosphites, in fact, analysis have shown the presence of magnesium nitrate, potassium nitrate, potassium chloride and metal phosphate [180,182]. Apart from these elements, BPS contains polyphenolic and tannin-based compounds [150]. The retarding effect of BPS is because all the above-mentioned components act as an endothermic coating that absorbs heat energy, as well as catalyse the dehydration of the cellulose structure and form an insulating carbonaceous char [183].

TABLE 7: FLAMMABILITY PARAMETERS OF COTTON FABRIC TREATED WITH BPS [180]

		BPS concentrations		
Flammability parameter	**Control**	**1:0**	**1:1**	**1:2**
Add on (%)	-	4.5	3.5	2
LOI	18	30	28	26
Horizontal flammability				
Warp way burn rate (mm/min)	75	7.5	8	14
Vertical flammability				
Observed burning rate (mm/min)	250	16.6	21.8	29.4
Flame time (s)	60	4	7	10
Afterglow time (s)	0	900	680	500

Basak et al. have studied the use of BPS to improve the fire behaviour of cotton, jute, paper and corn husk fibre with different concentrations and pH conditions mainly [180,182–186]. The first study consisted of treating bleached cotton fabric with BPS at different concentrations, non-

diluted (1:0) and diluted (1:1 and 1:2) maintaining a material to BPS ratio 1:10. Prior to treatment, the fabric was mordanted with 5% tannic acid and 10% alum, and then treated for 30 min maintaining an alkaline pH. The burning behaviour of the control and the treated samples were evaluated by LOI, horizontal and vertical flammability tests (Table 7).

The results showed that because cotton is purely cellulosic, it catches flame quickly, however, with the application of BPS the LOI increase significantly to almost 1.7 times higher than the control sample. As expected, with increasing concentration, the add-on and LOI increase, so it is better not to dilute the solution. For horizontal flammability, the burning rate is reduced 10 times providing additional time to escape or extinguish the flame. On the other hand, in vertical flammability the reduction is even higher (about 15 times) for non-diluted BPS. In addition, BPS treated cotton shows a reduction of flame time and an increase of afterglow time with respect to concentration. It should be noted that combustion with afterglow is not as severe because the temperature is much lower than a flame combustion, so it is beneficial if the burning with flame is reduced with the simultaneous increase of burning with afterglow time. Finally, in TGA it was observed that the degradation temperature is 50°C lower than the control sample due to BPS reduce the pyrolysis and dehydration temperature of cellulose. It also increases the char residue, so BPS improve the overall thermal resistance of cotton fabric.

Afterwards it was studied the effect of pH in BPS treatment of cotton fabric [183]. The supplied sap had a pH of 7.5, so it was tested as is, acidic (pH 5) and alkaline (pH 10) with the addition of acetic acid and soda ash, respectively, and the rest of the treatment conditions were the same. The LOI value increased to 28 with acidic BPS solution and under neutral conditions the index remained unchanged. In contrast, at alkaline pH, LOI value increased to 30 and in the vertical flammability test, the sample burned initially with flame followed by afterglow for 900 s, while the others completely burnt with flame. In addition, it showed a slow thermal decomposition and the temperature generated was lower (200°C). Therefore, the presence of alkali has provided more thermal stability and helped to increase the add-on. In cone calorimeter, the treatment increased the sample ignition time from 7 s to 14 s and delayed the flame out time. Also, the amount of carbonaceous char mass is higher which helps to absorb the generated heat during the burning cycle. However, the BPS treatment increase the total average smoke, carbon monoxide and decrease the carbon dioxide release. It has been reported that phosphate-based FR and chlorine tend to increase the smoke formation [187,188], so the persistence of afterglow and smoke is a drawback of BPS treatment. In conclusion, the effect of the pH on BPS treatment is an important variable to consider due to it is shown that alkaline condition increases the add-on and show a self-extinguishment against flame, but the smoke production and the strong afterglow must be solved.

For this reason, it has been studied the use boric acid (BA) and phosphorus-based chemicals to hinder the afterglow and smoke production. Basak et al. studied the addition of 1-3% boric acid to BPS for the treatment of bleached cotton fabric [186]. The fabric was mordanted and treated with BPS, BA and the mixed formulations of BPS and BA under the same conditions to compare the flammability behaviour. In this case the pH was maintained neutral. Table 8 show the results of add-on, LOI and vertical flammability.

TABLE 8: FLAMMABILITY PARAMETERS OF COTTON FABRIC TREATED WITH BPS AND BA [186]

		Treatments			
Flammability parameter	**Control**	**BPS**	**3% BA**	**BPS+1%BA**	**BPS+3%BA**
Add on (%)	-	5	6.5	7.4	9
LOI	18	28	29	34	42
Vertical flammability					
Observed burning rate (mm/min)	186.6	55.8	280	46.6	-
Flame time (s)	60	10	60	-	-
Afterglow time (s)	30	295	0	360	50
	Completely burnt with flame	Burnt initially with flame followed by afterglow	Burnt with blue colour flame	Partially burnt	Fire retardant

It is observed that the boric acid increases the LOI value to 29, but the fabric burns completely with a blue colour flame in 60 s and no afterglow. BPS treated cotton shows resistance against flame with flame for 10 s, but strong afterglow and smoke. On the other hand, BPS+1%BA show an increase in LOI, and BA improve the resistance against flame, but the afterglow is still severe. Finally, the addition of 3%BA to BPS shows significant effect in fire resistance, high LOI, no flame, lower afterglow, and the treated cotton has self-extinguish property with a char length of 140mm. In the TGA curves, it was observed that 3% BA cotton fabric showed lower degradation rate, catalysed cellulose dehydration by decreasing the temperature to around 300℃ and produced a thick insulating coating, but the combination of BPA and BA is better because it stops the afterglow of the fabric.

Afterwards, jute and corn husk fibre were treated with pure BPS, concentrated to half (2:1) and quarter (4:1), that is 100mL of extract turned into 50 ml and 25 ml, respectively, by evaporation of the desired volume [182,185]. The mordanted jute fabric was treated with an alkaline solution of BPS at 90℃, while the corn husk fabric was treated neutral and at room temperature. The results of the flammability tests are presented in Table 9. In both cases, the control samples catch flame easily and the LOI index is 21. However, the BPS treatment has a

significant effect in LOI and vertical flammability, and the improvement increases with concentration. Pure BPS has an effect in both types of fibre by increasing the LOI, reducing the after-flame time and increasing the afterglow, but the samples burn completely, and the burning rate is still high in corn husk fibre. When the concentration in BPS (2:1) is increased, no after flame is observed, afterglow increases and the burning rate is reduced, but the samples burn completely with afterglow. Finally, in the treatment concentrated to a quarter (4:1), the LOI increases to 40 and 32 for jute and corn husk fibre, respectively, the samples do not catch flame and the afterglow combustion stops in 40 s and 35 s, making the fibres self-extinguishing. Although both types of fibre have similar add-on values, the improvement in fire properties is greater in the case of jute. This can be justified due to the treatment applied to corn husk fibre was at neutral pH and it showed a rough, irregular and honeycomb appearance due to the presence of non-cellulosic carbon based encrusting substances on the surface of the fibre which generates less amount of residual char mass to protect the fibre.

TABLE 9: FLAMMABILITY PARAMETERS OF JUTE AND CORN HUSK FIBRE TREATED WITH BPS AT DIFFERENT CONCENTRATIONS [182,185]

	Jute				Corn husk fibre			
Flammability parameter	**Control**	**BPS 1:1**	**BPS 2:1**	**BPS 4:1**	**Control**	**BPS 1:1**	**BPS 2:1**	**BPS 4:1**
Add on (%)	-	3	5.7	8	-	4.5	6	8
LOI	21	33	36	40	21	24	28	32
Vertical flammability								
Observed burning rate (mm/min)	250	24.8	18.75	-	110	100	60	-
Flame time (s)	60	5	-	-	120	10	-	-
Afterglow time (s)	0	600	800	40	80	200	350	35

From banana cultivation, the use of banana peel powder (BPP) as flame retardant for polymers [189,190] or to treat natural fibres [191] has also been studied. BPP, which is mainly composed of cellulose (7-10%), hemicellulose (6-8%) and lignin (6-12%) has received attention as a natural additive due to its good thermal stability and high carbon content (almost 45%) which make it suitable as a carbonising agent [189]. For use in the treatment of natural fibres, the extract must be collected by mixing the powder with water, boil it and then filter the solution. Basak and Ali [191] treated cotton fabric with the solution as it is, concentrated to a half and to a quarter and obtained an add-on percentage of up to 17.3%, higher than BPS, however, the LOI increased only to 26. In the analysis of the composition, it was observed the presence of aromatic rings, C-O groups, phosphorous, silicon, magnesium, and potassium, however BPP does not possess enough affinity with cotton fabric because the char after combustion showed poor structural integrity thus obtaining a lower performance as a flame retardant [191].

On the other hand, the same article studied the use of pomegranate rind extract (PRE). This is another waste agricultural product that has been used as colorant for textiles, but its content in tannins, phenolic groups and nitrogen has made it promising for use as a flame retardant for cellulosic textiles. During fruit processing, peels and seed are obtained as by-products and, if not handled properly, can pose a problem of environmental contamination. Pomegranate accounts for about 26-30% of the total weight [192], and like BPP, it is necessary to boil the residue and then filter the solution to collect the extract. This extract has been used on jute and cotton, at different concentrations, pH and with other compounds such as sodium tri-polyphosphate (STPP) and sodium lignin sulfonate (SLS) [150,191,193–196]. As mentioned, it has been reported the presence of natural tannin-based compounds, aromatic rings, alkaloids, and protein groups that contain nitrogen, and high molecular weight phenolic groups, and these molecules assist in the self-extinguishing effect [150]. In addition, EDX analysis confirmed the presence of nitrogen, and other metallic elements such as potassium, chlorine, calcium and sulphur, and traces of chromium, copper, magnesium, aluminium, and silicon [150,196]. The effect of PRE is due to the aromatic phenolic groups act as intumescent barrier against heat and flame propagation, and the nitrogen compounds assist in char formation. Furthermore, PRE releases non-combustible gases as ammonia, nitrogen, and carbon dioxide and, on the other hand, metallic salts and oxides absorb moisture and catalyses the dehydration of cellulose, thus increasing the char formation [193]. This is confirmed by analysis of the morphology of the char residue, where it has been observed that the cotton fabric yarn is not damaged and the appearance is a hard, deep black char with small holes all over its surface, which may be due to the release of non-flammable gases [191].

Unlike other extracts, when the treatment is applied, it is not necessary to mordant the fibre to facilitate add-on as the tannin compounds act as mordant material. Furthermore, it can be applied as it is, but it has been found that hot condition for immersion is required to increase uptake and make the treatment more uniform [150]. The extract, such as it is, has an acidic pH of 4.5 and when the pH increases up to 10 it is observed that the LOI and add-on(%) increase reaching self-extinguishing behaviour. This fact has also been observed in the case of BPS and it is concluded that alkali attacks the primary hydroxyl group of cellulose thus forming soda cellulose and hindering the formation of flammable gases levoglucosan and pyroglucosan [193].

In the case of the treatment with concentrated PRE extract on cotton fabric at 90℃, it has been observed that the treatment considerably reduced the burning rate, decreasing by 75% for the solution as it is and up to 91% for the more concentrated 4:1 solution compared to the control cotton fabric [191]. Furthermore, thermogravimetry curves and LOI value revealed that the PRE extract increases the thermal stability because it is obtained a decrease of the mass loss peak by 60℃ due to it catalyses the pyrolysis phenomena and reduces the generation of flammable gases

and because it increases the LOI from 18 to 32 [194]. In the cone calorimeter analysis, cotton fabric burned within 45 s, while the 4:1 PRE treated fabric did not catch up the flame but combusted with afterglow and the pHRR was reduced 3.16 times and occurred 195 s later.

Finally, the use of PRE extract with other compounds such as STPP and SLS has been studied. Sodium tri-polyphosphate (STPP) is an eco-friendly phosphorous compound that has been added to PRE to study whether it can help with the afterglow of the cotton fabric with a comparatively lower add-on%. The bleached cotton fabric was treated with different concentrations of STPP (1, 2 and 3%), PRE with 2:1 concentration and the mixture of them [195]. It was observed that STPP alone does not improve the fire properties despite increasing the concentration, however, in the PRE+2%STPP mixture the cotton fibre resists flame and hinders afterglow propagation, obtaining a self-extinguishing material with a char length of 20 mm. When the concentration of STPP is increased to 3%, the cotton fabric obtains a classification in the vertical flammability test of V1 category as the afterglow lasts about 120 s, but the fact that it does not catch-up the flame corresponds with the V0 category. This effect is justified because the positive ions present in the PRE extract are deposited on the cotton fabric due to the negative charge of its surface. Then, these deposited positive ions attract the negative phosphate ions of the STPP, forming a mixture in which the PRE arrests the flame catch-up and the STPP stops the afterglow propagation.

On the other hand, sodium lignin sulfonate (SLS) which is a biobased branched chain lignin modified with sulfonic acid, has been used to study whether it could reduce the add-on% to achieve the self-extinguishment of the fabric. Bleached cotton fabric was treated with different concentrations of SLS (5, 7 and 10%), PRE and the mixture of them [196]. With SLS, all samples burned with flame and afterglow and the LOI did not increase enough to be considered as fire retardant, in fact the only difference with the control sample was that the char is much harder and blackish. However, the PRE and SLS mixture showed flame and afterglow resistance. Thermal stability improved with increasing SLS% concentration in the PRE, thus 10%SLS shows a char length of 40mm with a minimum afterglow time of 7-8 s. Fire retardant action may be attributed to the presence of polyphenolic and nitrogen compounds of the PRE and sulphur compounds of the SLS. The large molecular weight phenolic compounds assist to aromatize cellulose, promoting char formation and restricting the release of flammable volatiles during cotton pyrolysis. The nitrogen from the alkaloid groups of the PRE accelerates the dehydration process of the cellulose and generates more carbonaceous char and finally the sulphur may be converted into non-flammable sulphur dioxide or sulfuric acid thus also catalysing the dehydration process.

Other wastage product that has been studied to impart flame retardancy to natural fibres is the green coconut shells (GCSE). Increased consumption of coconut water and coconut pulp has led to an increase in the generation of shells, which account for up to 85% of the weight of the fruit, and in some regions these shells become waste despite their many uses [197]. GCSE has been used on paper, jute, and cotton, at different concentrations, pH and with boric acid [198–201]. To justify the retardant effect of this extract, phytochemical, gas chromatography-mass spectrometry (GC-MS), ATR-FTIR and EDX analyses, among others, have been carried out to determine the composition. GCSE presents aromatic rings, gallic acid, polyphenols, catechins and, in addition, phytochemical analysis revealed the presence of phenols, tannin, saponin, terpenoid, glycoside and flavonoids [198,199]. Regarding to EDX analysis, it reflected the presence of chlorine, potassium, calcium, sodium, phosphorus, magnesium, sulphur, nickel, aluminium and silicon, and these elements may be present in oxide or salt form [150,198,199,201]. The content of these elements varies according to the scientific paper, which is normal as it is a natural source, but different variety of GCSE has been used and not much difference has been observed [150]. The effect of the flame retardancy is due to all the above mentioned components jointly catalyse the pyrolysis of cellulose, cross-link the -OH groups and aromatize the structure and, as a result, more insulating char is formed [150]. In fact, the char showed structural integrity, light black colour, and small bubbles throughout the surface, confirming the intumescent effect of blowing agent compounds and high molecular weight polyphenols [150].

The solution after extraction presents a yellowish brown colour and a pH value of 4.5, for this reason it has been studied the effect of acid, neutral and alkaline pH in cotton and jute fabrics [198,199]. In both cases the solution was alkalised with anhydrous sodium carbonate, and applied unconcentrated and double concentrated at 90°C for 60 min. When the solution is concentrated, the add-on percentage increases and causes a greater improvement in LOI, for this reason, Table 10 shows the results of jute and cotton fibre with the double concentrated GCSE solution. After the application of the extract at pH 4.5, the LOI increases significantly, 28.6% for jute and 38.9% for cotton, and at pH 10 the improvement is even greater, 81% for jute and 72.2% for cotton. Comparing both types of fibre, it is observed that there is a higher affinity of the extract with jute fabric, because the add-on is greater with the same treatment conditions. Also, the pH effect is more noticeable in jute fibre, as both add-on and LOI increase more and even a self-extinguishing effect is achieved at alkaline pH. This fact could be attributed to the increase in jute swelling with increasing pH [198]. On the other hand, the TGA curves confirm that by increasing the pH, the thermal stability of the fabrics improves because the degradation temperature has gradually shifted towards lower temperatures and the amount of char mass remaining at higher temperatures, around 400°C, has increased [198,199].

TABLE 10: FLAMMABILITY OF UNTREATED AND GCSE TREATED JUTE AND COTTON FABRIC WITH DOUBLE CONCENTRATED SOLUTION [198,199]

	Jute				Cotton			
Flammability parameter	**Control**	**pH 4.5**	**pH 7**	**pH 10**	**Control**	**pH 4.5**	**pH 7**	**pH 10**
Add on (%)	-	6.15	7.42	9.18	-	4.98	5.19	5.97
LOI	21	27	34	38	18	25	28	31
Vertical flammability								
Flame time (s)	60	5	-	-	60	118	38	4
Afterglow time (s)	0	600	800	40	0	0	244	975

Basak and Ali [150] compared the effect of the banana peel powder (BPP) and pomegranate rind extract (PRE), explained above, with the coconut shell extract (GCSE) applied at different concentration at 90°C for 30 min without changing the pH. Analysing only the effect of the GCSE, it is observed that increasing the concentration to a quarter improves the fire properties with respect to the control cotton, but the fabric still catches the flame and burns completely with the afterglow, so it would be necessary to establish a combination of pH and concentration to achieve a self-extinguishing effect.

Lastly, Basak et al. studied the mixture of GCSE with boric acid (BA) in cellulosic paper [201]. It has been previously reported that the use of boric acid hinders afterglow and reduces smoke production, which is confirmed in this article because the paper is purely cellulosic and highly flammable and the addition of 2% BA results in a paper that does not catch-up flame and does not even show afterglow.

Another example of a plant-based extract is spinach juice (SJ), which is the solution extracted from fleshy green leaves of the spinach plant. When it is extracted, it has a deep green colour, but with time turns blackish green due to the poor lightfastness of the flavonoid and chlorophyll molecules when subjected to room temperature and open conditions [202]. The problem with respect the other extracts reviewed is that spinaches are used as food, so its use as a flame retardant would be unethical because of world hunger. In terms of composition, SJ contains different nutrients, potassium, calcium, sodium, nitrogen, silicon, proteins, vitamin K, vitamin A, vitamin B complex, antioxidant, polyphenolic aromatic rings, etc and the elements are present in the form of inorganic metallic salts or oxides [179,203]. The fire-retardant effect of the juice can be attributed to the presence of moisture which helps to absorb heat and, on the other hand, to the mineral salts, which delay the thermal decomposition of cellulose by contributing to the dehydration process, releasing non-flammable gases and increasing the formation of char. TGA analysis corroborates this fact, as the SJ powder curve showed that 30% of the char mass remained at 750°C, in addition to a lower rate of weight loss [202].

The SJ solution has been applied in cotton fabric at different concentrations and with and without mordanted process. In both cases the solution was alkalised to pH 10 with soda ash and applied at 90ºC for 30 min. In the first study the solution was diluted with water at 1:2, 1:1 and only SJ 1:0, and as expected, the thermal stability of the cotton increases with concentration [202]. After the application of SJ, the LOI increased from 18 to 26, 28 and 30, respectively, and the burning time passed from completely burnt by flame in 60 s to only afterglow for 400 s for the 1:0 solution. It should be noted that the afterglow is still a problem, but in a real life situation it provides longer escape time from the hazards and the environment is less dangerous due to the significantly lower temperature. In the horizontal test, the same conclusions were obtained, the burning rate was reduced 9 times compared to the control fabric, but no charring was observed due to the samples burned completely.

In the second article, the extracted juice was applied to a bleached and a premordanted cotton fabric [204]. Table 11 shows the flammability test results of control and SJ treated cotton fabric. First, comparing the control and mordanted fabric it is observed that the process does not influence the fire properties, in fact, the propagation rate remains unalterable. On the other hand, with SJ extract the mordanted process do not increase the add-on(%) of the treatment and in fact reduces the LOI value from 30 to 25. In addition, in the vertical flammability the cotton mordanted and SJ treated burnt completely with flame in 100 s, therefore, the process favours flame pick-up and accelerates flame propagation. In conclusion, it is not necessary to mordant the fabric, as the effect is counterproductive and reduces thermal stability. Regarding to the morphology of the char, the treated fabric shows a hard intact structure of closed cells with small pockets of gases that prevent the flow of volatiles into the flame and these observations confirmed the condensed phase intumescent mechanism.

TABLE 11: FLAMMABILITY RESULTS OF CONTROL AND SJ TREATED COTTON [204]

Flammability parameter	Control	Mordanted	SJ treated	Mordanted+SJ
Add on (%)	-	2	8	8
LOI	18	19	30	25
Vertical flammability				
Flame time (s)	60	60	-	100
Afterglow time (s)	15	-	345	-
Burning rate (mm/min)	250	250	43.5	150

In summary, plant-based treatments have shown that concentrated solutions and alkaline pHs favour the add-on%, thus improving fire resistance properties and that, in some cases, suppressants, such as boric acid, can be applied to minimise smoke and afterglow.

The development of intumescent coating with biobased compounds has also been studied. The advantages of this method are that the treatment does not change the properties of the fibre and the thickness, composition and functionality of the layers can be controlled to meet the fire properties. Cheng et al. developed an intumescent coating using three biobased compounds: phytic acid (PA), chitosan (CH) and biochar (BC) [205]. Biochar (BC) is a carbon-rich material that can be obtained from agricultural waste and contains P, N and S elements that can induce flame retardant mechanism [36]. The treatment was applied to a cotton fabric with the layer-by-layer (LBL) method. Table 12 shows the composition, add-on (%) and the results obtained in LOI and cone calorimeter test.

TABLE 12: COMPOSITION, ADD-ON, LOI AND CONE CALORIMETER DATA FOR COTTON FABRIC TREATED WITH PHYTIC ACIDM CHITOSAN AND BIOCHAR[205]

Sample	PA (%)	CH (%)	BC (%)	Add-on (%)	LOI	pHRR (kW/m^2)
COT	0	0	0	0	18.6	66.3
PA-COT	10	0	0	8.2	19.8	32.3
PA/CH-COT	10	2	0	30.2	40.2	26.5
PA/BC-COT	10	0	5	11.5	36	64.8
PA/CH/BC (5%)-COT	10	2	5	35.8	54	9
PA/CH/BC (7.5%)-COT	10	2	7.5	45.3	64.1	7.7
PA/CH/BC (10%)-COT	10	2	10	47.7	66.8	13.3

Results showed that the combination of the three components significantly improved the fire properties. Compared to untreated fabric, the PA/CH/BC (7.5%) sample showed a reduction of pHRR by 88.39% and an increase in LOI by 244.6%. In addition, the char residue increased from 0 to 90.8%. It was concluded that the intumescent coating acts in the condensed phase promoting the formation of a phosphorus-rich carbon layer that hinders the propagation of fire.

Another example of the use of phytic acid in cotton fabric was the study of Feng. et al. [206] who synthetised ammonium phytate (APA) using phytic acid (PA) and urea and applied it at different mass concentrations 5, 10 and 20%. Also was studied the permanence of the treatment after 10, 20, 30, 40 and 50 laundering cycles. The LOI value increased from 17.8% to 43.2% for the fabric treated with 20% APA and, after 50 laundering cycles, decreased to 24.7%. In the cone calorimeter test, the untreated sample shows a sharp HRR peak reaching 195.1 kW/m^2 at 22 s, representing the fast combustion of cotton. One the other hand, the treated sample does not show much variation throughout the test, reaching a pHRR of 10.7 kW/m^2, no flame and a very gentle combustion. The residue was 36.24% after test and the CO_2/CO ratio significantly declined from 86.18 to 3.05, thus demonstrating the excellent ability of APA to hinder the combustion.

In addition, phytic acid and urea have been applied to hemp fibres [207]. Before the treatment, the fibres used underwent a steam explosion refining step after a soda impregnation in which most of the hemicellulose was removed, and then passed a bleaching process. The exploded (HF) and bleached exploded (BHF) were phosphorylated in an aqueous solution at different concentrations of urea (1-20 wt%) and phytic acid (0.32-6.26 wt%) for 1 h at room temperature. After treatment, it was observed that the grafting of phytic acid is achieved in the presence of urea and that P% and N% increase with the concentration of both reagents. Regarding to %P content, fibres with contents below <0.2 wt% ignite and burn, with about 0.5 wt% became self-extinguishing and with contents above 0.5 wt% they are totally non-combustible. Furthermore, comparing both types of fibres, it is observed that the P and N content is higher in bleached fibres and, consequently, the fire properties are better. This is because delignification makes cellulose more accessible for phosphorous and nitrogen grafting. However, it was obtained a decrease in mechanical strength of 80% in fibres with high phosphorous content to a decrease in cellulose crystallinity and possible local damage.

4.3 CONCLUSIONS

Following the criteria used for the choice of the plastic matrix retardant additive, it is decided to select a biomolecule-based fabric treatment. Because of its availability in the Canary Islands, because it is a waste product and because of its effect, it was decided to use banana pseudostem sap for the treatment of the natural fibre fabric. As for the treatments of synthetic origin, APTES was selected because the percentage of reagent required is small and because it could improve the mechanical properties of the composite.

5. FIRE TESTS

Designers must ensure that materials achieve a wide range of parameters such as mechanical strength, chemical resistance, aesthetic appearance, among others, to be satisfactory in use and marketable. However, it is not considered that if a product is involved in a real fire and its performance is inadequate, it can cause loss of life and/or property. For this reason, fire behaviour should be included in the list of design criteria.

First, it is essential to consider that the fire test carried out, and the performance requirements achieved are relevant for the product and its final use. For example, a test for a specific purpose should be reproducible, but it should be noted that high-reproducibility tests can be misleading if they are not relevant to the product and the end-use situation.

There are many fire tests, which may be divided into various categories (Figure 3). They are often considered as separate properties, and the standards may imply this belief. However, most of these parameters are interrelated, and failure to acknowledge this can result in misleading conclusions and potentially unsafe situations.

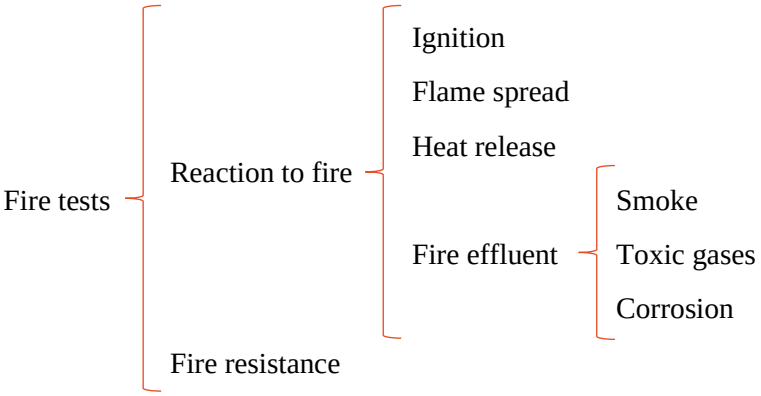

FIGURE 3: TYPES OF FIRE TESTS [208]

The first is the ignition test, which determines the probability of starting the fire, which is very important because without ignition there can be no fire. However, protection against identified ignition sources cannot guarantee that fire will not occur due to secondary ignitions, and the consequences of that ignition and fire growth need to be kept in mind. Continuing with flame spread, it may be considered as a series of staggered ignitions caused by radiant heat and pilot flames, both of which may be generated by the flame front itself [208]. Many of these tests imply the application of flames to products and materials. Different types, sizes, flame times as well as different specimen types, shapes and orientations are used, but most determine product's ability to sustain combustion beyond the ignition source. Then, rate of heat release is probably

the most important property because if the heat generated by the material burning exceeds the amount of heat needed to cause ignition, the fire will sustain itself. Finally, smoke, toxic, and corrosive gases are determined as “fire effluent” and depend on the material burning, the rate of burning fire model and the fire environment. On the other hand, fire resistance is the ability to prevent the passage of heat, smoke, and fire gases into a defined fire environment. Polymer products are rarely required to meet fire resistance requirements on their own, although they may be used in composite systems.

In turn, there are different scales of tests, ranging from laboratory scale to full scale with the fabrication of scenarios that reproduce for example the conditions in a room during a fire. Each scale provides different levels of information that needs to be interpreted to design effective fire protection strategies. In this case, as the work is focused on the development of a composite, the tests carried out are at laboratory scale and include ignition, flame propagation and heat release tests. The following sections describe each test carried out during this thesis and the basic concepts necessary for their understanding.

5.1 LOI

The limiting oxygen index (LOI) determines the minimum oxygen concentration necessary to sustain a stable flaming combustion of a material under certain conditions. It represents the percentage concentration of oxygen at which a small specimen will only just burn downwards in a candle like manner. The procedure is according to UNE-EN ISO 4589 and consists of clamping a test piece vertically at its base inside a glass chimney of specified dimensions. Then, the upper edge of the test specimen is ignited and burns in a candle-lie manner and a mixture of oxygen and nitrogen is metered through the base of the chimney (Figure 4). The aim of the test is to determine the minimum oxygen concentration in the gas mixture that enables a steady burning for 3 minutes or 50 mm [209]. Materials with LOI values less than 21% are classified as combustible and those with LOI greater than 21 are classed as self-extinguishing because their combustion cannot be sustained at ambient temperature without an external energy contribution [210]. Nevertheless, it is necessary to consider that the LOI value decrease as temperature increases and melting and dripping of a polymer during the test may cause a specimen to extinguish and give misleading high values.

This test is probably one of the best-known tests because it gives good repeatability, is useful for quality control and indicates the potential flammability of a material. However, it should be noted that it does not predict the performance of a material under fire conditions and should not

be used to extract conclusions of the behaviour of flame retardants, so the flammability assessment should be carried out in conjunction with other tests.

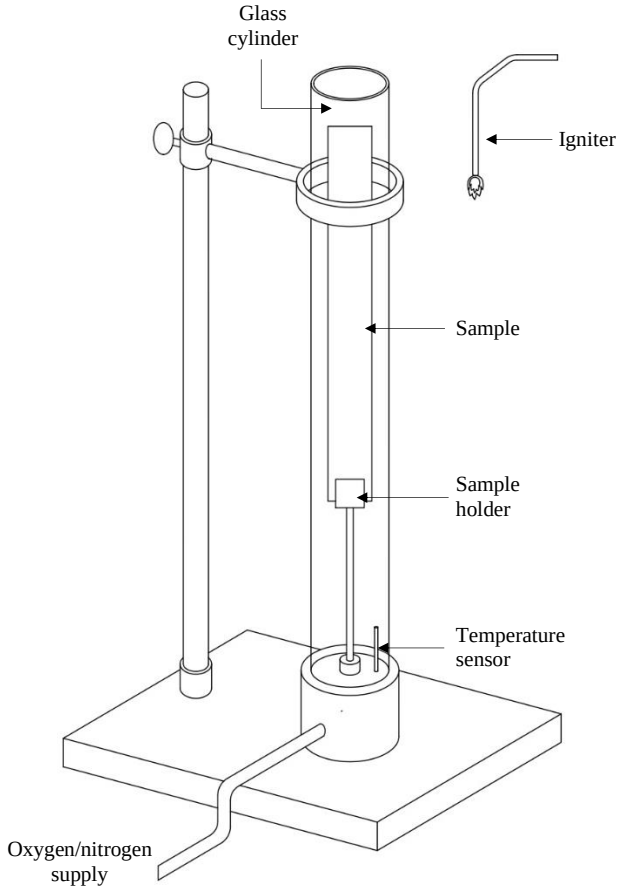

FIGURE 4: SCHEMATIC REPRESENTATION OF LIMITING OXYGEN INDEX TEST

5.2 UL94

The UL94 test is a test procedure and classification system for determining the flammability of thermoplastics and silicones developed by Underwriters Laboratories and is one of the most widely used. The benefits of these tests are that they are simple, practical, and useful for determining ignition and flame spread. Moreover, they have been adopted as international and national standards and are used to specify materials for many applications. UL94 contains: 94HB, 94V, 94VTM, 94-5V, 94HBF and 94HF. The 94HB describes the Horizontal Burn Method. Methods 94V and 94VTM are used for Vertical Burn, 94V is a more stringent test than 94HB and the difference to 94VTM is that 94VTM is used for very thin materials. The 94-5V test is similar to 94V test and is used in enclosures for products that do not move easily or are attached to a conduit system. The 94HBF and HF tests are horizontal tests and are used for non-structural foam materials i.e., acoustical foam. In this work we focused on 94HB and 94V which are described below.

The 94HB is generally considered the easiest test to pass and would typically be acceptable for portable, attended, intermittent-duty, household-use appliance enclosures or for decorative parts [211]. The test uses 1"x5" specimen held in a horizontal position at one end with marks at 1" and 5" from the free end. A flame is applied for 30 second or until the flame front reaches the 1" mark (Figure 5). If combustion continues, it is quantified the time between the 1" and 5" and then the propagation speed is calculated. If combustion stops before the 5" mark, the time of combustion and the damaged length between two marks are recorded. Depending on the thickness of the specimen, the material will be classified as the following table.

TABLE 13: MATERIAL CLASSIFICATION IN UL 94 HB TEST [212]

Test Criteria	Burning rate in V	Flammability rating
Test specimen thickness 3-13 mm	≤40 mm/min	HB
Test specimen thickness <3	≤75 mm/min	HB
Flame is extinguished before first mark	≡ 0 mm/min	HB

The 94V test measures the ability of a vertically oriented plastic part to extinguish the flame after ignition and its dripping behaviour under controlled laboratory conditions. A small burner flame is applied to the free end of the specimen for two 10 seconds intervals separated by the time it takes for the flame to cease burning after the first application. If the material drips on the Bunsen burner, it is placed at 45 degrees to prevent them from falling in. It is quantified the burning time of each specimen, the total burning time for 5 specimens, burning and afterglow times after second flame application, cotton ignited by flaming drips and combustion up to holding clamp. Then the material is rated as the following table.

TABLE 14: MATERIAL CLASSIFICATION IN UL 94 V TEST [212]

Test Criteria	V-0	V-1	V-2
Burning time of each individual test specimen (s)	≤10	≤30	≤30
Total burning time (s) (5 flame applications)	≤50	≤250	≤250
Burning and afterglow times after second flame application (s)	≤30	≤60	≤60
Dripping of burning specimens	No	No	Yes
Combustion up to holding clamp	No	No	No

Figure 5 shows a scheme of both tests: a) Horizontal 94HB b) Vertical 94V.

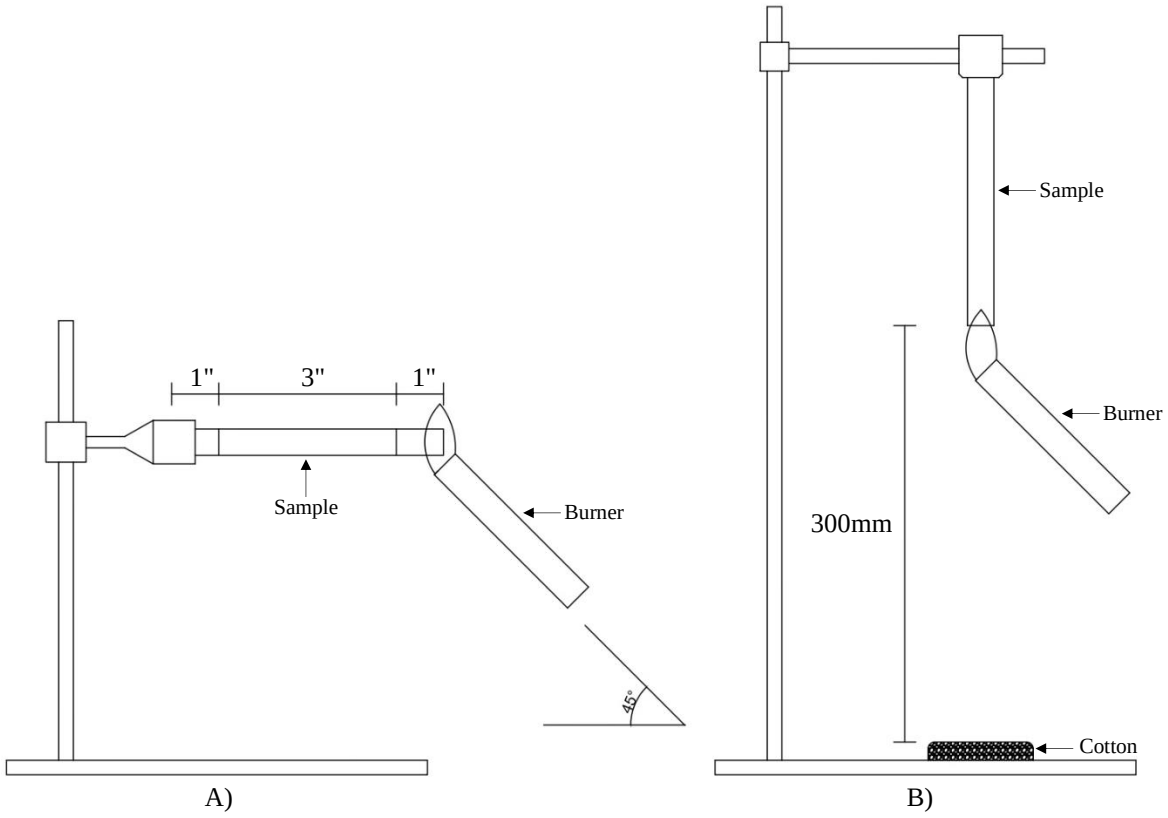

FIGURE 5: SCHEME OF UL94 TEST. A) HORIZONTAL 94HB B) VERTICAL 94V

5.3 CONE CALORIMETER

The cone calorimeter is a bench-scale testing device to measure the fire reaction of materials, specially heat release. It is the most widely used instrument for investigation the fire behaviour of materials because it provides abundant information with relatively small samples. In fact, it is used for research and as a standard test and is widely used to quantify flammability parameters in material development projects, prior to industry specific tests. The cone is established as the principal technique for the measurement of several fire and flammability hazard parameters for early or well-ventilated fires. For example, for measuring the heat release rate (HRR) and the effective heat of combustion from a burning polymer under a controlled radiant heat source (ISO 5660 part 1). In addition, it can be used to determine smoke generation as described in standard ISO 5660 part 2. Lastly, part 3 of the standard examines the measurement limitations and applications of the cone calorimeter and presents a set of guidelines that help to standardize its use.

The apparatus consists of a conical electric heater that applies controlled levels of radiance from 0 to 100 kW/m^2 to stimulate forced-fire conditions. The specimen (100x100 mm and up to 50mm thick) is mounted in a sample holder, usually horizontally, under the cone on a load cell recording its mass during the experiment. Samples can be tested with and without a retaining

frame and it affects the result, as well as the thermal insulation on the back of the sample. The specimen is ignited with or without an electric spark, and air passes through the apparatus, because tests are typically carried out under well-ventilated, due to is the worst-case scenario for flammability. The fire effluent gases travel upward into an instrument hood system where gas samples are collected.

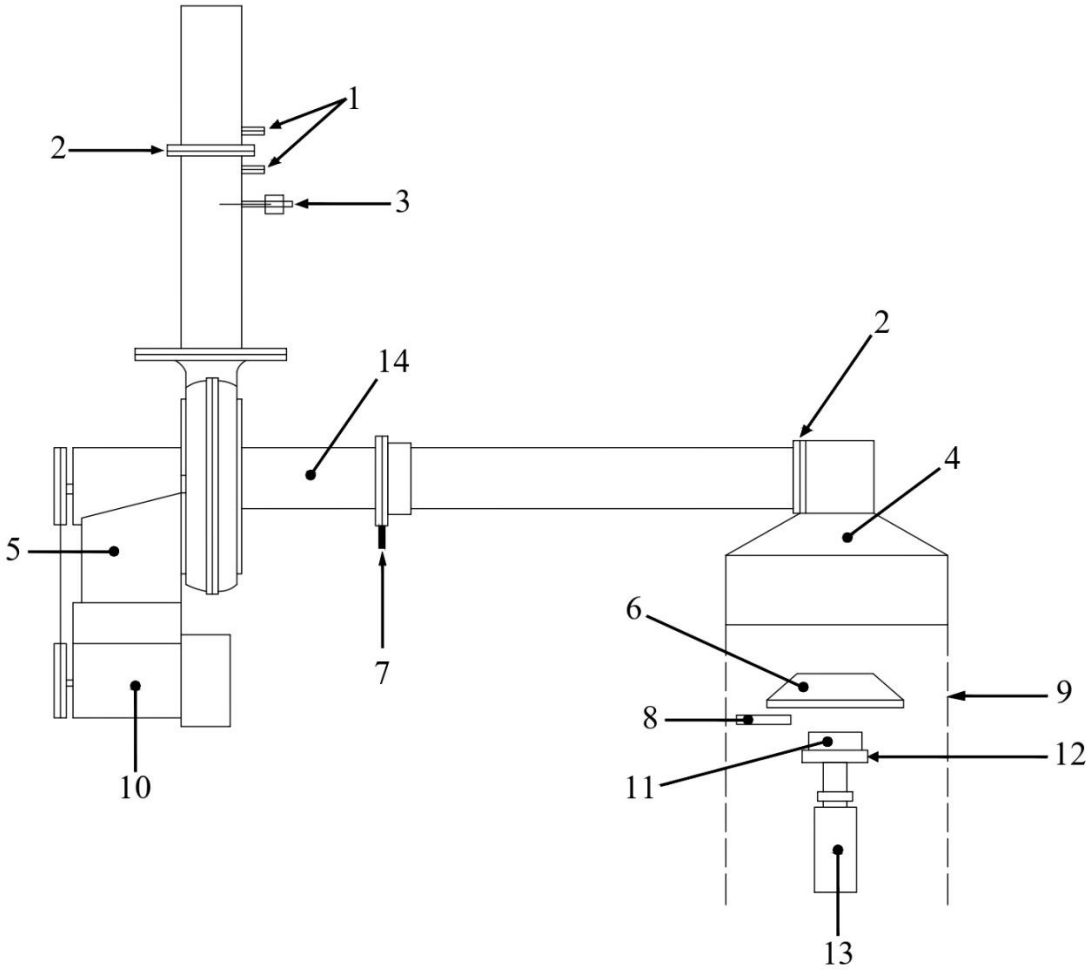

1 Pressure ports
2 Orifice plate
3 Termocouple (located on stack centreline)
4 Hood
5 Blower
6 Heater
7 Gas sampling ring probe
8 Spark plug
9 Optional screens
10 Blower motor
11 Retainer frame and specimen
12 Specimen holder
13 Weighing device
14 Smoke measurement section

FIGURE 6: CONE CALORIMETER SCHEME [213]

Cone calorimeter records parameters such as sample mass loss, heat flux, oxygen, CO_2 and CO concentrations in exhaust duct, and fire effluent flow as a function of time. With these variables are calculated various flammability parameters, including heat release rate (HRR), total heat released (THR), time to ignition (TTI), mass loss rate (MLR), total smoke release (TSR), and effective heat of combustion (EHC). The heat release rate (HRR) is the rate at which fire releases

energy and is determined by measurement of the oxygen consumption derived from the oxygen concentration and the flow rate in the combustion product stream [213]. The total heat released (THR) is the integral of the HRR with respect to the time and represents the total heat output up to that point [12]. Time to ignition (TTI) characterizes the ease of ignition of the material by defining how quickly the flaming combustion occurs when the material is exposed to a heat source [214]. The mass loss rate (MLR) represents the speed of mass loss due to pyrolysis and is controlled by the net heat flux, decomposition temperatures, heat transfer and residual mass [12]. The total smoke release (TSR) is the smoke production result from incomplete combustion and is strongly dependent on the material, fire scenario and cone calorimeter set-up [215]. Finally, the effective heat of combustion (EHC) is a very intrinsic property of the tested material, it indicates the energy released per unit of mass burned [216] and tends to be very noisy because it is divided by mass loss rate. Of these the most widely reported in the literature are peak of heat release rate (pHRR), time to peak HRR (ttpHRR), THR and TTI.

Figure 7 shows an example curve of HRR vs time and the variables usually reported. In addition, the shape of the graph also provides information of the behaviour of the material and ash formation [12]. Moreover, a great deal of information is obtained by observing the combustion of the samples in the cone calorimeter and relating it to the heat release data.

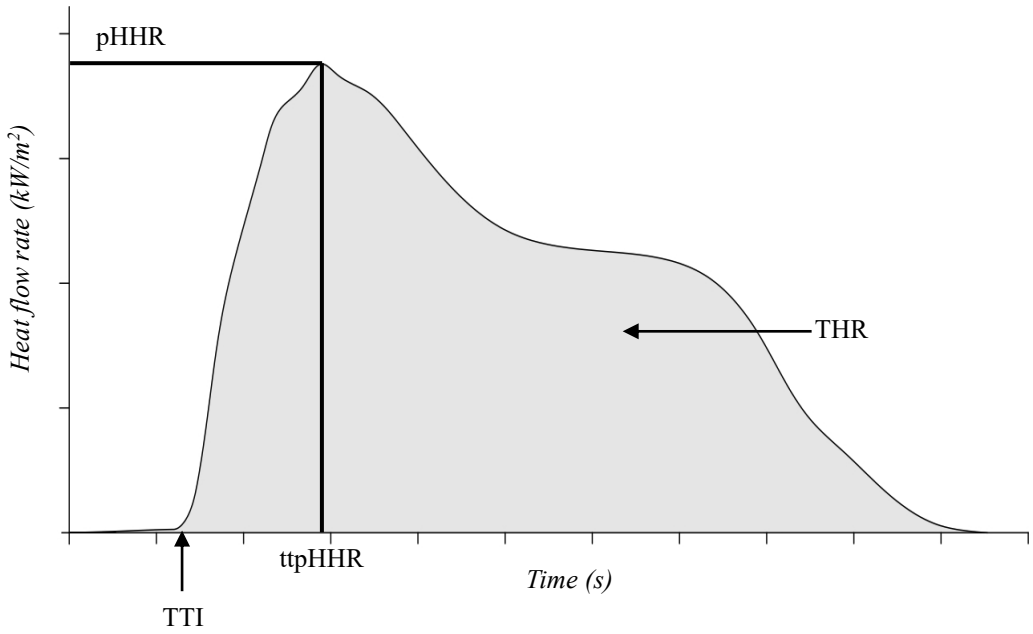

FIGURE 7: HEAT RELEASE RATE VS TIME CURVE AND VARIABLES USUALLY REPORTED

To simplify the interpretation of cone calorimeter data some derived parameters have been introduced as FIGRA, Fire Growth Rate, and MARHE, Maximum Average Rate of Heat Emission. These indices are considered derived parameters because are deduced from the

maximum HRR and are used for regulatory purposes. FIGRA is a parameter used to classify the fire properties of construction products and is defined as the growth of the burning intensity. It represents the maximum value of the function (heat release rate)/(elapsed test time) which is usually equal to the ratio of the pHRR to the time at peak occurrence and the unit is W/s. The higher the value of the index, the higher the fire risk, because it indicates a high pHRR value at a very low ignition time, so FIGRA represents a heat acceleration parameter [149].

On the other hand, the MARHE parameter is an important index as it is one of the requirements to be fulfilled by materials in the railway applications standard EN45545-2 and can be considered a good measure of the propensity to fire development under real scale conditions. It is determined by calculating the Average Rate of Heat Emission (ARHE), defined as the cumulative integral of heat emission divided by time, and its maximum value over the test period represents the MARHE. From the HRR values, the ARHE is calculated according to the following equation [217]:

$$ARHE\ (t_n) = \frac{\sum_2^n \left((t_n - t_{n-1}) \cdot \frac{q_n + q_{n-1}}{2} \right)}{t_n - t_0}$$

t_n: time, q_n: heat release rate at t_n

This parameter is selected because is not greatly affected by normal experimental variation or measurement noise and has proven to be a fairly robust measure of the propensity for fire development under real scale conditions. As well as the LOI, these indices try to concentrate the relevant information into a single number so they should be studied in conjunction with other parameters because it can be misleading [12].

5.4 MICROSCALE COMBUSTION CALORIMETRY

Micro-scale combustion calorimetry (MCC), also known as Pyrolysis-combustion flow calorimetry (PCFC), is a technique that reproduces solid and gas state phases of flaming combustion in a non-flaming test by controlled pyrolysis of the sample in an inert gas stream followed by high temperature oxidation of the volatile pyrolysis products [218]. One of the advantages of this test is that allows the measurement of heat release capacity and other parameters of milligram scale samples. As in cone calorimetry, the oxygen consumption method is used for the determination of the heat of combustion of the pyrolysis products.

The sample is placed in an inert, heat resistant crucible and heated under a controlled temperature programme in an inert atmosphere. The sample is pyrolyzed and the decomposition gases rise to the combustor section, where are burnt with the oxygen (Figure 8). Therefore, MCC

reproduces the chemical processes of polymeric materials in the solid phase state in the pyrolysis section and the gas phase state in the combustor section. Next, the flow meter and O_2 analyser record the flow rate and the oxygen concentration during the burning process to calculate then the specific heat release as a function of the temperature. The peak of the specific heat release and the temperature of the peak are also reported for their usefulness in assessing the fire behaviour of materials. Also curve fitting software can be applied to calculate the heat release capacity and total heat release.

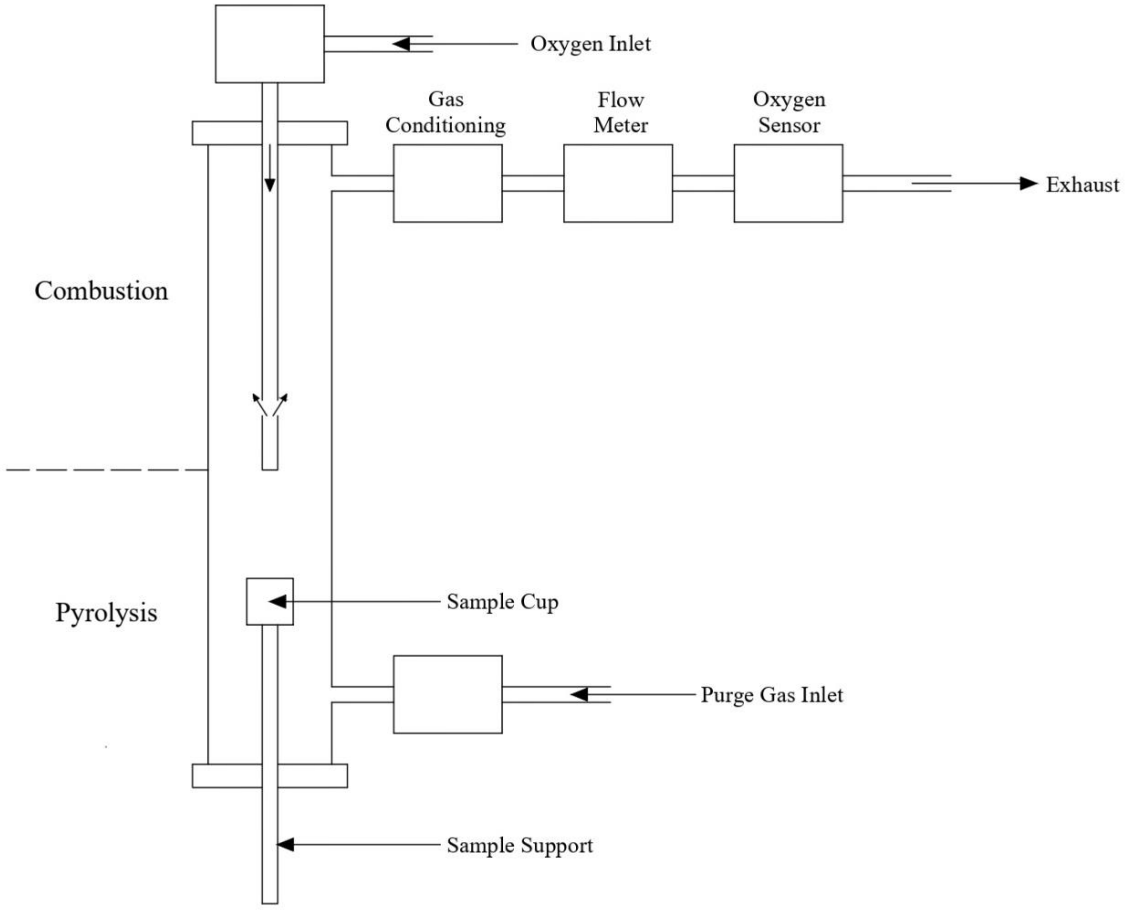

FIGURE 8: MICROSCALE COMBUSTION CALORIMETY SCHEME

MCC is a valuable technique thanks to its effective design, relatively low cost, sample size and ease of use. However, it has some limitations because it does not consider physical phenomena such as melting, dripping, shrinking, etc. and does not cover all flammability aspects like smoke release, so it needs to be used in combination with other tests [219].

5.5 TEXTILES

To study the fire behaviour of textiles, there is a wide variety of tests depending on their application. In this case, it is going to be used as a composite reinforcement, so the test to be

carried out should provide information about the flammability of the fabric and allow to compare the effect of the different treatments. The test that has been carried out is an ignitability test in accordance with UNE-EN ISO 11925-2:2020. This standard is one of the tests used as part of the Euroclass, European reaction to fire classification of construction materials. This standard specifies a method for the determination of the ignitability of products by direct application of small flame, with zero radiation and using samples in vertical orientation.

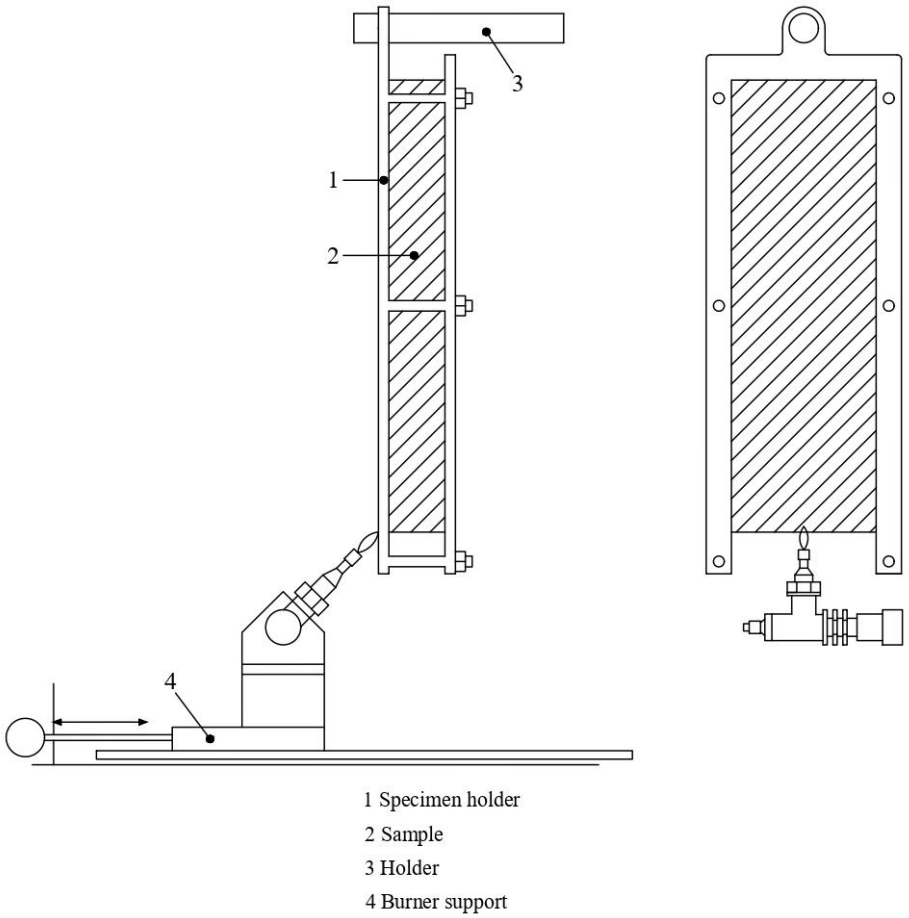

FIGURE 9: SCHEME OF UNE-EN-ISO 11925. SUPPORT AND BURNER POSITION [220]

The procedure and the equipment used are similar to the UL94 test. The test takes places inside a test chamber where the test specimen is mounted vertically (Figure 9). The test specimen is 250x90 mm and is subjected to edge and/or surface exposure from a small gas flame. The height of the flame is 20mm and is applied for 15 or 30 seconds. During the test, time of ignition, burning droplets and whether the flames reach the top marking of the test specimen within a prescribed time is registered. In this case, the results are used to make a comparison of the different treatments applied to natural fibres.

6. INDEX OF TABLES AND FIGURES

7. REFERENCES

1. Plastics Europe. Plastics - the Facts 2022. 2022.
2. Tiseo I. Global plastics industry - Statistics & Facts Statista [Internet]. 2021;Available from: https://www.statista.com/topics/5266/plastics-industry/#dossierKeyfigures
3. The Geneva Association. World Fire Statistics. 2014.
4. Brushlinsky NN, Ahrens M, Sokolov SV, Wagner P. World fire statistics. 2021.
5. Federal Aviation Administration. In-flight Fires. Advisory Circular. 2014.
6. Royal Aeronautical Society. Smoke, fire and fumes in transport aircraft: past history, current risks and recommended mitigation. 2018.
7. Uddin F. Flame-retardant fibrous materials in an aircraft. 2016.
8. Morgan AB, Gilman JW. An overview of flame retardancy of polymeric materials: application, technology, and future directions. Fire Mater 2013;37:259–79.
9. Károlyné P, Hugó M. Plastics : their behaviour in fires. Elsevier; 1991.
10. Laoutid F, Bonnaud L, Alexandre M, Lopez-Cuesta JM, Dubois Ph. New prospects in flame retardant polymer materials: From fundamentals to nanocomposites. Materials Science and Engineering: R: Reports 2009;63:100–25.
11. Dewaghe C, Lew CY, Claes M, Belgium SA, Dubois P. Fire-retardant applications of polymer–carbon nanotubes composites: improved barrier effect and synergism. In: Polymer–Carbon Nanotube Composites. Elsevier; 2011. page 718–45.
12. Schartel B, Hull TR. Development of fire-retarded materials - Interpretation of cone calorimeter data. Fire Mater 2007;31:327–54.
13. Kim Y, Lee S, Yoon H. Fire-Safe Polymer Composites: Flame-Retardant Effect of Nanofillers. Polymers (Basel) 2021;13:540.
14. Cortés D, Gil D, Azorín J, Vandecasteele F, Verstockt S. A Review of Modelling and Simulation Methods for Flashover Prediction in Confined Space Fires. Applied Sciences 2020;10:5609.
15. Buezas Sierra N. GUÍA: PLÁSTICOS Y FUEGO. Informe de Novedades Tecnológicas. 2010; Available from: http://www.observatorioplastico.com/ficheros/publicaciones/126155543Guia_plasticos_fuego_2010_encrip.pdf
16. Flameretardants-Online. Fire initiation and combustion process [Internet]. Available from: https://www.flameretardants-online.com/fires/fire-initiation
17. International Organization for Standardization. ISO 13943. Fire safety-vocabulary. 2018.
18. Hull TR, Law RJ, Bergman A. Chapter 4 - Environmental Drivers for Replacement of Halogenated Flame Retardants. In: Polymer Green Flame Retardants. Elsevier; 2014. page 119–79.

19. Shah AUR, Prabhakar MN, Song J Il. Current advances in the fire retardancy of natural fiber and bio-based composites – A review. International Journal of Precision Engineering and Manufacturing - Green Technology 2017;4:247–62.
20. Babrauskas V, Fuoco R, Blum A. Flame Retardant Additives in Polymers: When do the Fire Safety Benefits Outweigh the Toxicity Risks? [Internet]. Elsevier B.V.; 2014. Available from: http://dx.doi.org/10.1016/B978-0-444-53808-6.00003-2
21. Fábelová L, Loffredo CA, Klánová J, Hilscherová K, Horvat M, Tihányi J, et al. Environmental ototoxicants, a potential new class of chemical stressors. Environ Res 2019;171:378–94.
22. Routti H, Atwood TC, Bechshoft T, Boltunov A, Ciesielski TM, Desforges JP, et al. State of knowledge on current exposure, fate and potential health effects of contaminants in polar bears from the circumpolar Arctic. Science of The Total Environment [Internet] 2019;664:1063–83. Available from: https://doi.org/10.1016/j.scitotenv.2019.02.030
23. Chevrier J, Harley KG, Bradman A, Gharbi M, Sjödin A, Eskenazi B. Polybrominated Diphenyl Ether (PBDE) Flame Retardants and Thyroid Hormone during Pregnancy. Environ Health Perspect [Internet] 2010;118:1444–9. Available from: https://ehp.niehs.nih.gov/doi/10.1289/ehp.1001905
24. Harley KG, Marks AR, Chevrier J, Bradman A, Sjödin A, Eskenazi B. PBDE concentrations in women's serum and fecundability. Environ Health Perspect 2010;118:699–704.
25. Harley KG, Chevrier J, Schall RA, Sjödin A, Bradman A, Eskenazi B. Association of prenatal exposure to polybrominated diphenyl ethers and infant birth weight. Am J Epidemiol 2011;174:885–92.
26. Hendriks HS, Meijer M, Muilwijk M, van den Berg M, Westerink RHS. A comparison of the in vitro cyto- and neurotoxicity of brominated and halogen-free flame retardants: Prioritization in search for safe(r) alternatives. Arch Toxicol 2014;88:857–69.
27. Shaw SD, Blum A, Weber R, Kannan K, Rich D, Lucas D, et al. Halogenated flame retardants: Do the fire safety benefits justify the risks? Rev Environ Health 2010;25:261–305.
28. Molefe DM, Labuschagne J, Focke WW, van der Westhuizen I, Ofosu O. The effect of magnesium hydroxide, hydromagnesite and layered double hydroxide on the heat stability and fire performance of plasticized poly(vinyl chloride). J Fire Sci 2015;33:493–510.
29. Lenza J, Merkel K, Rydarowski H. Comparison of the effect of montmorillonite, magnesium hydroxide and a mixture of both on the flammability properties and mechanism of char formation of HDPE composites. Polym Degrad Stab 2012;97:2581–93.
30. Huo S, Song P, Yu B, Ran S, Chevali VS, Liu L, et al. Phosphorus-containing flame retardant epoxy thermosets: Recent advances and future perspectives. Prog Polym Sci 2021;114:101366.

31. Levchik S. Phosphorus-Based FRs. In: Non-Halogenated Flame Retardant Handbook. Hoboken, NJ, USA: John Wiley & Sons, Inc.; 2014. page 17–74.
32. Araby S, Philips B, Meng Q, Ma J, Laoui T, Wang CH. Recent advances in carbon-based nanomaterials for flame retardant polymers and composites. Compos B Eng 2021;212:108675.
33. Mazela B, Batista A, Grześkowiak W. Expandable Graphite as a Fire Retardant for Cellulosic Materials—A Review. Forests 2020;11:755.
34. Kiliaris P, Papaspyrides CD. Polymer/layered silicate (clay) nanocomposites: An overview of flame retardancy. Prog Polym Sci 2010;35:902–58.
35. Koedel J, Seibt S, Callsen C, Puchtler F, Weise M, Weidinger A, et al. DNA as a Natural Flame Retardant for Cellulose Acetate Polymer Mixtures. Chemistry Select 2021;6:3605–9.
36. Costes L, Laoutid F, Brohez S, Dubois P. Bio-based flame retardants: When nature meets fire protection. Materials Science and Engineering R: Reports [Internet] 2017;117:1–25. Available from: http://dx.doi.org/10.1016/j.mser.2017.04.001
37. Real Academia Española. Mineral [Internet]. Available from: https://dle.rae.es/mineral
38. Hull TR, Witkowski A, Hollingbery L. Fire retardant action of mineral fillers. Polym Degrad Stab 2011;96:1462–9.
39. Ceresana. Flame Retardants Market Report. 2022.
40. Sauerwein R. Mineral Filler Flame Retardants. In: Non-Halogenated Flame Retardant Handbook. Hoboken, NJ, USA: John Wiley & Sons, Inc.; 2014. page 75–141.
41. Rothon R, Hornsby P. Fire Retardant Fillers for Polymers. In: Polymer Green Flame Retardants. Elsevier; 2014. page 289–321.
42. Evans KA. Properties and uses of oxides and hydroxides. In: Downs AJ, editor. Chemistry of aluminium gallium, indium and thallium. Blackie Academic & Professional; 1993. page 248–91.
43. Krewski D, Yokel RA, Nieboer E, Borchelt D, Cohen J, Harry J, et al. Human Health Risk Assessment for Aluminium, Aluminium Oxide, and Aluminium Hydroxide. Journal of Toxicology and Environmental Health, Part B 2007;10:1–269.
44. Kool M, Soullié T, van Nimwegen M, Willart MAM, Muskens F, Jung S, et al. Alum adjuvant boosts adaptive immunity by inducing uric acid and activating inflammatory dendritic cells. Journal of Experimental Medicine 2008;205:869–82.
45. Farzad RH, Hassan A, Piah MAM, Jawaid M. Electrical and flammability properties of alumina trihydrate filled polypropylene/ethylene propylene diene monomer composites as insulators in cable applications. Polym Eng Sci 2014;54:493–8.
46. Parida MR, Mohanty S, Biswal M, Nayak SK, Rai S. Influence of aluminum trihydrate (ATH) particle size on mechanical, thermal, flame retardancy and combustion behavior of polypropylene composites. J Therm Anal Calorim 2023;148:807–19.

47. El-Sabbagh A, Steuernagel L, Meiners D, Ziegmann G, Toepfer O. Optimization of Flame Retardant Content with Respect to Mechanical Properties of Natural Fiber Polymer Composites: Case Study of Polypropylene/Flax/Aluminum Trihydroxide. Polym Compos 2016;37:3310–25.
48. Witkowski A, Stec AA, Richard Hull T. The influence of metal hydroxide fire retardants and nanoclay on the thermal decomposition of EVA. Polym Degrad Stab 2012;97:2231–40.
49. Hoffendahl C, Fontaine G, Duquesne S, Taschner F, Mezger M, Bourbigot S. The combination of aluminum trihydroxide (ATH) and melamine borate (MB) as fire retardant additives for elastomeric ethylene vinyl acetate (EVA). Polym Degrad Stab 2015;115:77–88.
50. Xu Z sheng, Yan L, Chen L. Synergistic Flame Retardant Effects between Aluminum Hydroxide and Halogen-free Flame Retardants in High Density Polyethylene Composites. Procedia Eng 2016;135:631–6.
51. Pan Y, Han L, Guo Z, Fang Z. Improving the flame-retardant efficiency of aluminum hydroxide with fullerene for high-density polyethylene. J Appl Polym Sci 2017;134.
52. Yan-hui Z, Zhi-wen Q, Zi-hao C, Ya-lan L. Study on Flame Retardant of Environmentally Friendly HDPE Sheath Material. J Phys Conf Ser 2021;1965:012095.
53. Almeida Pinto U, Visconte LLY, Gallo J, Nunes RCR. Flame retardancy in thermoplastic polyurethane elastomers (TPU) with mica and aluminum trihydrate (ATH). Polym Degrad Stab 2000;69:257–60.
54. Sabaruddin FA, Samat N. Effect of Coupling Agent on the Mechanical Properties of Flame Retardant PP/ATH Nanocomposites. Adv Mat Res 2013;812:241–5.
55. Ramazani SAA, Rahimi A, Frounchi M, Radman S. Investigation of flame retardancy and physical–mechanical properties of zinc borate and aluminum hydroxide propylene composites. Mater Des 2008;29:1051–6.
56. Sabaruddin FA, Samat N, Habibah AIHD. The Effects of Coupling Agent on the Flame Retardant Properties of PP/ATH Nanocomposites. Adv Mat Res 2015;1115:406–9.
57. Mohammadi M, Khodamorady M, Tahmasbi B, Bahrami K, Ghorbani-Choghamarani A. Boehmite nanoparticles as versatile support for organic–inorganic hybrid materials: Synthesis, functionalization, and applications in eco-friendly catalysis. Journal of Industrial and Engineering Chemistry 2021;97:1–78.
58. El Hage R, Viretto A, Sonnier R, Ferry L, Lopez-Cuesta JM. Flame retardancy of ethylene vinyl acetate (EVA) using new aluminum-based fillers. Polym Degrad Stab 2014;108:56–67.
59. Li X, Fang S. Effect of Boehmite and Vermiculite on Flame Retardancy and Mechanical Properties of PET. Polymer Korea 2022;46:463–9.
60. Li X. Influence of melamine cyanurate and boehmite on flame retardancy of PA6. Iranian Polymer Journal 2022;31:975–81.

61. Camino G, Maffezzoli A, Braglia M, De Lazzaro M, Zammarano M. Effect of hydroxides and hydroxycarbonate structure on fire retardant effectiveness and mechanical properties in ethylene-vinyl acetate copolymer. Polym Degrad Stab 2001;74:457–64.
62. Karger-Kocsis J, Lendvai L. Polymer/boehmite nanocomposites: A review. J Appl Polym Sci 2018;135:45573.
63. Droval G, Aranberri I, Ballestero J, Verelst M, Dexpert-Ghys J. Synthesis and characterization of thermoplastic composites filled with γ-boehmite for fire resistance. Fire Mater 2011;35:491–504.
64. Monti M, Camino G. Thermal and combustion behavior of polyethersulfone-boehmite nanocomposites. Polym Degrad Stab 2013;98:1838–46.
65. Zhang J, Ji Q, Zhang P, Xia Y, Kong Q. Thermal stability and flame-retardancy mechanism of poly(ethylene terephthalate)/boehmite nanocomposites. Polym Degrad Stab 2010;95:1211–8.
66. Laachachi A, Ferriol M, Cochez M, Lopez Cuesta JM, Ruch D. A comparison of the role of boehmite (AlOOH) and alumina (Al2O3) in the thermal stability and flammability of poly(methyl methacrylate). Polym Degrad Stab 2009;94:1373–8.
67. Cai Y, Zhao M, Wang H, Li Y, Zhao Z. Synthesis and properties of flame-retardant poly(vinyl alcohol)/pseudo-boehmite nanocomposites with high transparency and enhanced refractive index. Polym Degrad Stab 2014;99:53–60.
68. Borm PJ, Robbins D, Haubold S, Kuhlbusch T, Fissan H, Donaldson K, et al. The potential risks of nanomaterials: a review carried out for ECETOC. Part Fibre Toxicol 2006;3:11.
69. Pilarska AA, Klapiszewski Ł, Jesionowski T. Recent development in the synthesis, modification and application of Mg(OH)2 and MgO: A review. Powder Technol 2017;319:373–407.
70. Ropp RC. Group 16 (O, S, Se, Te) Alkaline Earth Compounds. In: Encyclopedia of the Alkaline Earth Compounds. Elsevier; 2013. page 105–97.
71. Liu SP. Flame retardant and mechanical properties of polyethylene/magnesium hydroxide/montmorillonite nanocomposites. Journal of Industrial and Engineering Chemistry 2014;20:2401–8.
72. Liu R, Xia W, Otitoju TA, Wu W, Wang S, Li S, et al. Effect of oleic acid on improving flame retardancy of brucite in low-density polyethylene composite. J Appl Polym Sci 2022;139:51862.
73. Lim HM, Yun J, Hyun M, Yoon Y, Lee DJ, Whang CM, et al. Magnesium hydroxide flame retardant and its application to a low-density polyethylene/ethylene vinyl acetate composite. Journal of Ceramic Processing Research 2009;10:571–6.

74. Ma Y, Chen M, Liu N, Dang P, Xu Y, Chen X, et al. Combustion characteristics and thermal properties of high-density polyethylene/ethylene vinyl-acetate copolymer blends containing magnesium hydroxide. Journal of Thermoplastic Composite Materials 2017;30:1393–413.
75. Peng H, Zhao W, Wang Y. Aluminum phosphate modified brucite and its flame retardant and smoke suppression performance on ethylene-vinyl acetate resin. Polym Adv Technol 2021;32:142–52.
76. Chen W, Li H, Li L, Wang X. Reinforcing Condensed Phase Flame Retardancy through Surface Migration of Brucite@Zinc Borate-Incorporated Systems. ACS Omega 2020;5:28186–95.
77. Qiu L, Xie R, Ding P, Qu B. Preparation and characterization of Mg(OH)2 nanoparticles and flame-retardant property of its nanocomposites with EVA. Compos Struct 2003;62:391–5.
78. Chen X, Yu J, Guo S, Lu S, Luo Z, He M. Surface modification of magnesium hydroxide and its application in flame retardant polypropylene composites. J Mater Sci 2009;44:1324–32.
79. Pilarska A, Bula K, Myszka K, Rozmanowski T, Szwarc-Rzepka K, Pilarski K, et al. Functional polypropylene composites filled with ultra-fine magnesium hydroxide. Open Chem 2015;13.
80. Yang Y, Niu M, Dai J, Bai J, Xue B, Song Y, et al. Flame-retarded polyethylene terephthalate with carbon microspheres/magnesium hydroxide compound flame retardant. Fire Mater 2018;42:794–804.
81. Genovese A, Shanks RA. Structural and thermal interpretation of the synergy and interactions between the fire retardants magnesium hydroxide and zinc borate. Polym Degrad Stab 2007;92:2–13.
82. Hollingbery LA, Hull TR. The fire retardant effects of huntite in natural mixtures with hydromagnesite. Polym Degrad Stab 2012;97:504–12.
83. Hollingbery LA, Hull TR. The fire retardant behaviour of huntite and hydromagnesite - A review. Polym Degrad Stab 2010;95:2213–25.
84. Terzi E, Kartal SN, Pişkin S, Stark N, Kantürk Figen A, White RH. Colemanite: A Fire Retardant Candidate for Wood Plastic Composites. Bioresources 2018;13.
85. Kaynak C, Isitman NA. Synergistic fire retardancy of colemanite, a natural hydrated calcium borate, in high-impact polystyrene containing brominated epoxy and antimony oxide. Polym Degrad Stab 2011;96:798–807.
86. Cavodeau F, Viretto A, Otazaghine B, Lopez-Cuesta JM, Delaite C. Influence of colemanite on the fire retardancy of ethylene-vinyl acetate and ethylene-methyl acrylate copolymers. Polym Degrad Stab 2017;144:401–10.
87. Waclawska I, Stoch L, Paulik J, Paulik F. Thermal decomposition of colemanite. Thermochim Acta 1988;126:307–18.

88. Galwey AK. Structure and order in thermal dehydrations of crystalline solids. Thermochim Acta 2000;355:181–238.
89. Bilici İ. The Effect of Colemanite on Thermal Properties of Recycled Polyethylene. Acta Phys Pol A 2019;135:922–4.
90. Ning Y, Guo S. Flame-retardant and smoke-suppressant properties of zinc borate and aluminum trihydrate-filled rigid PVC. J Appl Polym Sci 2000;77:3119–27.
91. Pi H, Guo S, Ning Y. Mechanochemical improvement of the flame-retardant and mechanical properties of zinc borate and zinc borate-aluminum trihydrate-filled poly(vinyl chloride). J Appl Polym Sci 2003;89:753–62.
92. Isitman NA, Kaynak C. Effect of partial substitution of aluminum hydroxide with colemanite in fire retarded low-density polyethylene. J Fire Sci 2013;31:73–84.
93. Zhang X, Wang Z, Liu H. Preparation and properties of zeolite/brucite/polypropylene composite fire retardant materials-cobalt. In: 2nd International Conference on Material Engineering and Application. 2015.
94. Liu Z, Zhang Y, Li N, Wen X, Nogales LA, Li L, et al. Study of nanocarbon black as synergist on improving flame retardancy of ethylene-vinyl acetate/brucite composites. J Therm Anal Calorim 2019;136:601–8.
95. Zhang A, Zhang Y, Lv F, Chu PK. Synergistic effects of hydroxides and dimethyl methylphosphonate on rigid halogen-free and flame-retarding polyurethane foams. J Appl Polym Sci 2013;128:347–53.
96. Camino G, Duquesne S, Delobel R, Eling B, Lindsay C, Roels T. Mechanism of Expandable Graphite Fire Retardant Action in Polyurethanes. 2001. page 90–109.
97. Wang X, Kalali EN, Wan JT, Wang DY. Carbon-family materials for flame retardant polymeric materials. Prog Polym Sci 2017;69:22–46.
98. Focke WW, Badenhorst H, Mhike W, Kruger HJ, Lombaard D. Characterization of commercial expandable graphite fire retardants. Thermochim Acta 2014;584:8–16.
99. Chung DDL. Exfoliation of graphite. J Mater Sci 1987;22:4190–8.
100. Focke WW, Muiambo H, Mhike W, Kruger HJ, Ofosu O. Flexible PVC flame retarded with expandable graphite. Polym Degrad Stab 2014;100:63–9.
101. Zhu H, Zhu Q, Li J, Tao K, Xue L, Yan Q. Synergistic effect between expandable graphite and ammonium polyphosphate on flame retarded polylactide. Polym Degrad Stab 2011;96:183–9.
102. Xie R, Qu B. Synergistic effects of expandable graphite with some halogen-free flame retardants in polyolefin blends. Polym Degrad Stab 2001;71:375–80.
103. Oulmou F, Benhamida A, Dorigato A, Sola A, Messori M, Pegoretti A. Effect of expandable and expanded graphites on the thermo-mechanical properties of polyamide 11. Journal of Elastomers & Plastics 2019;51:175–90.

104. Khalili P, Tshai KY, Kong I. Natural fiber reinforced expandable graphite filled composites: Evaluation of the flame retardancy, thermal and mechanical performances. Compos Part A Appl Sci Manuf 2017;100.
105. Chen X, Wu H, Luo Z, Yang B, Guo S, Yu J. Synergistic effects of expandable graphite with magnesium hydroxide on the flame retardancy and thermal properties of polypropylene. Polym Eng Sci 2007;47:1756–60.
106. Chen X, Yu J, Lu S, Wu H, Guo S, Luo Z. Combustion Characteristics of Polypropylene/Magnesium Hydroxide/Expandable Graphite Composites. Journal of Macromolecular Science, Part B 2009;48:1081–92.
107. Li Z, Qu B. Flammability characterization and synergistic effects of expandable graphite with magnesium hydroxide in halogen-free flame-retardant EVA blends. Polym Degrad Stab 2003;81:401–8.
108. Jeong SH, Park CH, Song H, Heo JH, Lee JH. Biomolecules as green flame retardants: Recent progress, challenges, and opportunities. J Clean Prod 2022;368:133241.
109. Agbor VB, Cicek N, Sparling R, Berlin A, Levin DB. Biomass pretreatment: Fundamentals toward application. Biotechnol Adv 2011;29:675–85.
110. Mngomezulu ME, John MJ, Jacobs V, Luyt AS. Review on flammability of biofibres and biocomposites. Carbohydr Polym 2014;111:149–82.
111. Vanholme R, Demedts B, Morreel K, Ralph J, Boerjan W. Lignin Biosynthesis and Structure. Plant Physiol 2010;153:895–905.
112. Ferdous D, Dalai AK, Bej SK, Thring RW. Pyrolysis of lignins: Experimental and kinetics studies. Energy and Fuels 2002;16:1405–12.
113. Zhao J, Xiuwen W, Hu J, Liu Q, Shen D, Xiao R. Thermal degradation of softwood lignin and hardwood lignin by TG-FTIR and Py-GC/MS. Polym Degrad Stab 2014;108:133–8.
114. Canan C, Cruz FTL, Delaroza F, Casagrande R, Sarmento CPM, Shimokomaki M, et al. Studies on the extraction and purification of phytic acid from rice bran. Journal of Food Composition and Analysis 2011;24:1057–63.
115. Zheng Z, Liu Y, Dai B, Meng C, Guo Z. Fabrication of cellulose-based halogen-free flame retardant and its synergistic effect with expandable graphite in polypropylene. Carbohydr Polym 2019;213:257–65.
116. Bajwa DS, Rehovsky C, Shojaeiarani J, Stark N, Bajwa S, Dietenberger MA. Functionalized Cellulose Nanocrystals: A Potential Fire Retardant for Polymer Composites. Polymers (Basel) 2019;11:1361.
117. Yu Y, Fu S, Song P, Luo X, Jin Y, Lu F, et al. Functionalized lignin by grafting phosphorus-nitrogen improves the thermal stability and flame retardancy of polypropylene. Polym Degrad Stab 2012;97:541–6.

118. De Chirico A, Armanini M, Chini P, Cioccolo G, Provasoli F, Audisio G. Flame retardants for polypropylene based on lignin. Polym Degrad Stab 2003;79:139–45.
119. Song P, Cao Z, Fu S, Fang Z, Wu Q, Ye J. Thermal degradation and flame retardancy properties of ABS/lignin: Effects of lignin content and reactive compatibilization. Thermochim Acta 2011;518:59–65.
120. Laoutid F, Duriez V, Brison L, Aouadi S, Vahabi H, Dubois P. Synergistic flame-retardant effect between lignin and magnesium hydroxide in poly(ethylene-co-vinyl acetate). Flame Retardancy and Thermal Stability of Materials 2019;2:9–18.
121. Zhang T, Yan H, Shen L, Fang Z, Zhang X, Wang J, et al. A phosphorus-, nitrogen- and carbon-containing polyelectrolyte complex: preparation, characterization and its flame retardant performance on polypropylene. RSC Adv. 2014;4:48285–92.
122. Alongi J, Blasio A Di, Cuttica F, Carosio F, Malucelli G. Bulk or surface treatments of ethylene vinyl acetate copolymers with DNA: Investigation on the flame retardant properties. Eur Polym J 2014;51:112–9.
123. European Bioplastics. Bioplastics facts and figures. 2022.
124. Kongkraireug N, Chuayjuljit S, Chaiwutthinan P, Larpkasemsuk A, Boonmahitthisud A. Use of Magnesium Hydroxide as Flame Retardant in Poly(Lactic Acid)/High Impact Polystyrene/Wood Flour Composites. Key Eng Mater 2018;773:311–5.
125. Yanagisawa T, Kiuchi Y, Iji M. Enhanced Flame Retardancy of Polylactic Acid with Aluminum Tri-Hydroxide and Phenolic Resins. Kōbunshi Rombun Shū 2009;66:49–54.
126. Cao Y, Ju Y, Liao F, Jin X, Dai X, Li J, et al. Improving the flame retardancy and mechanical properties of poly(lactic acid) with a novel nanorod-shaped hybrid flame retardant. RSC Adv 2016;6:14852–8.
127. Erdem A, Dogan M. Production and Characterization of Green Flame Retardant Poly(lactic acid) Composites. J Polym Environ 2020;28:2837–50.
128. Costes L, Laoutid F, Khelifa F, Rose G, Brohez S, Delvosalle C, et al. Cellulose/phosphorus combinations for sustainable fire retarded polylactide. Eur Polym J 2016;74:218–28.
129. Yin W, Chen L, Lu F, Song P, Dai J, Meng L. Mechanically Robust, Flame-Retardant Poly(lactic acid) Biocomposites via Combining Cellulose Nanofibers and Ammonium Polyphosphate. ACS Omega 2018;3:5615–26.
130. Zhang R, Xiao X, Tai Q, Huang H, Hu Y. Modification of lignin and its application as char agent in intumescent flame-retardant poly(lactic acid). Polym Eng Sci 2012;52:2620–6.
131. Costes L, Laoutid F, Aguedo M, Richel A, Brohez S, Delvosalle C, et al. Phosphorus and nitrogen derivatization as efficient route for improvement of lignin flame retardant action in PLA. Eur Polym J 2016;84:652–67.

132. Ferry L, Dorez G, Taguet A, Otazaghine B, Lopez-Cuesta JM. Chemical modification of lignin by phosphorus molecules to improve the fire behavior of polybutylene succinate. Polym Degrad Stab 2015;113:135–43.
133. Laoutid F, Karaseva V, Costes L, Brohez S, Mincheva R, Dubois P. Novel Bio-based Flame Retardant Systems Derived from Tannic Acid. J Renew Mater 2018;6:559–72.
134. Chen S, Wu F, Hu Y, Lin S, Yu C, Zhu F, et al. A fully bio-based intumescent flame retardant for poly(butylene succinate). Mater Chem Phys 2020;252:123222.
135. Faruk O, Bledzki AK, Fink HP, Sain M. Biocomposites reinforced with natural fibers: 2000-2010. Prog Polym Sci 2012;37:1552–96.
136. Mohammed L, Ansari MNM, Pua G, Jawaid M, Islam MS. A Review on Natural Fiber Reinforced Polymer Composite and Its Applications. Int J Polym Sci 2015;2015:1–15.
137. Data Bridge Market Research. Global Natural Fibers Market - Industry Trends and Forecast to 2029 [Internet]. 2022 [cited 2022 Aug 28]. Available from: https://www.databridgemarketresearch.com/reports/global-natural-fibers-market
138. El-Sabbagh A, Attia T, Ramzy A, Steuernagel L, Ziegmann G. Towards selection chart of flame retardants for natural fibre reinforced polypropylene composites. Compos B Eng [Internet] 2018;141:1–8. Available from: https://doi.org/10.1016/j.compositesb.2017.12.020
139. Horrocks AR. An Introduction to the Burning Behaviour of Cellulosic Fibres. Journal of the Society of Dyers and Colourists 2008;99:191–7.
140. Chapple S, Anandjiwala R. Flammability of natural fiber-reinforced composites and strategies for fire retardancy: A review. Journal of Thermoplastic Composite Materials 2010;23:871–93.
141. Galaska ML, Horrocks AR, Morgan AB. Flammability of natural plant and animal fibers: a heat release survey. Fire Mater 2017;41:275–88.
142. Kozłowski R, Władyka-Przybylak M. Flammability and fire resistance of composites reinforced by natural fibers. Polym Adv Technol [Internet] 2008;19:446–53. Available from: https://onlinelibrary.wiley.com/doi/abs/10.1002/pat.1135
143. Chai MW, Bickerton S, Bhattacharyya D, Das R. Influence of natural fibre reinforcements on the flammability of bio-derived composite materials. Compos B Eng 2012;43:2867–74.
144. Mouritz AP, Gibson AG. Fire Properties of Polymer Composite Materials. Springer; 2007.
145. Arao Y, Nakamura S, Tomita Y, Takakuwa K, Umemura T, Tanaka T. Improvement on fire retardancy of wood flour/polypropylene composites using various fire retardants. Polym Degrad Stab 2014;100:79–85.
146. Kandola BK. Chapter 5. Flame Retardant Characteristics of Natural Fibre Composites. 2012. page 86–117.
147. Zaikov GE, Lomakin SM. Ecological issue of polymer flame retardancy. J Appl Polym Sci 2002;86:2449–62.

148. Malucelli G. Biomacromolecules and bio-sourced products for the design of flame retarded fabrics: Current state of the art and future perspectives. Molecules2019;24.
149. Kozłowski RM, Muzyczek M. Improving the flame retardancy of natural fibres [Internet]. In: Handbook of Natural Fibres. Elsevier; 2020. page 355–91.Available from: https://linkinghub.elsevier.com/retrieve/pii/B9780128187821000109
150. Basak S, Ali SW. Fire-resistant behavior of cellulosic textile material functionalized with biomolecules. In: Advances in Functional and Protective Textiles. Elsevier; 2020. page 63–80.
151. Research and Markets. Global Textile Flame Retardants Market (2022 to 2030) - Size, Share & Trends Analysis Report. 2022.
152. Alongi J, Malucelli G. Cotton flame retardancy: state of the art and future perspectives. RSC Adv 2015;5:24239–63.
153. Wang D, Zhong L, Zhang C, Zhang F, Zhang G. A novel reactive phosphorous flame retardant for cotton fabrics with durable flame retardancy and high whiteness due to self-buffering. Cellulose 2018;25:5479–97.
154. Yang Z, Wang X, Lei D, Fei B, Xin JH. A durable flame retardant for cellulosic fabrics. Polym Degrad Stab 2012;97:2467–72.
155. Szolnoki B, Bocz K, Sóti PL, Bodzay B, Zimonyi E, Toldy A, et al. Development of natural fibre reinforced flame retarded epoxy resin composites. Polym Degrad Stab 2015;119:68–76.
156. Maksym L, Prabhakar MN, Jung-il S. Preparation of a novel bio-flame-retardant liquid for flame retardancy of natural fibers and their composites. Journal of Industrial Textiles 2022;51:7153S-7171S.
157. Gaan S, Sun G. Effect of phosphorus and nitrogen on flame retardant cellulose: A study of phosphorus compounds. J Anal Appl Pyrolysis 2007;78:371–7.
158. Gaan S, Sun G. Effect of phosphorus flame retardants on thermo-oxidative decomposition of cotton. Polym Degrad Stab 2007;92:968–74.
159. Gaan S, Sun G, Hutches K, Engelhard MH. Effect of nitrogen additives on flame retardant action of tributyl phosphate: Phosphorus–nitrogen synergism. Polym Degrad Stab 2008;93:99–108.
160. Liao Y, Chen Y, Zhang F. A biological reactive flame retardant for flame retardant modification of cotton fabric. Colloids Surf A Physicochem Eng Asp 2021;630:127601.
161. Chen Y, Liao Y, Wan C, Zhang G, Zhang F. Synthesis of a novel P-N reactive ammonium phosphate-based flame retardant for durable finishing of cotton fabric. Colloids Surf A Physicochem Eng Asp 2022;634:127967.
162. Zhang F, Gao W, Jia Y, Lu Y, Zhang G. A concise water-solvent synthesis of highly effective, durable, and eco-friendly flame-retardant coating on cotton fabrics. Carbohydr Polym 2018;199:256–65.

163. Luo X, Li Z, Shen J, Liu L, Chen H, Hu Z, et al. A facile strategy to achieve efficient flame-retardant cotton fabric with durable and restorable fire resistance. Chemical Engineering Journal 2022;430:132854.
164. Li S, Zhong L, Huang S, Wang D, Zhang F, Zhang G. A novel flame retardant with reactive ammonium phosphate groups and polymerizing ability for preparing durable flame retardant and stiff cotton fabric. Polym Degrad Stab 2019;164:145–56.
165. Weil ED, Levchik S v. Flame Retardants in Commercial Use or Development for Textiles. J Fire Sci 2008;26:243–81.
166. LeVan SL, Tran HC. The role of boron in flame retardant treatments. In: 1st International conference on wood protection with diffusible preservatives. Nashville, Tennessee: Forest Products Research Society; 1990. page 39–41.
167. Wang Q, Li J, Winandy JerroldE. Chemical mechanism of fire retardance of boric acid on wood. Wood Sci Technol 2004;38.
168. Ozcifci A, Toker H, Baysal E. Fire properties of laminated veneer lumber treated with some fire retardants. Wood Research 2007;52:37–46.
169. Nagieb ZA, Nassar MA, El-Meligy MG. Effect of Addition of Boric Acid and Borax of Fire-Retardant and Mechanical Properties of Urea Formaldehyde Saw Dust Composites. International Journal of Carbohydrate Chemistry 2011.
170. Pedieu R, Koubaa A, Riedl B, Wang XM, Deng J. Fire-retardant properties of wood particleboards treated with boric acid. European Journal of Wood and Wood Products 2012;70:191–7.
171. Rejeesh CR, Saju KK. Effect of chemical treatment on fire-retardant properties of medium density coir fiber boards Machining Simulation using CATIA V5 View project. Wood and Fiber Science [Internet] 2017;49:332–7. Available from: https://www.researchgate.net/publication/316455732
172. Yu L, Cai J, Li H, Lu F, Qin D, Fei B. Effects of Boric Acid and/or Borax Treatments on the Fire Resistance of Bamboo Filament. Bioresources 2017;12.
173. Xie Y, Hill CAS, Xiao Z, Militz H, Mai C. Silane coupling agents used for natural fiber/polymer composites: A review. Compos Part A Appl Sci Manuf 2010;41:806–19.
174. Sajna VP, Mohanty S, Nayak SK. A study on thermal degradation kinetics and flammability properties of poly(lactic acid)/banana fiber/nanoclay hybrid bionanocomposites. Polym Compos 2017;38:2067–79.
175. Samyn F, Murariu O, Bonnaud L, Duquesne S. Preparation and flame retardancy of flax fabric/polybenzoxazine laminates. Fire Mater 2021;45:366–78.
176. Członka S, Strąkowska A, Pospiech P, Strzelec K. Effects of Chemically Treated Eucalyptus Fibers on Mechanical, Thermal and Insulating Properties of Polyurethane Composite Foams. Materials 2020;13:1781.

177. Basak S, Samanta KK. Thermal behaviour and the cone calorimetric analysis of the jute fabric treated in different pH condition. J Therm Anal Calorim 2019;135:3095–105.
178. Ortega Z, Benítez AN, Monzón MD, Hernández PM, Angulo I, Marrero MD. Study of Banana Fiber as Reinforcement of Polyethylene Samples Made by Compression and Injection Molding. J Biobased Mater Bioenergy 2010;4:114–20.
179. Basak S, Ali SW. Sustainable fire retardancy of textiles using bio-macromolecules. Polym Degrad Stab 2016;133:47–64.
180. Basak S, Samanta KK, Chattopadhyay SK, Narkar RS, Mahangade R. Flame retardant cellulosic textile using banana pseudostem sap. International Journal of Clothing Science and Technology 2015;27:247–61.
181. Basak S, Samanta KartickK, Saxena S, Chattopadhyay SK, Narkar R, Mahangade R, et al. Flame resistant cellulosic substrate using banana pseudostem sap. Polish Journal of Chemical Technology 2015;17:123–33.
182. Basak S, Samanta KK, Chattopadhyay SK, Narkar R. Self-extinguishable ligno-cellulosic fabric using banana pseudostem sap. 2015.
183. Basak S, Saxena S, Chattopadhyay S, Narkar R, Mahangade R. Banana pseudostem sap: A waste plant resource for making thermally stable cellulosic substrate. Journal of Industrial Textiles 2016;46:1003–23.
184. Basak S, Samanta KK, Chattopadhyay SK, Narkar R. Thermally stable cellulosic paper made using banana pseudostem sap, a wasted by-product. Cellulose 2015;22:2767–76.
185. Kambli ND, Samanta KK, Basak S, Chattopadhyay SK, Patil PG, Deshmukh RR. Characterization of the corn husk fibre and improvement in its thermal stability by banana pseudostem sap. Cellulose 2018;25:5241–57.
186. Basak S, Samanta KK, Chattopadhyay SK, Saxena S, Narkar & R. Banana pseudostem sap and boric acid-A new green intumescent for making self-extinguishing cotton fabric. 2018.
187. Horrocks AR. Flame retardant/resistant textile coatings and laminates. In: Advances in Fire Retardant Materials. Elsevier; 2008. page 159–87.
188. Park CY, Choi CH, Lee JH, Kim S, Park KW, Cho JH. Evaluation of formaldehyde emission and combustion behaviour of wood based composite subjected to different surface finishing method. Bioresources 2013;8:5515–23.
189. Kong F, Nie B, Han C, Zhao D, Hou Y, Xu Y. Flame Retardancy and Thermal Property of Environment-Friendly Poly(lactic acid) Composites Based on Banana Peel Powder. Materials 2022;15:5977.
190. Kong F bei, He Q lin, Peng W, Nie S bin, Dong X, Yang J nian. Eco-friendly flame retardant poly(lactic acid) composites based on banana peel powders and phytic acid: flame retardancy and thermal property. Journal of Polymer Research 2020;27:204.

191. Basak S, Wazed Ali S. Fire resistant behaviour of cellulosic textile functionalized with wastage plant bio-molecules: A comparative scientific report. Int J Biol Macromol 2018;114:169–80.
192. Mo Y, Ma J, Gao W, Zhang L, Li J, Li J, et al. Pomegranate Peel as a Source of Bioactive Compounds: A Mini Review on Their Physiological Functions. Front Nutr 2022;9.
193. Basak S, Ali SW. Leveraging flame retardant efficacy of pomegranate rind extract, a novel biomolecule, on ligno-cellulosic materials. Polym Degrad Stab 2017;144:83–92.
194. Basak S, Wazed Ali S. Wastage pomegranate rind extracts (PRE): a one step green solution for bioactive and naturally dyed cotton substrate with special emphasis on its fire protection efficacy. Cellulose 2019;26:3601–23.
195. Basak S, Ali SW. Sodium tri-polyphosphate in combination with pomegranate rind extracts as a novel fire-retardant composition for cellulosic polymer. J Therm Anal Calorim 2019;137:1233–47.
196. Basak S, Ali SW. Sodium Lignin Sulfonate (SLS) and Pomegranate Rind Extracts (PRE) Bio-macro-molecule: A Novel Composition for Making Fire Resistant Cellulose Polymer. Combustion Science and Technology 2022;194:3206–24.
197. Ayrilmis N, Jarusombuti S, Fueangvivat V, Bauchongkol P, White RH. Coir fiber reinforced polypropylene composite panel for automotive interior applications. Fibers and Polymers 2011;12:919–26.
198. Teli MD, Pandit P, Basak S. Coconut shell extract imparting multifunction properties to ligno-cellulosic material. Journal of Industrial Textiles 2018;47:1261–90.
199. Teli M, Pandit P. Development of thermally stable and hygienic colored cotton fabric made by treatment with natural coconut shell extract. Journal of Industrial Textiles 2018;48:87–118.
200. Basak S, Ali SW. Fire-resistant behavior of cellulosic textile material functionalized with biomolecules. In: Advances in Functional and Protective Textiles. Elsevier; 2020. page 63–80.
201. Basak S, Patil PG, Shaikh AJ, Samanta KK. Green coconut shell extract and boric acid: new formulation for making thermally stable cellulosic paper. Journal of Chemical Technology & Biotechnology 2016;91:2871–81.
202. Basak S, Samanta KK, Chattopadhyay SK. Fire retardant property of cotton fabric treated with herbal extract. The Journal of The Textile Institute 2015;106:1338–47.
203. Lomnitski L, Bergman M, Nyska A, Ben-Shaul V, Grossman S. Composition, Efficacy, and Safety of Spinach Extracts. Nutr Cancer 2003;46:222–31.
204. Basak S, Samanta KK, Saxena S, Chattopadhyay SK, Parmar MS. Self-extinguishable cellulosic textile from Spinacia oleracea. Indian J Fibre Text Res 2017;42:215–22.

205. Cheng X, Shi L, Fan Z, Yu Y, Liu R. Bio-based coating of phytic acid, chitosan, and biochar for flame-retardant cotton fabrics. Polym Degrad Stab 2022;199.
206. Feng Y, Zhou Y, Li D, He S, Zhang F, Zhang G. A plant-based reactive ammonium phytate for use as a flame-retardant for cotton fabric. Carbohydr Polym 2017;175:636–44.
207. Antoun K, Ayadi M, el Hage R, Nakhl M, Sonnier R, Gardiennet C, et al. Renewable phosphorous-based flame retardant for lignocellulosic fibers. Ind Crops Prod 2022;186:115265.
208. Keith P. Testing for Fire. In: Brown R, editor. Handbook of Polymer Testing. Physical Methods. CRC Press; 1999. page 659–95.
209. Asociación Española de Normalización. UNE-EN ISO 4589-2. Plásticos. Determinación del comportamiento al fuego mediante el índice de oxígeno. Parte 2: Ensayo a temperatura ambiente. 2017.
210. John MJ. Flammability performance of biocomposites. In: Koronis G, Silva A, editors. Green Composites for Automotive Applications. Elsevier; 2019. page 43–58.
211. Boedeker Plastics. UL94 Overview [Internet]. [cited 2022 Jun 15];Available from: https://www.boedeker.com/Technical-Resources/Technical-Library/UL94-Fire-Retardant-Testing-Overview
212. Underwriters Laboratories. Burning tests for plastic materials [Internet]. [cited 2022 Jun 15];Available from: https://www.ul.com/services/combustion-fire-tests-plastics
213. International Organization for Standardization. ISO 5660-1. Reaction to fire tests. Heat release, smoke production and mass loss rate. Part 1: Heat release rate (cone calorimeter method) and smoke production rate (dynamic measurement). 2015.
214. Benzarti K, Colin X. Understanding the durability of advanced fibre-reinforced polymer (FRP) composites for structural applications. In: Advanced Fibre-Reinforced Polymer (FRP) Composites for Structural Applications. Elsevier; 2013. page 361–439.
215. Babrauskas V. The generation of CO in bench-scale fire tests and the prediction for real-scale fires. Fire Mater 1995;19:205–13.
216. Aqlibous A, Tretsiakova-McNally S, Fateh T. Waterborne intumescent coatings containing industrial and bio-Fillers for fire protection of timber materials. Polymers (Basel) 2020;12.
217. Didane N, Giraud S, Devaux E. Fire performances comparison of back coating and melt spinning approaches for PET covering textiles. Polym Degrad Stab 2012;97:1083–9.
218. Lyon RE, Walters RN. Pyrolysis combustion flow calorimetry. J Anal Appl Pyrolysis 2004;71:27–46.
219. Xu Q, Mensah RA, Jin C, Jiang L. A critical review of the methods and applications of microscale combustion calorimetry for material flammability assessment. J Therm Anal Calorim 2022;147:6001–13.

220. Asociación Española de Normalización. UNE-EN ISO 11925. Ensayos de reacción al fuego. Inflamabilidad de los productos cuando se someten a la acción directa de la llama. Parte 2: Ensayo con una fuente de llama única. 2021.

CHAPTER 3

MATERIALS AND METHODS

TABLE OF CONTENTS

During the development of this thesis, polymer composites have been manufactured with different matrices and additives to improve fire properties. As the same tests have been carried out at all stages, this chapter summarises the materials and methods used .The first part describes the polymeric matrices, flame retardant additives and reinforcement, as well as some of their most important characteristics. Followed by the techniques used to obtain the composites, the characterization tests with theoretical concepts necessary for understanding and analysis and finally the methodology used to optimise the results.

1. MATERIALS

1.1 POLYMERS

The polymeric matrices used are a non-biodegradable polymer, polypropylene (PP), and a biodegradable polymer, polybutylene succinate (PBS). The reason for using polypropylene for this thesis is due to natural fibre composites have their main applications in the transport industry and PP is the most widely used polymer in this field [1]. On the other hand, as the reinforcement and additives are of natural origin, the use of a biodegradable polymer has been added to the study to provide an additional environmental value to the composite. In addition, PBS is a polymer that has not been investigated in depth in terms of fire resistance and is also presented as an alternative to PP due to its similar mechanical properties.

Polypropylene is a thermoplastic polymer of the polyolefin group and is obtained by chain-growth polymerization from the monomer propylene. It is a polymer used in a wide variety of applications, in fact, it is the second-most widely produced commodity plastic after polyethylene [2]. Among its many advantages, PP has no stress cracking problems and offers excellent electrical and chemical resistance at higher temperatures. In addition, it has lower density, higher melting point and higher rigidity and hardness compared to polyethylene [3]. However, due to the chemical constitution of the polymer, it is easily flammable, so flame retardancy is an important requirement to accomplish.

Polypropylene used in this project are Luban HP5101R (named PP1101S) and Luban HP1151K (named PP1151K) in pellets from Orpic, both homopolymers. The main difference between both grades is the fluency, being 24g/10 min and 3g/10 min, respectively. Table 1 shows some of their properties of the technical data sheet.

TABLE 1. PROPERTIES OF POLYPROPYLENE PP1101S AND PP1151K

Material	PP1101S	PP1151K
MFR (g/10 min) *230 °C/2.16 kg	24	3
Density (g/cm^3)	0.91	0.91
Tensile Modulus (MPa) *1 mm/min	1500	1750
Charpy notched impact strength (kJ/m^2)	2.5	5
Heat Deflection Temperature (°C)	85	99

Polybutylene succinate (PBS) is a semi-crystalline thermoplastic polymer of the polyester family and is one of the most important biodegradable polyesters, as well as being a very promising biopolymer because its mechanical properties are comparable to those of high-density polyethylene and isotactic polypropylene [4]. It is synthesised by the polycondensation of succinic acid and 1-4-butanediol and both monomers are usually synthesized from petroleum-based feedstock, but it is possible to produce them from fermentation of bio-based feedstocks [5]. In addition to its biodegradability, it has many interesting properties, such as excellent processability and thermal and chemical resistance.

PBS used in this project is BioPBS FZ91 in pellets from PTT MCC Biochem Company and is partially bio-based because the succinic acid is from renewable resources. Table 2 shows some properties of the technical data sheet.

TABLE 2. PROPERTIES OF POLYBUTYLENE SUCCINATE BIOPBS FZ91

Material	BioPBS FZ91
MFR (g/10 min) *190 °C/2.16 kg	5
Density (g/cm^3)	1.26
Melting point (°C)	115
Heat Deflection Temperature (°C)	95
Flexural Modulus (MPa)	650
Izod impact strength (kJ/m^2)	10

1.2 FLAME RETARDANTS

To select the most suitable additives for the composite from those reviewed in Chapter 2, it is necessary to consider that the decomposition temperature of the flame retardant must be above the polymer processing temperature, but also below or at the decomposition temperature of the polymer. This is because the flame retardant must act before the polymer starts to decompose [6]. Polypropylene has a melting point between 130-171°C, depending on the type, and the thermal degradation occurs in the range of 350 to 500°C in the presence of nitrogen and between 250-450°C in the presence of oxidising atmosphere [7]. In addition, the extrusion temperatures used

are around 210-240°C according to PP1101S technical datasheet. For this reason, brucite, boehmite and colemanite have been selected among the retardants of mineral origin, lignin from biobased compounds and expandable graphite as a synergistic agent.

Brucite is a hydroxide mineral composed mainly by magnesium hydroxide ($Mg(OH)_2$) and is often used as a precursor to magnesia (MgO), but in recent years its use as a flame retardant has been studied. The use of magnesium hydroxide has been studied in detail along with aluminium hydroxide ($Al(OH)_3$) because of their low cost, toxicity, and corrosion, in addition to lower smoke emissions. In fact, aluminium hydroxide is the most widely sold, with a current market share of 38% [8], but its mineral form is not pure enough for direct use. However, in the case of magnesium hydroxide, there are natural sources of brucite that are pure enough to be used only with grinding and physical beneficiation processes [9]. Another advantage is that its decomposition temperature is 300-320°C, compared to 180-200°C for $Al(OH)_3$, which is too low for processing with polypropylene [6]. For these reasons, brucite is selected for use as natural flame retardant for polypropylene. The brucite used was superfine brucite powder HQ-1250 kindly supplied by Fengcheng City Heqi Brucite Mining with a $Mg(OH)_2$ content ≥94%, a particle size between 0.9 and 8 μm, and a density of 2.3-2.4 g/cm^3.

On the other hand, the decomposition of aluminium hydroxide in certain conditions occur in two stages with the formation of an intermediate, the aluminium oxide-hydroxide AlO(OH). This compound is found in mineral form as boehmite, is stable at higher temperatures and starts to decompose at 340°C [9], making it suitable for use in polypropylene. The drawback is that the enthalpy of decomposition and volatile release are significantly less, 560 kJ/g compared to 1300 kJ/g of $Al(OH)_3$ [6], so its effect is expected to be lower than that of brucite. The boehmite used was ACTILOX B30, kindly supplied by Nabaltec, with an AlO(OH) content of 99%, a particle size between 0.7 and 4.2 μm and a bulk density of 0.6 g/cm^3.

Lastly, colemanite is a borate mineral composed of $Ca_2B_6O_{11}\cdot 5H_2O$ and is widely used in ceramics, glass, and detergents. The use of this additive is promising due to its relatively high decomposition temperature, around 350°C [10], and its ability to release structural water due to endothermic degradation. Colemanite can act like zinc borate (ZnB), and even be more effective, with the advantage that it has no heavy metals in its composition and is five times cheaper than ZnB and three times cheaper than $Mg(OH)_2$ [11]. Furthermore, colemanite showed promise as a new synergistic agent with other flame retardant because it decomposes into CaO and B_2O_3 that can react with flame retardants or form a thermally resistant layer on the surface of composite materials [12]. For this reason, colemanite is selected to study its interaction with the polymeric matrices and flame retardant additives. The colemanite used was purchased from Potclays Ltd,

with a colemanite content of 65-95%, dolomite 10-20% and ulexite 2-6%, and a density of 2.4 g/cm^3.

From the biobased aromatic products, lignin was selected, which is the second most abundant organic polymer after cellulose and is one of the main constitutes of plants and fibres. Moreover, it is an important waste stream in the pulp and paper industry, of which only 2% is used in industrial applications [13], so its use as a retardant would represent a revalorisation of the waste. It should be noted that the flame-retardant effect of lignin depends on the thermal conditions, the origin, and the extraction process [14], as they affect the molecular weight and the presence of other components. The lignin used was UPM BioPiva 199, a softwood kraft lignin purchased from UPM Biochemicals with a molecular weight of 5000 g/mol, a solids content of 90% and less than 2% sulphur content.

The use of expandable graphite (EG) as a flame retardant has also been studied. Expandable graphite prepared from natural graphite by chemical treatment has been widely used as flame retardant for a wide range of polymers [15–18]. It is generally prepared by exposing flake graphite to concentrated sulphuric acid in combination with strong oxidants [17]. As a graphite derivative, it has low cost, high availability, electrical conductivity and, most importantly, acts as a flame retardant. EG, when exposed to heat, expands generating a porous physical layer on the surface that isolates the polymer matrix from heat and oxygen, but a high loading is necessary to obtain a satisfactory effect [19]. For this reason, EG needs to be combined with other flame retardants, so in this work it is studied whether EG has a synergistic effect with the other additives. The EG used was PX 250 kindly supplied by James Durrans Group which is a high purity source material, with neutral pH, particle size over 300µm by 80% and an expansion temperature of 185°C.

Finally, to observe the effect of flame retardants, it is necessary to compare composites with the same amount of combustible material, so an inert additive or one that does not provide any retardant effect to the plastic matrix is used. In this case, calcium carbonate ($CaCO_3$) purchased from Intra Laboratories with a purity of 98.25% and density of 2.65 g/cm^3 is used.

1.3 Reinforcement

The reinforcing material used in the composites is a technical linen fabric. This reinforcement has been developed to improve vibration absorption and mechanical properties, reduce the weight, and improve the aesthetics. The linen fabric used is FlaxDry BL with a density of 200g/m^2 and 2x2 twill structure (Figure 1).

FIGURE 1: FLAXDRY BL 200 G/M^2

2. METHODS

This section describes in detail the techniques used for the manufacture of the composites, as well as the characterization tests.

2.1 COMPOSITES PREPARATION

To achieve a good mixture between polymers and additives, it is necessary to reduce the size of the plastic particles, as flame retardants come in powder form. For this purpose, cryogenic grinding is used. Pellets are first immersed in liquid nitrogen (-190°C) for 10 min to make them brittle. Then they are grounded using a Wedco SE-12-TC Pilot grinding machine, which consists of two parallel plates, 500µm apart, where one rotates at a speed of 10000 rpm. Subsequently, polymers and additives are mixed using a Prism Pilot 3 high speed mixer at 2000 rpm for 4 min and dried at 80°C for 24h prior to compounding.

FIGURE 2: POLYPROPYLENE IN PELLETS AND POWDER

Compounding was carried out using a Collin ZK25X30D co-rotating twin screw extruder with a screw diameter of 25mm (Figure 3). The extruder barrel consisted of five heating zones, with a sixth at the die, set to 180/190/190/190/190/190°C for PP blends and

110/165/165/165/165/165℃ for PBS blends. In addition, the screw speed was set at 250rpm for all samples and the feeding speed was modified depending on the fluency of the mixture varying from 11 to 20 rpm. The filament was quenched in a water bath and then passed through a pelletizer. It was observed that some blends absorbed water from the cooling bath, so pellets were dried at 80℃ for 24h.

FIGURE 3: TWIN SCREW EXTRUDER COLLIN ZK25

For characterization, the plates were manufactured by compression moulding using a Collin hot plate press model P200P. In the case of blends, the moulds used were 1, 2 and 3mm thick aluminium frames, depending on the test to be performed (Figure 4). The samples were covered with Teflon sheets to avoid contamination. From these plates, samples were cut by punching, CNC machining, or CNC laser cutting.

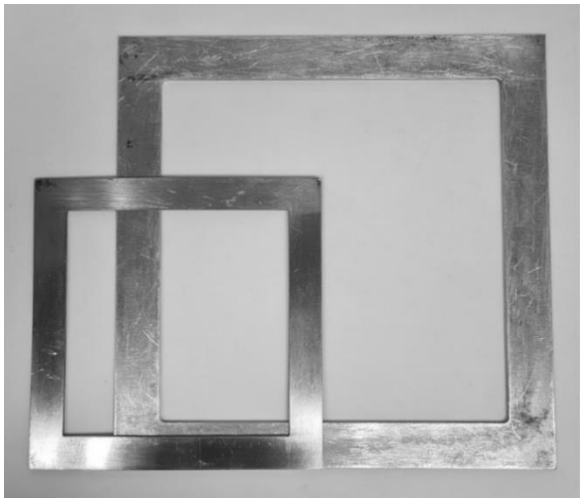

FIGURE 4: ALUMINIUM FRAMES FOR COMPRESSION MOULDING

During the trials, it was observed that the additive affects the parameters of the compression moulding process, so they vary depending on the part to be manufactured as shown in the following table.

TABLE 3: COMPRESSION MOULDING PROCESS PARAMETERS

Composite	Temperature (°C)	Pressure (bar)
PP without additive	190	10
PP with additive	190	35
PBS without additive	145	10
PBS with additive	145	35

2.2 PRELIMINARY CHARACTERIZATION

Firstly, the density of the mixtures was determined to study how the additives affect the density of the material and, consequently, the composite. For this purpose, two samples of the plates obtained by compression moulding were used. The equipment to measure the density was the Electronic Densimeter MDS-300 of Alfa Mirage. Its measurement method is based on the hydrostatic balance, which is a direct application of the Archimedes principle. By classical definition, consists of weighing an object of known mass (M_m) while is suspended in a liquid (M_L) with controlled density (ρ_L). The difference between both weights is equivalent to the mass of the displaced liquid, therefore the density of the material (ρ_m) is calculated with the following equation [20]:

$$\rho_m = \frac{M_m}{M_m - M_L} \cdot \rho_L$$

Then, the analysis of the ash content in polymers was carried out using a muffle furnace. The method is based on UNE-EN ISO 3451-1 standard, specifically Method A-Direct Calcination [21]. The method consists in place a known amount of sample (M_s), previously dried, into a dried/pre-weighted porcelain crucible and introduce it in a muffle furnace at 600°C for 24 hours. After that, the crucible is cooled to room temperature in a desiccator and weighted to determine the ash residue (M_{ash}). The ash result is expressed as %ash.

$$\%ash = \frac{M_{ash}}{M_s} \cdot 100$$

The results obtained are the average of three determinations. The objective of this test, in addition to the percentage, is to observe the appearance, structure and hardness of the char, due to during fire it plays an important role in terms of protection. In the case of minerals, it is also possible to determine the real percentage of additive in the composite or mixture considering the decomposition reactions or the experimental ash values of the additives.

2.3 MICROSCOPY

Two different types of microscopy techniques have been used in this thesis, the optical and the scanning electron microscopy (SEM). The optical microscopy has been used mainly to study the natural fibre textile and the effects of the treatments. The microscope used is the Olympus BX51 optical microscope with objectives from 2x to 100x.

Furthermore, scanning electron microscopy (SEM) is a technique that uses the interactions occurring between electrons and matter and provides information about the topography and composition of the sample. In this case, SEM was used to observe the additive particles as well as tensile tests factures. For the additives, the powder was spread on a double-sided copper tape. For the factures, a small piece of each specimen was cut to the same size and placed vertically on the copper tape (Figure 5 B). To improve the imaging, all samples were coated with a gold layer using a sputter coater under vacuum and argon gas. Then, the samples were observed using a JEOL JSM-6500F FEGSEM.

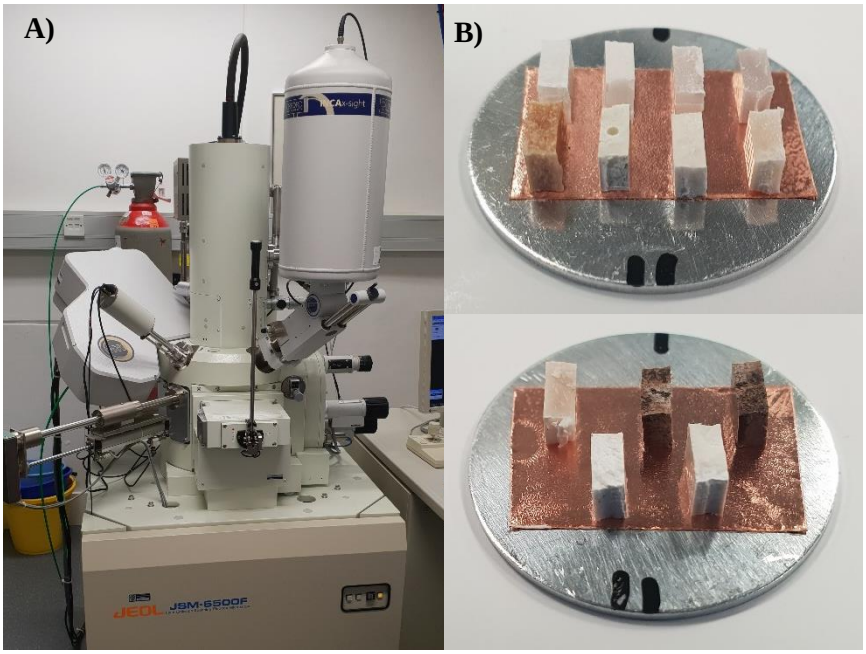

FIGURE 5: A) SEM MICROSCOPE JEOL JSM-6500F B) TENSILE TEST FACTURES ON 30MM SEM STUBS

2.4 THERMAL PROPERTIES

The International Confederation for Thermal Analysis and Calorimetry (ICTAC) defines the thermal analysis as “a group of techniques in which a property of a sample is monitored against time or temperature while the temperature of the sample, in a specified atmosphere, is programmed” [22]. Each technique evaluates different physical changes, consequently, different techniques or a combination of them must be used depending on the purpose. In this case the

techniques studied are Differential Scanning Calorimetry (DSC), Thermogravimetric Analysis (TGA) and Dynamic Mechanical Analysis (DMA).

2.4.1 DSC

Differential Scanning Calorimetry (DSC) is a technique that measures the quantity of heat that is either absorbed or released by a substance due to a physical or a chemical change when it is heated, cooled, or held isothermally at constant temperature. The change suffered by the substance alters its internal energy, which is defined as enthalpy (H) when it is at constant pressure [23]. The processes that are frequently measured are melting, evaporation, glass transition, curing, crystallization, and decomposition. Therefore, this technique is used to study how additives and fibres influence these processes.

This technique consists of two capsules inside a furnace, one with the sample to be analysed and the other empty as a reference capsule. Each crucible is placed on top of an individual heater and are heated or cooled together according to a controlled temperature program. If any difference is detected between the temperature measured in both capsules due to the physical or chemical processes, the individual heaters are corrected to maintain the same temperature. Therefore, when an exothermic or endothermic process takes places, the instrument compensates the energy required to maintain the same temperature in both capsules while registers the heat flow vs temperature (Figure 6).

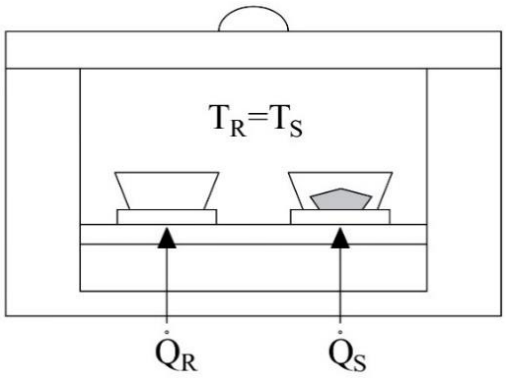

FIGURE 6: SCHEMATIC DIAGRAM OF DSC. MODIFIED FROM EHRENSTEIN ET AL. [23]

The tests of the blends were carried out in a Perkin Elmer Pyris 6 DSC. For each test, between 9.5 and 10.5 mg of sample was cut, weighted, and sealed in an aluminium sample pan. PP samples were subjected to a first heating from 30 to 250°C at 10°C/min, then hold for 2 min, cooling from 200 to 30°C at 10°C/min and finally second heating from 30 to 250°C at 10°C/min. PBS samples were subjected to a first heating from 30 to 170°C at 10°C/min, hold for 2 min, cooling from 170

to 30°C at 10°C/min and second heating from 30 to 170°C at 10°C/min. The purpose of performing two heating ramps is to eliminate the effect of processing history.

From the heating curves are determined onset ($T_{onset,\ m}$), end ($T_{end,\ m}$) and melting (T_m) temperatures, enthalpy of fusion (ΔH_m), which is the area under the curve, and partial areas (X_1, X_2, X_3) (Figure 7). In the cooling curve, onset ($T_{onset,\ c}$) and crystallization (T_c) temperatures, and enthalpy (ΔH_c) of crystallization (Figure 8).

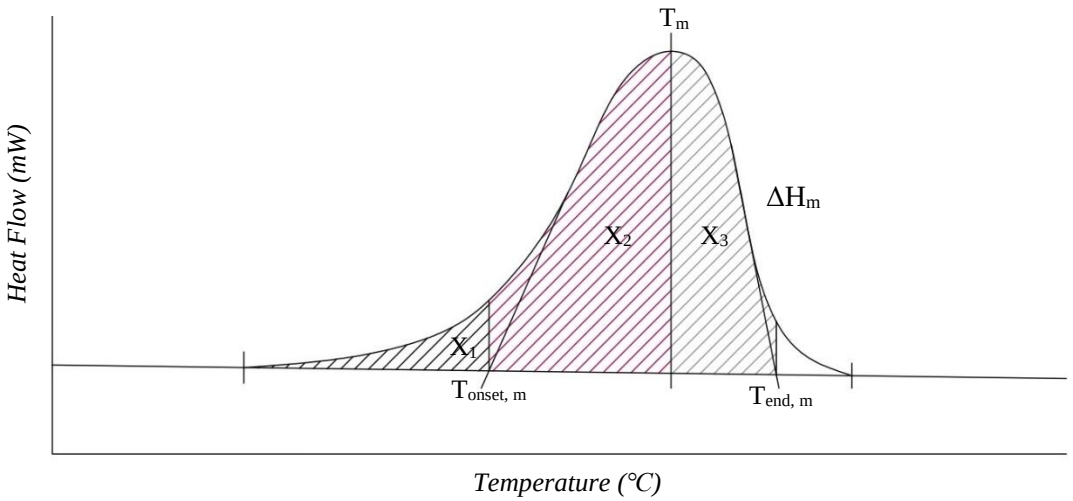

FIGURE 7: EXAMPLE OF MELTING CURVE IN DSC

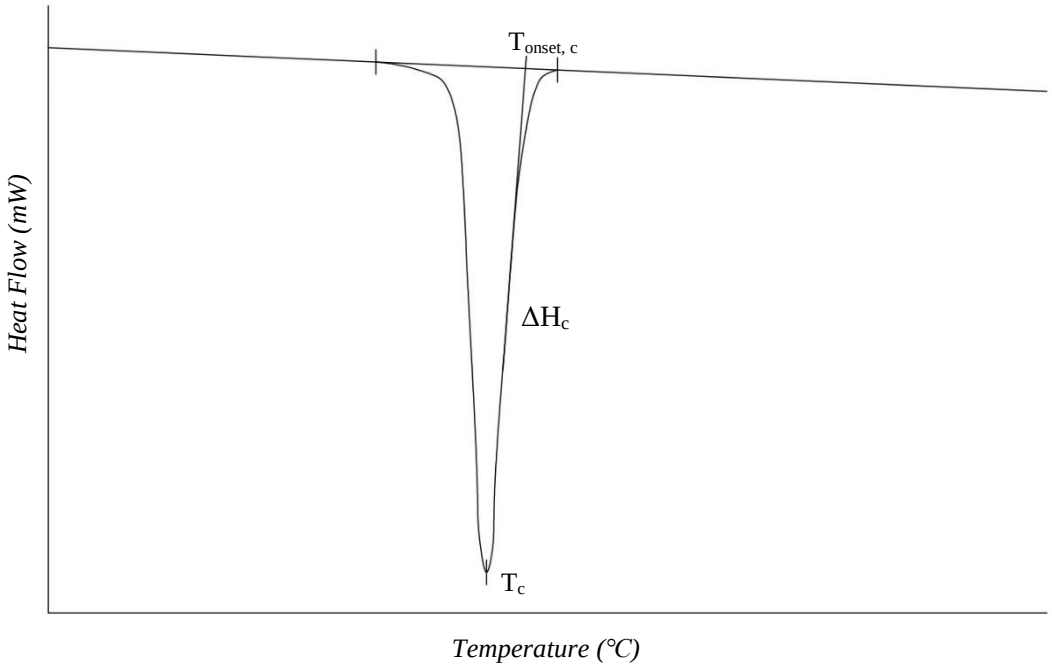

FIGURE 8: EXAMPLE OF COOLING CURVE IN DSC

Finally, the percentage of crystallinity (w_c) was determined using the second melting curve, dividing the enthalpy of fusion by the reference value of the polymer 100% crystalline. In the

case of samples with additives, it is necessary to correct the formula due to the samples are not 100% polymer.

$$w_c = \frac{\Delta H_m}{\Delta H_m^0} \cdot \frac{100}{W_p}$$

ΔH_m: Heat of fusion sample (J/g)

ΔH_m^0: Heat of fusion of 100% crystalline material (J/g)

W_p: Percentage of polymer in parts per unit

The reference value used for polypropylene 100% crystalline is 207 J/g [23]. However, in the case of PBS, quite different values are reported. The value of 110 J/g is often used, but it is an estimated value calculated based on the group contribution method proposed by van Krevelen [24]. On the other hand, values between 200 and 230 J/g have also been reported [25,26]. Righetti et al. [27] determined the enthalpy of melting of 100% crystalline PBS using DSC and XRD techniques and obtained a result of 195±10 J/g, which confirms the ΔH_m^0 values reported close to 200 J/g. In conclusion, the reference value used for PBS 100% crystalline is 200 J/g.

2.4.2 TGA

Thermogravimetric analysis (TGA) is a technique for the measurement of thermal stability of materials and composition e.g., polymer, additive, or filler content. In addition, to understand the behaviour of a material in a fire, this test yields understanding of decomposition of the materials. TGA measures the change in mass of a sample as a function of temperature, time or both when is subjected to a controlled temperature program in a controlled atmosphere [28]. The results of a TGA test are plotted as mass in mg or percentage against temperature or time, in case of isothermal experiments. Another useful representation is the derivative curve with respect to temperature or time because it shows the rate at which the mass changes. Several different effects can cause changes of sample mass, e.g., sublimation, evaporation, decomposition, or chemical reaction, among others. These changes are shown as steps in the graph, usually due to loss of material, although an increase in mass can also occur when the sample reacts with the surrounding atmosphere. For this reason, one of the crucial factors of this test is the choice of purge gas because it can be inert gases such as nitrogen, helium and argon, or oxidizing gases such as oxygen or air. In addition, it is important to consider that the extent of heat transfer to the specimen depends on the gas flow rate [29].

The equipment consists of a sample suspended on an extremely sensitive scale that measures mass change inside of a programmable furnace to control the heat up rate of the sample. The sample is suspended on a beam which is held constant by an electromagnetic force feedback

system. With this system, the equipment determines the mass of the sample by the force required to maintain the beam horizontally [29]. In addition, the balance is isolated to maximize the sensitivity, accuracy, and precision of weighing. In the first two stages of the thesis dynamic TGA tests were performed on a Mettler Toledo TGA/DTA 851e^{o} under O_2 gas at 50 mL/min. The samples were subjected to a temperature ramp from 40 to 600°C with a heating rate of 5°C/min. The reason for using oxygen instead of nitrogen is because decomposition indicates processes that can occur before ignition.

Because the samples studied are generally blends of polymers and additives, the curves show multi-step losses of mass. In these cases, TGA curves often do not have a section between the steps where the mass remains constant due to the overlapping changes of mass. Taking this into account, the main points to be determined for each step are the starting point or onset (A) and the endpoint (B), with the respective temperatures and mass, and the left limit temperature (T_L), which is the temperature where the weight loss starts. In addition, it is determined the peak of maximum degradation (P) with the derivative curve. When two steps overlap, the mass at the midpoint (m_i) can also be determined by using the derivative curve, where m_i is the smallest value of the curve between the two steps [29]. Figure 9 shows the typical curve of a sample with two steps and no overlapping.

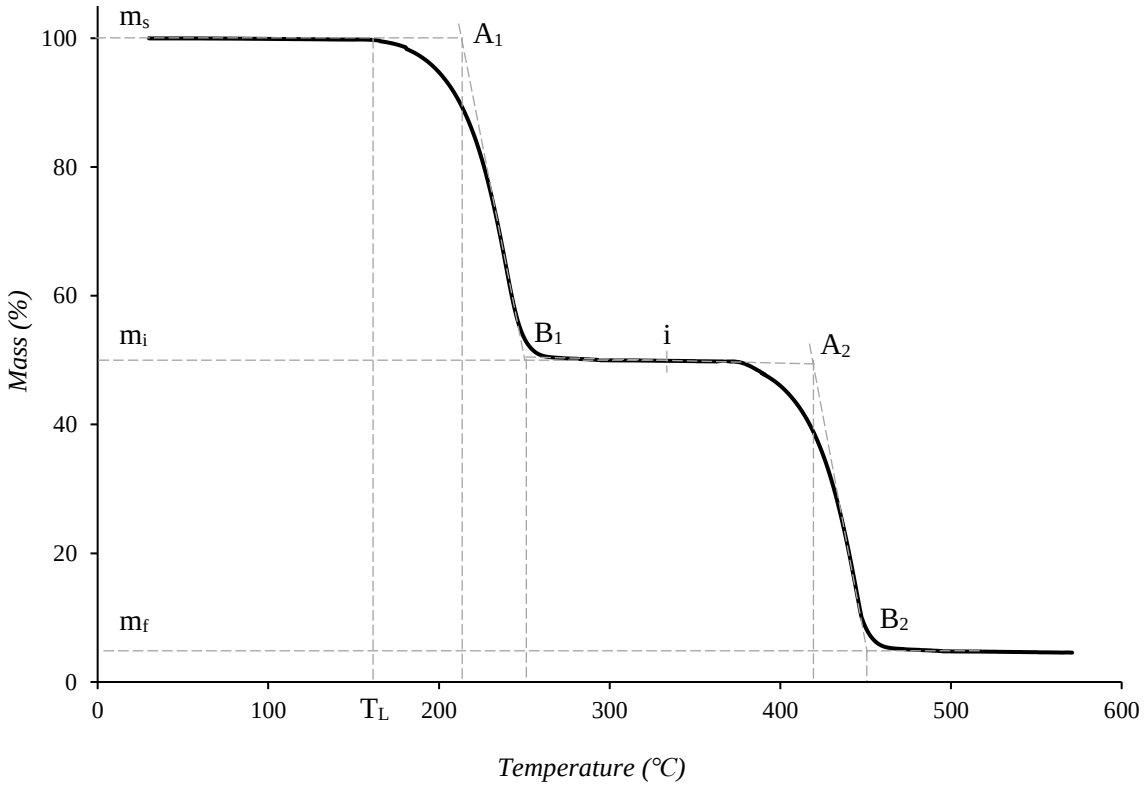

FIGURE 9: TGA CURVE WITH DETERMINED PARAMETERS. MODIFIED FROM EHRENSTEIN ET AL. [29]

2.4.3 DMA

Dynamic Mechanical Analysis (DMA), also called Dynamic Mechanical Thermal Analysis (DMTA), is a technique used to study and characterize the viscoelastic behaviour of a material with respect to temperature, humidity, vibration frequency, dynamic or static strain amplitude, or other parameter against time [30]. The test consists of a system of clamps for mechanical testing such as tension, compression, flexure, and shear. All DMA configurations consist of a moving clamp and one or more stationary clamps, where the movable part applies force and displace the sample according to the mechanical movement to be tested. In dynamic testing a minor oscillation, usually sinusoidal, is applied to the sample by the movable clamp at the specified force as a function of time and temperature. The applied mechanical load (stress) causes a corresponding deformation (strain) whose amplitude and phase shift can be determined [31] (Figure 10).

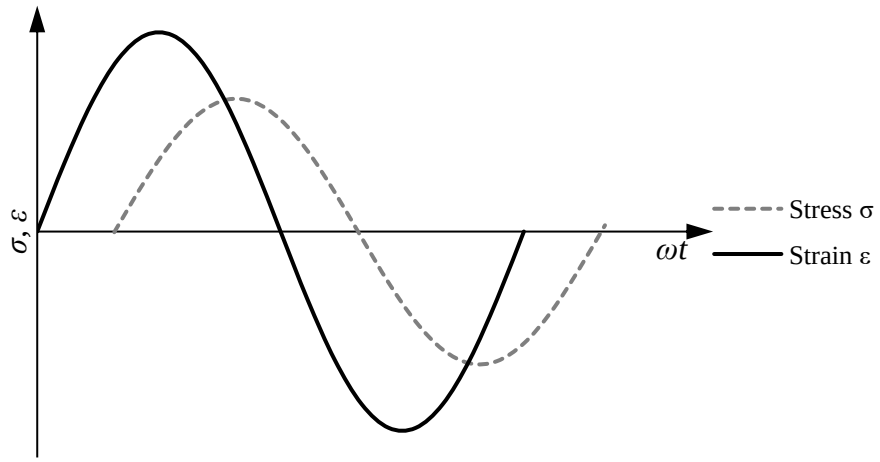

FIGURE 10: SINUSOIDAL OSCILLATION AND RESPONSE IN DMA. MODIFIED FROM EHRENSTEIN ET AL. [31]

The complex modulus (E*) is the ratio of the stress amplitude to the strain amplitude and represents the stiffness of the material [31]. It is composed of the storage modulus (E') and the loss modulus (E"). The storage modulus (E') is the real part of E* and is defined in UNE-EN ISO 6721-1 as the stiffness of a viscoelastic material and is proportional to the maximum energy stored during a loading cycle [32]. In the same standard, the loss modulus (E") is the imaginary part of the complex modulus and is proportional to the energy dissipated during a loading cycle. It represents the ability of the material to disperse mechanical energy through internal molecular motions, which cannot be recovered, for example, energy lost as heat. It should be noted that these are dynamic elastic characteristics and are material specific, so their magnitude is critically dependent on the frequency as well as the measurement conditions and the history of the specimen [31]. In addition to these parameters, it is also determined the loss factor (tan δ) which is the ratio of loss modulus to storage modulus [32]. It is a dimensionless parameter and is a measure of

energy lost, expressed as recoverable energy, and represents mechanical damping or internal friction in a viscoelastic system [31].

$$\tan \delta = \frac{E''}{E'}$$

One of the important applications of DMA is the determination of the glass transition temperature (T_g) of polymers, because it offers the highest sensitivity for its determination [33]. T_g is defined as the temperature of amorphous polymers at which the material transitions from glassy state or energy elastic state to rubber or entropy elastic state [31]. In the glassy state the molecules are "locked", whereas in the rubbery region the polymer chains can flow more easily in comparison. This change is detected in the DMA by the drop in the storage modulus (E') and the reaching of a maximum in the loss modulus (E'') (Figure 11). It can also be quantified by the maximum of the loss factor tan δ, but the temperature obtained is higher with respect to the loss modulus. Another commonly used technique for T_g determination is DSC because it reflects changes in the specific heat of the polymer at the glass-rubber transition, but it is a less sensitive technique for this application [30].

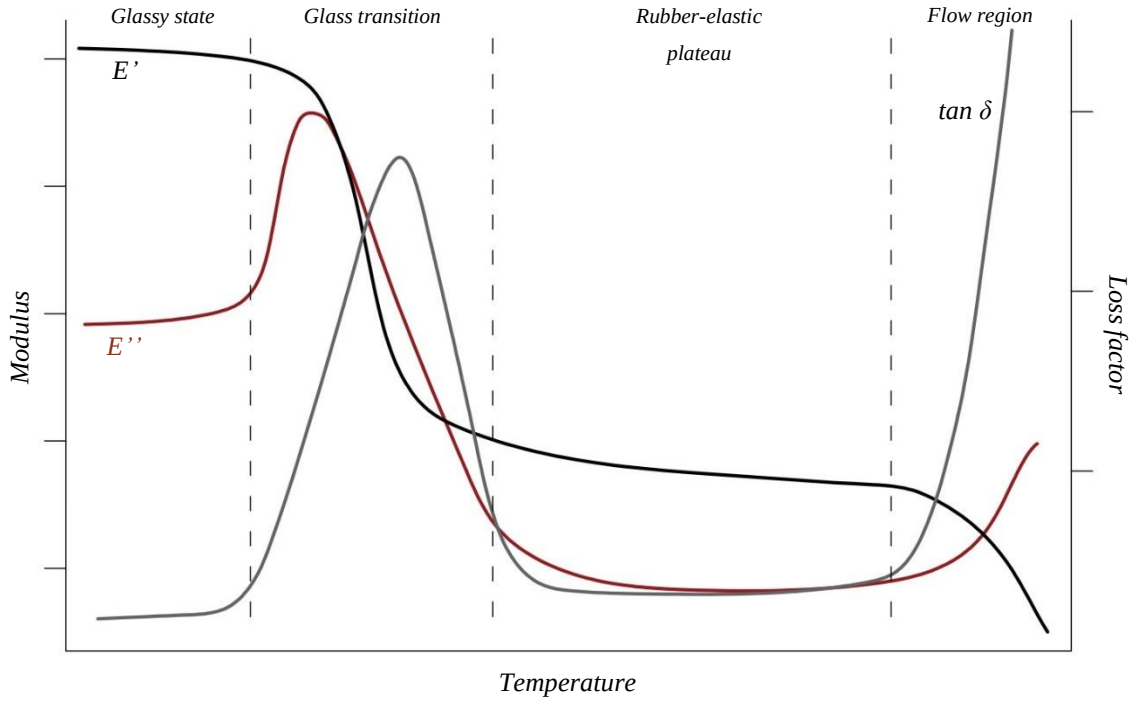

FIGURE 11: DMA CURVE. MODIFIED FROM METTLER TOLEDO [34]

In this case, the T_g is determined using the maximum of the loss modulus and is studied how it is affected by the different additives. Several authors and standards recommend the evaluation of T_g based on this peak. For example, Rieger J. gives three arguments why T_g should be

determined at the maximum of E''[35]. Firstly, E" is the measure of dissipated energy so the temperature of the maximum is the transition temperature in question, while tan δ is from the physical point of view a derived variable. Secondly, the value of the maximum does not depend on whether the material is pure or a mixture and lastly, Peleg demonstrated that the temperature at the maximum of tan δ, especially in the case of smeared glass transitions, does not coincide with the softening temperature at which the shear or tensile modulus drops to low values [36].

The main types of test modes are temperature and frequency sweep. In this case temperature scanning is used to observe how the material will behave mechanically in an environment where the temperature increases, as in the case of a fire. The equipment used to perform the tests is a Triton Technology Tritec 2000 DMA with a single cantilever clamp (Figure 12). The temperature program was from -50 to 165°C for PP samples and from -50 to 110°C for PBS samples at a scan rate of 2°C/min. The frequency was set at 1 Hz and the displacement at 0.05 mm.

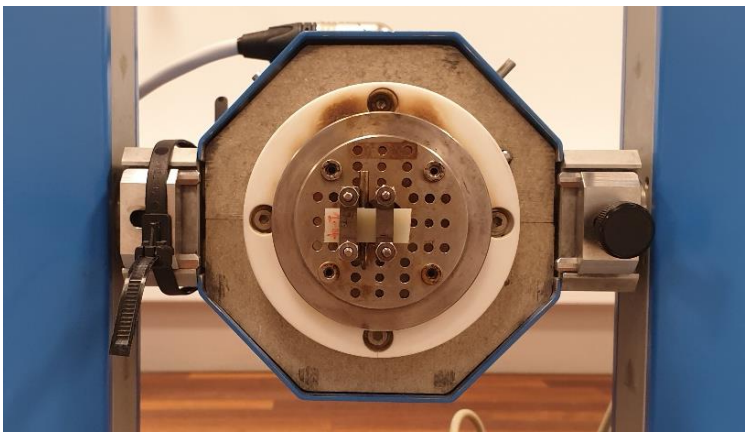

FIGURE 12: TRITEC 2000 DMA WITH SINGLE CANTILEVER CLAMP AND A SAMPLE

2.5 Oscillatory Rheology

Rheology is the study of the flow and deformation of matter and describes the interrelation between force, deformation, and time [37]. The study of the rheological properties plays a significant role in this case because the polymers studied are additivated with flame retardants at high loads and the viscosity of the material increases considerably. Consequently, the results obtained provide the tools to adjust the processing conditions of the polymers according to the composite to be manufactured. There are different techniques to measure the rheological properties of materials such as melt flow index (MFI), capillary rheology, oscillatory rheology, and vibrating viscometers, among others. In this case the technique used is the oscillatory rheology because it measures the viscosity at very low shear rates, thus covering compression moulding and extrusion, techniques used for the manufacture of composites.

The oscillatory rheology is a non-destructive test where the sample is twisted while it is measured how stiff, or mobile it is as a function of temperature, time, shear, or frequency. The sample is mounted between two parallel circular metal plates and the upper plate oscillates horizontally, typically in a sinusoidal mode. As in DMA, a sinusoidal deformation is applied, and the material response is measured as the phase angle δ or shift between the deformation and response. The magnitude and phase lag of the transmission will depend on the viscoelastic properties of the specimen. For example, in viscous materials the stress is dissipated by friction, while in elastic materials it is transmitted [38]. The ratio of this transmission gives the complex modulus (G*) which defines the overall stiffness of the sample. The complex modulus (G*) can be separated into two components, the storage modulus G' (real part) and the loss modulus G" (imaginary part). The storage modulus is the elastic component, which indicates the amount of energy stored and represent the solid or gel like behaviour. On the other hand, the loss modulus is the viscous component, which indicates the amount of energy dissipated and represents the viscous or liquid behaviour. Therefore, a larger value of G' compared to G" means that in that region the material exhibits elastic behaviour [38]. When both moduli are plotted, there is sometimes and intersection of the curves, named crossover frequency or cross-over point, which means that the elastic and viscous behaviour are the same. This point is an important rheological parameter due to is inversely proportional to the relaxation time [38]. Figure 13 shows an example of typical viscoelastic behaviour where at low frequencies the material exhibits viscous behaviour, followed by a cross-over point around 42Hz to pass to a solid or elastic behaviour.

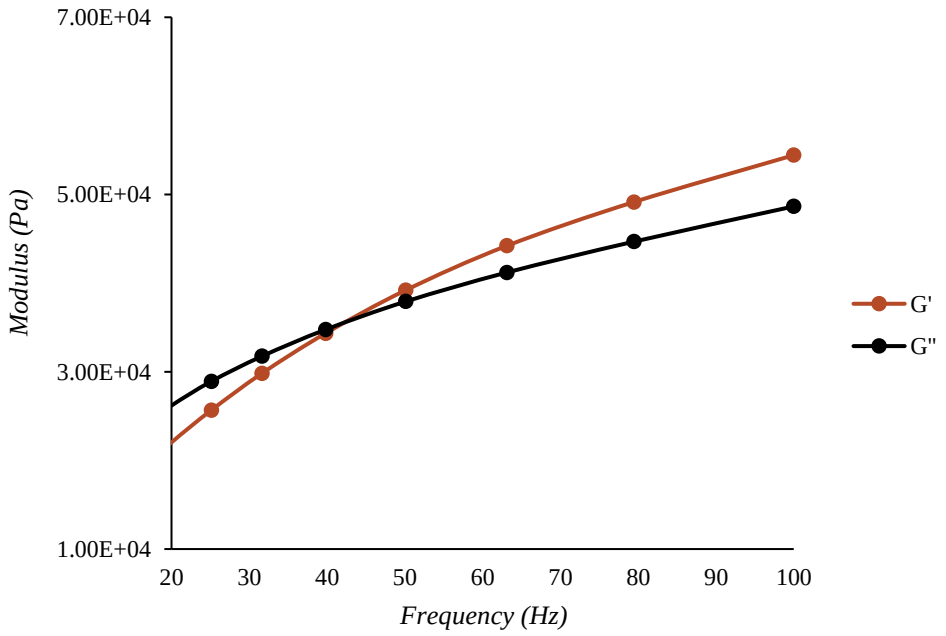

FIGURE 13: GRAPH OF STORAGE AND LOSS MODULUS VS FREQUENCY IN OSCILLATORY RHEOLOGY

There are different modes of measurement as frequency sweep, stepped viscosity, strain sweep and flow temperature ramp, among others. In this case the mode used is the frequency sweep, which consists of monitor the polymer response while the frequency increase at a constant amplitude (displacement) and temperature. Frequency sweep tests were performed using a TA Instruments ARG2 parallel plate rheometer over the range of 100 to 0.1 Hz (Figure 14). The gap between plates was set to 1 mm and the diameter of the sample was 25 mm, which was extracted with a punch from the compression moulded plates. PP samples were tested at 170, 190 and 210 ℃, and PBS samples at 120, 140 and 160℃ to study the effect of the temperature in the viscosity of the materials. The storage modulus (G') and the loss modulus (G") were measured, and the G cross-over point was also determined, if applicable. The Cox-Merz transformation was used to obtain the viscosity curves and the zero-shear viscosity was extrapolated from the data using Carreau Model.

FIGURE 14: TA INSTRUMENTS ARG2

2.6 MECHANICAL TEST

As mentioned above, to obtain a fireproof material with natural flame retardants, it is necessary to use high loadings, so the mechanical properties are compromised. For this reason, it is especially important to determine their properties to know in which industrial applications they can be used. First, to determine the mechanical properties of the developed composites, it is necessary to extract or cut the samples for each test from the plates manufactured by compression moulding. The methods used were punching and laser cutting, and the geometry and size of the specimens are in accordance with UNE Standards.

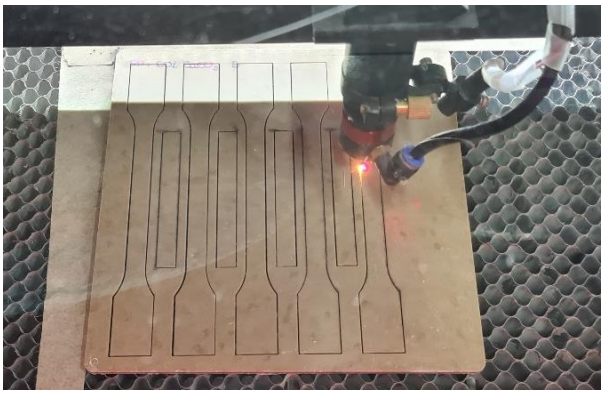

FIGURE 15: LASER CUTTING OF THE COMPRESSION MOULDED PLATES

2.6.1 TENSILE TEST

Tensile testing is a destructive test process that measures the force required to break a composite or plastic specimen and the extent to which the specimen stretches or elongates to that breaking point [39]. The tensile tests were carried out according to the procedure described in the UNE-EN ISO 527-1 and UNE-EN ISO 527-2 standards. The equipment employed to perform the test of the blends is an Instron Universal Tensile Tester 5564 with a load cell of 5kN and a constant crosshead speed of 20 mm/min (Figure 17). For each blend, at least five replicates of 1BA samples were tested.

In the tensile test, the specimen is elongated along its principal axis, at constant speed, until failure or until the stress (load) reaches a specified value. The values measured during the test are the load supported and the elongation of the specimen, and then the stress (σ), strain (ε) and elastic modulus (E_t) are calculated. shows the stress-strain graph for polypropylene.

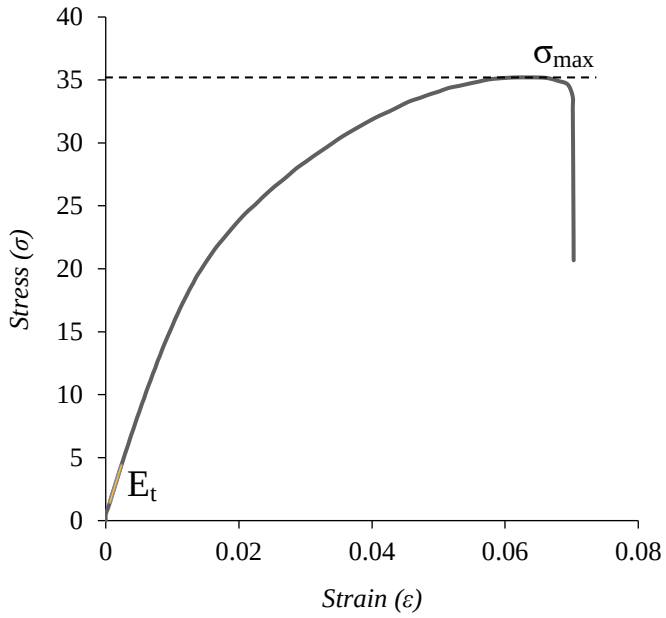

FIGURE 16: STRESS-STRAIN GRAPH OF POLYPROPYLENE

The elastic modulus (E_t) is calculated as the slope of the curve in the elastic deformation region, between 0.0005 and 0.0025 of the strain. In addition, it is determined the value of the maximum strength (σ_{max}), which is the highest stress value recorded.

2.6.2 FLEXURAL TEST

Flexural test measures the force required to bend a material and determine the resistance to flexing or stiffness. The flexural tests were carried out based on the UNE-EN ISO 178 standard using an Instron Universal Tensile Tester 5564 with a load cell of 5kN (Figure 17). The three-point testing fixture was set at a span of 64mm and a speed of 2 mm/min, which was applied until failure or a deflection of 8.5mm. At least five specimens with sample dimensions of 80x10x2 mm were tested per group.

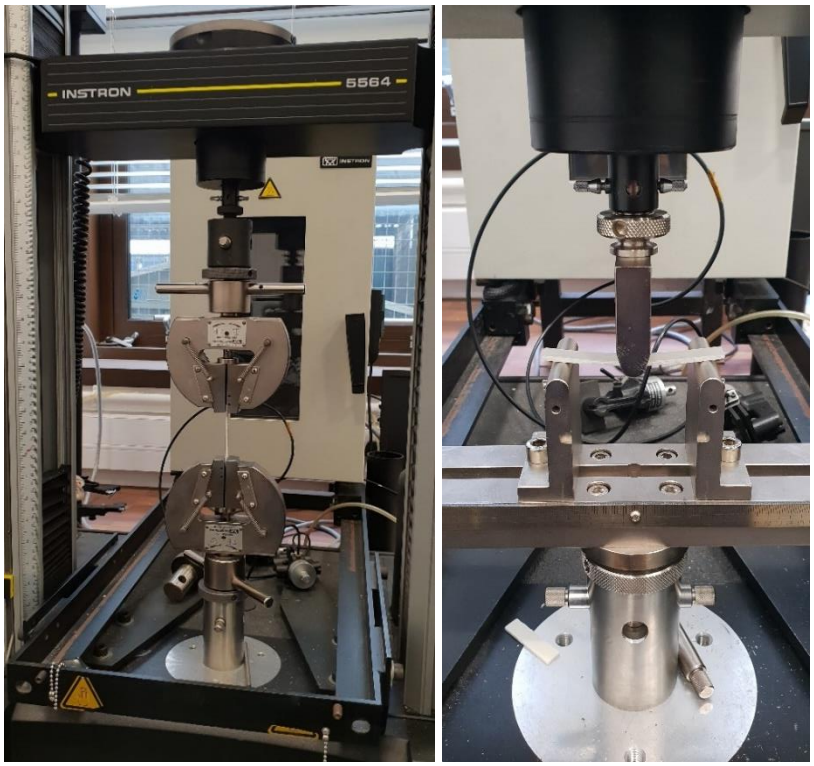

FIGURE 17: INSTRON UNIVERSAL TENSILE TESTER 5564

The values measured during the test are the load applied and the displacement, and then the stress (σ_f), strain (ε_f) and flexural modulus (E_f) are calculated. As the tensile test, the flexural modulus (E_f) is calculated as the slope of the curve stress-strain in the elastic deformation region.

2.6.3 IMPACT TEST

The toughness or impact strength is the amount of energy that a material can absorb before rupturing [40]. Impact test is used for quality control and to compare relative toughness of engineering materials. The plastic samples are subjected to high-speed loading and the response

behaviour is observed. The impact tests carried out on the blends are based on UNE-EN ISO 179-1 and UNE-EN ISO 179-2 standards. Charpy impact strength was measured using the Instron Ceast Resil Impactor Model 6958.000 and at least five un-notched specimens with sample dimensions of 80x10x2 mm were tested per group.

2.7 FIRE TESTS

Due to this work is focused on develop a composite reinforced with natural fibres and additivated with natural flame retardants, the fire tests performed are at laboratory scale.

2.7.1 UL94

The reaction to fire study was carried out based on the procedure developed by Underwriters Laboratories, which is described in Chapter 2, section 4.2. The blends were tested in a lab-made equipment (Figure 18). The device consists of a combustion chamber equipped with a gas extraction device at the top, and inside there is a Bunsen burner with a support that allows it to be positioned at 0 or 45º depending on the material to be tested. In addition, the support is coupled to a rail that allows it to be moved from the outside of the chamber. For the vertical test 94V, a specimen holder with a Hoffman clamp was used and for 94HB, a laboratory stand with a laboratory clamp. The gas used was butane, the flame 2 cm high and the application time was 10 seconds for 94V and 30 seconds for 94HB, as described in the procedure.

FIGURE 18: FIRE TEST LAB-MADE EQUIPMENT

In the vertical test the burning time, afterglow and dripping were recorded. In addition, due to the typology of the materials, the propagation speed was determined by marking the specimens every two centimetres and quantifying the time taken for the flame to reach each mark (Figure

19). In the horizontal test it is recorded the burning rate and if flame extinguished before the first mark. To facilitate the analysis of the data, a video recording device has been introduced inside the chamber to record the tests. At least eight specimens with sample dimensions of 127x12.7x3mm were tested per material, five in vertical 94V and three in horizontal 94HB.

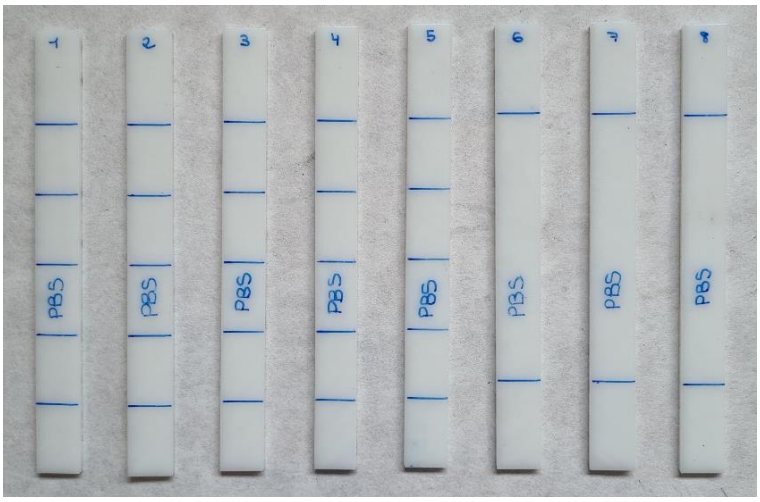

FIGURE 19: SAMPLES PREPARED FOR UL94 TESTS

2.7.2 CONE CALORIMETER

As well as the previous test, cone calorimeter test is described in Chapter 2, section 4.3: Cone calorimeter. The tests were carried out using a SGS Govmark Cone Calorimeter following ISO 5660. Specimens with dimensions 100x100x3mm were exposed to a constant heat flux of 25 kW/m^2 at 25 mm height and ignited with a spark igniter placed above the sample. The plaques were placed in the sample holder with the aluminium foil facing with a retainer frame, exposing 90 cm^2 of the sample surface to the radiation (Figure 20). In addition, glass wool was placed under the plate as insulating material.

FIGURE 20: CONE CALORIMETER SAMPLES WITH RETAINING FRAME

The test is performed until the heat release rate (HRR) decrease to 10 kW/m^2 or the mass loss or extinction coefficient are zero. During and after the test it is observed the formation of the char, its shape, colour, and hardness. The parameters analysed are those explained in Chapter 2, heat release rate (HRR) and its peak (p-HRR), total heat released (THR), time to ignition (TTI), mass loss rate (MLR), total smoke release (TSR), as well as the derived parameters Fire Growth Rate (FIGRA) and Maximum Average Rate of Heat Emission (MAHRE). Each test was performed at least twice, and the averages are presented in the results.

2.8 OPTIMIZATION

To determine the best additives and their percentage for the composite, an optimization was carried out with the results of the mechanical and fire tests. The optimization algorithm employed is based on a genetic algorithm which is described in detail by Paz et al. [41–43]. The fitness function evaluation is determined by the Kriging metamodel, which is an interpolation method. In this case, Matlab Kriging Toolbox developed by Lophaven et al. [44] was used. First, the Kriging metamodel is created based on the experimental data obtained. Among the available correlation models, the generalized exponential is used because it is the most flexible in terms of the form of the function and is often used when the spatial correlation between data is unknown [41]. In addition, the regression model is polynomial which allows varying the order from 2 to 0 depending on the number of data and their distribution, with two being the most accurate. Once the metamodel is created, the genetic algorithm proceeds with the optimization using 100 generations, each one with 100 individuals. Then, the fitness value of each individual proposed by the genetic algorithm is calculated following the estimations of the metamodel [41]. Once calculated, the genetic algorithm applies a tournament selection of 2 individuals, an arithmetic crossover with 50% probability, mutation with 60% probability, reparation, and elitism. When the algorithm finishes its evolution, the best additive/percentage is obtained and studied in the next stage to complete the feedback process.

The inputs of the program are the number of variables, specifying whether they are discrete or continuous, the number of restrictions (if applicable), the number of responses that define the objective, the function to optimize, whether the objective is to minimize or maximize, and lastly the limits of each variable (maximum and minimum) and of the restrictions. Since different additives and percentages, as well as response variables, have been used at each stage, in Chapter 4 it is specified the procedure and variables used to perform the optimization at each stage.

3. INDEX OF TABLES AND FIGURES

4. REFERENCES

1. Economics & Statistics Department. American Chemistry Council. Plastics and Polymer Composites in Light Vehicles. 2019.
2. Polymer Database. Properties of Polyolefins [Internet]. Available from: http://polymerdatabase.com/polymer%20classes/Polyolefin%20type.html
3. Colin Hindle. Polypropylene (PP) [Internet]. British Plastic FederationAvailable from: https://www.bpf.co.uk/plastipedia/polymers/PP.aspx
4. Polymerdatabase. Polybutylene Succinate (PBS) [Internet]. Available from: https://www.polymerdatabase.com/Polymer%20Brands/PBS.html
5. Niaounakis M. Introduction. In: Biopolymers: Processing and Products. Elsevier; 2015. page 1–77.
6. Hull TR, Witkowski A, Hollingbery L. Fire retardant action of mineral fillers. Polym Degrad Stab 2011;96:1462–9.
7. Esmizadeh E, Tzoganakis C, Mekonnen TH. Degradation Behavior of Polypropylene during Reprocessing and Its Biocomposites: Thermal and Oxidative Degradation Kinetics. Polymers (Basel) 2020;12:1627.
8. Ceresana. Market Study: Flame Retardants World Report (7 th edition) [Internet]. 2022. Available from: www.ceresana.com
9. Rothon R, Hornsby P. Fire Retardant Fillers for Polymers. In: Polymer Green Flame Retardants. Elsevier; 2014. page 289–321.
10. Kaynak C, Isitman NA. Synergistic fire retardancy of colemanite, a natural hydrated calcium borate, in high-impact polystyrene containing brominated epoxy and antimony oxide. Polym Degrad Stab 2011;96:798–807.
11. Terzi E, Kartal SN, Pişkin S, Stark N, Kantürk Figen A, White RH. Colemanite: A Fire Retardant Candidate for Wood Plastic Composites. Bioresources 2018;13.
12. Atikler U, Demir H, Tokatlı F, Tıhmınlıoğlu F, Balköse D, Ülkü S. Optimisation of the effect of colemanite as a new synergistic agent in an intumescent system. Polym Degrad Stab 2006;91:1563–70.
13. Kai D, Tan MJ, Chee PL, Chua YK, Yap YL, Loh XJ. Towards lignin-based functional materials in a sustainable world. Green Chemistry 2016;18:1175–200.
14. Costes L, Laoutid F, Brohez S, Dubois P. Bio-based flame retardants: When nature meets fire protection. Materials Science and Engineering R: Reports [Internet] 2017;117:1–25. Available from: http://dx.doi.org/10.1016/j.mser.2017.04.001
15. Zhu H, Zhu Q, Li J, Tao K, Xue L, Yan Q. Synergistic effect between expandable graphite and ammonium polyphosphate on flame retarded polylactide. Polym Degrad Stab 2011;96:183–9.

16. Khalili P, Tshai KY, Kong I. Natural fiber reinforced expandable graphite filled composites: Evaluation of the flame retardancy, thermal and mechanical performances. Compos Part A Appl Sci Manuf 2017;100.
17. Mazela B, Batista A, Grześkowiak W. Expandable Graphite as a Fire Retardant for Cellulosic Materials—A Review. Forests 2020;11:755.
18. Schirp A, Su S. Effectiveness of pre-treated wood particles and halogen-free flame retardants used in wood-plastic composites. Polym Degrad Stab 2016;126:81–92.
19. Wang X, Kalali EN, Wan JT, Wang DY. Carbon-family materials for flame retardant polymeric materials. Prog Polym Sci 2017;69:22–46.
20. Asociación Española de Normalización. UNE-EN ISO 1183-1. Plásticos. Métodos para determinar la densidad de plásticos no celulares. Parte 1: Método de inmersión, método del picnómetro líquido y método de valoración. 2019;
21. Asociación Española de Normalización. UNE-EN ISO 3451-1. Plásticos. Determinación del contenido en cenizas. Parte 1: Métodos generales. 2020;
22. Hill JO. For Better Thermal Analysis and Calorimetry. 3rd ed. 1991.
23. Ehrenstein GW, Riedel G, Trawiel P. Differential Scanning Calorimetry (DSC). In: Thermal Analysis of Plastics. München: Carl Hanser Verlag GmbH & Co. KG; 2004. page 1–110.
24. van Krevelen DW, te Nijenhuis K. Calorimetric Properties. In: Properties of Polymers. Elsevier; 2009. page 109–28.
25. Gan Z, Abe H, Kurokawa H, Doi Y. Solid-state microstructures, thermal properties, and crystallization of biodegradable poly(butylene succinate) (PBS) and its copolyesters. Biomacromolecules 2001;2:605–13.
26. Papageorgiou GZ, Bikiaris DN. Crystallization and melting behavior of three biodegradable poly(alkylene succinates). A comparative study. Polymer (Guildf) 2005;46:12081–92.
27. Righetti MC, di Lorenzo ML, Cinelli P, Gazzano M. Temperature dependence of the rigid amorphous fraction of poly(butylene succinate). RSC Adv 2021;11:25731–7.
28. Inan TY. Thermoplastic-based nanoblends. In: Recent Developments in Polymer Macro, Micro and Nano Blends. Elsevier; 2017. page 17–56.
29. Ehrenstein GW, Riedel G, Trawiel P. Thermogravimetry (TG). In: Thermal Analysis of Plastics. München: Carl Hanser Verlag GmbH & Co. KG; 2004. page 139–71.
30. Gearing J. Dynamic Mechanical (Thermal) Analysis. In: Brown R, editor. Handbook of Polymer Testing. Physical Methods. CRC Press; 1999. page 501–31.
31. Ehrenstein GW, Riedel G, Trawiel P. Dynamic Mechanical Analysis (DMA). In: Thermal Analysis of Plastics. München: Carl Hanser Verlag GmbH & Co. KG; 2004. page 236–99.
32. Asociación Española de Normalización. UNE-EN ISO 6721-1. Plásticos. Determinación de las propiedades mecano-dinámicas. Parte 1: Principios generales. 2020;

33. Wagner M, editor. The glass transition. In: Thermal Analysis in Practice Handbook. Mettler Toledo; 2009. page 225–51.
34. Mettler Toledo. DMA Curve Interpretation.
35. Rieger J. The glass transition temperature Tg of polymers—Comparison of the values from differential thermal analysis (DTA, DSC) and dynamic mechanical measurements (torsion pendulum). Polym Test 2001;20:199–204.
36. Peleg M. A note on the tan δ(T) peak as a glass transition indicator in biosolids. Rheol Acta 1995;34:215–20.
37. Malvern. A Basic Introduction to Rheology. 2016.
38. Miri T. Viscosity and Oscillatory Rheology. In: Practical Food Rheology: An Interpretive Approach. Wiley-Blackwell; 2010. page 7–28.
39. Saba N, Jawaid M, Sultan MTH. An overview of mechanical and physical testing of composite materials. In: Mechanical and Physical Testing of Biocomposites, Fibre-Reinforced Composites and Hybrid Composites. Elsevier; 2019. page 1–12.
40. Sun L, Gibson RF, Gordaninejad F, Suhr J. Energy absorption capability of nanocomposites: A review. Compos Sci Technol 2009;69:2392–409.
41. Paz R, Pei E, Monzón M, Ortega F, Suárez L. Lightweight parametric design optimization for 4D printed parts. Integr Comput Aided Eng 2017;24:225–40.
42. Paz R, Monzón MD. Optimization methodology for the material assignation in bioprinted scaffolds to achieve the desired stiffness over time. Int J Numer Method Biomed Eng 2019;35.
43. Bordón P, Paz R, Monzón MD. Evaluation of the Performance of Atomic Diffusion Additive Manufacturing Electrodes in Electrical Discharge Machining. Materials 2022;15:5953.
44. Lophaven SN, Nielsen HB, Søndergaard J. A Matlab Kriging Toolbox. Technical Report IMM-TR-2002-12. 2002.

CHAPTER 4

FLAME RETARDANCY OF POLYMERS

TABLE OF CONTENTS

1. INTRODUCTION

Several strategies exist to improve the flame retardant properties of polymers such as engineering approach, less flammable polymers, and addition of flame retardants (FR) [1]. Of these, the latter has been selected because it is a well-accepted method, cost effective and relatively easy to incorporate. Among the available flame retardants, those of natural origin are used because they provide additional environmental value to the composite under study and their use is relatively recent. FR additives have the disadvantage that they are not universal for all polymeric matrices, so the following additives have been selected from those reviewed in Chapter 2 considering the polymers to be used. The minerals brucite, boehmite and colemanite, the biobased compound lignin and, finally, expandable graphite. Since these additives have not been studied in detail, it is necessary to perform several cycles until the optimum percentage is obtained. For this reason, three stages have been carried out in this study. The procedure consists in establishing different additives at different percentages, performing the characterization, optimising the results, and finally executing an iterative process until the optimum solution is reached. The following diagram describes each stage with the polymeric matrices and additives used.

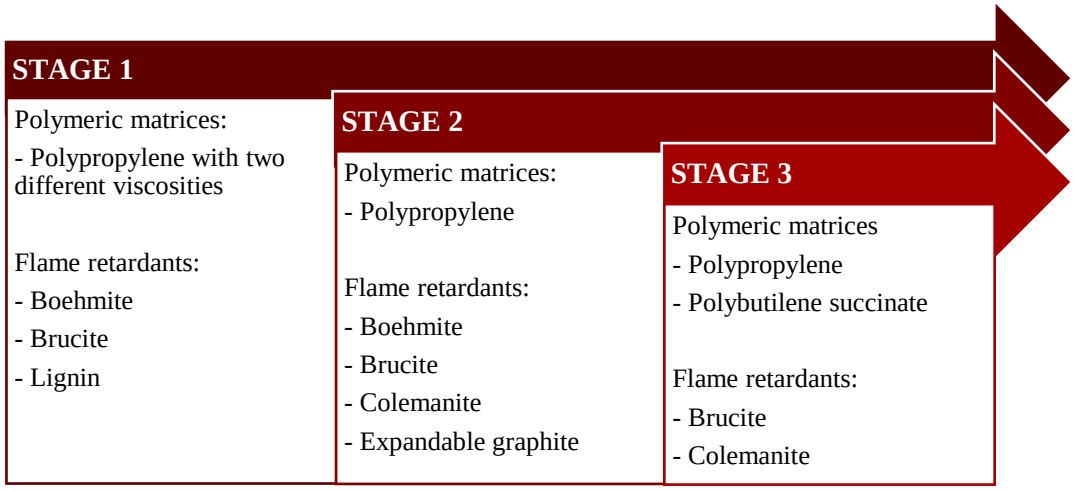

FIGURE 1: DIAGRAM OF THE STAGES CARRIED OUT TO IMPROVE THE FIRE PROPERTIES OF POLYMERS

Each stage carried out is described below, with results, discussion, optimization and, finally, conclusions that have led to the next stage. For the discussion of results, an ANOVA analysis was carried out to study the effect of the different additives and matrices. All materials and methods used are explained in detail in Chapter 3 and all the results are shown in the Annex.

2. STAGE 1

As shown in the diagram above, in the first stage the effect of boehmite, brucite and lignin on polypropylene is studied. According to the literature, minerals should be used up to 60-70% to obtain a fireproof material [2,3]. For this reason, boehmite and brucite were used at 45 and 60% to study their effect and tendency. On the other hand, some authors have shown that 20% lignin improves the fire properties of polypropylene. For this percentage, a reduction of the heat release rate (HRR) between 58 and 66% is obtained [4,5], so it was decided to study the effect of lignin at 10 and 20%. In addition, to test the effect of polymer viscosity, polypropylene was used at two different viscosities, PP1101S with MFR of 24 g/10 min and PP1151K with MFR of 3 g/10 min. The following table summarises all the mixtures studied, specifying matrix, additive, percentages, and nomenclature of the samples.

TABLE 1: MIXTURES OF PP AND FLAME RETARDANT ADDITIVES TESTED IN STAGE 1

Matrix	Additive	Percentage	Nomenclature
PP1101S	-	-	PP1101S
	Boehmite	45	PP1101S+45%Boeh
		60	PP1101S+60%Boeh
	Brucite	45	PP1101S+45%Bruc
		60	PP1101S+60%Bruc
	Lignin	10	PP1101S+10%Lig
		20	PP1101S+20%Lig
PP1151K	-	-	PP1151K
	Boehmite	45	PP1151K+45%Boeh
		60	PP1151K+60%Boeh
	Brucite	45	PP1151K+45%Bruc
		60	PP1151K+60%Bruc
	Lignin	10	PP1151K+10%Lig
		20	PP1151K+20%Lig

In this stage, due to the use of two polymeric matrices and three different additives, a multifactorial ANOVA analysis was performed to study the influence of each factor. To analyse the effect of the matrix, all the PP1101S samples were compared with all the samples with PP1151K because in both polymeric matrices the same mixtures were manufactured with the same percentages of additive. On the other hand, as the additives have been used at two percentage levels, not only the type of additive but also its proportion has an influence. For this reason, each group was compared independently, i.e., samples with 45%Boeh, with 60%Boeh, 45%Bruc, etc., analysing not only the effect of each additive, but also the percentage used.

2.1 COMPOSITE PREPARATION

Due to the flame retardants are in powder form, the particle size is an important aspect to consider to achieve a good distribution and homogeneity of the mixture. For this reason, a particle size analysis of the polymers was performed after cryogenic grinding. Figure 2 shows the results of the cumulative distribution (Q3) obtained with the Helos (H1533) & Cuvette analyser. It is observed that PP1151K, which corresponds to the more viscous PP, has a larger particle size distribution compared to PP1101S. D10, which is the point in the distribution curve where 10% of the particles fall, is 554.4 µm for PP1151K, whereas for PP1101S is 121.4 µm. Furthermore, D50 and D90 of PP1151K are 699.8 and 838.5 µm respectively, whereas for PP1101S they are 299.2 and 477.5 µm, so there is a significant difference in the particle size of the two matrices. This fact can be associated with the difference in mechanical strength and hardness of the materials, since the technical data sheet of the polymers indicates that the more viscous polymer has a Charpy notched impact strength of 5 kJ/m^2 compared to 2.5 kJ/m^2 of PP1101S. Therefore, PP1151K needs more force or more cycles to grind it into smaller particles. Taking this into account, a homogeneity analysis is performed after extrusion to verify the correct distribution of the additive particles in the samples with PP1151K.

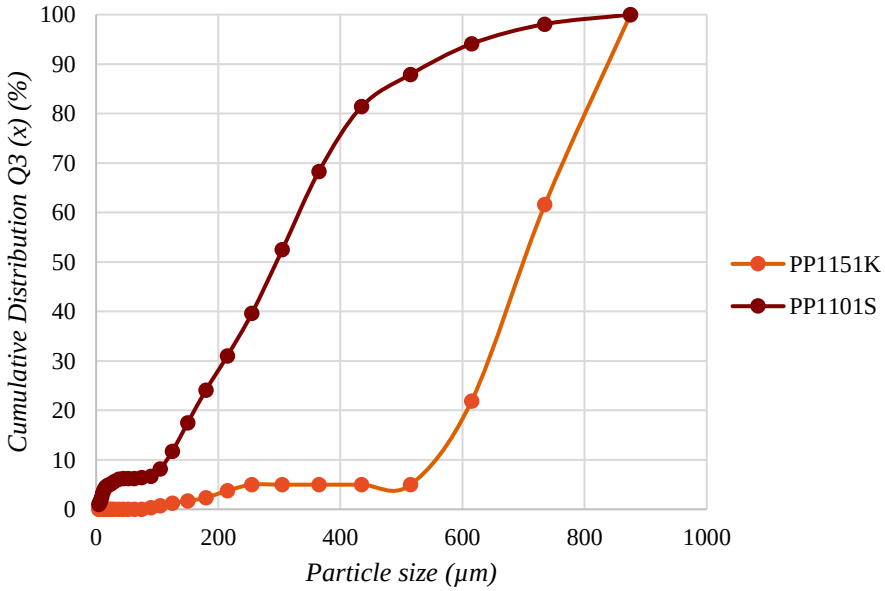

FIGURE 2: PARTICLE SIZE ANALYSIS OF PP1101S AND PP1151K

When the material was fed into the hopper of the extruder, it was observed that traces of additive remain in the bag used for drying, so the percentage may be reduced. Regarding the hopper, it has a paddle that rotates, which prevents the formation of a dome and the agglomeration of the particles, and favours mixing (Figure 3). In addition, the feeding system has two screws that also favour mixing.

FIGURE 3: FEEDING SYSTEM OF THE EXTRUDER

During the extrusion it was observed that, in the mixtures corresponding to 60%, the pressure increased due to the additive, but within normal operating parameters. The mixture PP1151K+60%Bruc, due to the higher viscosity of the polymer and the high additive load, presented a rougher surface and sometimes the filament broke during the process. This is due to the mixture behaves like a paste, does not flow properly and breaks. However, in the rest of the mixtures with minerals, there were no incidents, which can be associated with the lower density of the brucite particles with respect to boehmite. As this mineral has a lower density, its particles occupy more volume in the mixture, so there is less volume of plastic in proportion that can help in the flow of the mixture. Regarding the mixtures with lignin, steam was observed at the end of extrusion, and a toasted odour and colour, which may be associated with the beginning of the degradation of the additive.

Once the mixtures were obtained, the homogeneity test was carried out using a TGA. The PP1151K+60%Bruc sample was selected because of the larger polymer particle size that could hinder the mixing and because of the incidences encountered during extrusion. The TGA test was carried out on three different pellets in air from 30 to 600°C at 10°C/min. The curves were compared to observe if there were any differences, especially in the final percentage when the polymer had degraded and only the additive remained. Figure 4 shows the curves for each replicate and it is observed that at the end of the test there is practically no difference between them (0.55%), which leads to the conclusion that the extrusion is homogeneous. It should be noted that the final percentage is less than 60% of added additive, as the additive decomposes with temperature into the corresponding oxide (MgO) and therefore the quantity decreases.

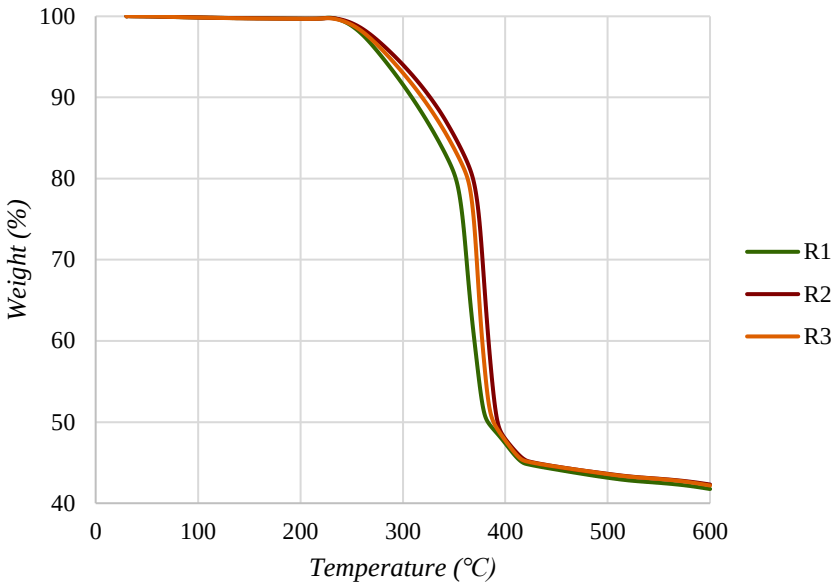

FIGURE 4: TGA OF PP1151K TO STUDY THE HOMOGENEITTY OF THE EXTRUSION

Once the homogeneity of the mixtures was verified, the plates for characterisation of the materials were manufactured by compression moulding. Some of the plates obtained are shown below (Figure 5). It is observed that the mixtures with boehmite acquire a light beige colour, while with brucite present a green beige and for lignin a dark brown. Visually, a small difference is observed between the PP1101S and PP1151K plates, which is more noticeable in plate G) PP1151K+60%Bruc. It is observed that the colour is not homogeneous as in plate C) PP1101S+60%Bruc because splay marks of the material can be seen running from the centre to the corners of the plate. Therefore, the particle distribution may differ between these parts, due to the high viscosity of the mixture, which hinders the fluency and consequently the homogeneity of the plate.

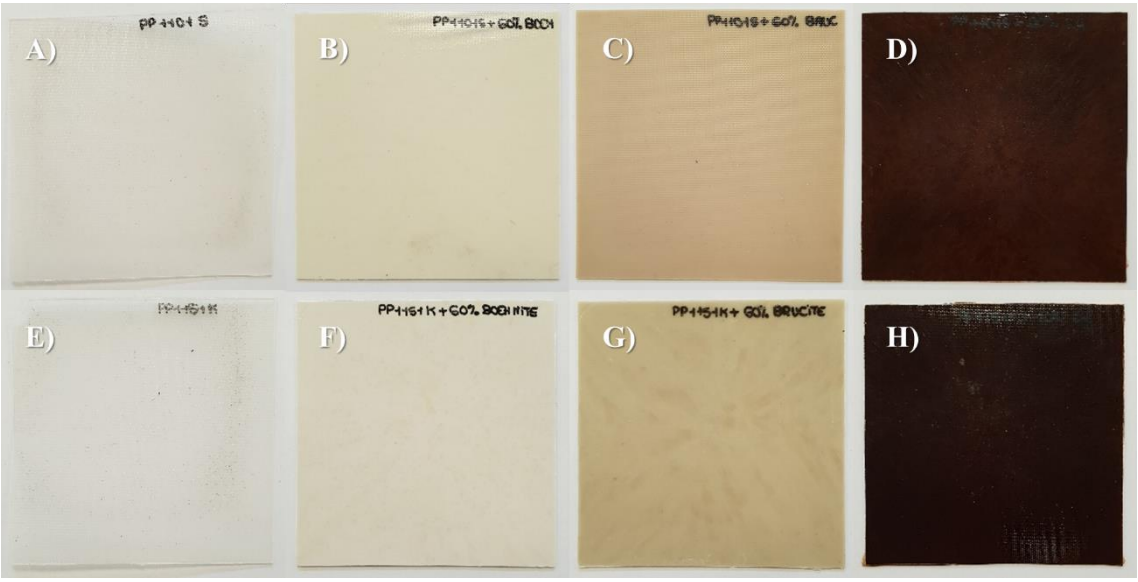

FIGURE 5: PLATES MANUFACTURED IN STAGE 1. A) PP1101S, B) PP1101S+60%BOEH, C) PP1101S+60%BRUC, D) PP1101S+20%LIG, E) PP1151K, F) PP1151K+60%BOEH, G) PP1151K+60%BRUC, H) PP11151K+20%LIG

2.2 PRELIMINARY CHARACTERIZATION

Next, the density and ash content of the samples was determined. Table 2 shows first the results obtained in the densimeter, then the results of the ash content, and finally the results of the estimated additive content ($\%ash_{est}$). The calculation of the estimated additive percentage can only be carried out for minerals since they do not decompose completely (they are converted into the corresponding oxide). For this calculation, the ash content obtained for the polymer ($\%ash_{PP}$) is subtracted from the average value of the mixture ($\%ash$), thus obtaining the ash content corresponding to the presence of additive in the composite. Then, this value is divided by the experimentally obtained ash value of the additive ($\%ash_{add}$), found at the end of the table, thus obtaining the estimated percentage of additive in the composite. With this, the experimental value of the additive is used instead of the theoretical value obtained from the decomposition reaction because these additives are not 100% pure, therefore, the real value is slightly higher.

$$\%add_{est} = \frac{(\%ash - \%ash_{PP})}{\%ash_{add}} \cdot 100$$

TABLE 2: RESULTS OF DENSITY AND ASH CONTENT OF STAGE 1 MIXTURES AND ADDITIVES

Sample		Density (g/cm^3)	Ash content (%)	Estimated additive content (%)
PP1101S		0.895 ± 0.003	0.09 ± 0.10	-
PP1101S+45%Boeh		1.287 ± 0.003	36.94 ± 0.24	43.18
PP1101S+60%Boeh		1.508 ± 0.004	49.02 ± 0.18	57.34
PP1101S+45%Bruc		1.235 ± 0.002	31.88 ± 0.57	44.52
PP1101S+60%Bruc		1.398 ± 0.003	42.02 ± 0.86	58.72
PP1101S+10%Lig		0.907 ± 0.010	0.14 ± 0.06	-
PP1101S+20%Lig		0.854 ± 0.016	0.36 ± 0.04	-
PP1151K		0.898 ± 0.002	0.08 ± 0.03	-
PP1151K+45%Boeh		1.291 ± 0.002	37.33 ± 0.21	43.64
PP1151K+60%Boeh		1.497 ± 0.006	49.17 ± 0.38	57.51
PP1151K+45%Bruc		1.235 ± 0.002	32.05 ± 0.44	44.76
PP1151K+60%Bruc		1.381 ± 0.009	41.88 ± 0.77	58.52
PP1151K+10%Lig		0.920 ± 0.003	0.15 ± 0.04	-
PP1151K+20%Lig		0.927 ± 0.010	0.30 ± 0.06	-
Boehmite		3 – 3.07 [6]	85.34 ± 0.12	-
Brucite		2.3 – 2.4 [6]	71.41 ± 0.20	-
Lignin		1.35 – 1.5 [7]	1.83 ± 0.01	-
p-value	**Matrix**	0.4413	0.3161	-
	Additive	0.0000	0.0000	-

In addition, the results of the multifactorial ANOVA analysis for matrix and additive are shown at the end of Table 2, and those with significant differences (p-value<0.05) are marked in red. The results obtained refer to the mixtures, the values obtained for the additives individually are not included in the statistical analysis. As for the p-value results, it is observed that the additive has a statistically significant effect on both density and ash content, while no differences are observed due to the matrix.

In terms of density, it is important to determine the density of the materials since in certain applications the weight of a part is key and in fact, the window of densities suitable for a given application is often quite small [8]. Firstly, it is observed that the additive has a significant effect because the density of the mixtures increases with the percentage of additive due to these have a higher density than polypropylene. However, for the PP1101S+20%Lig sample this trend is not observed since the density of the mixture is slightly lower than PP. In this sample, when the plates were cut, holes or air bubbles were observed inside the material, which may have caused an erroneous measurement of the density. Then, when comparing the different additives, it is observed that the blends with boehmite are the densest, followed by brucite and lignin, because they follow the trend of particle density. Finally, it is observed that there are no significant differences with respect to the matrix because the densities obtained for the same samples with the two polypropylenes are similar.

Regarding the study of the percentage of ash, the additives are analysed first, whose results are shown at the end of the table. To understand the difference between the different additives, it is necessary to consider their decomposition reaction. Brucite is the magnesium hydroxide mineral, so when it decomposes it forms magnesium oxide, and boehmite is the aluminium oxide-hydroxide mineral, and when it decomposes it forms aluminium oxide. Considering the reactions shown below and the molecular weights of the compounds, the ashes obtained with boehmite should be higher than those corresponding to brucite, which is confirmed experimentally by obtaining 85.3% compared to 71.4%. As mentioned above, the percentages obtained are slightly higher than those calculated theoretically because the minerals have not undergone a refining process and therefore present other metallic compounds that increase the ash content. As for lignin, it is observed that since it is an organic polymer composed of carbon, hydrogen, and oxygen, it is almost completely degraded by the action of temperature and the ash that remains is mainly due to the presence of sodium sulphate impurities in the lignin (Figure 6).

$$Mg(OH)_2 \rightarrow MgO + H_2O$$
$$2AlOOH \rightarrow Al_2O_3 + H_2O$$

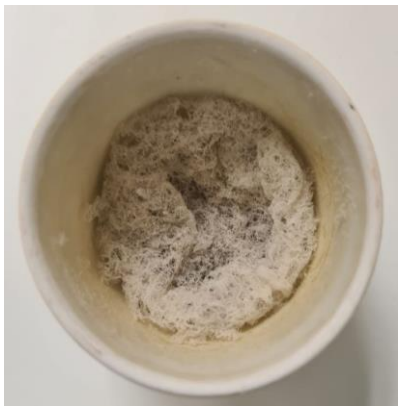

FIGURE 6: IMAGES OF THE ASHES FOR LIGNIN

Then, the analysis of the ash content of the PP mixtures with the additives is carried out. Firstly, the virgin PP samples do not differ significantly from each other and therefore the matrix does not affect the ash content either. Polypropylene, as it is composed of carbon and hydrogen, it decomposes completely and has a very low ash content due to the additives added by the manufacturer. As for the PP samples with additive, the ash content increases with the additive percentage and is higher in boehmite samples than in brucite samples due to the decomposition reactions mentioned above. Finally, in the lignin samples, the ash content is slightly higher than in the virgin polymer, because although the additive is completely degraded, the lignin impurities remain.

Lastly, the analysis of the estimated percentage of minerals shows a small reduction compared to the amount added. This is because of the traces of additive observed in the bag used for drying and that the particles were flying slightly at the entrance of the extruder. However, the reduction is not considered to be very significant.

2.3 SEM MICROSCOPY

In this first stage, SEM microscopic analysis of the additives and tensile test fractures was carried out. Figure 7 shows the images obtained from the additives at the same 2500x magnification. Firstly, it can be observed that boehmite presents a more homogeneous particle size compared to the other additives. The particles exhibit a similar structure with cubic and cuboid shapes, as reported by other researchers [9]. On the other hand, brucite presents different particles sizes with a layered structure. This structure has been reported by Pang et al. [10], who analysed the structure by TEM and justified that brucite exhibits one layer of magnesium cations sandwiched between every two layers of hydroxyl groups. Finally, lignin particles are irregular in shape and sized and presents a structure of irregular granules linked together. The structure of

lignin depends on its origin, extraction process and subsequent treatment and, in this case, it is kraft softwood lignin and its structure corresponds to that reported in the literature [11].

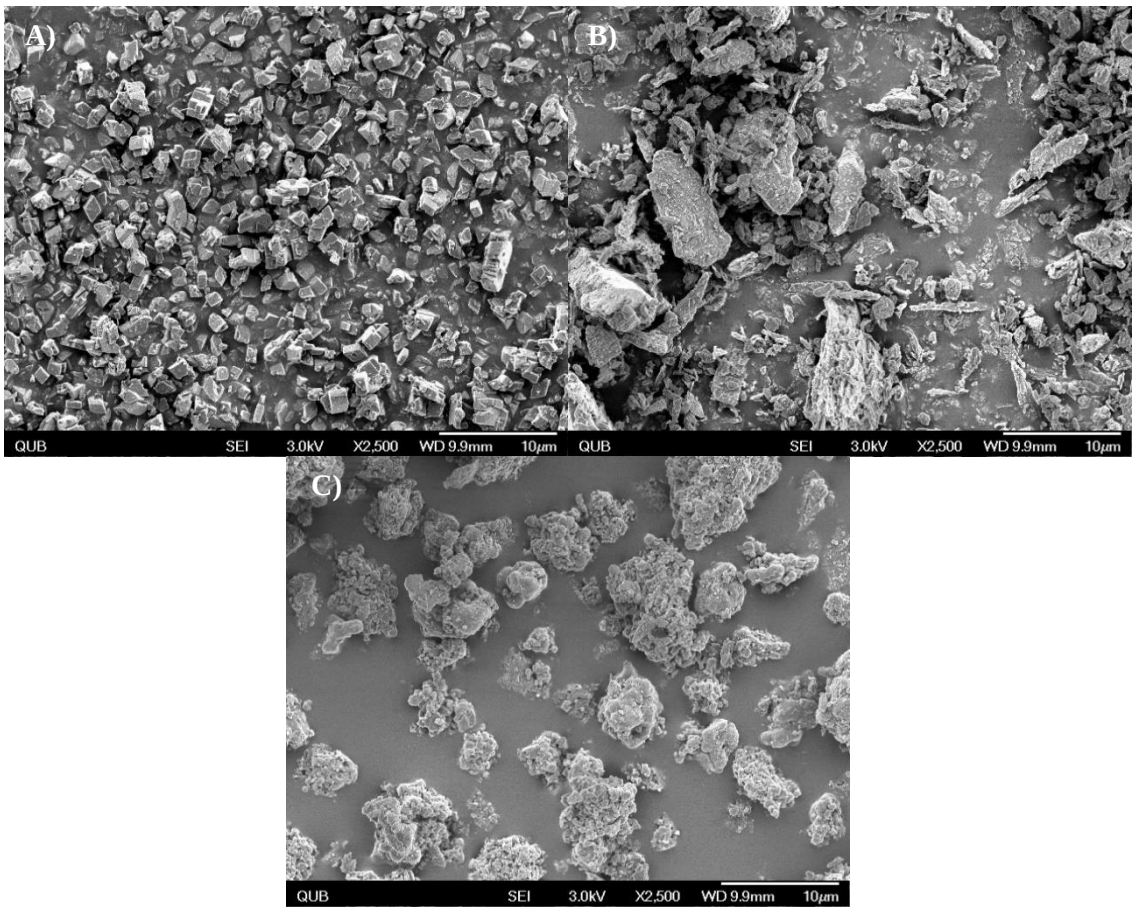

FIGURE 7: SEM IMAGES OF ADDITIVES OF STAGE 1. A) BOEHMITE, B) BRUCITE, C) LIGNIN

Figure 8 shows some of the fractures of the tensile test specimens of the three additives. The observation of this area of the specimen has been chosen because it allows us to know how the facture has been, if it has been produced by agglomeration of particles or if they are well adhered to the plastic. Firstly, a homogeneous distribution of the additives within the matrix is observed. In the PP1101S+45%Boehmite specimen (Figure 8A), the additive particles are integrated within the matrix, and it is shown that the plastic stretched until the fracture. In the specimen with brucite (Figure 8B), the laminar structure of the particles is clearly observed, and they are well adhered to the PP. In this case, the same elastic rupture does not occur, the fracture has broken all at once without plastic deformation. Finally, in the mixture with lignin, it can be observed that the particles have acquired a more regular spherical shape when mixed with the polypropylene, due to the processing and heating of the particles during extrusion. As the samples with brucite, the breakage of the specimen has occurred without plastic deformation because no stretching of the polymer can be observed.

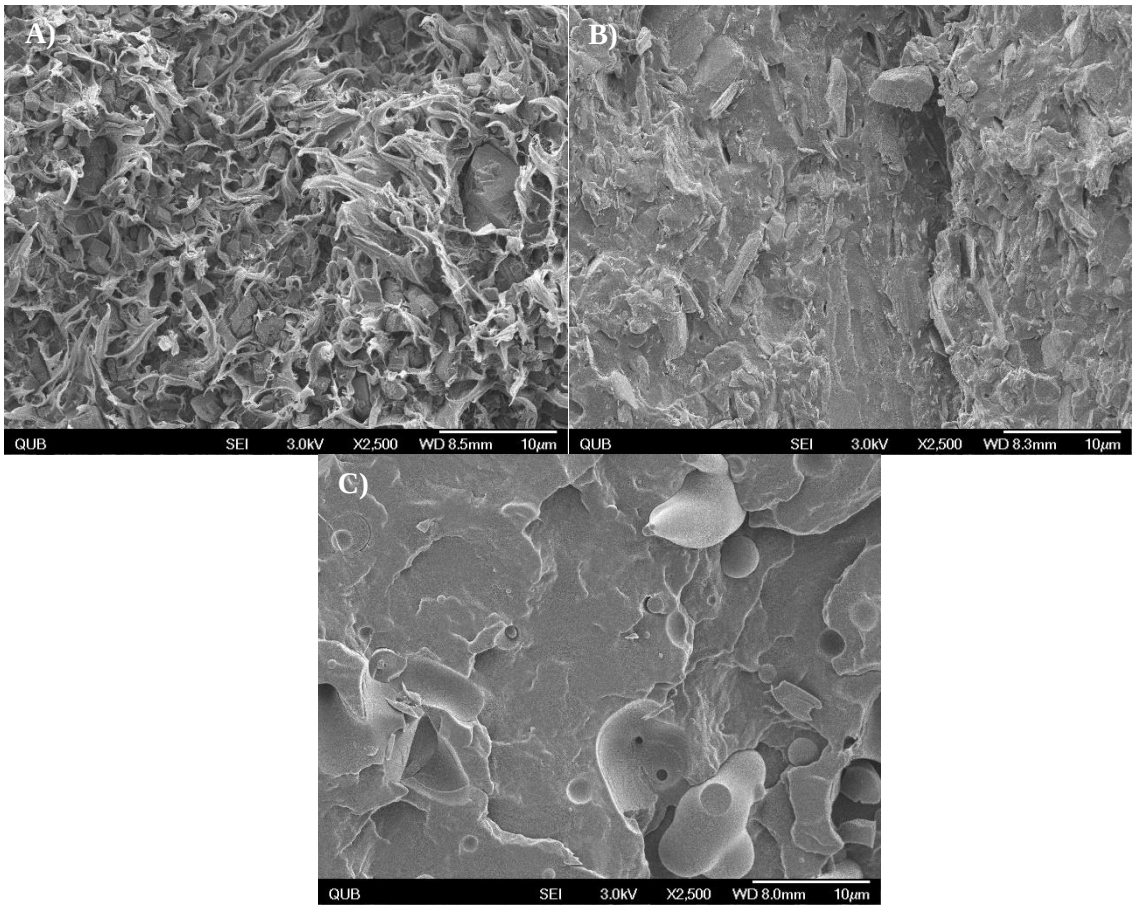

FIGURE 8: SEM IMAGES OF TENSILE TEST FRACTURES OF STAGE 1. A) PP1101S+45%BOEHMITE, B) PP1101S+45%BRUCITE, C) PP1101S+20%LIGNIN

2.4 THERMAL PROPERTIES

Flame retardant additives are compounds that generally modify the thermal properties of polymeric matrices. For this reason, DSC, TGA and DMTA were carried out to observe how boehmite, brucite and lignin influence these properties.

2.4.1 DSC

As explained in Chapter 3, DSC tests have been performed with two heating ramps to eliminate the effect of the processing history. The results obtained for the second heating and cooling curves are shown below together with the results of the multifactorial ANOVA analysis.

First, Table 3 shows the temperature results of the second melting curve, onset temperature ($T_{onset,m}$), end temperature ($T_{end,m}$) and melting temperature (T_m), as well as the range of the curve. The range of the curve, which corresponds to the difference between the onset and end temperatures, has been calculated because it provides information of the size distribution of the polymer crystals. At the onset temperature, the smaller and less perfect crystals start to melt, and as the temperature increases, the thicker crystals melt until the end temperature is reached, at

which all the larger crystals have melted. Therefore, if the difference between the temperatures is small, it means that there is a more homogeneous distribution of crystal size, so the range reflects the uniformity of the structure [12]. In addition, the last rows of Table 3 show the p-value results of the multifactorial ANOVA analysis.

TABLE 3: DSC RESULTS OF SECOND MELTING CURVE FOR STAGE 1. PART 1

Sample		$T_{onset,m}$(°C)	$T_{end,m}$(°C)	Range (°C)	T_m (°C)
PP1101S		153.33	169.85	16.52	163.67
PP1101S+45%Boeh		152.30	166.79	14.49	164.50
PP1101S+60%Boeh		151.83	167.74	15.91	164.87
PP1101S+45%Bruc		156.15	168.01	11.86	165.00
PP1101S+60%Bruc		155.44	167.73	12.29	164.70
PP1101S+10%Lig		154.62	169.94	15.32	163.50
PP1101S+20%Lig		155.04	169.96	14.92	165.66
PP1151K		161.05	168.49	7.44	165.57
PP1151K+45%Boeh		155.50	167.06	11.56	164.35
PP1151K+60%Boeh		152.94	167.37	14.43	164.72
PP1151K+45%Bruc		156.95	167.50	10.55	164.33
PP1151K+60%Bruc		156.10	166.92	10.82	164.04
PP1151K+10%Lig		156.43	168.69	12.26	165.40
PP1151K+20%Lig		156.59	167.83	11.24	163.60
p-value	**Matrix**	0.0432	0.0245	0.0186	0.9779
	Additive	0.2607	0.0217	0.4836	0.9992

In the DSC test, it is observed that the matrix has a significant effect on the onset and end temperatures and on the range, while the additive only influences the end temperature. Furthermore, the peak temperature or melting temperature is not significantly affected by either of the two factors, in fact the temperatures are in the range 163.5 to 165.7°C. Analysing the matrix, it is observed that, on average, the onset temperature of the samples with PP1101S is lower than those with PP1151K, 154.1°C versus 156.5°C, and the end temperatures are slightly higher, 168.6°C versus 167.7°C. Consequently, the range of the curve is larger in the PP1101S samples, which means that the crystal size distribution is larger and less uniform. This fact is due to PP115K has nucleant, which generates more nuclei at the same cooling conditions, hence the structure is finer, and the range is smaller.

Next, the effect of the additives is analysed. On the one hand, it is observed that in the PP1101S matrix, boehmite decreases both the onset and end temperatures and slightly reduces the range, so this additive shifts the curve to the left, encompassing smaller crystals with a slight

improvement in the uniformity of the structure. On the other hand, both brucite and lignin reduce the range by increasing onset temperatures, so it is concluded that these additives make the size of the crystals more homogeneous, being better with brucite additive. In the case of the samples with PP1151K, when comparing the samples with and without additives, a significant difference is obtained in onset temperature and curve range. The samples with additive show a decrease in onset temperature of about 5ºC on average and an increase in range of about 4ºC with respect to unfilled PP1151K. However, when comparing the curves, this tendency is not observed (Figure 9) and this is due to the value obtained for the onset temperature of virgin PP1151K. The onset temperature, which is the melting extrapolated onset temperature, for Ehrenstein et al. is defined as "intersection of the extrapolated linear section of the falling peak edge with the baseline extrapolated from temperatures below the peak" [12]. As the peak geometry is sharper in the PP1151K sample, that intersection is more vertical, so the onset line is further away from the beginning of the curve and the temperature is higher. However, visually it can be seen that, as in PP1101S, the virgin matrix covers a larger range and that the addition of the flame retardants reduces this range. Then, when comparing the three additives, the same trend is obtained as for PP1101S. Brucite is the additive with the lowest temperature range, followed by lignin and boehmite. Therefore, it is concluded that additives alter crystal formation by decreasing the size range and making the crystalline structure finer, so they can act as nucleants.

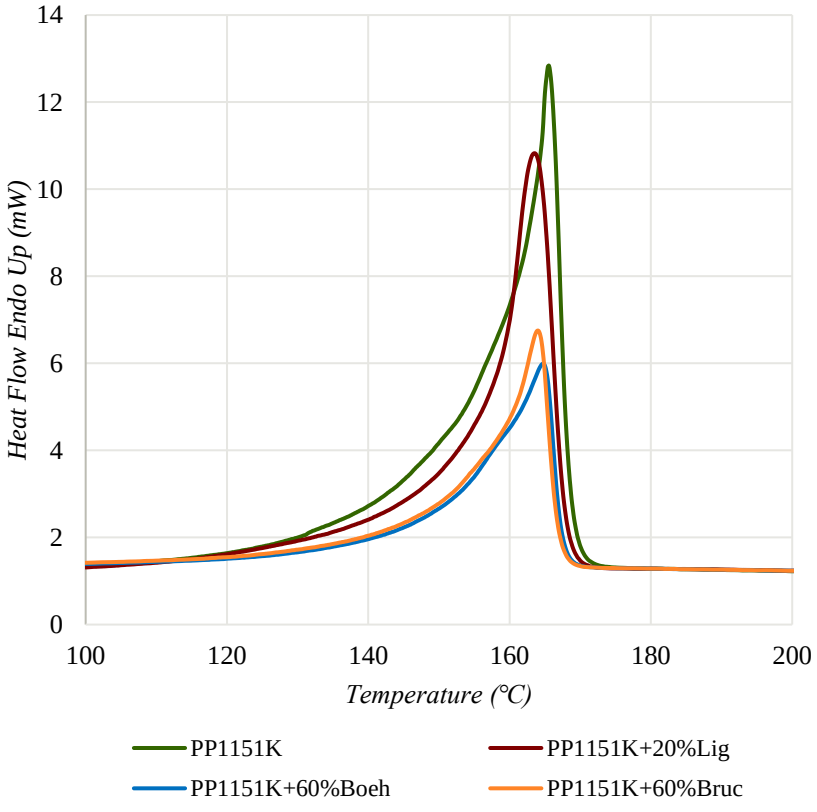

FIGURE 9: DSC MELTING CURVES OF PP1151K SAMPLES

Table 4 below shows the results of the partial areas, enthalpy of fusion and percentage crystallinity. The analysis of the partial areas is performed because it provides information on the size distribution of the polymer crystals and allows to determine whether the additives have any influence. X_1 represents the percentage of area under the curve between the start until the onset temperature, X_2 between the onset and the peak and X_3 between the peak and the end. For the areas, a significant effect of the matrix is obtained in X_1 and X_2 and of the additive in X_2 . In X_1 it is observed that the samples with PP1151K have a larger area in this section because the geometry of the peak is sharper (Figure 9). For this reason, the onset line is more vertical in these samples and the area to the left of the line is larger. This fact is clearly seen when comparing the two PP grades, in PP1101S the onset is 153.33℃ and X_1 is 31.71%, however as the onset of PP1151K is 161.05℃, the area increases to 57.44%. In the case of X_2 is the opposite, the area for PP1101S samples is larger than for PP1151K due to the difference in the onset temperature. In X_2 a significant difference is also obtained for the additive. It is observed that in the minerals, the area increases with respect to the percentage of additive, being higher in the samples with boehmite. Therefore, it is concluded that both boehmite and brucite favour the formation of crystals in the size range between the onset and peak temperature. As for lignin, the area also increases but with no clear trend with respect to the percentage. Lastly, no significant effect or trend is observed in X_3 for both factors.

TABLE 4: DSC RESULTS OF SECOND MELTING CURVE FOR STAGE 1. PART 2

Sample		X_1(%)	X_2 (%)	X_3 (%)	ΔH_m (J/g)	w_c (%)
PP1101S		31.71	42.68	24.63	77.41	37.38
PP1101S+45%Boeh		30.06	48.95	19.99	54.35	47.42
PP1101S+60%Boeh		23.68	61.64	13.59	42.33	51.10
PP1101S+45%Bruc		36.55	47.73	14.30	53.83	47.26
PP1101S+60%Bruc		34.66	49.73	14.32	41.44	50.03
PP1101S+10%Lig		30.88	40.43	27.67	77.63	41.65
PP1101S+20%Lig		30.57	51.20	17.14	65.99	39.83
PP1151K		57.64	27.60	13.36	87.57	42.28
PP1151K+45%Boeh		40.49	45.71	12.64	51.93	45.59
PP1151K+60%Boeh		29.24	57.29	12.42	39.28	47.41
PP1151K+45%Bruc		43.86	39.73	15.05	49.22	43.21
PP1151K+60%Bruc		42.86	42.48	13.49	40.26	48.60
PP1151K+10%Lig		39.00	44.84	14.86	85.98	46.13
PP1151K+20%Lig		40.21	38.05	20.60	72.96	44.04
p-value	**Matrix**	0.0061	0.0353	0.1299	0.5048	0.9933
	Additive	0.1261	0.0356	0.5235	0.0003	0.1759

Then, the enthalpy of fusion is analysed, which is significantly affected by the additives (p-value 0.0003). The additives used do not present any thermal effect in the temperature range of the test, melting, decomposition, etc., therefore, only the effects of the polymeric matrix are observed. For this reason, the enthalpy decreases with respect to the percentage of additive, since the lower the amount of polymer, the lower the enthalpy needed to melt it. Consequently, it is necessary to apply the correction in the calculation of the percentage of crystallinity (w_c) explained in Chapter 3 section 2.4.1. In crystallinity, although the effect of the matrix and the additives are not significant, there is a clear trend with respect to the additives. It is observed that in all cases the percentage of crystallinity increases with respect to virgin PP, which would confirm the nucleating effect observed previously in the range of the curve. Regarding to minerals, boehmite and brucite increase the crystallinity percentage with respect to the additive percentage used for the two matrices. The effect of boehmite on PP crystallinity has been studied by other authors such as Pedrazzoli et al. who, using boehmite from 2.5 to 10%, obtained an increase in crystallinity despite not correcting the formula with the polymer percentage [13] as well as Streller at al. in two studies with nanoboehmite [14,15]. Therefore, it is confirmed that boehmite has a nucleating effect on PP. The same applies to brucite, authors such as Cook M. and Cheng X. [16,17], among others, have verified the nucleating effect of brucite on PP, which confirms the findings of this study. Finally, with lignin the crystallinity percentage increases for 10%, but then decreases at 20% for both matrices. Since in other studies a decrease has been obtained with respect to the percentage of lignin used [18], that the reduction in the melting curve range was not very significant and that in the results the crystallinity apparently decreases at higher percentages, it is concluded that lignin does not act as a nucleating agent. Finally, when analysing the two matrices, as expected, the crystallinity of virgin PP1151K is higher than PP1101S due to the presence of nucleant in its composition. However, with additives, the difference between the two matrices is not observed. In fact, the values obtained for PP110S with boehmite and brucite are higher than those of PP1151K, which may be associated with the difference in viscosity. The nucleating action of the mineral filler is generally attributed to the existence of adsorption sites on the surface for the polymeric molecules [19]. Therefore, due to the high viscosity of PP1151K, the additive particles are more agglomerated, so the surface area accessible to the polymer is smaller and consequently the nucleating effect is reduced.

Lastly, it is studied the effect of the matrix and additives on the crystallisation curve. Table 5 shows the results of onset temperature ($T_{onset,c}$), enthalpy of crystallisation (ΔH_C), crystallisation temperature (T_C) and finally the difference between onset and peak temperatures. This last difference represents the crystallisation rate, because the smaller the difference, the higher the speed, and is calculated to study whether additives accelerate the formation of crystals of the polymer [20]. First, it is obtained that the additive significantly influences the onset temperature.

Boehmite and brucite increase the onset temperature up to 11.5°C due to their nucleating effect, because they favour the formation of crystals and, consequently, crystallisation occurs at higher temperatures. In the case of lignin, a reduction of the onset temperature is observed, which confirms that it does not act as a nucleant in PP. Comparing the matrices, virgin PP1151K has an onset temperature almost 7°C higher due to the nucleant of its composition. As in the melting, the effect of the additives is not as noticeable due to the viscosity of the matrix hinders their effect. Regarding to the crystallisation enthalpy, the same occurs as in the melting enthalpy, the additives reduce the percentage of polymer, so the enthalpy decreases with respect to the percentage of additive. Then, at the peak or crystallisation temperature, the same tendency is obtained as for the onset, the minerals increase the temperature due to their nucleating action with a more noticeable effect on the PP1101S matrix and the lignin decreases the temperature. Lastly, no significant differences are observed with respect to the matrix or additives in the crystallisation rate. In the case of the matrix, the difference between the $T_{onset,c}$ and T_C is lower in the samples with PP1151K, 3.38°C on average compared to 4.11°C for PP1101S, because the nucleant in its composition accelerates the formation of crystals. As for the additives, a clear trend is observed with boehmite since the difference between the temperatures decreases when the percentage of additive increases, so boehmite not only increases the amount of crystals, but it also favours their formation. On the other hand, brucite and lignin do not show a clear trend, so it is not possible to conclude whether they influence the crystallisation rate.

TABLE 5: DSC RESULTS OF COOLING CURVE FOR STAGE 1

Sample		$T_{onset,c}$ (°C)	ΔH_c (J/g)	T_c (°C)	$T_{onset,c}$-T_c
PP1101S		120.93	77.61	116.76	4.17
PP1101S+45%Boeh		128.89	54.60	125.62	3.27
PP1101S+60%Boeh		131.56	41.61	128.32	3.24
PP1101S+45%Bruc		127.65	53.75	124.20	3.45
PP1101S+60%Bruc		128.97	41.15	124.59	4.38
PP1101S+10%Lig		119.11	77.40	113.76	5.35
PP1101S+20%Lig		114.98	65.92	110.07	4.91
PP1151K		127.78	86.74	123.71	4.07
PP1151K+45%Boeh		128.41	51.54	125.06	3.35
PP1151K+60%Boeh		129.94	36.76	126.80	3.14
PP1151K+45%Bruc		127.21	48.59	122.97	4.24
PP1151K+60%Bruc		126.78	39.78	123.44	3.34
PP1151K+10%Lig		121.63	85.90	119.02	2.61
PP1151K+20%Lig		119.17	72.94	116.23	2.94
p-value	**Matrix**	0.3583	0.5730	0.9933	0.1766
	Additive	0.0097	0.0003	0.1759	0.9058

2.4.2 TGA

Firstly, the thermal stability of the flame retardants is studied in Figure 10 and it is observed that lignin is the additive with the lowest thermal stability, followed by brucite and boehmite. In addition to the graph, Table 6 shows the results obtained for the temperatures (left limit, 5%, onset and peak), the maximum mass loss rate and the final mass. The temperature at which the weight loss is 5% and the onset temperature have been determined because the curves have different shapes and steps, so analysing only the $T_{5\%}$ is not sufficient. The onset temperature was determined as the intersection of extrapolated starting mass with the tangent applied to the maximum slope of the TG curve according to Ehrenstein G. et al. [21].

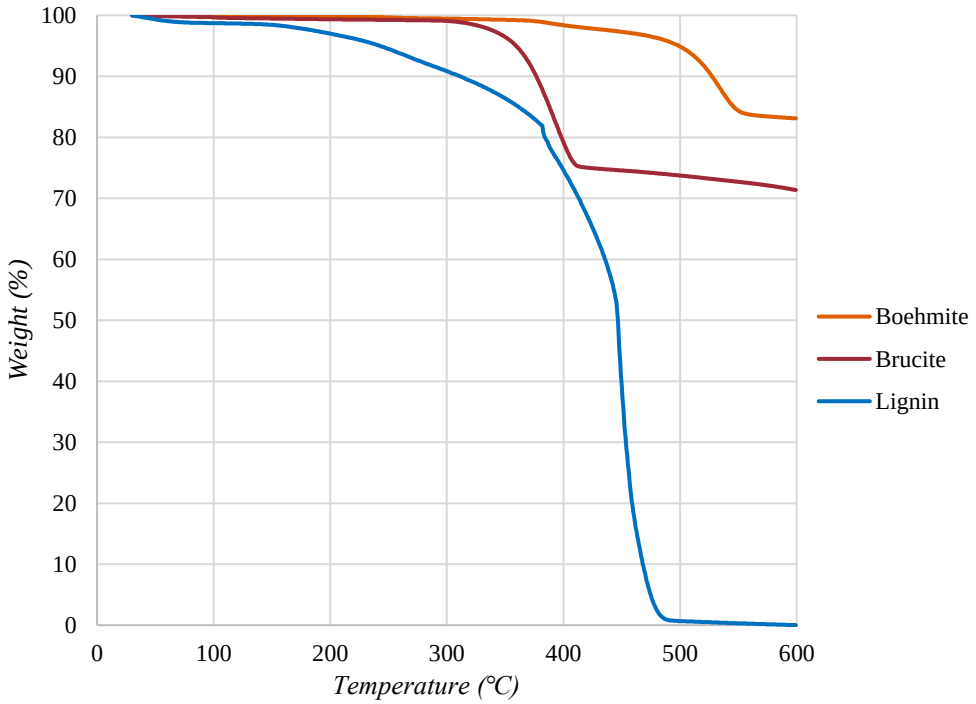

FIGURE 10: TGA CURVES OF BOEHMITE, BRUCITE AND LIGNIN

TABLE 6: RESULTS OF TGA TESTS OF FLAME RETARDANTS

Sample	T_L(°C)	$T_{5\%}$(°C)	T_{onset}(°C)	T_{peak}(°C)	Rate (%/°C)	m_F (%)
Boehmite	333.3	498.7	492.5	536	0.293	83.10
Brucite	285.6	359.3	357.1	392	0.491	71.35
Lignin	146.0	242.0	432.4	448	3.362	0.00

In the case of lignin, TGA curve shows that degradation occurs over a wide temperature range in several steps because lignin is composed by various oxygen functional groups that have different thermal stabilities [22]. The first step from 20 to 125°C corresponds to the release of humidity with a weight loss of 1.37%. Then, from 140 to 382°C with a weight loss of 16.83%, it

is produced the start of the thermal decomposition of lignin macromolecule with a T_L (left limit temperature) of 146°C and $T_{5\%}$ around 242°C. Subsequently, the degradation rate increases, obtaining the main peak at 448°C at a mass loss rate of 3.36%/°C. This step ranges from 382 to 478.5°C with a weight loss of 81% and corresponds to depolymerization reactions that forms various volatile products, whose nature and amount depend on lignin composition [23]. Finally, the degradation products are completely decomposed up to 600°C obtaining 0% of char residue. On the other hand, the TGA curve of brucite shows a single step, with a T_L of 285.6°C and $T_{5\%}$ of 359.3°C, so it is more thermally stable because its degradation/decomposition occurs at higher temperatures than that of lignin. The peak of maximum degradation occurs at 392°C with a mass loss rate of 0.49%/°C and corresponds to the decomposition of brucite into magnesium oxide. Although this peak occurs at a lower temperature than in lignin, it occurs at a lower rate and the sample is not completely degraded. After the end temperature of the step (409.6°C approximately), the sample continues to lose weight due to the remaining $Mg(OH)_2$ residues obtaining a final weight of 71.35% which corresponds to the ashes that would form a protective layer of the polymer. Finally, the degradation of boehmite also presents a single step, it starts at 333.3°C with a $T_{5\%}$ of 498.7°C and weight loss of 15.81%. In this case, the degradation peak occurs at higher temperature (536°C) with a mass loss rate of 0.29%/°C, lower than that of the other additives, making boehmite the most thermally stable additive. As in brucite, the final mass of ash is composed of the corresponding oxide.

Next, the effect of the different additives on the thermal stability of the mixtures is studied. To facilitate the analysis, the effect of each additive is studied separately, so Figure 11 shows the curves obtained for the samples of the two PP matrices and boehmite . Firstly, pure PP show a single degradation step, while the mixtures show two degradation steps. Both matrices present similar behaviour with small differences in T_L, $T_{5\%}$ and T_{onset} (Table 7). The most noticeable difference is in the zone of maximum degradation because in sample PP1101S it occurs at 351.3°C at a mass loss rate of 2.07%/°C, while in PP1151K it occurs at 341.3°C at 1.90%/°C. Then, in the samples with boehmite, two degradation steps are observed, the first one corresponds to the degradation of PP and the second one to the decomposition of the additive. With 45% boehmite, an increase in thermal stability is obtained because the onset and peak temperatures increase. However, this stability does not increase with the percentage of additive, since at 60% boehmite these temperatures decrease, obtaining even lower values than the unfilled PP. Shen-Peng Lui et al. obtained the same trend and justified that the decrease occurs because the agglomeration of the particles causes a deterioration of the thermal stability [24]. In fact, this would justify that in the sample with PP1151K even lower temperatures are obtained because the viscosity is higher, which makes mixing more difficult and favours the formation of agglomerations. Then, between 500-540°C the boehmite decomposes into aluminium oxide. Finally, in terms of final weight, the

samples with 45% boehmite have a 35.4% of sample weight while with for 60% boehmite 45.9% on average, which corresponds to the weight of ash that can act as a protective layer for the plastic.

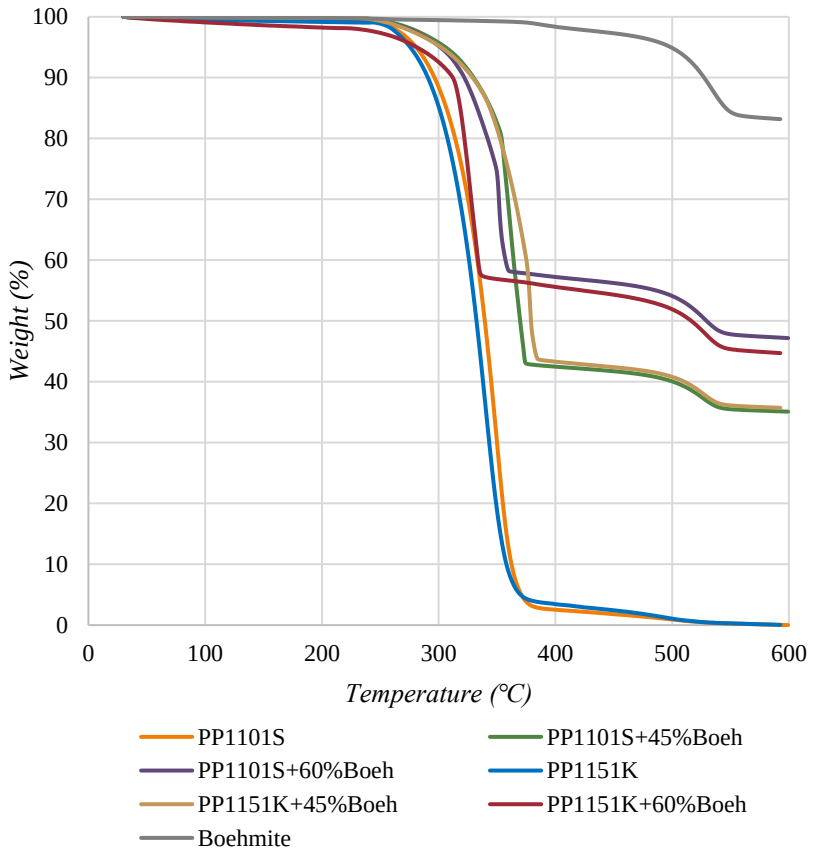

FIGURE 11: TGA CURVES OF STAGE 1 BOEHMITE SAMPLES

TABLE 7: RESULTS OF TGA TESTS OF BOEHMITE SAMPLES STAGE 1

Sample	T_L(°C)	$T_{5\%}$(°C)	T_{onset}(°C)	T_{peak}(°C)	Rate (%/°C)	m_F (%)
PP1101S	237.7	280.7	307.0	351.3	2.071	0.00
PP1101S +45%Boeh	234.4	305.3	344.8	361.3	2.070	35.09
PP1101S +60%Boeh	231.1	301.3	342.7	352.0	3.627	47.19
PP1151K	243.7	275.6	301.0	341.3	1.897	0.00
PP1151K +45%Boeh	234.4	302.0	318.5	378.7	3.433	35.68
PP1151K +60%Boeh	224.7	281.3	311.6	326.7	1.814	44.63

Next, in the samples with brucite, it is observed that the 45% samples degrade in one step and the 60% samples have two steps (Figure 12). Thus, with the 45% brucite, the degradation of the components occurs almost at the same time, so the retarding effect of brucite is activated at the ideal temperature to improve the thermal properties of PP. However, in the samples with 60%

brucite the same behaviour is not observed, the degradation occurs in two phases where the first one corresponds to the polypropylene and the second one to the additive. Furthermore, the PP1101S+60%Bruc sample shows a lower thermal stability than unfilled PP, which is not in accordance with what was expected due to the better thermal stability of the brucite compared to PP.

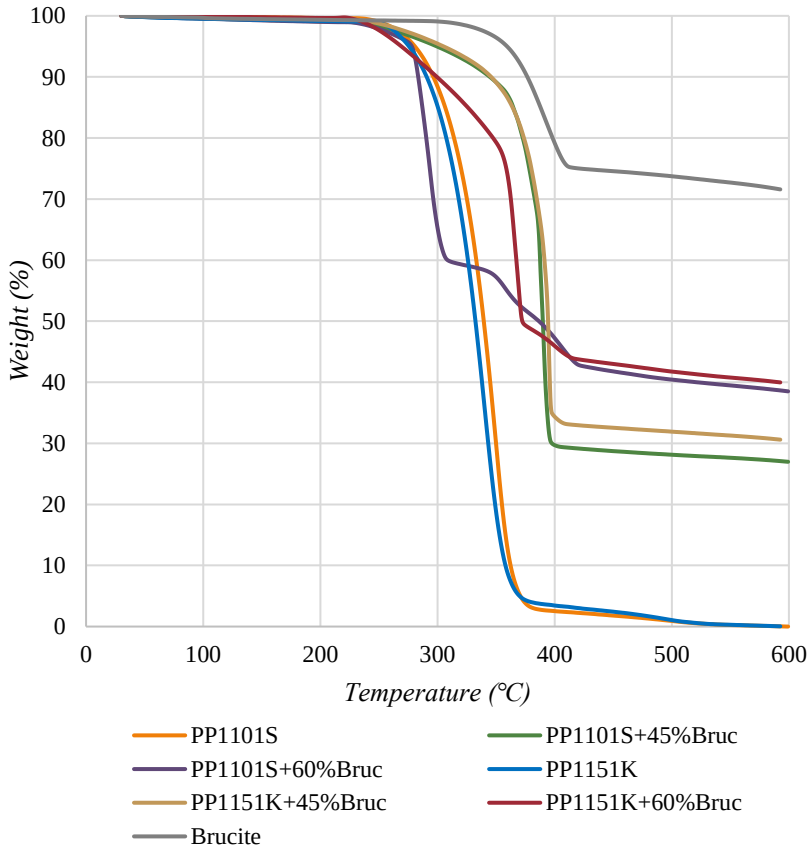

FIGURE 12: TGA CURVES OF STAGE 1 BRUCITE SAMPLES

TABLE 8: RESULTS OF TGA TESTS OF BRUCITE SAMPLES STAGE 1

Sample	T_L(°C)	$T_{5\%}$(°C)	T_{onset}(°C)	T_{peak}(°C)	Rate (%/°C)	m_F (%)
PP1101S +45%Bruc	222.7	299.3	378.9	391.3	4.881	26.98
PP1101S +60%Bruc	228.5	278.0	279.1	294.0	1.733	38.51
PP1151K +45%Bruc	226.9	304.7	365.7	395.3	6.934	30.47
PP1151K +60%Bruc	227.3	269	347.4	378.7	3.433	35.67

Table 8 shows the results obtained in the samples with brucite. First, it can be observed that in the 45% brucite samples, the thermal stability is improved because, although degradation starts earlier than with PP, degradation occurs at a slower rate and the additive shifts the curve to the

right. In these samples, the temperatures increase except for the T_L, which is reduced by 11°C on average with respect to those obtained with PP. The most significant increase corresponds to the maximum degradation temperature, which increases approximately 40°C with respect to unfilled PP. This is because the decomposition reaction of brucite is endothermic, so the reaction removes heat from the polymer and delays the thermal degradation of the material. In addition, the relatively high heat capacity of the magnesium oxide compared to the polymer matrix contributes to reduce the available thermal energy [25]. On the other hand, different behaviours are obtained in the 60% brucite samples. As in the case of the samples with boehmite, it is observed that despite increasing the percentage of additive, the thermal stability does not increase. On the one hand, in the PP1101S+60%Bruc the curve shifts to the left, obtaining a reduction in T_{onset} of almost 28°C and in T_{peak} of 57.3°C with respect to PP1101S, so the thermal stability of this mixture is significantly lower than that of PP1101S. On the other hand, in PP1151K+60%Bruc, the thermal stability is intermediate between the samples with 45%Bruc and the unfilled PP1151K. The degradation starts about 10°C earlier than in PP1151K, but as it occurs at a slower rate, the peak of maximum degradation is reached at 378.7°C, i.e., about 27°C higher than in PP1151K. Finally, between 350 and 410°C the remaining brucite decomposes into magnesium oxide. In summary, brucite apparently improves the thermal stability of polypropylene, but due to the discrepancy obtained in the samples PP1101S+60%Bruc, it is necessary to observe if this difference in thermal stability of both matrices will affect the fire tests.

Finally, the samples with lignin are studied in Figure 13. First, it is observed that degradation occurs in two steps. Due to the degradation range of lignin is from 150 to 500°C, the first step corresponds to the degradation of the matrix and lignin and the second to the degradation of lignin only. In the first step, it is observed that although the additive starts to degrade earlier than PP, it improves the thermal stability of the material because all the curves are shifted towards higher temperatures. In the left limit temperature (Table 9), an increase is obtained with respect to unfilled PP in all mixtures, but this does not increase with respect to the percentage of additive. This is because lignin degradation occurs at 150°C and the higher the percentage, the more significant the effect. Then, at $T_{5\%}$, T_{onset} and T_{peak} there is an increase compared to unfilled PP (Table 6Table 7) and the higher the percentage, the higher the temperature. This upward trend with the percentage of additive is due to the peak of lignin degradation occurs at 90-100°C higher than PP (448°C versus 341.3-351.3°C) , so the higher the amount, the greater the effect. However, although degradation occurs at higher temperatures, lignin accelerates the degradation rate which is a negative effect. Finally, in the second step from 270 to 450°C, the most complex components of lignin are degraded, leaving a small residue that finishes decomposing up to 600°C. Therefore, lignin improves the thermal stability of the mixture but does not leave residue such as minerals that can act as a protective layer of the polymer.

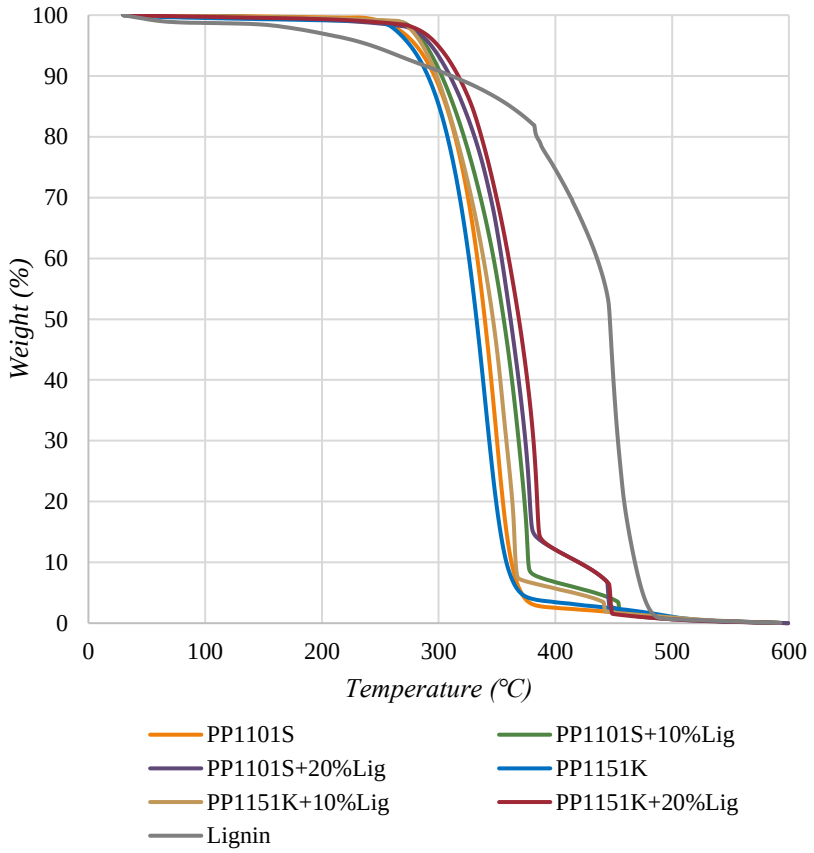

FIGURE 13: TGA CURVES OF STAGE 1 LIGNIN SAMPLES

TABLE 9: RESULTS OF TGA TESTS OF LIGNIN SAMPLES STAGE 1

Sample	T_L(°C)	$T_{5\%}$(°C)	T_{onset}(°C)	T_{peak}(°C)	Rate (%/°C)	m_F (%)
PP1101S +10%Lig	260.2	289.0	309.6	376.0	3.695	0.00
PP1101S +20%Lig	252.2	293.3	323.1	378.0	3.264	0.00
PP1151K +10%Lig	256.6	286.0	303.6	365.3	4.436	0.00
PP1151K +20%Lig	245.2	299.3	323.9	384.7	4.030	0.00

2.4.3 DMTA

PP blends were tested by DMTA to study the thermo-mechanical stability and to determine the glass transition temperature (T_g). First, the effect of temperature on the samples with PP1101S is analysed in Figure 14, where the storage modulus (E') is plotted as a function of temperature. The graph shows that the storage modulus decreases with respect to temperature for all samples. Initially, the decrease is less significant because this is the glassy state zone, where the material is stiffer so there is less molecular movement. However, from T_g (glass transition zone), which is around 7°C, there is an inflection point from which the drop in properties is more significant

because there is greater inter-molecular movement, i.e., greater loss of energy in the form of heat. In general, it is observed that the flame retardant additives increase the storage modulus with respect to virgin PP up to 140°C, after which the samples with lignin have a lower modulus. This increase is because the incorporation of rigid particles restricts the movement of the molecular chain providing stiffness to the material and, consequently, increases the modulus [13]. Therefore, it is concluded that up to 140°C all the samples with PP1101S and flame retardant additives have better thermo-mechanical stability, which is beneficial in case of fire.

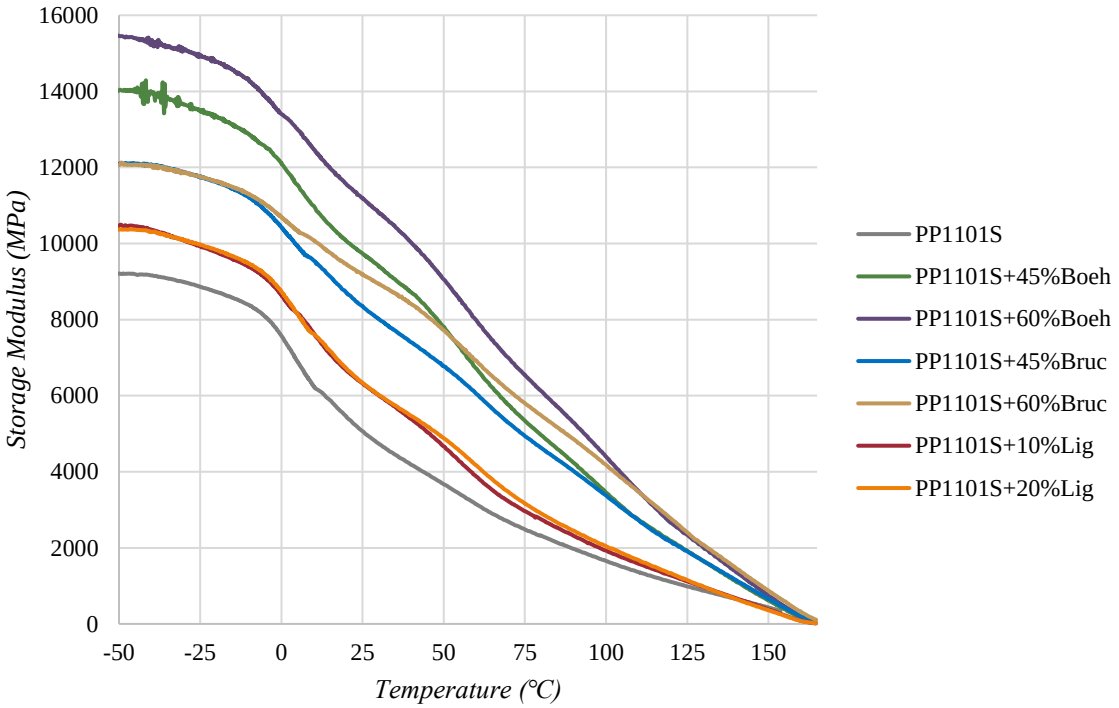

FIGURE 14: STORAGE MODULUS VS TEMPERATURE OF PP1101S SAMPLES OF STAGE 1

Then, comparing the different additives, the PP1101S+60%Boeh sample shows the highest E' value, making it the stiffest and the most thermo-mechanical stable mixture of the PP1101S samples. This is followed by the PP1101S+45%Boeh and PP1101S+60%Bruc samples. The PP1101S+45%Boeh sample has a higher storage modulus up to 50°C, at which point it crosses over with the PP1101S+60%Bruc. This crossover means that the PP1101S+45%Boeh sample is stiffer than PP1101+60%Bruc at the beginning (from -50 to 50°C) but as it loses mechanical properties more quickly, it is overtaken above this temperature by PP1101S+60%Bruc. In conclusion, because of the interest in higher stability at higher temperatures due to the application of the material, PP1101S+60%Bruc would be selected from these samples. Then there is the PP1101S+45%Bruc, which is equal in the initial zone (-50 to 0°C) to the PP1101S+60%Bruc sample. This sample, as with the PP1101S+60%Bruc, loses mechanical properties more slowly than PP1101S+45%Boeh, so it reaches similar E' values at around 110°C. Therefore, the samples with brucite, although they have a lower thermo-mechanical stability in the initial part, their

properties decrease more slowly with respect to the temperature, so at high temperatures they are on a par with boehmite samples. Finally, there are the samples with lignin, which have a higher stiffness than PP1101S up to 140°C, but the increase in the percentage of additive has no influence, as the curves obtained for both percentages are similar.

The results obtained for the samples with PP1151K are shown in Figure 15. As with PP1101S, the storage modulus decreases with temperature and this decrease is more significant from the glass transition which in this case is around 8°C. In this matrix, it is observed that the samples with lignin do not improve the thermo-mechanical stability because the curves obtained are very similar to those of PP1151K, obtaining even lower values in some ranges, as in the case of PP1151K+20%Lig from -50 to approximately 10°C. On the other hand, it is observed that in the samples with boehmite and brucite, the storage modulus increases considerably with respect to PP1151K, and it also increases with the percentage of additive. This is because when stiff particles are incorporated into the matrix, the higher the percentage, the greater the stiffness. Furthermore, comparing boehmite and brucite, it is observed that the samples with brucite have a higher storage modulus than those with boehmite at the same percentages of additive, so it is concluded that with the PP1151K matrix, the samples with the highest thermo-mechanical stability correspond to the samples with brucite.

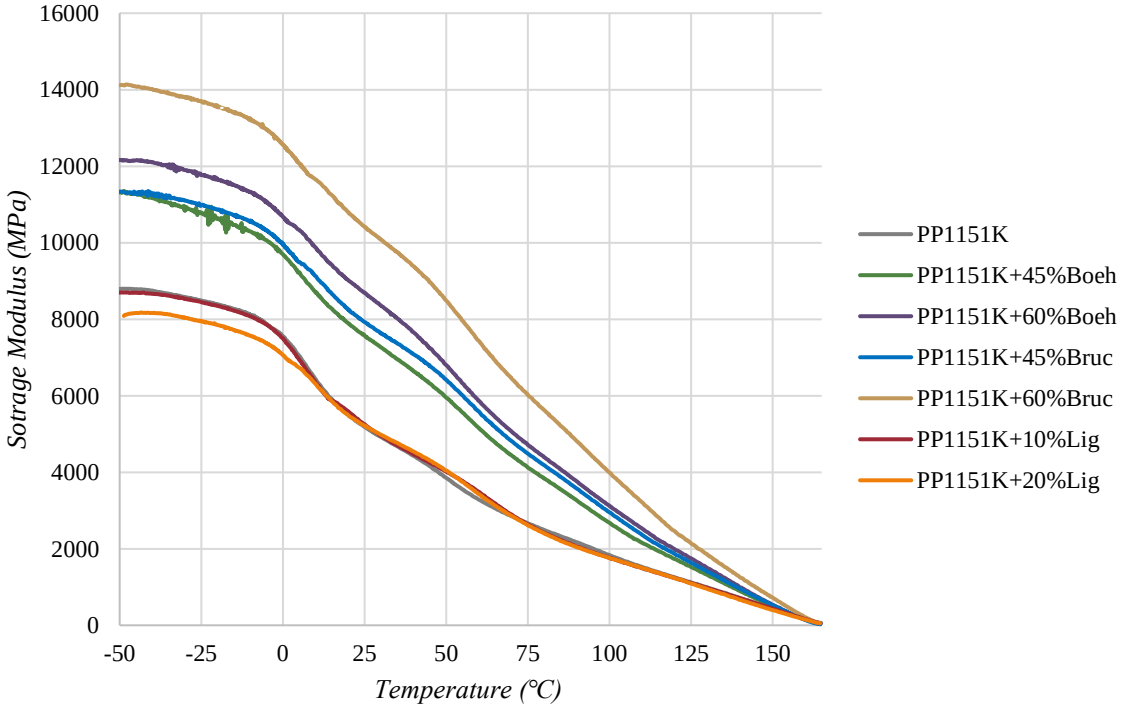

FIGURE 15: STORAGE MODULUS VS TEMPERATURE OF PP1151K SAMPLES OF STAGE 1

Table 10 shows the results of the storage modulus at room temperature (20°C), 100°C and 150°C for both matrices and the p-values. In the statistical analysis it is obtained that the additive

has a statistically significant effect on E' while the matrix does not have an influence. The additive has a significant effect because it is observed that at the three temperatures the modulus changes not only by the type of additive, but also by the percentage. At 20ºC, the storage modulus increases with the percentage of additive in the samples with minerals, while with lignin no differences are observed. In fact, in the PP1151K matrix, the results obtained in the samples with lignin are similar to those of the unfilled PP. As for the minerals, it is obtained that with the PP1101S matrix, the samples with boehmite have the highest E' values, 19% more than the brucite mixtures, while with PP1151K it is the brucite with approximately 12% more. Next, at 100ºC the same trend is obtained while at 150ºC it changes. At this temperature, it is observed that the mixtures with brucite are the most stable for the two matrices because they have the highest storage modulus values. This is because the loss or drop in modulus is slower in these samples, so from 110-115 ºC the mixtures with brucite outperform those with boehmite. On the other hand, in the case of lignin, it is observed that in both matrices a decrease in properties is obtained with respect to unfilled PP, which is counterproductive. In summary, boehmite and brucite significantly improve the mechanical stability of polypropylene with respect to temperature, while lignin worsens at higher temperatures.

TABLE 10: DMTA RESULTS OF STAGE 1 SAMPLES

Sample		$E'_{20ºC}$(MPa)	$E'_{100ºC}$(MPa)	$E'_{150ºC}$(MPa)	T_g (ºC)
PP1101S		5453.7	1654.7	431.3	4.94
PP1101S+45%Boeh		10067.7	3451.3	616.6	6.12
PP1101S+60%Boeh		11561.4	4396.9	740.8	8.58
PP1101S+45%Bruc		8710.0	3377.7	656.1	9.00
PP1101S+60%Bruc		9458.1	4184.3	880.3	8.50
PP1101S+10%Lig		6661.9	1928.0	378.9	7.36
PP1101S+20%Lig		6723.0	2047.1	360.9	6.17
PP1151K		5505.7	1836.2	437.6	7.60
PP1151K+45%Boeh		7900.2	2681.5	492.2	7.65
PP1151K+60%Boeh		9025.3	3125.8	535.6	9.84
PP1151K+45%Bruc		8251.4	2952.6	529.3	9.24
PP1151K+60%Bruc		10805.2	3997.5	724.2	7.32
PP1151K+10%Lig		5592.8	1759.0	434.1	7.07
PP1151K+20%Lig		5495.7	1761.9	399.4	9.76
p-value	**Matrix**	0.1351	0.0581	0.1122	0.1274
	Additive	0.0080	0.0016	0.0104	0.2578

Table 10 also shows the results obtained for the glass transition temperature (T_g). As previously explained, T_g in DMA test can be determined at the drop of the storage modulus (E'),

at the peak of the loss modulus (E'') or at the peak of tan δ, and in this case it has been determined as the peak of E''. Figure 16 shows the curves of the loss modulus versus temperature of the samples with PP1151K matrix and in some samples, they present two peaks. The first transition, which corresponds to the T_g, is called Betha transition or β-relaxation (T_β) and is considered a major transition of many polymers due to the physical properties change drastically when the material goes from glassy state to rubber-elastic state [26,27]. In fact, in rubbers and some semicrystalline materials represents the lower operating temperature [26]. The second peak is the alpha transition (T_α), which is a second-order transition that represents the movements of the polymer chains in the crystalline section below melting [26,28]. As this transition corresponds to the crystalline part of the polymer, the higher the crystallinity of the material, the higher the peak intensity. For this reason, this transition is more noticeable in the samples with minerals, especially with additive percentages of 60% because they are the ones that present a higher percentage of crystallinity.

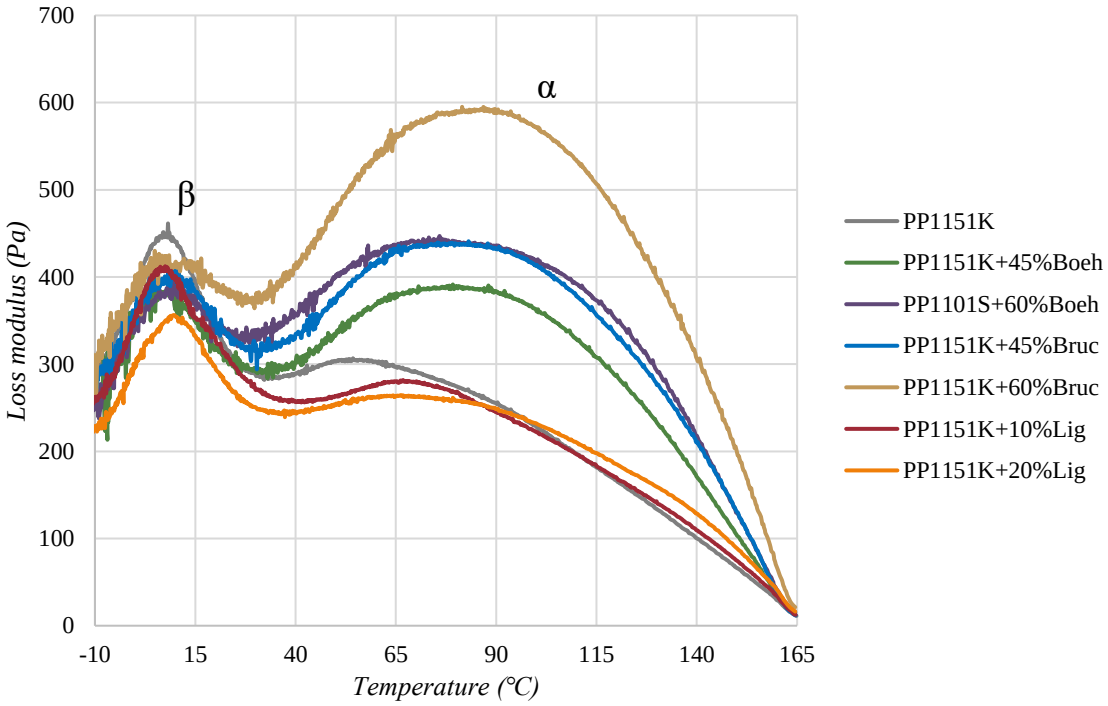

FIGURE 16: LOSS MODULUS VS TEMPERATURE OF PP1151K SAMPLES OF STAGE 1

Since the curves obtained show significant noise especially in the first transition due to the high stiffness of the mixtures, the data were fitted to a polynomial function and the maximum was calculated from this function to determine the T_g. Despite this, no clear trend has been obtained with respect to the type of matrix, additive or percentage and in fact neither the matrix nor the additive has a statistically significant effect on the T_g. Overall, in most samples, T_g is higher in the samples with additives compared to unfilled PP, indicating that the incorporation of additives

restricts the movement of the polymer chains [29]. With boehmite, there is an upward trend with respect to the percentage for both matrices, which agrees with the observations of Pedrazzoli et al. [29]. On the other hand, for brucite the T_g increases for 45% but then decreases, being this drop more significant in PP1151K+60%Bruc. This fact could be justified because the T_α transition observed in Figure 16, being more significant, affects the intensity of the betha transition, so it would be necessary to do more tests to confirm this decrease with respect to the percentage of brucite. In the case of lignin, the trends are opposite for both matrices, so it is not possible to draw conclusions.

2.5 RHEOLOGY

To study the viscosity of the mixtures and the effect of two polymeric matrices and additives, an oscillatory rheology test was carried out at three temperatures 170, 190 and 210℃. First, a comparison of the two matrices is shown in Figure 17. The graph represents the curves obtained for the storage modulus (G') and loss modulus (G'') at 210℃ versus frequency.

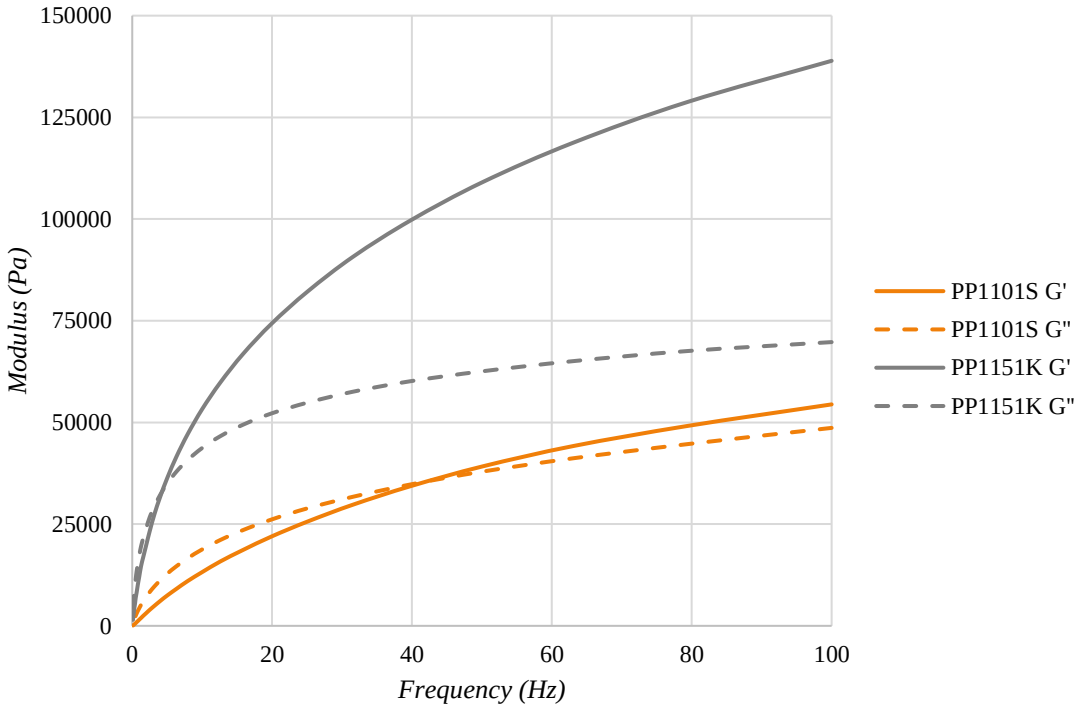

FIGURE 17: OSCILLATORY RHEOLOGY CURVES OF PP1101S AND PP1151K AT 210 ℃

In this graph it is observed that the curves of PP1151K (grey lines) show higher values than those of PP1101S (orange lines) due to its higher viscosity. PP1151K sample presents a cross-over point at low frequencies (4.259 Hz) and, from that point on, the difference between both curves (G' and G'') increases as the frequency increases. The cross-over point represents that the samples up to 4.259 Hz presents a liquid dominant behaviour because G'' is higher than G', then at 4.259 Hz the liquid and solid behaviour are equal and from 4.259 Hz onwards the solid

behaviour predominates (G'>G''). On the other hand, in the PP1101S matrix, the cross-over point of PP1101S occurs at intermediate frequencies (42.34 Hz), and the difference between both curves is not so significant, so in this matrix the solid and liquid behaviour do not differ so much. Therefore, in the frequency range studied (0.1 to 100 Hz), the PP1151K matrix presents mostly solid behaviour and high modulus values, which would make its processing difficult due to its high viscosity.

Then, this problem is accentuated at lower temperatures and with the addition of flame retardants, especially in the case of samples with an additive content of 60%. With the additives, samples with PP1151K show cross-over points at even lower frequencies and at higher modulus. Figure 18 shows the curves obtained for PP1151K and PP1151K+60%Boeh at 170 and 190°C.

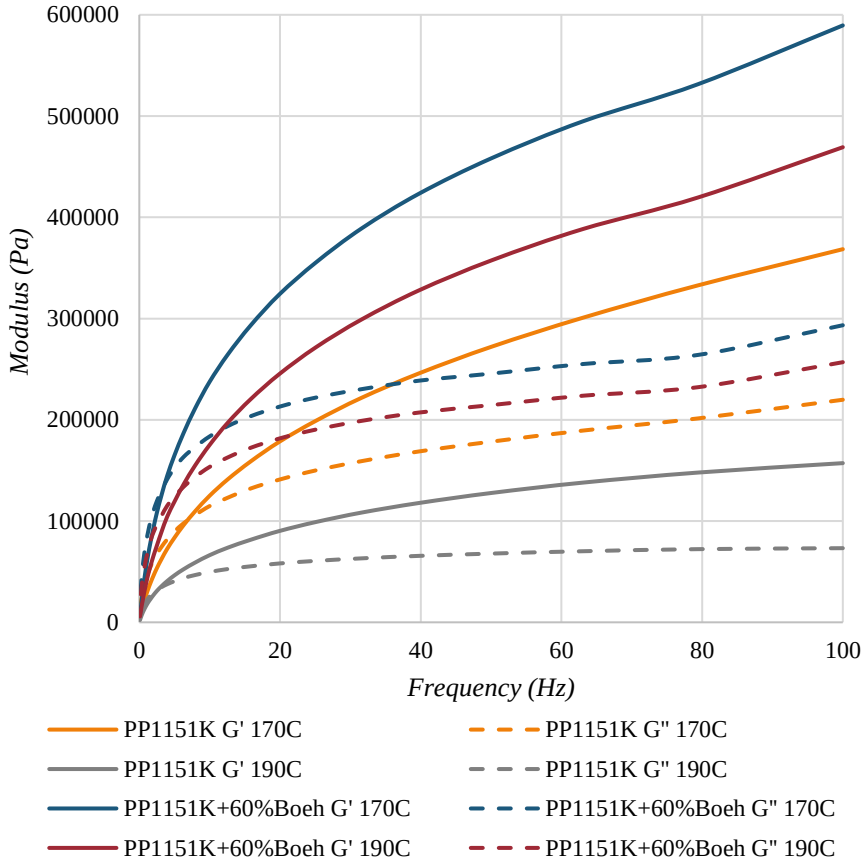

FIGURE 18: OSCILLATORY RHEOLOGY CURVES OF PP1151K AND PP1151K+60%BOEH AT 170 AND 190 °C

Compared to the previous sample at 210°C (Figure 17), the cross-over point of PP1151K moves to 1.73 and 2.82 Hz at 170 and 190°C, respectively. Moreover, the difference between the curves G' and G'' increases at lower temperatures, at 100 Hz the difference between the G' and G'' modulus at 170, 190 and 210°C is 148.7, 84 and 69.2 Pa, respectively. Therefore, as expected, PP1151K at lower temperatures behaves even more like a solid, which makes it difficult to flow and even if the temperature increases its viscosity is still very high. In the sample with 60% Boeh

this fact is aggravated. It is observed that the G' modulus at 100 Hz increases compared to unfilled PP1151K by 60% at 170℃ and 198.5% at 190℃, so although the temperature increases, it does not improve the fluency of the 60%Boeh samples as much as in PP1151K. In conclusion, although the method used for the manufacturing is compression moulding and the fluency of the material is not as important as in other techniques, the PP1151K matrix is discarded for the following stages because its high viscosity could hinder the adhesion of the matrix with the natural fibre as it is more difficult for it to flow and pass through the holes in the fabric correctly.

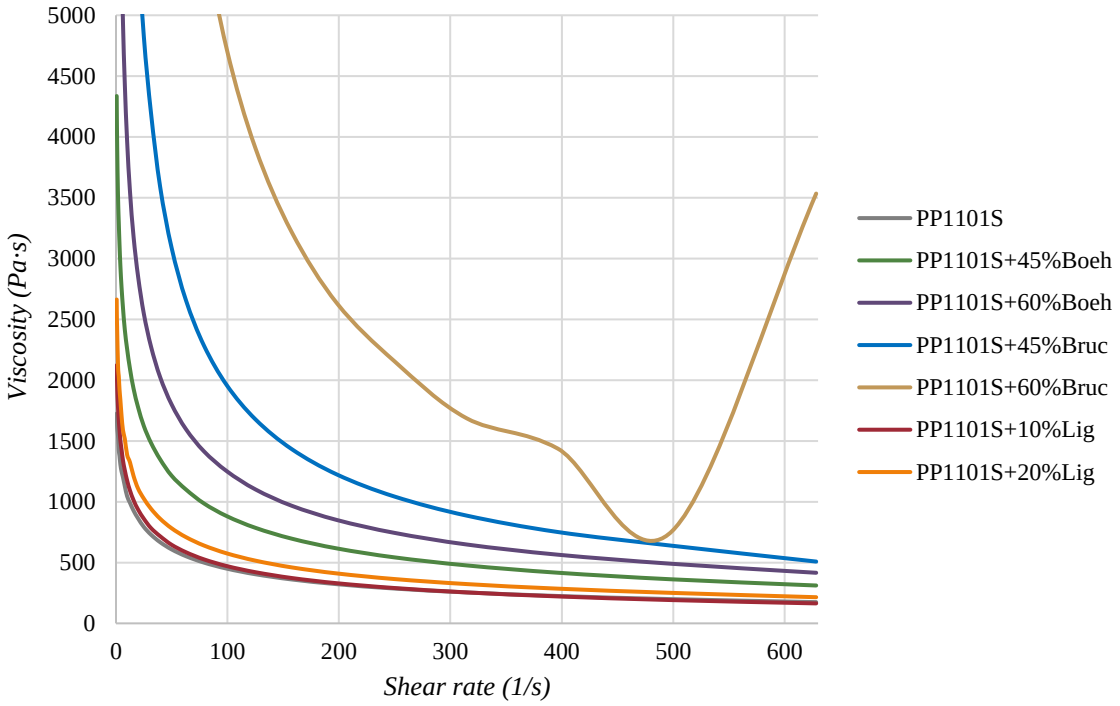

FIGURE 19: VISCOSITY CURVES OF PP1101S SAMPLES OF STAGE 1 AT 190 ℃

Then, the comparison of the samples with PP1101S as matrix is carried out. The Cox-Merz transformation is used to obtain the viscosity versus shear rate curves from oscillatory rheology data. Figure 19 shows the curves for all the additives at 190℃ because this is the temperature used in compression moulding. The curves obtained at 170 and 210℃ are shown in the Annex. First, the samples exhibit shear thinning, high viscosity at low shear rates that decreases with the increasing shear rate [30]. Starting with the lower viscosity curves, it can be seen that the samples with 10% lignin show a very similar viscosity to unfilled PP1101S, followed by the 20% lignin samples with a slightly higher viscosity. Therefore, at 190℃ the lignin does not significantly modify the viscosity of the mixture. In fact, Tahir I. et al. studied the blend of PP with lignin at 5, 15 and 35%, and the additive did not have a significant effect because they stated that the addition of lignin did not require any modification of the injection process parameters, except for a slight increase in pressure [18]. The curves for boehmite at 45% and 60% are then obtained. The results show that the incorporation of boehmite increases the viscosity with increasing boehmite content,

especially in the low shear rate region. This increase is due to boehmite particles act as non-interacting rigid particles in dilute suspension with high hardness and high percentage. Finally, the highest viscosity curves correspond to brucite, with the 60% curve being much higher than the PP1101S curve. The sample with 60% brucite has a different geometry from 400 s^{-1} onwards due to turbulences produced in the sample by the particles and their high percentage [31]. Samples with brucite have a higher viscosity compared to boehmite because of the larger particle size and lower density, which leads to a higher surface area. In conclusion, brucite considerably increases the viscosity of the mixture and has a dominantly solid behaviour over the frequency range as shown in Figure 20. The cross-over point is at 1.09 Hz at 190°C, so it is better to process it at higher temperature to facilitate flowability as the crossover point is at 6.56 Hz at 210°C and the G' and G'' curves are significantly lower.

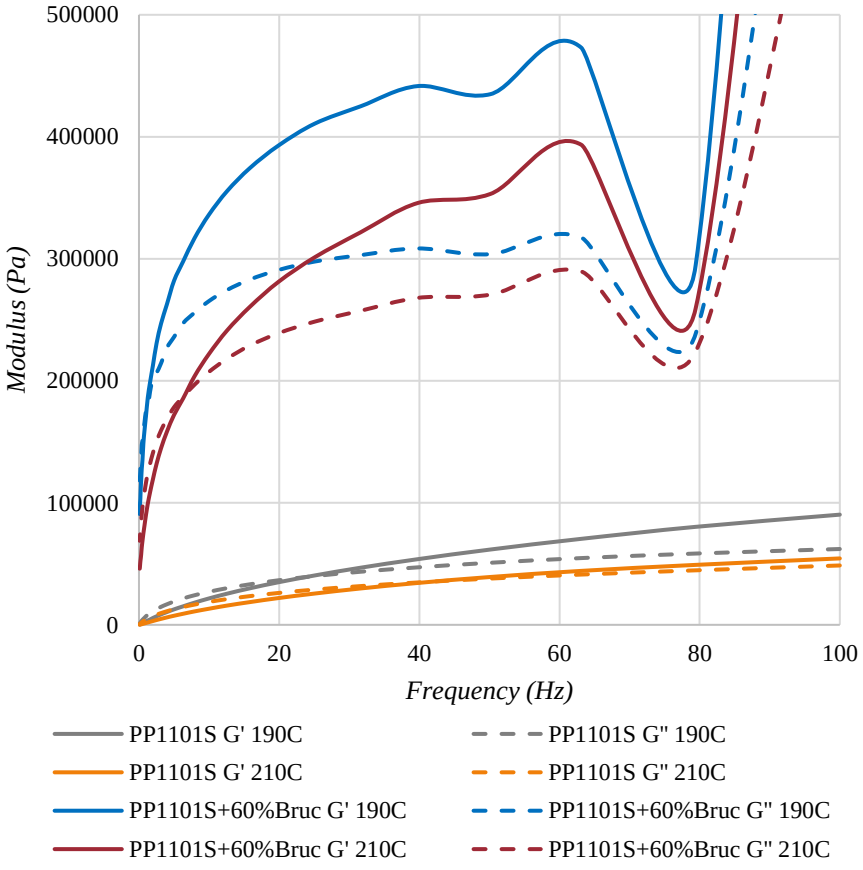

FIGURE 20: OSCILLATORY RHEOLOGY CURVES OF PP1101S AND PP1101S+60%BRUC AT 190 AND 210 °C

2.6 MECHANICAL TESTS

Regarding the mechanical tests, the results of the tensile test are analysed first. Figure 21 shows the elastic modulus and the maximum tensile strength of the PP1101S (grey colour) and PP1151K (red colour) mixtures with their standard deviation. In addition, the totality of the results together with the p-values of the matrix and additives can be found in Annex I. Firstly, no significant differences are observed due to the matrix in the elastic modulus, so an overall analysis

of the effect of the additives is carried out. During the test, it was observed that when the flame retardants were added to the polypropylene, its breaking behaviour changed from plastic deformation until breakage to sudden breakage without plastic deformation. This behaviour is justified because the particles decrease the polymer content in the cross-section of the specimen, so there is less material that is deformable, and breakage occurs directly. Then, it is observed that the elastic modulus increases with boehmite and brucite and remains unchanged with lignin. The modulus increases with the minerals due to the stiffness of the particles and, for this reason, it increases with the percentage of additive. Furthermore, samples with brucite have a higher modulus because their density is lower than boehmite, 2.3-2.4 g/cm^3 versus 3-3.5 g/cm^3 for boehmite [6], therefore the particles occupy more volume and provide more stiffness to the cross-section of the specimen. As for lignin, it is observed that the elastic modulus increases slightly, but this is not a significant difference, due to the low stiffness of the lignin particles.

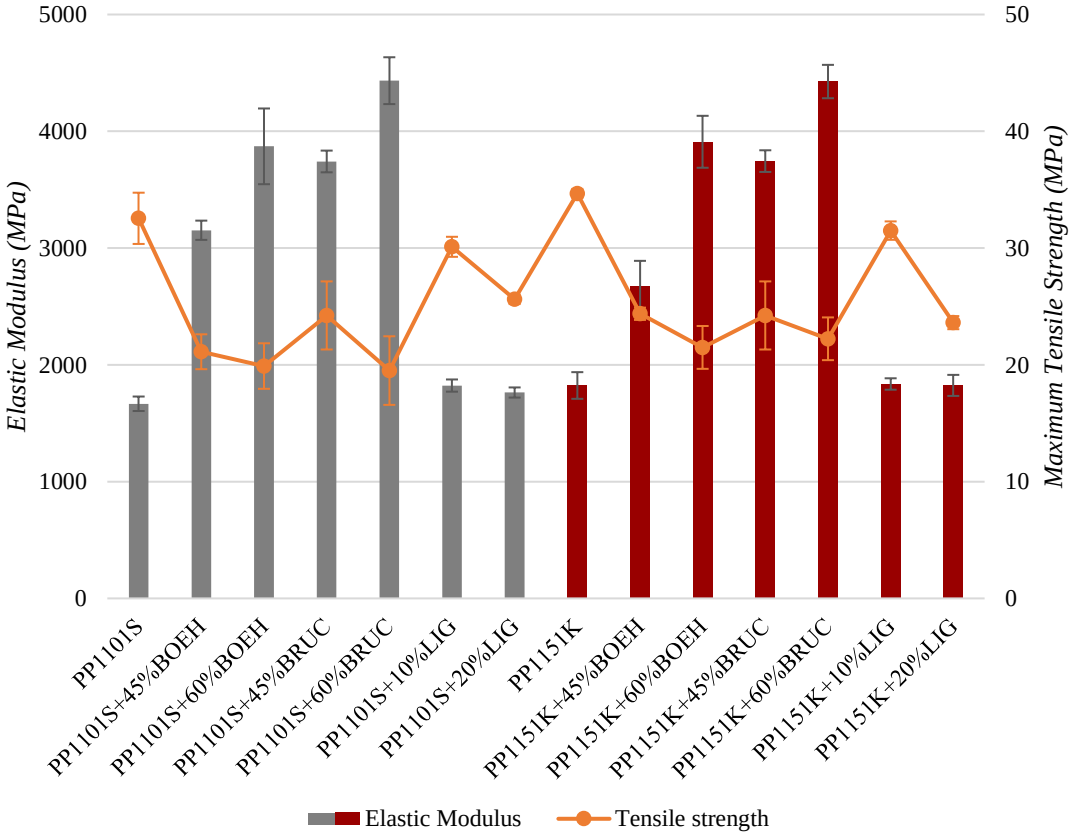

FIGURE 21: TENSILE TEST RESULTS OF STAGE 1

On the other hand, in the maximum tensile strength both matrix and additive have a statistically significant effect. In the case of the matrix, samples with PP1151K have slightly higher strength compared to PP1101S, 26 MPa versus 24.9 MPa on average, because this PP grade has superior mechanical properties as indicated in the technical data sheet. As for the additives, lignin influences the value of the maximum tensile strength because it decreases with

the percentage of additive reaching a reduction of 33% for the sample PP1151K+20%Lig. This is due to the poor adhesion between the matrix and the particles, which increases the chances of failure. Stress is transferred to the lignin particles inefficiently and the particles are not very strong, so increasing the percentage increases the chances of failure at lower stresses [32]. Compared to minerals, lignin affects the strength value as much as minerals, despite its lower percentage due to its lower density. In fact, density is a key aspect in the maximum tensile strength. Without good adhesion to the matrix, the particles do not act as a whole, and it is the plastic particles that resist the force. For this reason, the lower the density of the additive, the lower the amount of polymer in the effective section and the lower the resistance. Therefore, lignin considerably affects the maximum tensile strength because its density is between 1.35 and 1.5 g/cm3 (Table 2) so the total volume occupied by its particles in the mixture is almost as large as in the minerals. Regarding to minerals, the same tendency is obtained as in lignin, the strength decreases with the percentage of additive due to the decrease of the effective area of the polymer.

TABLE 11: FLEXURAL AND IMPACT TEST RESULTS OF STAGE 1

Sample		Flexural Modulus (MPa)	Impact strength (kJ/m^2)
PP1101S		1484.5 ± 42.5	28.42 ± 0.89
PP1101S+45%Boeh		2904.8 ± 67.3	21.34 ± 6.27
PP1101S+60%Boeh		4010.5 ± 164.3	6.72 ± 1.09
PP1101S+45%Bruc		2905.3 ± 107.6	8.78 ± 1.90
PP1101S+60%Bruc		4117.6 ± 67.2	5.32 ± 1.07
PP1101S+10%Lig		1869.5 ± 12.3	26.10 ± 1.06
PP1101S+20%Lig		1665.6 ± 28.0	25.97 ± 5.16
PP1151K		1955.1 ± 121.1	38.61 ± 1.29
PP1151K+45%Boeh		2715.9 ± 35.9	36.81 ± 1.24
PP1151K+60%Boeh		3539.9 ± 115.0	13.84 ± 1.97
PP1151K+45%Bruc		3161.7 ± 87.0	16.64 ± 2.40
PP1151K+60%Bruc		4331.1 ± 128.0	6.93 ± 0.99
PP1151K+10%Lig		1949.5 ± 84.4	30.82 ± 2.47
PP1151K+20%Lig		1729.8 ± 78.7	28.98 ± 1.51
p-value	**Matrix**	0.2226	0.0000
	Additive	0.0000	0.0000

In the case of the flexural properties, only the type of additive has a significant influence (Table 11). It is observed that with minerals the flexural modulus increases with the additive percentage because the particles add stiffness to the composite. Comparing both additives, the modulus of brucite is higher than boehmite, as well as in the elastic modulus, due to the lower

density of brucite particles. On the other hand, 10% lignin in PP1101S increases the modulus but when the percentage increases to 20%, the modulus decreases. In the case of PP1151K, 10% lignin does not significantly alter the flexural modulus, but when increased to 20%, the flexural modulus decreases, reaching a value lower than that of PP without additive. Comparing the results with those reported in the literature, it is observed that no clear trend is obtained with respect to the percentage. For example. Toriz et al. did not obtain a linearity with respect to the percentage for both elastic and flexural modulus [32]. However, Chen et al. obtained a decrease with respect to percentage in PP [33] and Sameni et al. obtained an increase in HDPE matrix [34]. Therefore, it is not possible to determine that lignin has a trend with respect to percentage based on the data obtained in this stage and in the literature.

In terms of impact resistance, both the matrix and the additives have a significant influence (Table 11). Firstly, it is observed that the samples with PP1151K have a higher impact strength than PP110S. As indicated in the technical data sheets, the PP1151K matrix has a nucleating agent in its composition, has a higher viscosity and higher impact strength, for this reason, the samples with this matrix have higher impact resistance. For the additives, the conclusions obtained are the same as for the maximum tensile strength. The impact strength decreases with respect to the percentage for the three additives. For minerals, the values obtained for brucite are lower due to its lower density compared to boehmite. As for lignin, it does not reduce the strength so significantly because, as seen in the tensile and impact tests, the particles are not as stiff as the minerals. Consequently, lignin does not embrittle the polymer matrix as much and the reduction obtained is due to the reduction of the effective area.

2.7 FIRE TESTS

The results and discussion of the UL94 test are shown below. Figure 22 shows a graph of the horizontal propagation speed of all the samples studied and all the results are reported in the Annex. In this test, the factor that significantly influences the speed is the type of additive. It is observed that boehmite and brucite decrease the propagation speed and the higher the percentage, the lower the speed. Comparing both additives, the response is more satisfactory for brucite as it ensures the sample not propagate the flame when used at 60% in both matrices. This effect is expected as brucite absorbs more heat from the medium due to its higher enthalpy of decomposition, 1450 kJ/g for brucite versus 560 kJ/g for boehmite [2], and because it releases more water that better dilutes the flammable gases of combustion. As for lignin, it reduces the propagation speed, but the effect is not very significant compared to virgin PP, so it would be discarded as a flame retardant to be used in future stages. In summary, the samples with boehmite

and brucite in the two matrices and PP1101S+20%Lig are classified as HB in the flammability rating of the 94HB test because their propagation speed is lower than 40 mm/s.

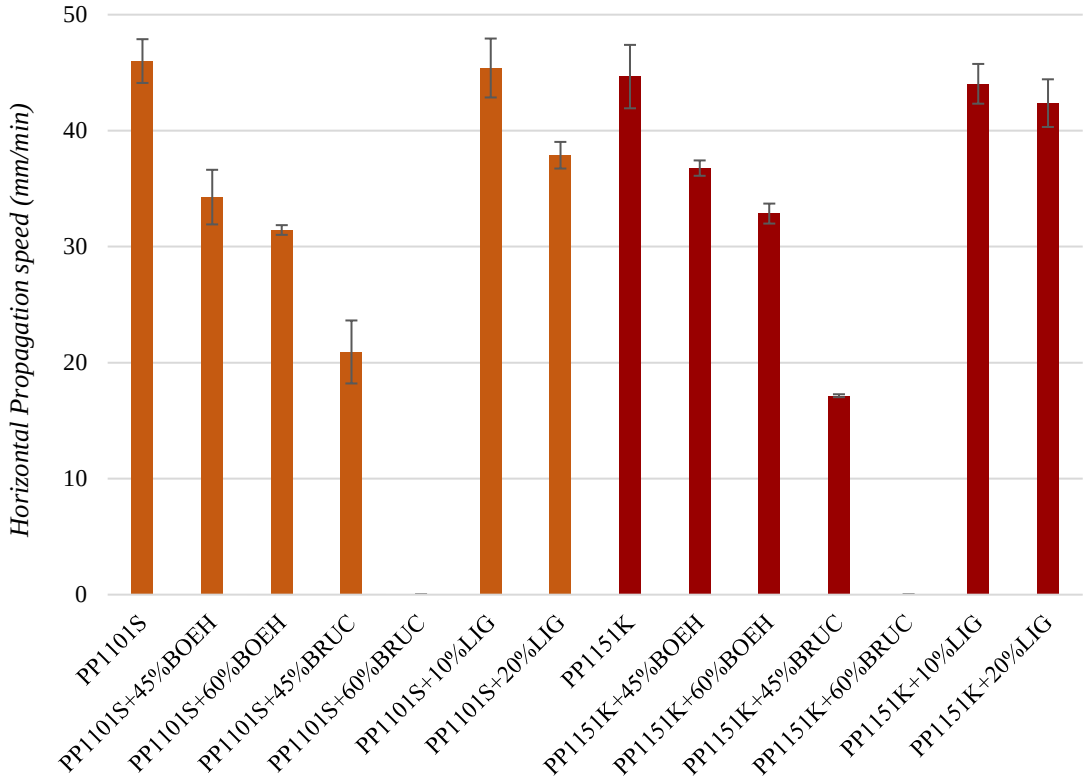

FIGURE 22: RESULTS OF HORIZONTAL TEST 94 HB OF STAGE 1 SAMPLES

As for the vertical test, it was not possible to classify the samples in the 94V test criteria because the flame times are longer than those required. For this reason, in order to study the effect of the additives, the vertical propagation speed was determined, and the results are shown in Figure 23. In this test, similar conclusions were obtained as in the horizontal test, except that in the ANOVA statistical test it was determined that both factors, matrix and additive, have a statistically significant effect on the vertical propagation speed. On the one hand, it was found that the matrix influences the speed mainly because of the difference obtained in the lignin samples. The propagation speed was about 25 mm/s higher on average in the samples with PP1101S compared to PP1151K. This is due to the presence of bubbles in the plates, which on the one hand favoured combustion because of the trapped air and on the other hand modified the density. Density is important because it modifies the weight of the sample, the propagation time decreases at lower weights because there is less material to burn and consequently the material burns faster [35,36]. On the other hand, boehmite and brucite reduce the propagation speed and it decreases with respect to the percentage of additive, being better in brucite. In fact, samples with 60% boehmite show equivalent results to those with 45% brucite. Although the samples studied do not pass the test, the 60% brucite sample shows a reduction in velocity of approximately 48%,

which is a considerable improvement. Finally, the results obtained for the lignin samples are the opposite of those expected because the speed increases. For this reason, lignin is discarded for the next stage.

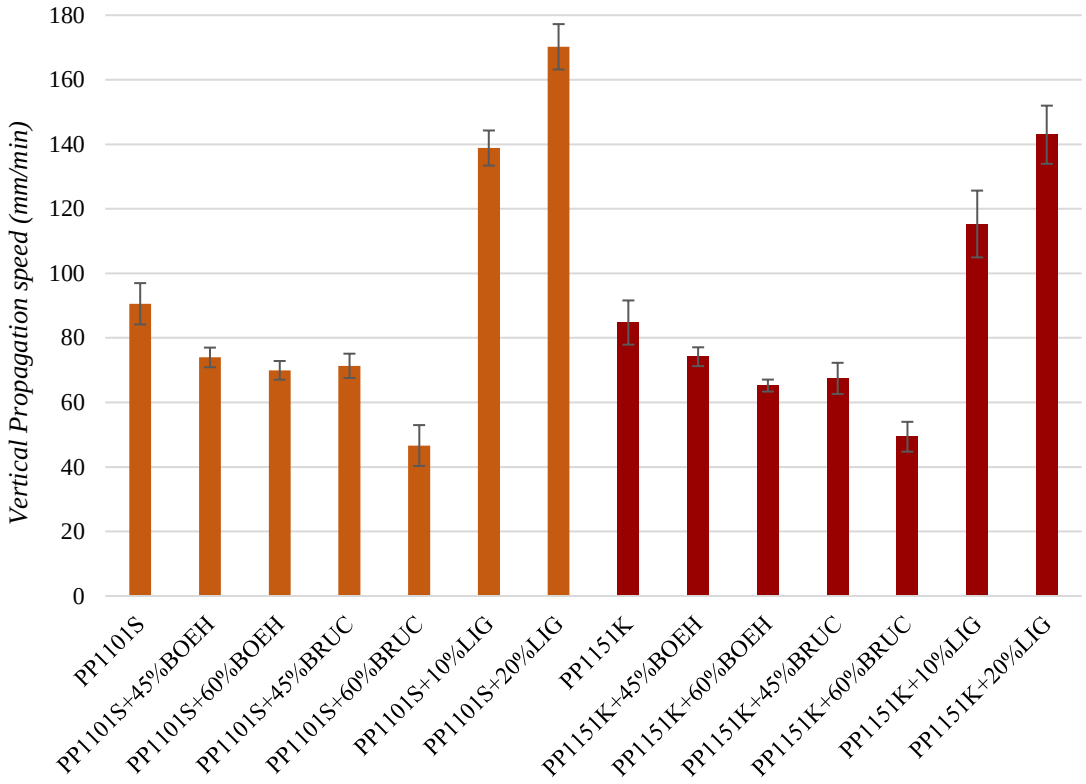

FIGURE 23: RESULTS OF VERTICAL TEST 94V OF STAGE 1 SAMPLES

To obtain further results on fire properties, the LOI test, which is explained in detail in Chapter 2 Section 5.1, was carried out by the IMDEA Materials Institute. Among the mixtures studied, PP1101S samples with the highest percentages of additive, 60%Boeh, 60%Bruc and 20%Lignin, were analysed. Samples with the PP1151K matrix were not analysed because due to the high viscosity of the blends it was discarded for the following stages. Table 12 shows the results obtained and confirms that brucite is the additive with the best properties and the sample is classified as self-extinguishing (LOI > 21). On the other hand, the samples with boehmite and lignin are classified as combustible, with lignin being the worst.

TABLE 12: LOI RESULTS OF STAGE 1 PP1101S SAMPLES

Sample	LOI value
PP1101S	17.6
PP1101S+60%Boeh	20.8
PP1101S+60%Bruc	24.4
PP1101S+20%Lig	18.6

2.8 OPTIMIZATION

With the results obtained, it has been observed that, despite the high additive percentages used, it has not been possible to pass the UL94 test criteria and the mechanical properties of the material have decreased considerably. To overcome this situation, synergistic additive mixtures can be used, which is a combination of additives in which the retarding effect is greater than the sum of the effect of the individual components. For this reason, it was decided to study the possibility of developing synergistic mixtures using a second additive to improve the effect of the main additive or additive 1, boehmite or brucite, or to complement it by making up for some of its deficiencies. The search for this second additive could lead to better fire retardant properties with a lower percentage of total additive and with a lower effect on the mechanical properties. For this purpose, the optimum percentage of boehmite or brucite in the synergistic mixture is first calculated. Since both the maximum stress and impact strength are significantly reduced, to obtain a balance between mechanical and fire properties, an optimisation of the results was carried out by restricting a minimum of maximum tensile strength while minimising the propagation speed. For this purpose, following the method described in Chapter 3 Section 2.8, the values of maximum strength were introduced as constraint and the horizontal propagation speed as objective. As the objective was to develop synergistic mixtures with boehmite and brucite separately, the optimisation for each additive was performed independently. Table 13 shows how the data for boehmite was entered. Firstly, the percentage of additive as a variable (V1) as this is what the program calculates, then the maximum strength as a constraint (R1) and finally the objectives, elastic modulus (O1), impact strength (O2), flexural modulus (O3) and propagation speed (O4). Then, it was established that the maximum strength cannot be less than 75% of the value obtained for the virgin PP1101S, which is 25.161 MPa, and the objective to be minimised was O4, propagation speed. For the rest of the objectives, the programme just calculates the estimated value for the optimum percentage obtained, but these other objectives did not influence on the optimisation search.

TABLE 13: INPUTS FOR OPTIMIZATION OF BOEHMITE PERCENTAGE IN STAGE 1

	V1	R1	O1	O2	O3	O4
Sample	**% addit**	**Maximum strength (MPa)**	**Elastic Modulus (MPa)**	**Impact strength (kJ/m^2)**	**Flexural Modulus (MPa)**	**Propagation speed (mm/s)**
PP1101S	0	33.55	1666.6	28.42	1484.5	46.00
PP1101S +45%Boeh	45	21.12	3152.6	21.34	2904.8	33.56
PP1101S +60%Boeh	60	19.90	3871.3	6.72	4010.5	31.47

Figure 24 shows the result obtained for boehmite which is 30.89% approximate to **30%**. Then, the result obtained for the constraint is shown, followed by the rest of the values of the mechanical properties and finally the result of the objective function, which in this case is the horizontal propagation speed. For brucite, the optimum additive percentage was 40.29%, approximate to **40%**.

```
The estimated optimal design is: 30.872852
The estimated constraint 1 of the optimum is: 25.162563
The estimated response 1 of the optimum is: 2696.812590
The estimated response 2 of the optimum is: 22.974146
The estimated response 3 of the optimum is: 2489.266939
The estimated response 4 of the optimum is: 37.564099
The estimated value of the objective function of the optimum is: 37.564099
Calculation time: 0.391993 s
```

FIGURE 24: RESULT OF THE OPTIMIZATION OF BOEHMITE AT STAGE 1

2.9 CONCLUSIONS

The conclusions drawn at this stage are summarised below:

- During extrusion, it was observed that the mixtures corresponding to 60% additive increase the pressure, but within normal operating parameters, and it is possible to obtain a mixture with high viscosity PP (MFI 4g/10 min) and 60% mineral additive with good homogeneity.

- Since the additives have a higher density than PP, the density of the mixture increases with respect to the percentage of additive.

- In DSC test, it was observed that boehmite and brucite act as a nucleant of PP because they increase the percentage of crystallinity, favour the formation of crystals, and improve the homogeneity of the crystals structure.

- In TGA test, it was observed that lignin is the additive with the lowest thermal stability, followed by brucite and boehmite. In general, the additives improve the thermal stability of the samples although it does not improve with respect to the percentage because a decrease was observed with the samples at 60%.

- The samples with mineral additives have a higher maximum storage modulus than the virgin PP over the temperature range tested in DMTA test, therefore, they improve the thermo-mechanical stability, which is beneficial because they are more resistant and allow people to escape in case of fire before material failure occurs.

- In oscillatory rheology, it was observed that the viscosity of the mixtures increases with respect to the percentage, being highest for brucite, followed by boehmite and lignin. In addition, PP1151K matrix is discarded for the following stages due to its high viscosity could hinder the manufacturing of the composites with the natural fibre fabric.

- Additives significantly influence the mechanical properties. Minerals increase the elastic and flexural modulus, while lignin has no significant influence. On the other hand, the maximum tensile and impact strength decrease with respect to the percentage, being higher with brucite. Therefore, the additives used stiffen the material and make it less resistant.

- In the UL94 test, it was observed that the samples do not pass the test but brucite was the additive with the highest fire retardant effect on polypropylene. On the other hand, lignin was discarded for the next stage because it increases the vertical propagation speed.

- Finally, since the fire resistance results were not satisfactory, synergistic blends were considered for the next stage. As the additives significantly affect the mechanical properties, an optimisation of the results was carried out by restricting a minimum value of maximum tensile strength while minimising the propagation speed. As a result, the optimum additive percentage for boehmite is 30% and for brucite 40%.

3. STAGE 2

3.1 CONFIRMATION OF OPTIMAL VALUES

Before proceeding to the second stage, a verification of the calculated optimum percentages was carried out, so a batch of 500 g of boehmite at 30% and brucite at 40% were extruded. These mixtures were then characterised by tensile test and UL94, and the results obtained (Table 14) were added to the optimisation to make a feedback process and verify the percentages. The same procedure described in Section 2.8 was followed and for boehmite the optimum percentage based on the established criteria was 34.88%, which was approximated to **35%**, and for brucite **40%** was confirmed. The percentage of boehmite increased since the value obtained for the maximum strength was higher than expected, 27.16 MPa instead of the 25.16 MPa calculated in the optimisation. In the case of brucite, the 40% is confirmed because the value obtained for the maximum strength is similar. It is also observed that the horizontal propagation speed values of both additives are higher than expected, so the propagation speed-percentage of additive relation is not linear.

TABLE 14: RESULTS FOR THE CONFIRMATION OF OPTIMAL ADDITIVE PERCENTAGES

Sample	Elastic Modulus (MPa)	Tensile strength (MPa)	Horizontal propagation speed (mm/s)
PP1101S+30%Boeh	2455.9 ± 25.4	27.16 ± 0.19	41.43 ± 0.88
PP1101S+30.87%Boeh*	2696.8	25.16	37.56
PP1101S+34.88%Boeh**	2666.8	25.16	38.94
PP1101S+40%Bruc	3231.4 ± 71.5	25.05 ± 0.5	32.42 ± 1.18
PP1101S+40.3%Bruc*	3017.4	25.16	23.22

*ESTIMATED VALUES FROM OPTIMISATION OF STAGE 1

** ESTIMATED VALUES FROM THE PRELIMINARY OPTIMISATION OF STAGE 2

Once the optimum additive percentages for boehmite and brucite were determined, the synergistic mixtures to be studied were established. For the choice of the second additive, the main component of boehmite and brucite, AlO(OH) and $Mg(OH)_2$ respectively, was considered because there are few articles about synergistic mixtures with these minerals. Furthermore, it was stipulated that the total additive content should be less than 60% to see if it is possible to achieve an improvement in the fire properties with a lower additive content and less impairment of the mechanical properties. After reviewing the state of the art, colemanite and expandable graphite were selected as options for the second additive (Chapter 2 Section 3.2). Colemanite was chosen because zinc borates have been widely used together with aluminium and magnesium hydroxides [37–39], and promising results have been obtained, so colemanite, being a hydrated calcium borate of mineral origin, could be the natural alternative. Furthermore, colemanite has been used

both individually and mixed with other additives from 1 to 30% depending on the polymer and the main additive with good flame retardancy results [40–42]. Regarding to expandable graphite, it is usually necessary to combine it with other flame retardants to obtain a fireproof material and it is usually used from 2.5 to 12.8% [43,44]. Expandable graphite is an additive that has a lower density compared to minerals and, due to the action of temperature, expands and increases in volume, so it is not possible to use it at very high percentages as there would not be enough plastic volume to cover all the additive particles. Therefore, considering that the main additives, boehmite and brucite were at 35 and 40% respectively and that the total additive content should be less than 60%, 10 and 15% were set for colemanite and 10% for expandable graphite. In this case it is not possible to increase the percentage of expandable graphite because the volume of plastic that would be in the mixture was estimated and compared to the volume of total additive and it was concluded that there would not be sufficient volume of polymer to adequately cover all the particles. In addition to the above mixtures, it is necessary to study the mixtures of colemanite and expandable graphite individually with polypropylene to determine their effect and to verify whether they act as synergistic mixtures with boehmite and brucite. For this purpose, the percentages 10 and 20% were established for both additives. Table 15 summarises all the mixtures studied, specifying additive, percentages, and nomenclature of the samples. From here on, as the high viscosity matrix has been discarded, the nomenclature of PP1101S becomes PP.

TABLE 15: MIXTURES OF PP AND FLAME RETARDANT ADDITIVES TESTED IN STAGE 2

Matrix	Additive 1	Percentage	Additive 2	Percentage	Nomenclature
PP	Boehmite	30	-	-	PP+30%Boeh
		35	-	-	PP+35%Boeh
		35	Colemanite	10	PP+35%Boeh +10%Col
		35		15	PP+35%Boeh +15%Col
		35	Expandable graphite	10	PP+35%Boeh +10%EG
	Brucite	40	-	-	PP+40%Bruc
		40	Colemanite	10	PP+40%Bruc +10%Col
		40		15	PP+40%Bruc +15%Col
		40	Expandable graphite	10	PP+40%Bruc +10%EG
	Colemanite	10	-	-	PP+10%Col
		20	-	-	PP+20%Col
	Expandable graphite	10	-	-	PP+10%EG
		20	-	-	PP+20%EG

3.2 COMPOSITE PREPARATION

During the extrusion there were difficulties with the expandable graphite samples. In the PP+20%EG, the filament was rough and had difficulty flowing, resulting in filament breakage. In fact, it was not possible to extrude the whole batch. Also, in the PP+40%Bruc+10%EG sample, the filament was more fragile, it broke, and it was not possible to pelletise. For this reason, both mixtures were processed afterwards to obtain pellets. These difficulties arose, in addition to the lower density of the expandable graphite particles, because the starting temperature of expansion of the graphite is 185°C according to the technical data sheet. For this reason, at the extrusion temperature (190°C), the expansion has started, the particles have increased in volume and there is not enough plastic volume to adequately cover all the graphite. Therefore, the mixture of expandable graphite with brucite at these percentages and polypropylene as matrix is difficult to apply at industrial level due to processing difficulties.

Next, the plates were manufactured by compression moulding and some of the plates are shown below (Figure 25). The first image (Sample A) shows that colemanite changes the colour of the boehmite plate and turns grey. In the case of brucite (Sample B), the piece darkens to a khaki green colour like the 20% colemanite plate (Sample C). Finally, despite the difficulties in extrusion, the mixture with expandable graphite (Sample D) had good visual characteristics, smooth surface, and homogeneous colour.

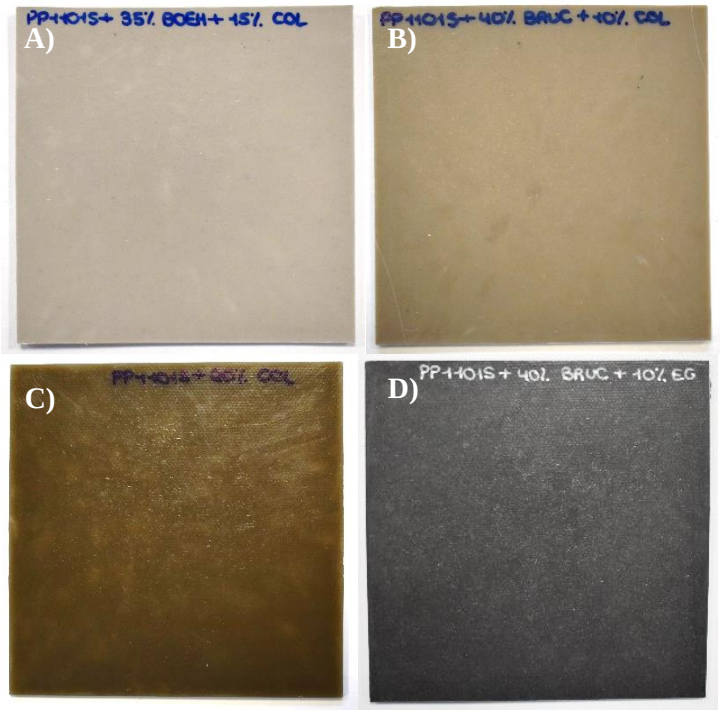

FIGURE 25: PLATES MANUFACTURED IN STAGE 2. A) PP+35%BOEH+15%COL, B) PP+40%BRUC+10%COL, C) PP+20%COL, D) PP+40%BRUC+10%EG

3.3 PRELIMINARY CHARACTERIZATION

Table 16 shows the results for density, ash content and ANOVA analysis. In this case, the statistical test is a simple ANOVA analysis because only the effect of the additive is studied. In addition, the estimated percentage is not determined in this stage because, as it is a mixture of additives, it is not possible to discern which quantity corresponds to which additive. Regarding the density results, it is observed that it increases with the percentage of additive due to their higher density compared to PP. In the case of the mixtures of expandable graphite and minerals (boehmite and brucite), a small decrease is observed compared to the samples with only mineral due to the expansion of the EG particles observed during the extrusion. The same effect is observed in the samples with 10 and 20%EG, the density has an upward trend, but the increase is lower than what corresponds to the density of the additive due to the expansion observed.

TABLE 16: RESULTS OF DENSITY AND ASH CONTENT OF STAGE 2 MATERIALS

Sample	Density (g/cm^3)	Ash content (%)
PP+30%Boeh	1.103 ± 0.004	22.77 ± 0.15
PP+35%Boeh	1.122 ± 0.010	27.86 ± 0.27
PP+35%Boeh +10%Col	1.244 ± 0.010	37.05 ± 0.19
PP+35%Boeh +10%EG	1.097 ± 0.023	31.19 ± 0.28
PP+40%Bruc	1.186 ± 0.002	28.65 ± 0.91
PP+40%Bruc +10%Col	1.265 ± 0.011	37.37 ± 1.26
PP+40%Bruc +15%Col	1.323 ± 0.008	40.87 ± 0.86
PP+40%Bruc +10%EG	1.105 ± 0.022	30.57 ± 1.05
PP+10%Col	0.947 ± 0.002	6.16 ± 0.13
PP+20%Col	1.011 ± 0.003	14.14 ± 0.24
PP+10%EG	0.893 ± 0.017	0.81 ± 0.10
PP+20%EG	0.933 ± 0.011	0.73 ± 0.05
Colemanite	2.42 [6]	78.15 ± 0.64
Expandable graphite	1.8-2.25 [45–47]	5.22 ± 0.96
p-value	0.0744	0.0127

In the determination of the ash content, it is observed that the higher the percentage of the minerals, the higher the ash content, because they decompose completely into the corresponding oxide. According to the decomposition reaction of colemanite [48], the ash content should be around 78.09%, which is confirmed experimentally. In the case of expandable graphite, the ash content is small because it is mainly composed of carbon, 0.81% for PP+10%EG and 0.73% for

PP+20%EG, but when mixed with the minerals, a higher content is obtained. This fact is more significant with boehmite, because in the sample PP+35%Boeh the ash content is 27.86% and when 10%EG is added, it increases to 31.19%. This means that when the additives are combined, the resulting ash content is higher than when both are summed individually. This fact could be because they react to form a heavier compound or due to their retarding effect, they prevent the polymer from decomposing completely, leaving an undegraded remnant. Analysing the ashes visually, it is observed that the samples with expandable graphite present a granular ash with no cohesion (Figure 26 A and B). However, when mixed with boehmite (Figure 26 G), the structure is more compact on the surface and the expandable graphite has expanded inside, which would help in flame retardancy. The same happens for mixtures with boehmite and colemanite, the resulting ash is greater than the sum of the individual ashes. Visually comparing samples D) PP+35%Boeh, E) PP+35%Boeh+10%Col and F) PP+35%Boeh+15%Col, it is observed that the higher the colemanite content, the larger the holes on the surface. These holes can help in the release of water generated in the decomposition of the minerals, helping with the dilution of combustible gases, and reducing the amount of heat inside the material, but no improvement in the cohesion or hardness of the ash is observed. Therefore, from the appearance of the ashes it is expected that the boehmite/expandable graphite mixture will have a better fire behaviour.

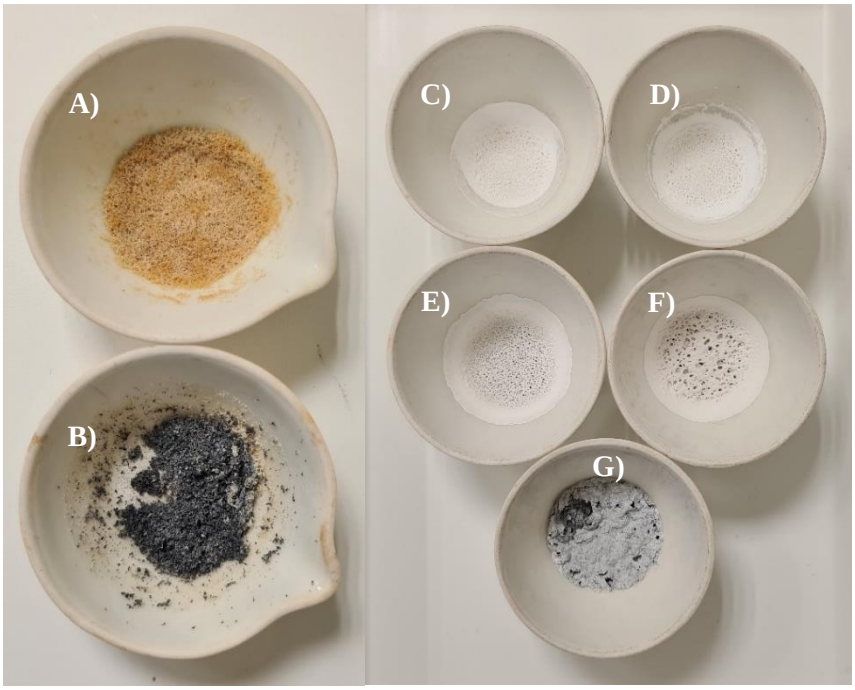

FIGURE 26: IMAGES OF THE ASHES FOR THE EXPANDABLE GRAPHITE AND BOEHMITE SAMPLES. A) PP+10%EG, B) PP+20%EG, C) PP+30%BOEH, D) PP+35%BOEH, E) PP+35%BOEH+10%COL, F) PP+35%BOEH+15%COL, G) PP+35%BOEH+10%EG

In the case of brucite, the same result is obtained, the mixtures with colemanite and expandable graphite have a higher ash content. Figure 27 shows that with the addition of

colemanite, the ashes present a more cohesive surface that would help to protect the plastic from heat and fire. In the case of expandable graphite, the surface is similar to that of boehmite but with a lower hardness, so from the appearance of the ashes, a better result is expected with colemanite. In summary, the mixtures studied could act as a synergistic mixture, but fire tests are necessary to confirm this.

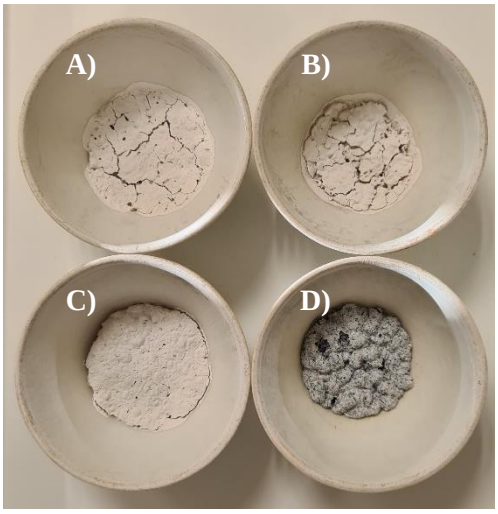

FIGURE 27: IMAGES OF THE ASHES FOR BRUCITE SAMPLES. A) PP+40%BRUC, B) PP+40%BRUC+10%COL, C) PP+40%BRUC+15%COL, D) PP+40%BRUC+10%EG

3.4 THERMAL PROPERTIES

As in the previous stage, DSC, TGA and DMTA tests are carried out to study the influence of colemanite and expandable graphite on the thermal properties of the material.

3.4.1 DSC

The results obtained for the second heating curve together with the results of the ANOVA analysis are shown in Table 17. Firstly, it is obtained that the additive has a significant influence in the onset temperature and enthalpy of fusion. In the onset temperature, it is observed that when colemanite and expandable graphite are added to boehmite and brucite, the temperature increases and consequently, the range of the curve decreases. This decrease means that these additives, colemanite and expandable graphite, reduce the range of crystal size and, therefore, the distribution is more homogeneous. Then, when colemanite and expandable graphite are studied individually, the same conclusions can be drawn. Both additives increase the onset temperature and decrease the end temperature with respect to the values obtained for the matrix in Stage 1 (Table 3), so the range of the curve decreases, being greater the effect of the expandable graphite. In conclusion, these additives improve the homogeneity of the polymer crystals, so they could act as nucleants.

TABLE 17: DSC RESULTS OF SECOND MELTING CURVE FOR STAGE 2

Sample	$T_{onset,m}$(°C)	$T_{end,m}$(°C)	Range (°C)	T_m (°C)	ΔH_m (J/g)	w_c (%)
PP	153.33	169.85	16.52	163.67	77.41	37.38
PP+30%Boeh	154.51	167.69	13.18	162.82	67.12	46.29
PP+35%Boeh	153.28	167.87	14.59	162.19	62.15	46.17
PP+35%Boeh +10%Col	157.09	167.12	10.03	163.99	55.54	48.76
PP+35%Boeh +15%Col	156.65	166.85	10.20	163.43	51.78	50.00
PP+35%Boeh +10%EG	157.07	167.03	9.96	163.98	59.21	51.98
PP+40%Bruc	156.47	166.83	10.36	163.48	57.32	46.13
PP+40%Bruc +10%Col	158.12	166.85	8.73	163.33	46.49	44.90
PP+40%Bruc +15%Col	157.43	167	9.57	163.57	43.91	47.12
PP+40%Bruc +10%EG	157.66	166.91	9.25	163.84	52.98	51.17
PP+10%Col	156.69	168.46	11.77	162.54	89.94	48.25
PP+20%Col	156.35	168.33	11.98	163.58	80.91	48.84
PP+10%EG	157.51	167.37	9.86	163.77	90.31	48.45
PP+20%EG	157.39	167.65	10.26	164.08	80.88	48.82
p-value	0.0244	0.1520	0.0535	0.2125	0.0003	0.8627

Then, in the melting temperature, no significant effect of the additive is obtained, and no trend can be determined because the differences are less than one degree. On the other hand, the additive has a significant influence on the enthalpy of fusion. It is observed that in the blends with boehmite and brucite, a lower enthalpy is obtained at a higher percentage of additive as in Stage 1 due to the lower amount of polymer. When colemanite and expandable graphite are added to these main additives, the same trend is obtained, the enthalpy decreases as the total percentage of additive increases and the decrease is more significant with colemanite. On the other hand, the samples with colemanite and expandable graphite individually do not follow the same trend with respect to the percentage of additive. It is observed that the enthalpy increases at 10% and then decreases at 20% by about 9 J/g due to the lower percentage of polymer with respect to the previous sample, but the value is still higher than that of virgin PP. This increase compared to PP is justified by the increase in crystallinity obtained. For both colemanite and expandable graphite, a higher crystallinity percentage is obtained than for the PP+35%Boeh and PP+40%Bruc samples, despite the lower percentage of additive. For this reason, as there is a greater amount of polymer and higher crystallinity, it is necessary to provide more heat for the melting of the material. On the other hand, it is observed that despite increasing the additive percentage of colemanite and expandable graphite, the crystallinity does not increase accordingly, so apparently both additives

increase the formation of crystals, but to a certain extent. Comparing the results obtained with the literature, Oulmou et al. used expandable and expanded graphite in PA11 and obtained an increase in crystallinity for both, but no clear trend with respect to the percentage of additive used [49]. On the other hand, the article by Şahin T. concludes that colemanite does not act as a nucleant because the correction of the percentage of polymer in the crystallinity calculation was not applied [50]. However, applying the formula in Chapter 3 Section 2.4.1 with the percentages by weight added, an increase with respect to the percentage of additive is obtained. Therefore, both additives seem to act as nucleating agents in polymers.

Next, comparing the results for boehmite and brucite with those obtained in the previous stage, it is observed that there is a trend with respect to the percentage. The graph in Figure 28 plots the percentage of crystallinity versus the percentage of additive and it is observed that for both additives the data fit a straight line with high regression values, so it is concluded that there is a linear trend for boehmite and brucite. Then, when colemanite and expandable graphite are added to these minerals, the crystallinity increases, except in the sample PP+40%Bruc+10%Col, which is because these additives act as a support for crystal formation. Comparing both additives, it is observed that the expandable graphite favours more the formation of crystals and for this reason the samples with the highest crystallinity are PP+35%Boeh+10%EG with 51.98% and PP+40%Bruc+10%EG with 51.17%.

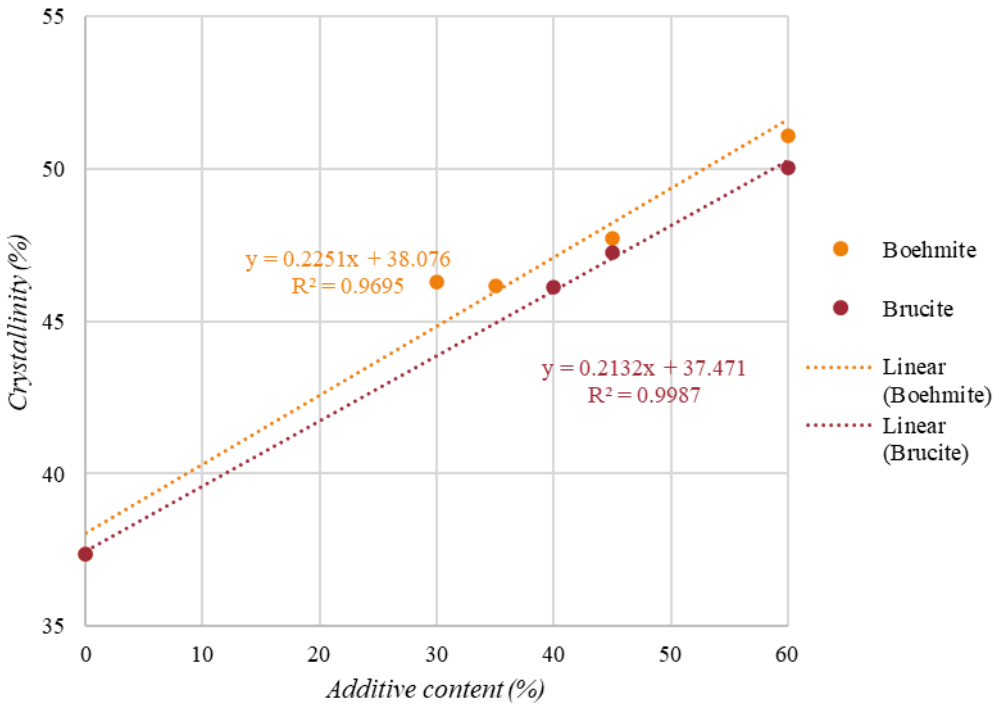

FIGURE 28: CRYSTALLINITY VS ADDITIVE CONTENT FOR BOEHMITE AND BRUCITE SAMPLES

Finally, the effect of additive on the cooling curve is analysed and it is observed that it has no significant influence on any of the variables analysed (Table 18). As in Stage 1, the mixtures with boehmite and brucite increase the $T_{onset,c}$ and T_c because they favour the formation of crystals, so crystallisation occurs at higher temperatures. However, when colemanite is added to the minerals, both temperatures decrease and the difference between them increases. Analysing colemanite individually, it is observed that both temperatures are the lowest of all the mixtures studied in this stage and they are also lower that those obtained in the PP. Therefore, there is a controversy in the results between the melting and crystallisation curves to be able to conclude that colemanite acts as a nucleant, so it is necessary to carry out tests at other percentages or other characterization techniques to confirm. In contrast, when expandable graphite is added to boehmite and brucite, the $T_{onset,c}$ and T_c increase, obtaining the highest of all the mixtures studied in Stage 2. Onset temperatures increase to around 128℃ and peak temperatures to 124℃, but the rate of crystal formation does not accelerate. Analysing individually the expandable graphite, the same conclusions are obtained, the temperatures increase and the rate decreases. In conclusion, expandable graphite acts as a nucleant in polypropylene because it increases the percentage of crystallinity, improves size homogeneity, and increases the crystallisation curve temperatures, but it does not accelerate the crystal formation.

TABLE 18: DSC RESULTS OF COOLING CURVE FOR STAGE 2

Sample	$T_{onset,c}$(℃)	T_c (℃)	$T_{onset,c}$-T_c
PP	120.93	116.76	4.17
PP+30%Boeh	125.13	121.08	4.05
PP+35%Boeh	126.19	123.29	2.90
PP+35%Boeh +10%Col	125.55	122.22	3.33
PP+35%Boeh +15%Col	126.10	122.06	4.04
PP+35%Boeh +10%EG	128.61	124.20	4.41
PP+40%Bruc	125.76	122.50	3.26
PP+40%Bruc +10%Col	123.88	120.73	3.15
PP+40%Bruc +15%Col	124.64	121.26	3.38
PP+40%Bruc +10%EG	127.48	123.35	4.13
PP+10%Col	119.06	115.32	3.74
PP+20%Col	120.93	115.63	5.30
PP+10%EG	125.52	121.17	4.35
PP+20%EG	126.55	121.10	5.45
p-value	0.8321	0.5442	0.1103

3.4.2 TGA

The effect of colemanite and expandable on the thermal stability of polypropylene is studied. Firstly, the results obtained for colemanite are analysed and compared with the results obtained in the Stage 1. Colemanite, like boehmite and brucite, is a mineral that decomposes endothermically under the action of temperature and releases water [48]. Compared to the additives studied in section 2.4.2, colemanite act in a similar range to brucite because its maximum degradation temperature is 398°C compared to 392°C for brucite (Table 19). The main differences between both additives are observed at the beginning and in the final mass percentage. Colemanite starts to release water earlier because its T_L is 255.6°C compared to brucite whose T_L is at 285.6°C (Table 6), but the onset occurs at about 38°C higher. Then, colemanite undergoes the major mass loss attributed to dehydration, which starts at around 395°C to 426°C with the peak of degradation at 398°C at a mass loss rate of 1.37%/°C. Therefore, degradation occurs faster than for boehmite and brucite. In terms of decomposition, colemanite decomposes by two mechanisms [51]. In the former, the structural OH groups form water and in the latter the hydrogen bonds formed between water and boron chains are broken. The second step is accompanied by the release of water vapour, appropriately termed explosive dehydration, which is typically observed during thermal decomposition of hydrated crystalline solid [52]. The water molecules formed are trapped tightly within the crystal structure as internal water which upon heating causes the crystal to explode under internal vapour pressure [42], and for this reason the peak degradation rate obtained is 2.8 higher in colemanite than in brucite. Regarding the final mass, ash remains due to the product obtained in the decomposition reaction [48].

TABLE 19: RESULTS OF TGA TESTS OF COLEMANITE AND EXPANDABLE GRAPHITE SAMPLES

Sample	T_L(°C)	$T_{5\%}$(°C)	T_{onset}(°C)	T_{peak}(°C)	Rate (%/°C)	m_F (%)
PP	237.7	280.7	307.0	351.3	2.071	0.00
PP+10%Col	209.0	246.0	267.2	335.3	5.511	5.50
PP+20%Col	210.3	248.7	263.2	341.3	4.654	15.20
Colemanite	255.6	395.3	393.2	398.0	1.368	77.32
PP+10%EG	211.0	239.3	260.9	305.3	2.868	6.48
PP+20%EG	202.9	242.7	252.9	254.7	18.487	16.04

Then, when colemanite is added to PP, the curve shifts towards lower temperatures compared to unfilled PP (Figure 29). The PP+10%Col and PP+20%Col samples have a similar behaviour at the beginning with similar temperatures (Table 19) and from 300°C is when they separate. It is observed that the PP+20%Col sample has a slightly higher thermal stability because the peak temperature is about 6°C higher than the PP+10%Col sample, degradation occurs at a slower rate and generates more ash that can act as a protective layer for the polymer.

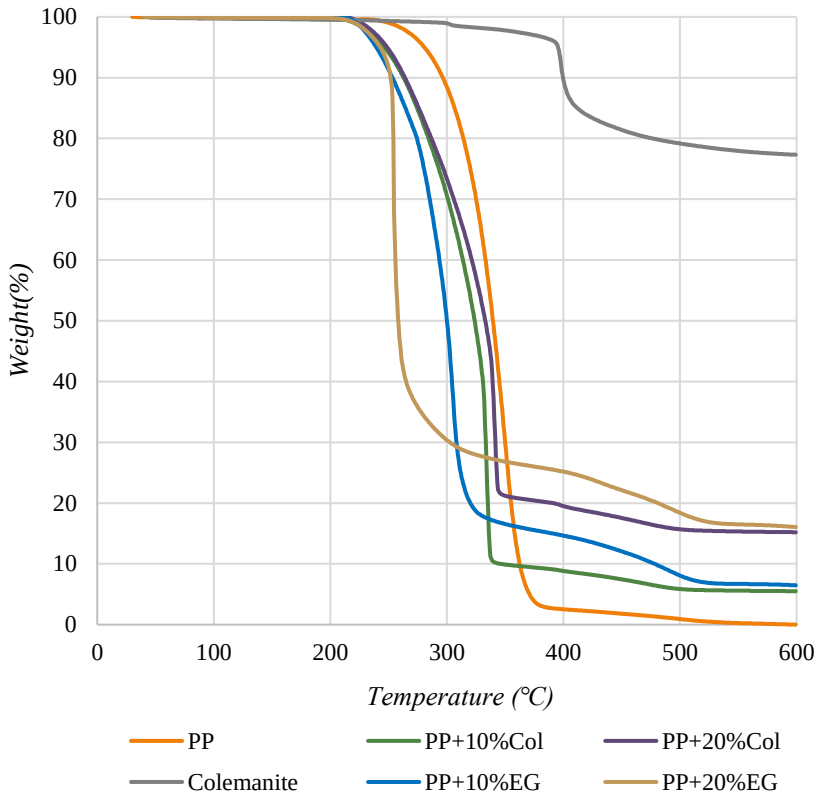

FIGURE 29: TGA CURVES OF COLEMANITE AND EXPANDABLE GRAPHITE SAMPLES

On the other hand, since it was not possible to obtain satisfactory TGA results for the expandable graphite additive, only its effect on PP degradation is analysed. Firstly, it is observed that this additive worsens the thermal stability because the curves move towards lower temperatures with respect to PP and the slope at the point of maximum degradation is much greater (Table 19). Apart from $T_{5\%}$, a decrease in temperatures is obtained with respect to the percentage of additive, reaching a decrease of almost 100°C at the peak of maximum degradation, which is not beneficial for the desired application. This decrease can be attributed to the presence of sulphuric acid inside the expandable graphite sheets due to the synthesis process, whereby the release of acid degradation products may facilitate PP degradation at lower temperatures [49]. Furthermore, the release of these products catalyses the degradation and results in a degradation rate almost 9 times faster than unfilled PP. Finally, the final mass is similar to that obtained for colemanite for the same additive percentages and differs from that observed in the ash content test because in TGA the test ended at 600°C, while in the other the sample remained at this temperature for several hours, allowing the EG to finish degrading.

Figure 30 below shows the TGA curves obtained for the boehmite samples and Table 20 the results for temperatures, peak rate, and final mass. Firstly, it is observed that samples with boehmite degrade in several stages. The samples with only boehmite have two steps, the first one

corresponds to PP degradation, which is more significant, and the second one corresponds to the decomposition of the additive. When colemanite is added to boehmite, a third stage is observed around 400°C due to the dehydration of colemanite, but this change is not so noticeable due to the low percentage of colemanite added. Finally, when expandable graphite is added, its degradation occurs simultaneously with the other two components, so its degradation cannot be differentiated from the others.

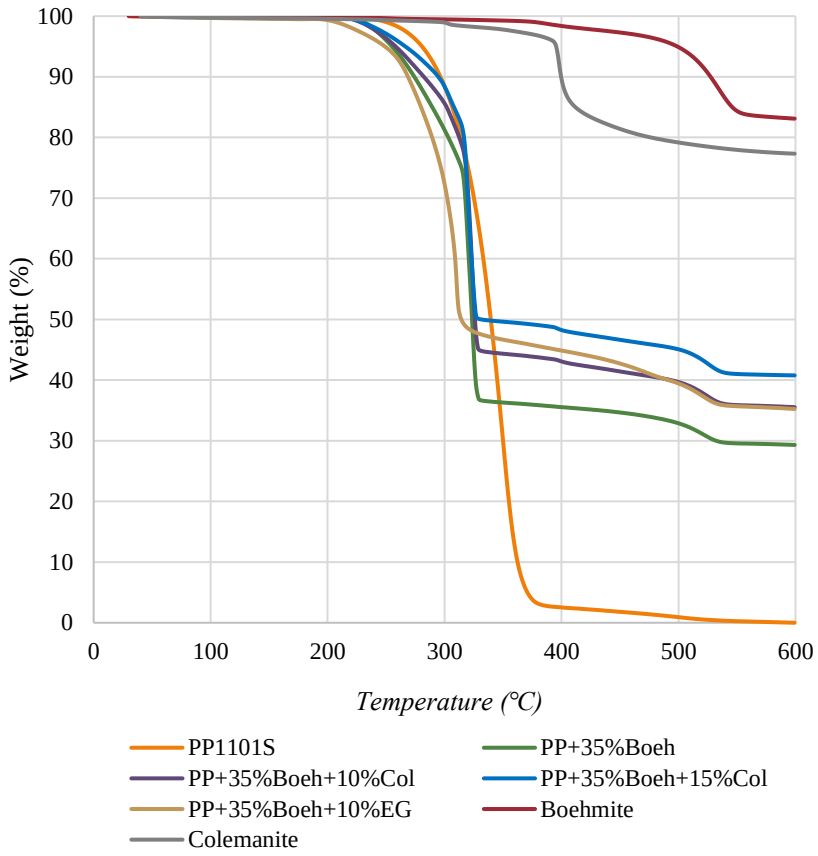

FIGURE 30: TGA CURVES OF BOEHMITE MIXTURES STAGE 2

Next, comparing the results obtained for all the mixtures with PP, it is observed that the thermal stability of the material is not improved because all the curves have shifted to the left. The degradation of the material starts earlier since both T_L and $T_{5\%}$ have decreased, being more significant in the PP+35%Boeh+10%EG sample (Table 20). In the case of the samples with colemanite, the $T_{5\%}$ increases with the percentage added with respect to the PP+35%Boeh samples, but the values are still lower than those obtained for PP. On the other hand, in the T_{onset}, a slight increase in temperature is obtained, between 2 and 5°C, so the mixtures slightly delay the onset of maximum degradation. However, they accelerate the degradation rate and reduce the peak temperature between 27 and 40°C, depending on the mixture. Therefore, the samples with boehmite studied in this second stage do not improve the thermal stability of the material. Finally, it should be noted that the sample with the lowest thermal stability is PP+35%Boeh+10%EG

because all temperatures decrease with respect to the PP+35%Boeh and PP samples, which agrees with the results observed previously for the samples with only expandable graphite.

TABLE 20: RESULTS OF TGA TESTS OF BOEHMITE SAMPLES STAGE 2

Sample	T_L(°C)	$T_{5\%}$(°C)	T_{onset}(°C)	T_{peak}(°C)	Rate (%/°C)	m_F (%)
PP+35%Boeh	211.6	254.7	308.9	324.0	3.807	29.31
PP+35%Boeh +10%Col	209.6	258.0	310.9	323.3	3.906	35.53
PP+35%Boeh +15%Col	207.0	266.3	311.9	320.0	3.761	40.77
PP+35%Boeh +10%EG	190.3	248.7	260.4	310.7	3.408	35.24

Lastly, the results obtained for the samples with brucite are analysed. Figure 31 shows that all the mixtures studied decrease the thermal stability of the material because they degrade at lower temperatures than PP1101S. The PP+40%Bruc sample presents a curve with two differentiated steps, the first step from approximately 260 to 325°C, corresponds to the degradation of PP, and the second one from 350 to 412°C to the decomposition of brucite. Thus, the degradation of PP occurs about 40-50°C earlier, which is not beneficial for the intended application of this material.

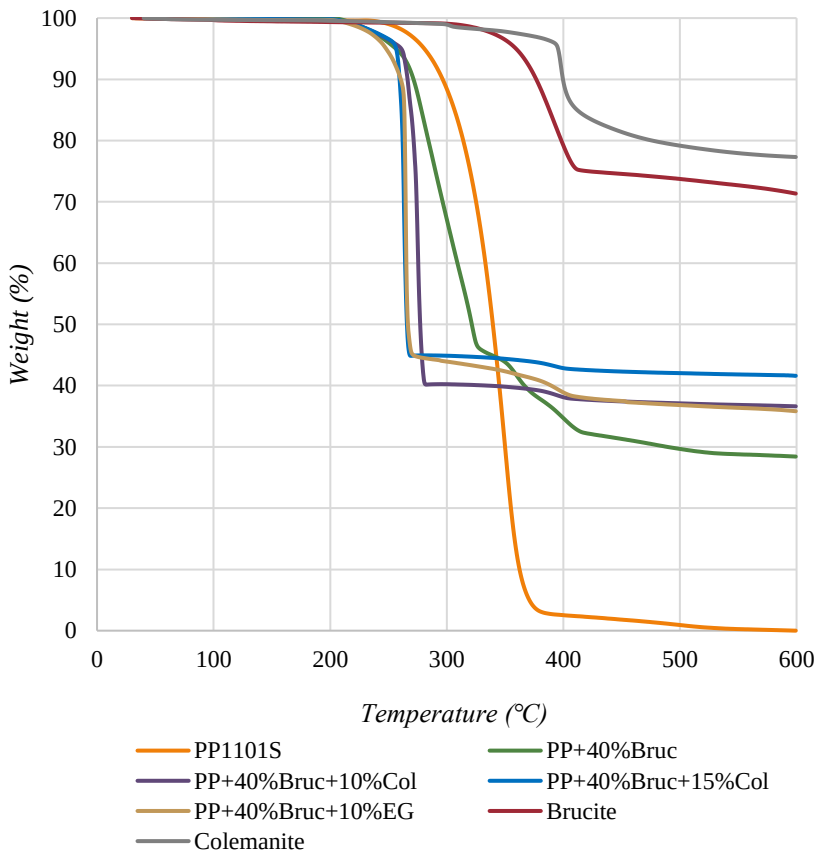

FIGURE 31: TGA CURVES OF BRUCITE MIXTURES STAGE 2

When both colemanite and expandable graphite are added, this is worsened. In these mixtures, the beginning of degradation does not change much as the initial temperatures, T_L, $T_{5\%}$ and T_{onset} differ by less than 10°C with respect to PP+40%Bruc (Table 21), however, the peak temperature is significantly reduced. On average, the peak is reduced by 54°C with respect to PP+40%Bruc and 83°C with respect to PP1101S, and the degradation rate increases considerably, therefore, the mixtures with brucite have a low thermal stability with respect to the rest of the samples studied at this stage, except for PP+20%EG. In conclusion, the samples in this second stage do not improve the thermal stability of PP despite the fact that the decomposition temperatures of the additives are higher than that for PP. Therefore, it is necessary to perform the fire tests in order to determine whether these mixtures have a negative impact on the material properties.

TABLE 21: RESULTS OF TGA TESTS OF BRUCITE SAMPLES STAGE 2

Sample	T_L(°C)	$T_{5\%}$(°C)	T_{onset}(°C)	T_{peak}(°C)	Rate (%/°C)	m_F (%)
PP+40%Bruc	202.9	256.3	259.9	322.0	9.391	28.42
PP+40%Bruc +10%Col	201.4	261.0	267.5	275.3	7.534	36.62
PP+40%Bruc +15%Col	201.0	256.7	259.5	263.3	10.744	41.61
PP+40%Bruc +10%EG	202.3	248.0	262.8	265.3	16.665	35.82

3.4.3 DMTA

Firstly, the effect of temperature on the samples with colemanite and expandable graphite is analysed in Figure 32. The graph shows that the storage modulus versus temperature. Initially between approximately -50 and -5°C, the decrease in modulus is less significant because there is less molecular movement (glassy state zone). Then from the glass transition zone there is an inflection point from which the drop in properties is more significant because there is more intermolecular movement. Comparing the two additives, it is observed that the samples with expandable graphite have a higher storage modulus compared to unfilled PP over the whole temperature range and it increases with the percentage of additive. This trend has also been obtained by other authors such as Oulmou F. who used expandable graphite in PA11 and obtained an increase in modulus with respect to the percentage [49]. This increase is because the EG particles, as being rigid, restrict the movement of the polymeric chain providing rigidity to the material [13]. On the other hand, the samples with colemanite do not have a significant difference with respect to PP. The PP+10%Col is lower than PP in the initial part and then they equalise, and PP+20%Col is slightly higher at some temperatures, so colemanite at these percentages does not seem to significantly affect the thermo-mechanical stability of the material.

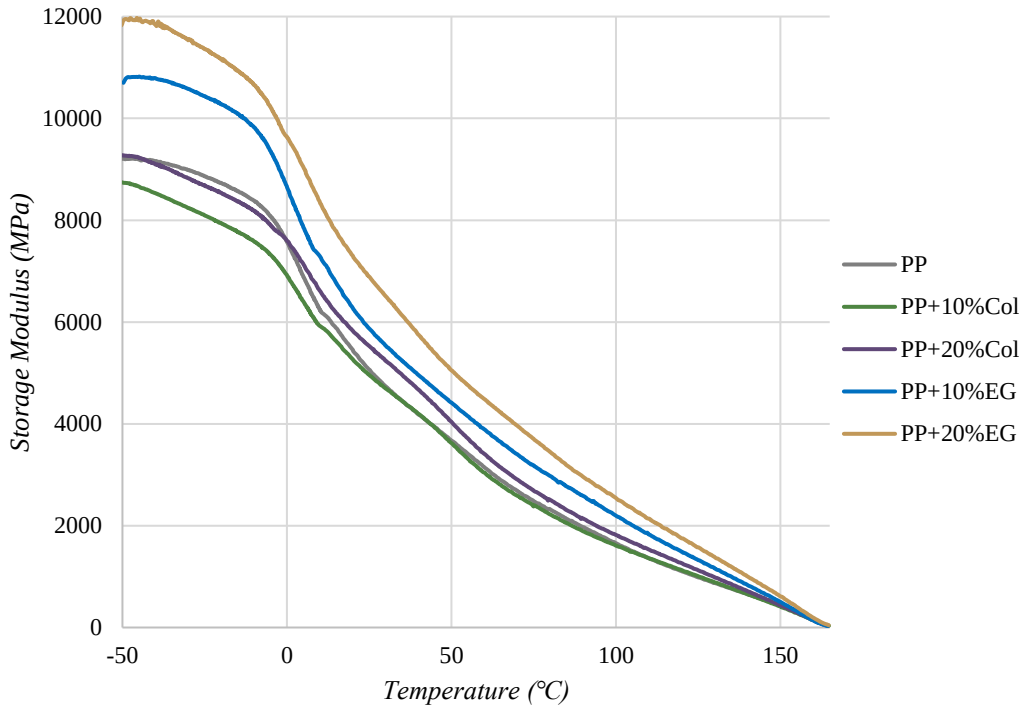

FIGURE 32: STORAGE MODULUS VS TEMPERATURE OF COLEMANITE AND EXPANDABLE GRAPHITE SAMPLES OF STAGE 2

Then, the results obtained for the mixtures with boehmite are analysed below in Figure 33. In this graph, as in Stage 1, it is observed that the storage modulus increases with the percentage of additive due to the incorporation of rigid particles restricts the movement of the molecular chain providing stiffness to the material. In fact, the sample with the highest thermo-mechanical stability corresponds to the PP1101S+60%Boeh sample from Stage 1. When colemanite or expandable graphite is added to the PP+35%Boeh mixture, it is observed that the storage modulus increases with respect to the sample with only boehmite, but the values are lower than those obtained for PP+45%Boeh despite having the same or even higher percentage of total additive. Therefore, the additives of this second stage do not significantly improve the stability of the boehmite. Comparing the Boeh+Col and Boeh+EG mixtures, it is observed that there are no significant differences between them. From higher to lower storage modulus, it is observed that PP+35%Boeh+10%Col and PP+35%Boeh+10%EG samples show similar behaviour especially in the temperature range up to about 50°C. Above this temperature, the PP+35%Boeh+10%EG sample shows a slightly higher storage modulus value, 3352 MPa vs 3020.8 MPa for PP+35%Boeh+10%Col. Therefore, at elevated temperatures the expandable graphite provides higher thermo-mechanical stability, which agrees with the results obtained previously for the PP and expandable graphite mixture. Subsequently, at around 12700 MPa storage modulus, about 500 MPa less than the previous mixtures, is the sample PP+35%Boeh+15%Col. This mixture, despite having 5% more additive, has a lower storage modulus, which leads to the conclusion that colemanite does not show a clear trend with respect to the percentage of additive.

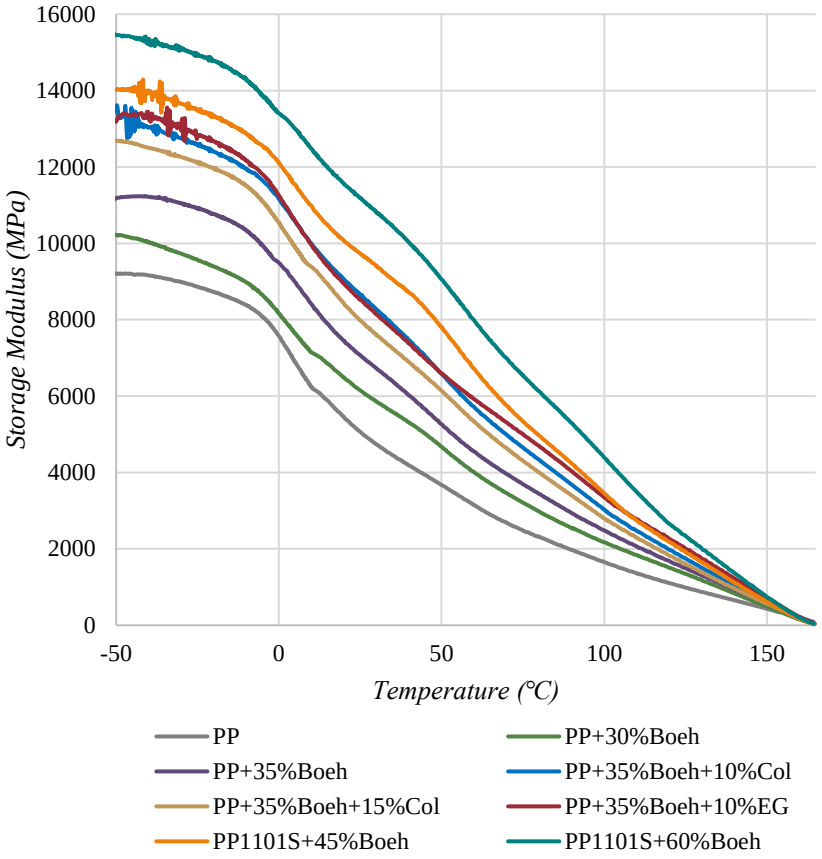

FIGURE 33: STORAGE MODULUS VS TEMPERATURE OF BOEHMITE SAMPLES OF STAGE 2

Figure 34 shows the curves for the samples with brucite. In this case, it is observed that the mixtures of this second stage present higher storage modulus values than those obtained for the mixtures with only brucite in almost all the temperature range. The most thermo-mechanical stable sample is PP+40%Bruc+15%Col, followed by PP+40%Bruc+10%EG and PP+40%Bruc+10%Col. These last two mixtures present a significant difference in the initial zone or glassy state zone, but from -10 degrees both curves are equal. Thus, in the mixtures with brucite, no differences were obtained in the performance between colemanite and expandable graphite, so the factor that influenced the modulus value was the percentage of additive, because a higher storage modulus was obtained with a higher total additive content. Then, when comparing these mixtures with those studied in the previous stage, it is observed that the PP+40%Bruc+15%Col has a modulus 3000 MPa higher than the PP+60%Bruc mixture at -50 degrees, which is quite a significant difference. However, as in the PP+60%Bruc mixture the loss of properties with respect to temperature occurs more slowly, there comes a point where the two curves cross. The crossover occurs at around 115C and it is at this temperature that the PP+60%Bruc sample has the highest storage modulus value, but as it is less than 100 MPa, it is considered that the difference is not very significant. Therefore, colemanite when combined with

brucite improves the material properties and the mixtures of this stage improve the thermo-mechanical stability of the material with respect to the mixtures of the previous stage.

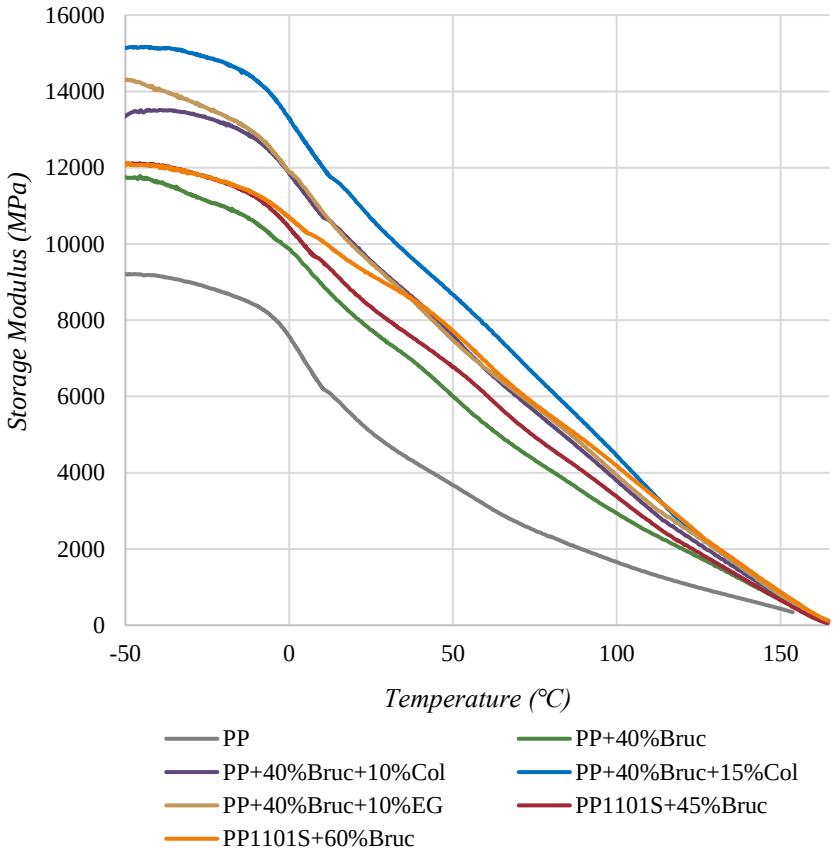

FIGURE 34: STORAGE MODULUS VS TEMPERATURE OF BRUCITE SAMPLES OF STAGE 2

Finally, Table 22 shows the results of the storage modulus at 20, 100 and 150°C and the value obtained for the glass transition temperature. As concluded from the graph above, colemanite does not significantly affect the properties of polypropylene because the values obtained are very similar. However, when mixed with boehmite and brucite, it does improve the thermal stability, especially in the mixtures with brucite, so it could be concluded that these additives complement each other when they act together. In the case of expandable graphite, it is observed that both individually and in mixtures, it improves the thermal stability of the material throughout the entire temperature range. In fact, the PP+20%EG mixture presents higher storage modulus values than the 30%Boeh mixture. It would therefore be necessary to verify whether the result obtained in the mixtures is the sum of the effect of the additives individually or whether there is a synergistic effect between them. Finally, comparing the samples with boehmite with those with brucite, it is observed that the storage modulus is higher with brucite, even with the same total percentage of additive, which is due to the density of the additives. The density of

brucite is lower than that of boehmite, so its particles occupy more volume and there is less polymer to provide flexibility to the material.

TABLE 22: DMTA RESULTS OF STAGE 2 SAMPLES

Sample	$E'_{20°C}$(MPa)	$E'_{100°C}$(MPa)	$E'_{150°C}$(MPa)	T_g (°C)
PP1101S	5453.7	1654.7	431.3	4.94
PP+10%Col	5271.4	1611.6	412.8	4.55
PP+20%Col	5827.7	1817.5	436.9	7.01
PP+10%EG	6287.9	2190.3	500.2	2.74
PP+20%EG	7301.0	2549.0	610.8	5.57
PP+30%Boeh	6486.9	2173.4	489.8	3.59
PP+35%Boeh	7449.2	2487.1	569.3	6.75
PP+35%Boeh +10%Col	9066.3	3020.8	614.1	6.27
PP+35%Boeh +15%Col	8436.1	2787.5	558.4	4.79
PP+35%Boeh +10%EG	8934.0	3352.0	715.5	4.64
PP+40%Bruc	8094.5	2933.5	668.2	5.07
PP+40%Bruc +10%Col	9975.3	3788.9	751.9	4.53
PP+40%Bruc +15%Col	11170.4	4440.9	752.2	5.04
PP+40%Bruc +10%EG	9895.1	3940.1	786.4	6.98
p-value	0.0180	0.0695	0.2837	0.4448

Finally, the T_g of all samples was determined using the loss modulus peak and the results are shown in Table 22. As in Stage 1, the loss modulus curves presented two peaks due to the betha (T_g) and alpha transitions, with the alpha transition being more noticeable. This transition, being associated with the movement of the chains in the crystalline phase, is more significant in the samples with higher crystallinity and can overshadow the one corresponding to betha or T_g. Furthermore, in the T_g region, the curves are noisy, which makes it difficult to determine the temperature accurately and to determine trends due to additives, so the results should be considered an approximation. In general terms, the glass transition temperatures are lower than in Stage 1 and do not differ significantly from those obtained for PP. Therefore, these mixtures have less influence on the movement of the polymer chains in the glass transition zone. In colemanite, T_g seems to increase with the percentage of additive when used individually and in mixtures with brucite. However, when mixed with boehmite, a decrease in T_g is obtained with the percentage of colemanite, which agrees with the trend previously observed in the storage modulus. In the figure, a decrease in the storage modulus was obtained for the sample PP+35%Boeh+15%Col, therefore,

as the sample is less rigid, it favours the movement of the polymeric chains and the T_g decreases. As for the expandable graphite, it is not possible to determine a clear trend since at the individual level and in the mixtures with minerals, different trends are observed, and these do not correspond to those observed in the storage modulus.

3.5 RHEOLOGY

To study the viscosity of the mixtures, an oscillatory rheology test was carried out at three temperatures 170, 190 and 210°C. Firstly, the effect of colemanite and expandable graphite in the viscosity of polypropylene is analysed in Figure 35. This graph shows the curves obtained at 210°C and shows that the viscosity increases with the percentage of additive used and that there are significant differences between the samples with colemanite and expandable graphite.

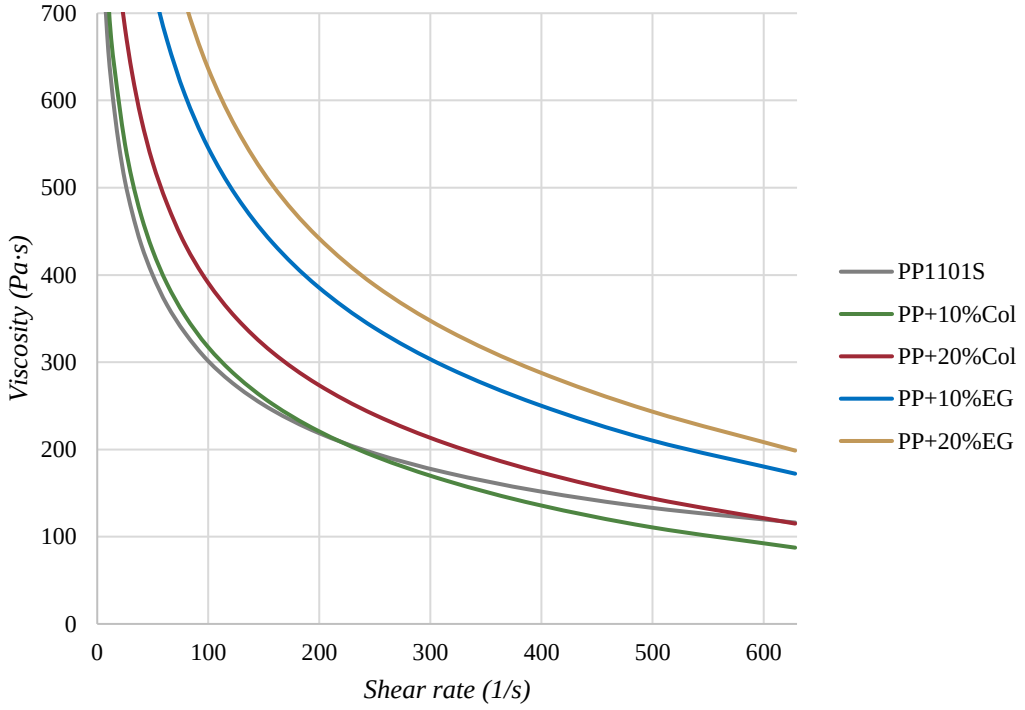

FIGURE 35: VISCOSITY CURVES OF PP SAMPLES WITH COLEMANITE AND EXPANDABLE GRAPHITE AT 210°C

In the case of colemanite, the PP+10%Col sample has a similar viscosity to unfilled PP and when increasing to 20%Col the viscosity increases by approximately 26%. Other authors such as Güldaş et al. [53] obtained an increase in the viscosity of PP even with an additive percentage of 5%, so it is necessary to study in detail the PP+10%Col sample to verify this trend. In the case of the samples with expandable graphite, the viscosity of the PP+10%EG sample is higher by 38% on average with respect to the 20% colemanite sample, despite having a lower additive proportion. This is mainly due to the particle type as well as the particle density. Expandable graphite particles

have a lower density than colemanite, which means that they occupy more volume and therefore make it more difficult for the material to flow. If there is also a slight expansion of the EG due to temperature, the volume occupied by the particles increases and the effect on the viscosity is aggravated. Subsequently, when increasing the percentage to 20%, the viscosity increases approximately 20% more with respect to PP+10%EG, which means that the increase in viscosity due to the expandable graphite is an important aspect to consider as it can make manufacturing more difficult.

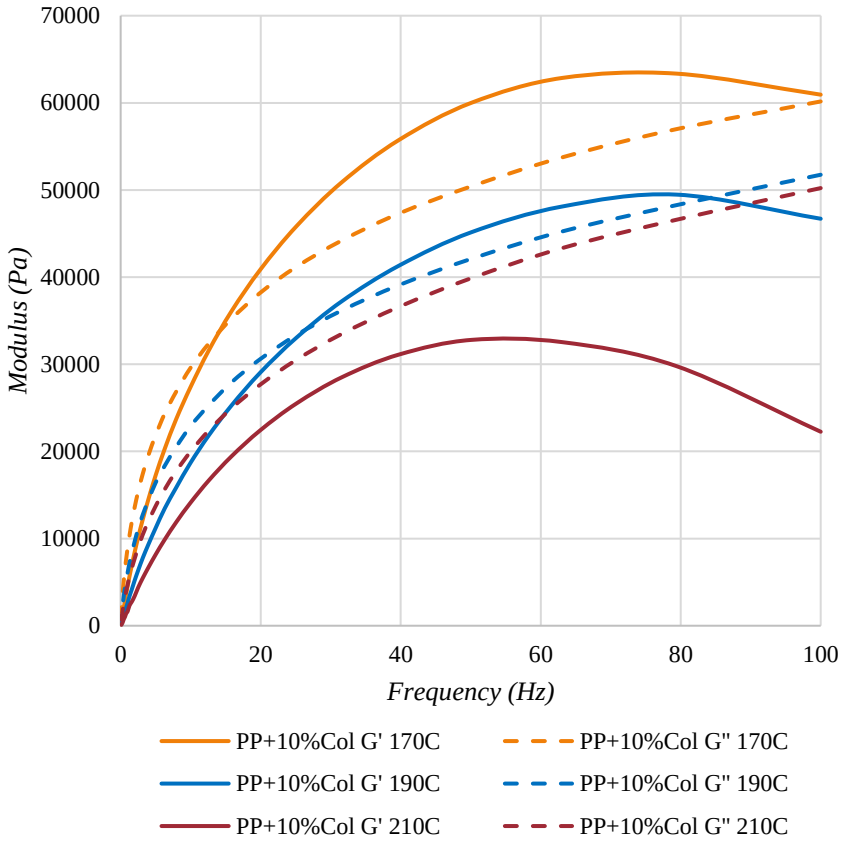

FIGURE 36: OSCILLATORY RHEOLOGY CURVES OF COLEMANITE SAMPLES AT 170°C

Figure 36 shows the G' and G'' curves obtained for the PP+10%Col sample at the three test temperatures. In the curve at 170°C, it is observed that the sample presents a liquid dominant behaviour up to 14.72 Hz (crossing point between G' and G") and this occurs at 33770 Pa. When the temperature increases to 190C, two crossover points are observed, the first at 26.55 Hz (34020 Pa) and the second at 83.05 Hz (48920 Pa). In the case of PP, there was only one crossover point at 23.82 Hz, which means that at this temperature the PP+10%Col sample has a wider range of liquid behaviour. Finally, at 210°C it is observed that the curve G" is higher than G' in the whole frequency range, so despite having a 10% additive, the sample presents a liquid dominant behaviour, while with PP it presented a crossover point at 42.34 Hz. For this reason, the PP+10%Col sample has a similar or even lower viscosity than PP at some temperatures.

Figure 37 shows the viscosity curves obtained for the boehmite samples. Following the trend observed in previous stages, in the samples with boehmite and colemanite, the percentage of additive influences the viscosity, since the higher the percentage, the higher the viscosity of the mixture. In the case of the sample with expandable graphite, PP+35%Boeh+10%EG has a higher viscosity than PP+35%Boeh+15%Col despite having 5% less additive because, as observed previously in the analysis of the effect of the two additives (Figure 35), expandable graphite increases more the viscosity of the material due to the size and density of its particles.

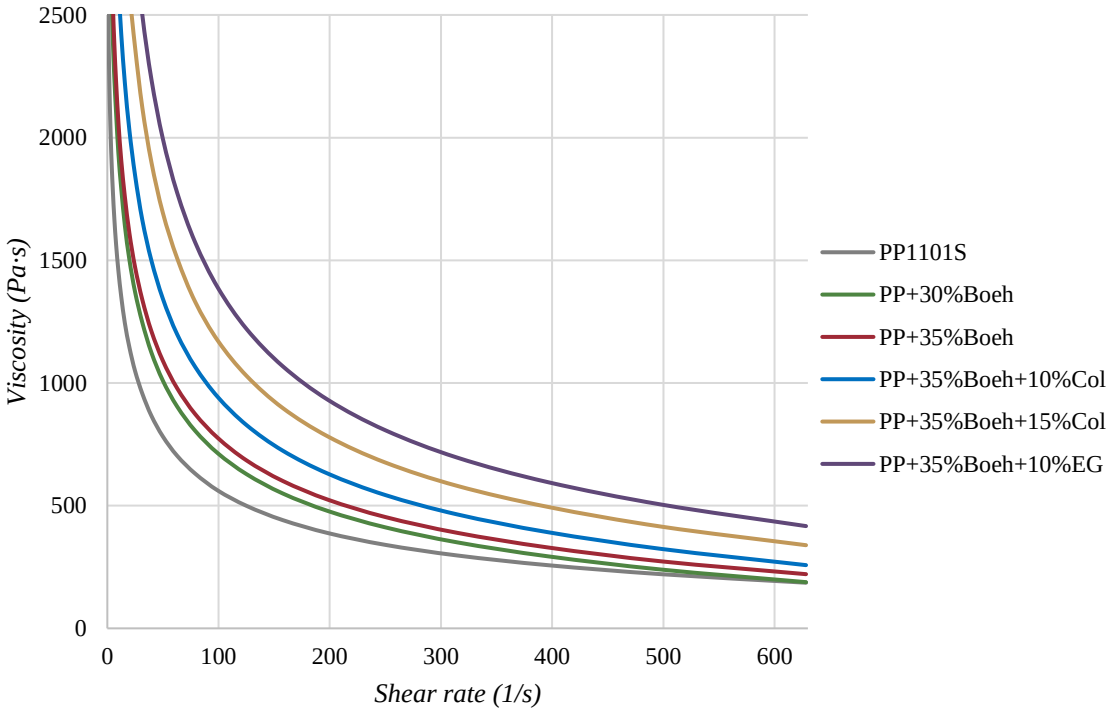

FIGURE 37: VISCOSITY CURVES OF BOEHMITE SAMPLES OF STAGE 2 AT 170ºC

On the other hand, the same trend is not obtained in the samples with brucite (Figure 38). In this case, the viscosity of the sample increases with respect to the percentage of total additive for all the mixtures studied. The sample with the highest viscosity is the one corresponding to PP+40%Bruc+15%Col because it has the highest percentage of additive and the curve shows turbulences in the final part as in the 60% brucite mixtures. Therefore, when brucite is mixed with expandable graphite at these percentages, the viscosity of the mixture increases with respect to PP+40%Bruc+10%Col due to the type of particles, but not so much as to exceed the sample with 15%Col. Finally, when comparing both boehmite and brucite mixtures, the brucite samples show a significantly higher viscosity than the boehmite sample despite having the same total additive percentage in some samples. This difference is because the main additive, boehmite and brucite, in addition to differing by 5%, the density of boehmite is higher than for brucite and consequently affects the viscosity of the mixture less.

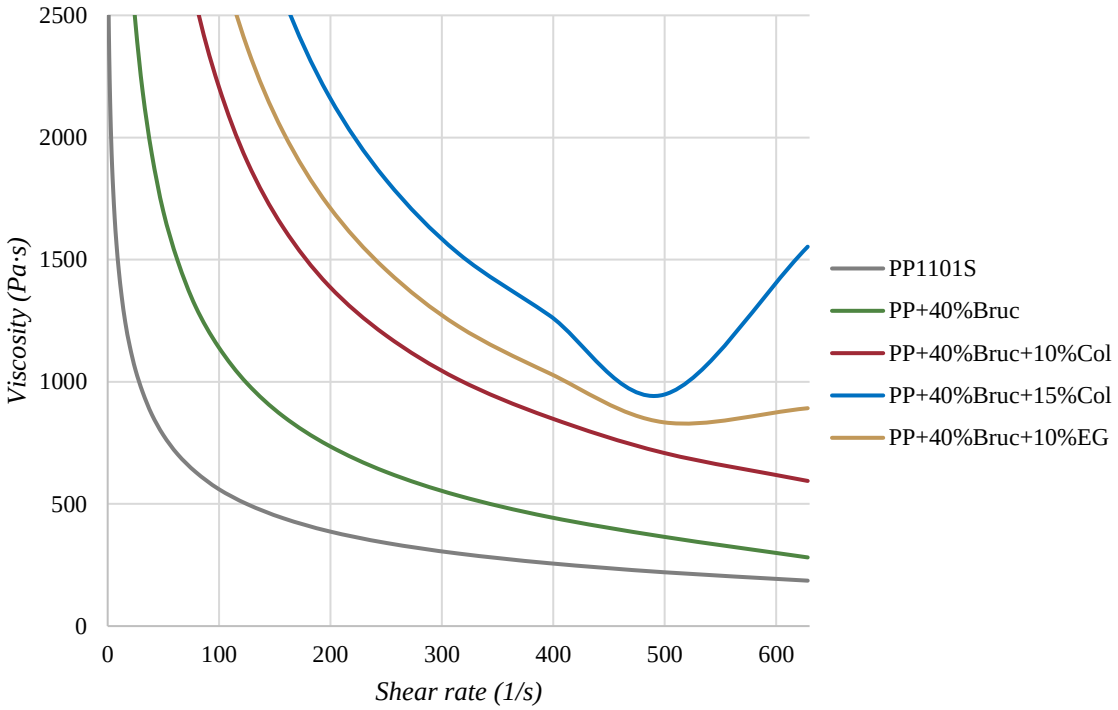

FIGURE 38: VISCOSITY CURVES OF BRUCITE SAMPLES OF STAGE 2 AT 170ºC

3.6 MECHANICAL TESTS

Regarding the mechanical test, the results of the tensile tests are analysed first. Figure 39 shows the tensile properties of the samples together with their standard deviation. As observed in the previous stage, the additive has a statistically significant effect on the elastic modulus and maximum tensile strength. Firstly, it is observed that in the samples with boehmite and colemanite, the higher the total percentage of additive, the higher the modulus, which is justified by the stiffness of the particles that confer rigidity to the material. However, this increase in the stiffness of the material is coupled with a decrease in the maximum tensile strength with respect to the percentage of additive, because the additives used make the material more brittle. This brittleness is justified because there is a poor adhesion between the polymer and the additive, so the stress is transferred inefficiently to the particles and there is less material in the cross section to resist the force. Then, when expandable graphite is added to boehmite, a slight increase in the elastic modulus is obtained, 2778.4 MPa compared to 2697.1 MPa for PP+35%Boeh, but the maximum tensile strength decreases considerably. Although the PP+35%Boeh+10%EG sample has a lower additive percentage, the strength decreases 2.26 MPa compared to PP+35%Boeh+15%Col and is also 8.57 MPa lower with respect to PP+35%Boeh. In fact, its strength is slightly lower than that obtained in Stage 1 for the PP+60%Boeh sample (Figure 21), which is contrary to the objective of using synergistic mixtures to not affect the mechanical properties as much. This significant decrease is because, as observed in the extrusion, the

expandable graphite started to expand so it occupies more volume in the specimen section and there is less volume of polymer to resist the force.

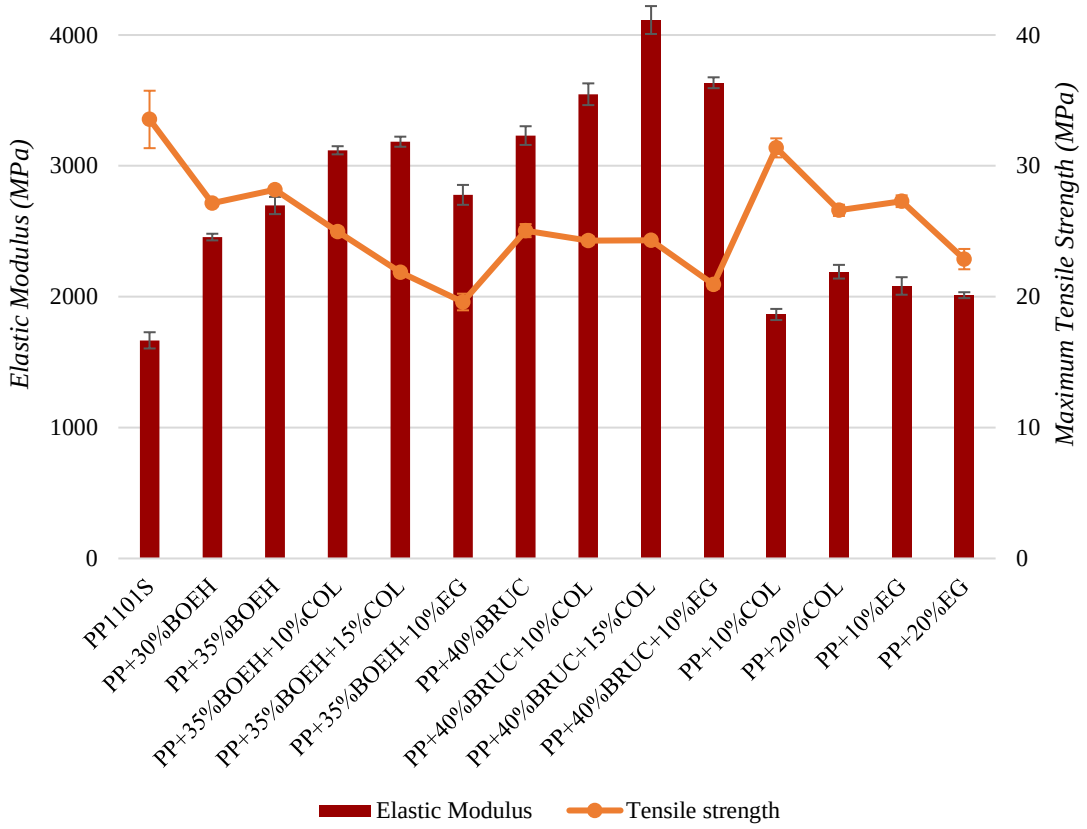

FIGURE 39: TENSILE TEST RESULTS OF STAGE 2

In the brucite samples, the elastic modulus increases with the percentage of additive and the module are higher than those for boehmite samples due to the lower density of brucite and colemanite mixture. Colemanite has a similar density to brucite (Table 2), so at the same total percentage, the particles (brucite and colemanite) occupy more volume and provide more stiffness to the specimen compared to boehmite and colemanite. On the other hand, in the results of the maximum stress, it is observed that it decreases with respect to the percentage, but slightly compared to boehmite samples. This difference could be justified by the fact that brucite and colemanite particles are more compatible with each other and adhere better to the polymer, so although the percentage of additive is increased, the tensile strength is not significantly reduced. This conclusion is also obtained in the elastic modulus. For the same level of colemanite addition, the elastic modulus of the samples with brucite increases more than in the samples with boehmite, because by adhering better, they reinforce the polymer better. In fact, other authors such as Isitman N. [54] have found that the partial substitution of the main additive by colemanite improved the ductility and toughness of the material, and in this case, it occurs better with brucite. Then, in the PP+40%Bruc+10%EG sample, the elastic modulus increases to values even slightly

higher than those obtained for PP+40%Bruc+10%Col. This increase can be attributed to the fact that EG also has some compatibility with brucite and therefore strengthens the material better than with boehmite. For this same reason, EG decreases the maximum tensile strength by 4.11 MPa compared to PP+40%Bruc, which is half of the decrease obtained with boehmite due to its better adhesion with the matrix. In summary, it is concluded that brucite may have a certain compatibility with colemanite and expandable graphite that allows them to adhere better to the polymer, but further tests are needed to confirm this interaction.

Finally, the effect of colemanite and EG on the tensile properties of polypropylene is studied. In the samples with colemanite, the same tendency is obtained as for the rest of the minerals studied. The elastic modulus increases with the percentage of additive while the maximum stress decreases, which agrees with what has been observed by other authors [50]. For the EG samples, the elastic modulus increases with respect to unfilled PP. When the percentage is increased to 20%, a small decrease is obtained compared to PP+10%EG, which agrees with what was observed in the extrusion process. As the percentage of EG increased, the filament did not become stiffer, it became a little more elastic and less resistant due to the expansion of the additive. For this reason, the maximum tensile strength diminishes with respect to the percentage of additive, obtaining a considerable decrease compared to PP1101S, 22.87 MPa versus 32.42 MPa of PP. This decrease is because as the particles occupy more volume, there is less polymer that can resist the tensile stress in the section of the specimen. Moreover, even if particle had not expanded, the same trend would have been obtained with respect to the percentage as reported by Oulmou F [49].

The results obtained in the flexural and impact test are analysed below (Table 23). In the flexural test, the modulus increases with the percentage of mineral additive due to the higher stiffness of the particles. In fact, the increase is greater when colemanite is added due to the greater stiffness of the mineral with respect to boehmite and brucite, which is also related to the hardness. From highest to lowest on the Mohs scale, colemanite has a hardness of 4.5 [55], followed by boehmite with 3.5 [6] and brucite with 2.5-3 [56]. In addition to the hardness, it is necessary to consider the total percentage of additive and the density of the particles to justify the trend. The flexural modulus obtained for the brucite samples are higher despite the greater hardness of boehmite, because the total percentage of additives are higher, and the density of the mixtures is lower. As observed in Stage 1, the greater the volume occupied by the additives, the greater the effect on the stiffness because there is a lower proportion of flexible material in the specimen section. In the case of expandable graphite, the same trend is obtained, the flexural modulus increases when added to boehmite and brucite because it increases the stiffness. Finally, expandable graphite increases the flexural modulus with respect to unfilled PP, but when the

percentage is increased, the modulus decreases slightly. This result agrees with what was observed experimentally during extrusion. The PP+20%EG showed a higher flexibility compared to the PP+10%EG sample because, due to the expansion of the particles, there is more movement between the graphite layers, which favours the flexibility of the material and the modulus decreases.

TABLE 23: FLEXURAL AND IMPACT TEST RESULTS OF STAGE 2

Sample	Flexural Modulus (MPa)	Impact strength (kJ/m^2)
PP1101S	1484.5 ± 42.5	32.42 ± 0.89
PP+30%Boeh	2651.6 ± 61.8	30.26 ± 3.34
PP+35%Boeh	2725.1 ± 25.1	28.26 ± 4.93
PP+35%Boeh+10%Col	3675.7 ± 78.6	16.18 ± 2.35
PP+35%Boeh+15%Col	3857.9 ± 138.4	13.38 ± 1.33
PP+35%Boeh+10%EG	3748.2 ± 155.1	8.92 ± 0.72
PP+40%Bruc	2885.9 ± 84.5	14.21 ± 1.86
PP+40%Bruc+10%Col	4472.5 ± 125.7	9.69 ± 0.61
PP+40%Bruc+15%Col	4851.0 ± 128.4	7.81 ± 0.47
PP+40%Bruc+10%EG	4263.3 ± 152.2	6.77 ± 0.45
PP+10%Col	2053.6 ± 132.8	30.90 ± 0.96
PP+20%Col	2375.6 ± 49.4	30.54 ± 0.68
PP+10%EG	2303.0 ± 74.6	22.31 ± 3.82
PP+20%EG	2272.5 ± 95.6	12.05 ± 1.32
p-value	0.0000	0.0000

Lastly, for the impact strength, the conclusions obtained are the same as for the maximum tensile strength. In the samples with minerals, the impact strength decreases with respect to the percentage of additive due to the reduction of the effective area. In this case, the key aspects are the total percentage of additive and the density of the particles. As the stress is not transferred efficiently to the particles, the smaller the polymer area, the lower the strength. For this reason, samples with brucite and colemanite have lower impact strength compared to boehmite because of their lower density. Comparing the results obtained with Stage 1 (Table 11), it can be observed that in the samples with boehmite, the addition of colemanite has a negative effect on the impact strength because the values are lower for the same total percentage of additive. A value of 16.18 kJ/m^2 was obtained for the PP+35%Boeh+10%Col compared to 21.34 kJ/m^2 for the PP+45%Boeh. However, with brucite colemanite it has had a beneficial effect because for higher values of additive percentage a higher impact strength has been obtained. For example, the PP+40%Bruc+10%Col has an impact strength of 9.69 kJ/m^2 compared to 8.78 kJ/m^2 for the PP+45%Bruc. On the other hand, the addition of expandable graphite has a very significant effect

on the impact strength. As can be seen in the results for both boehmite and brucite mixtures, when 10%EG is added, the lowest impact strength values of all the samples studied in Stage 2 are obtained. Even in the PP+20%EG sample, a strength of 12.05 kJ/m^2 is obtained which is 63% lower than PP1101S despite having only 20% additive. As mentioned above, the significant decrease in mechanical properties in the samples with expandable graphite is due to the expansion of the particles during processing. To avoid this, several alternatives could be used, such as lower the processing temperatures, which may not be feasible for a correct extrusion of the PP samples, use an expandable graphite with a higher expansion temperature or use a matrix with a lower melting point. Finally, in the samples with colemanite, a small decrease is obtained with respect to unfilled PP, but the increase of the additive percentage does not have a significant effect on the impact strength. This trend does not agree with the maximum tensile strength tendency obtained or reported by other authors [50], so it would be necessary to study colemanite with polypropylene at other percentages to determine the trend.

In summary, the use of synergistic mixtures shows promising mechanical results, especially in the case of colemanite with brucite, because it allowed to obtain materials with better mechanical properties at the same or even higher loading levels.

3.7 FIRE TESTS

Since the results obtained in the mechanical tests seem promising, fire tests are then carried out to study whether these additives also complement each other as flame retardants. For this purpose, the UL94 test has been carried out both horizontally and vertically following the procedure performed in the previous stage and the cone calorimeter test has been added to obtain more information on the effect of the mixtures.

3.7.1 UL94

First, the results obtained for the horizontal test are analysed. Figure 40 shows the horizontal propagation speed of all the samples studied and the totality of results are reported in the Annex. In this test, the additive has a statistically significant effect (p-value=0.0000). In the samples with boehmite, it is observed that the increase of the percentage to 35% and the addition of 10% colemanite do not significantly influence the speed and, in fact, these samples do not meet the test criteria. However, increasing the percentage of colemanite to 15% or adding 10% expandable graphite results in a decrease in speed of 17.7% and 14.4% respectively, and the criteria is met. This decrease is significant compared to the PP+35%Boeh sample, but it is not enough to justify the use of these mixtures. Compared to the values obtained for boehmite in Stage 1, it is observed that the speed of the sample PP+35%Boeh+15%Col remains practically unchanged with respect

to the sample PP1101S+45%Boeh (Figure 22) despite having 5% more additive, 33.98 mm/s versus 34.27 mm/s. In addition, for the sample PP+35%Boeh+10%EG the speed increases (35.37 mm/s). Therefore, it is concluded that neither colemanite nor expandable graphite act as synergistic additives with boehmite.

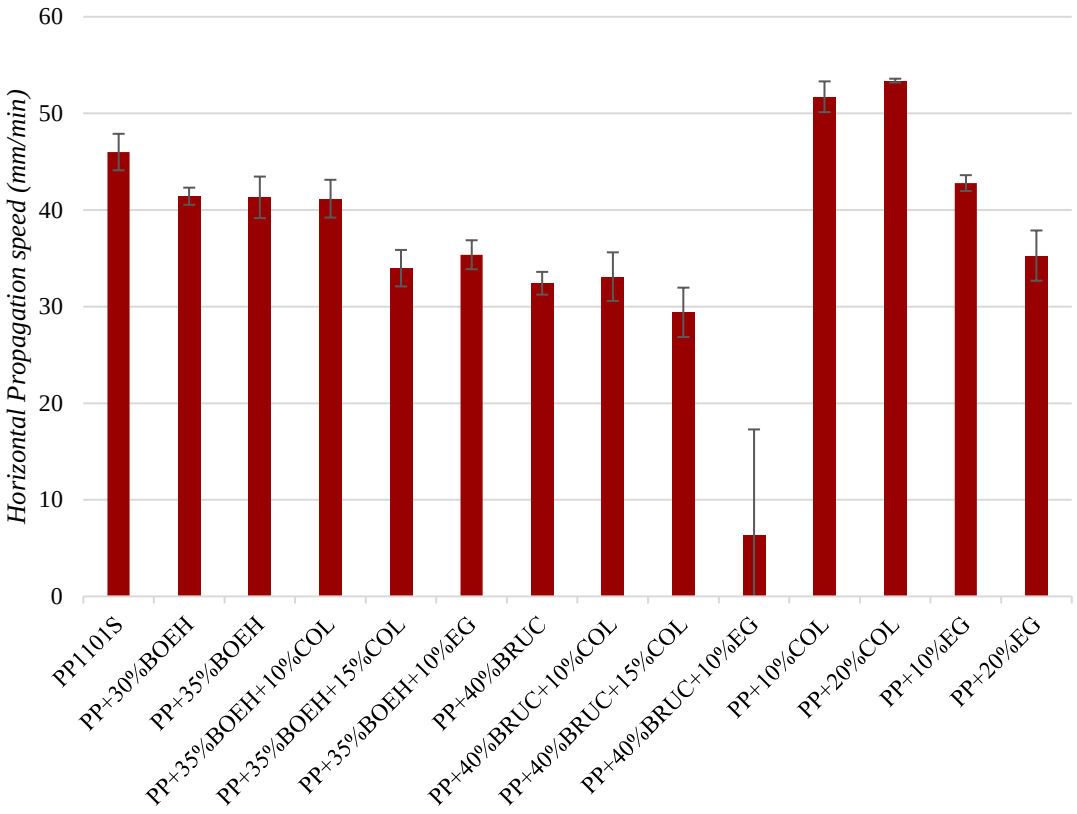

FIGURE 40: RESULTS OF HORIZONTAL TEST 94 HB OF STAGE 2 SAMPLES

On the other hand, in the samples with brucite, all the mixtures meet the criteria of the horizontal test. As with boehmite, the addition of 10% colemanite does not significantly affect the speed and when increased to 15%, the speed is reduced but not enough to justify the increase of the total additive percentage to 55%. In fact, when compared to Stage 1, none of the samples have a lower horizontal propagation speed than that obtained for the PP1101S+45%Brucite sample. In contrast, when 10% expandable graphite is added, the speed is significantly reduced to 6.32 mm/s on average. This sample has a higher standard deviation compared to the rest of the samples because of the three specimens studied, two did not propagate the flame and one did, but at a lower speed than the PP1101S+45%Bruc. Therefore, it seems that brucite and colemanite mixtures do not act as synergistic mixtures, but the expandable graphite seems to have a synergistic effect as reported by Chen X. et al [57,58]. Finally, when analysing the effect of colemanite individually, a negative effect is obtained since the speed is higher than for unfilled PP1101S (46 mm/s) and seems to increase with the percentage. These results are not in agreement with those obtained by other authors for other matrices [59,60], so further tests are needed to

confirm the effect of colemanite on polypropylene. In the case of expandable graphite, a decrease in speed is obtained with respect to the percentage of additive used, 7% for PP+10%EG and 23.3% for PP+20%EG with respect to PP1101S. Therefore, adding the effect of 40% brucite and 10% expandable graphite individually gives a higher speed than that obtained for PP+40%Bruc+10%EG, which would confirm that it is a synergistic mixture.

As the samples do not meet the criteria set by the UL94V test and it is not possible to determine the effect of the additives clearly with the flame times, the vertical propagation velocity was determined, and the results are shown in Figure 41.

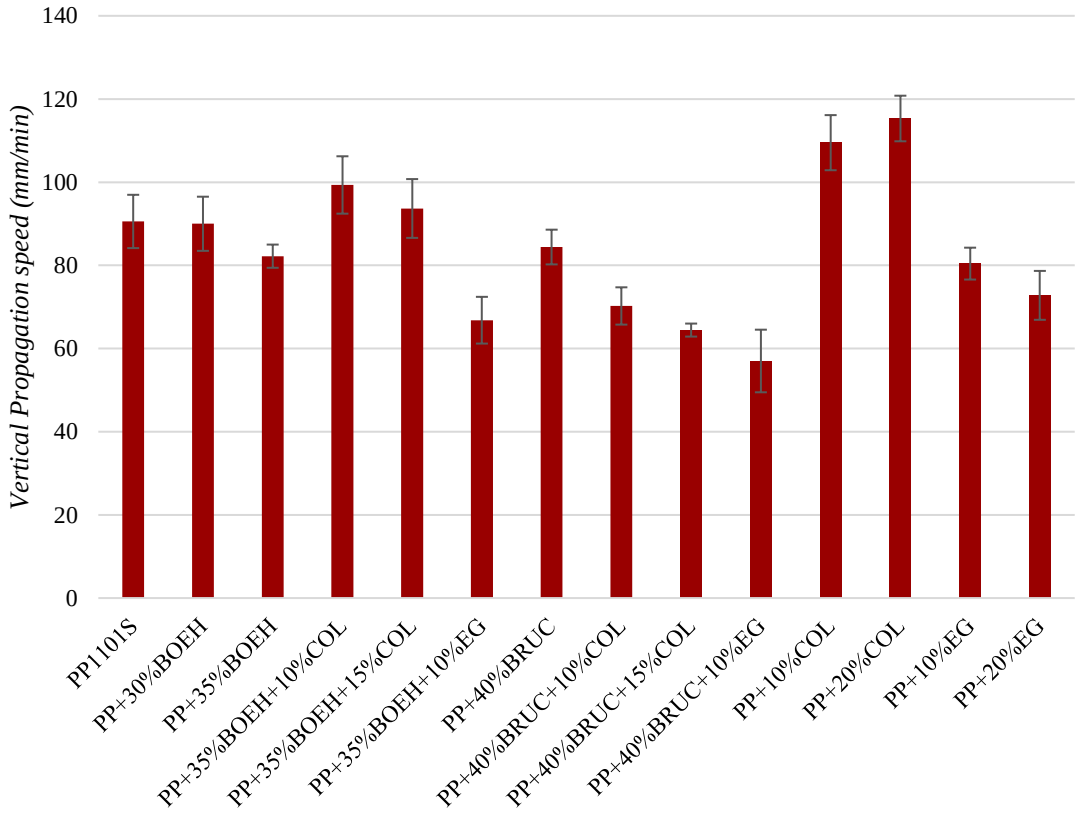

FIGURE 41: RESULTS OF VERTICAL TEST 94V OF STAGE 2 SAMPLES

In the samples with boehmite, it is observed that the propagation speed decreases with the percentage, but when colemanite is added the velocity increases. In the sample PP+35%Boeh+10%Col, the speed increased from 82.2 mm/s for PP+35%Boeh sample to 99.3 mm/s, which is a considerable augmentation. Then, with the addition of 15% colemanite, the speed diminished to 93.7 mm/s, but it is still higher than the PP+35%Boeh sample. In conclusion, as the vertical propagation speeds of boehmite/colemanite samples are even higher than for PP1101S, the mixture would be discarded from the study. In the case of the expandable graphite, the propagation speed decreases by 18.7% compared to PP+35%Boeh and its speed is similar to

the PP+60%Boeh sample, 66.8 mm/s versus 69.9 mm/s. This is a promising result for the boehmite/expandable graphite mixture but has the disadvantage that the mechanical properties decreased considerably. Therefore, between PP1101S+60%Boeh and PP+35%Boeh+10%EG, the former would be chosen for its better mechanical properties. Then, in the samples with brucite, a decrease of the speed with respect to the percentage is obtained and when colemanite is added, the speed follows the same trend. This decrease could be due to the lower fuel content or to the fact that both additives have a synergistic effect. In the results obtained for colemanite alone, it is observed that the speed increases with the additive percentage even to values higher than unfilled PP1101S. Taking this into account, adding colemanite to brucite mixture should increase the velocity as in the samples with boehmite, but it decreases. Therefore, brucite and colemanite could act as synergistic mixture, but further testing is needed to confirm. Finally, expandable graphite decreases the vertical propagation speed with respect to the additive percentage. When 10% of expandable graphite is added to brucite, the vertical propagation speed decreases to 57.01 mm/s, which is lower than the sum of the additives individually, so this mixture would also act as a synergistic mixture.

3.7.2 MCC

To confirm the results of the UL94 test, the microscale combustion calorimetry (MCC), which is described in Chapter 2 Section 5.4 was carried out. This test was performed by the Centre for Fire and Hazards Sciences (CFHS) Research Laboratory of the University of Central Lancashire. Samples weighing 2-3 mg were pyrolyzed from 75 to 740°C at 1°C/s in a nitrogen stream. The decomposition gases were then burnt in the combustor at 900°C in a 80/20 nitrogen/oxygen mixture. A minimum of 3 tests per sample were performed to ensure repeatability and the peak of heat release rate (pHRR), temperature of the peak (T_{peak}) and Total Heat Released (THR) values were determined. The samples tested to confirm the synergistic mixtures with brucite are PP+45%Bruc and PP+60%Bruc from Stage 1, and PP+40%Bruc+10%Col and PP+40%Bruc+10%EG from Stage 2. The sample with 10%Col has been selected instead of 15%Col to have the same total percentage of additive and thus eliminate the influence of the amount of plastic. The PP+35%Boeh+15%Col sample is also tested to confirm its different behaviour compared to brucite/colemanite mixture and because it also meets the total additive percentage of 50%. Figure 42 shows the HRR curves obtained and Table 24 the main results. According to pHRR results, the sample with the highest value is PP+45%Bruc and with a significant difference with respect to the following samples. This sample presents a higher value mainly because it has a higher proportion of combustible material (55% PP) and brucite, as not being in a sufficient percentage, does not improve the properties as much as in the other samples tested. This is followed by the samples PP+35%Boeh+15%Col, PP+60%Bruc and PP+40%Bruc+10%EG which have similar pHRR values. In this case the samples differ by 10%

of combustible material, but this difference does not influence the value obtained. Therefore, the boehmite/colemanite and brucite/expandable graphite mixtures in these proportions seem to equate the behaviour of the PP+60%Bruc sample despite having 10% more combustible material and with better mechanical properties, especially in the PP+35%Boeh+15%Col sample. This behaviour contradicts the conclusions obtained in the UL94 test in which none of the mixtures studied improved or equalled the properties with respect to the PP+60%Bruc, so further tests such as the cone calorimeter are needed to confirm the results. Finally, the PP+40%Bruc+10%Col sample presents the lowest pHRR value which is 35% lower than for the PP+60%Bruc and 47% lower than for the PP+45%Bruc. This significant reduction compared to the brucite-only samples would confirm that the brucite/colemanite mixture acts as a synergistic mixture, as better results are obtained with the combination of both additives.

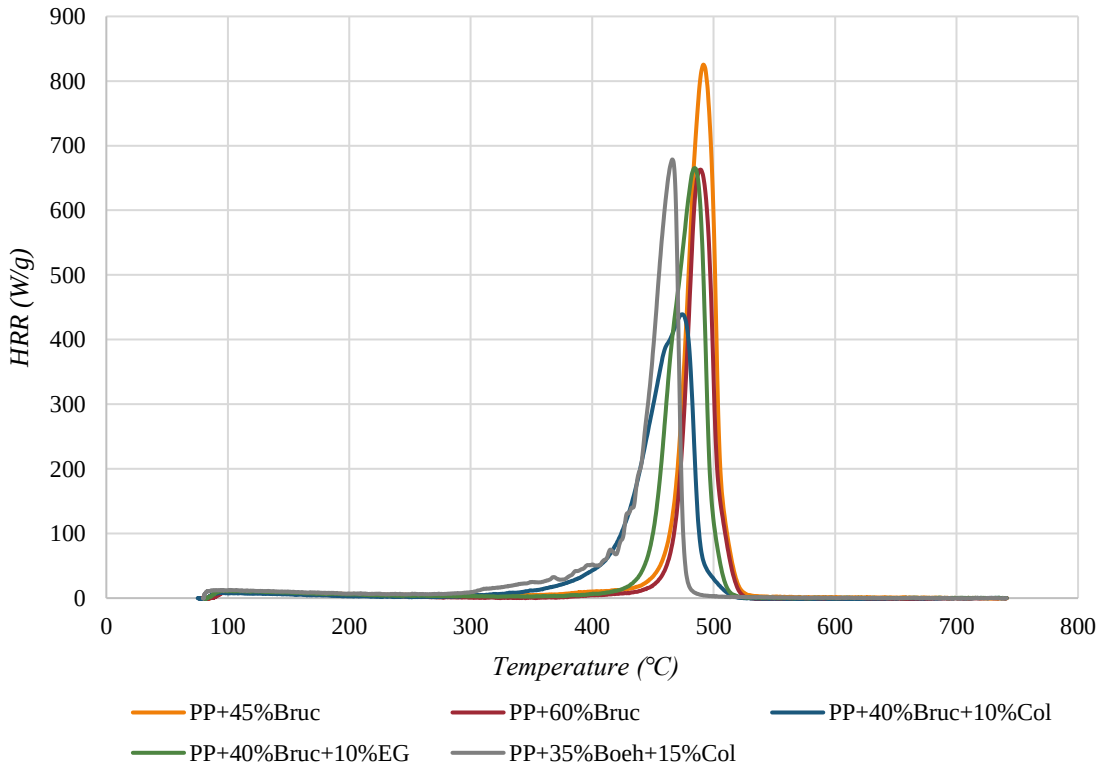

FIGURE 42: MCC TEST CURVES OF STAGE 2 SAMPLES

TABLE 24: MCC RESULTS OF STAGE 2

Sample	pHRR (W/g)	T_{peak} (°C)	THR (kJ/g)
PP+45%Bruc	820.83 ± 13.34	492.13 ± 0.53	27.22 ± 1.39
PP+60%Bruc	670.49 ± 16.71	490.66 ± 1.76	19.85 ± 0.46
PP+40%Bruc+10%Col	435.92 ± 3.14	472.74 ± 1.64	25.03 ± 1.38
PP+40%Bruc+10%EG	664.70 ± 2.23	484.60 ± 0.63	24.87 ± 0.14
PP+35%Boeh+15%Col	684.09 ± 28.30	467.37 ± 1.14	24.81 ± 0.55

Then when analysing the results obtained for the peak temperature, it is observed that it decreases when colemanite and expandable graphite are added. This decrease is due to the lower thermal stability of the mixtures, which agrees with the results obtained in the TGA (Table 8 and Table 21). Regarding to THR, a clear trend is observed with respect to the amount of polymer because the lowest value corresponds to PP+60%Bruc, the highest to PP+45%Bruc and the rest of the samples do not present significant differences because they have the same percentage of PP. In summary, when comparing the results with those obtained in the UL94 tests, the samples show different trends and therefore the conclusions change, so it is important to carry out different fire tests to be able to verify the behaviour of a material.

3.7.3 CONE CALORIMETER

As different trends and conclusions were obtained in the UL94 and MCC, the cone calorimeter (CC) test was carried out. The cone calorimetric test is the most effective and widely used to investigate the mechanism of action of flame retardant because it is sensitive to both chemical and physical phenomena, whereas the MCC is sensitive only to chemical phenomena. For this reason, the normalized pHRR values of both techniques do not always correlate well, especially when a protective layer is formed during combustion [61]. This is important to consider because the additives used in this research also act by the formation of a protective layer and this may be the reason why no differences were obtained between some samples in the MCC. In addition, the decrease in the pHRR due to flame retardants should be higher or at least equal to the decrease obtained in the MCC, so with this technique the difference between the samples could be better identified. The basis of the test is described in Chapter 2 Section 5.3 and the methodology in Chapter 3 Section 2.7.2. The samples tested are PP+60%Bruc, PP+40%Bruc+10%Col, PP+40%Bruc+10%EG and PP+35%Boeh+15%Col and a minimum of 3 tests were performed per sample to ensure repeatability.

Figure 43 shows the HRR curves and Table 25 the results of time to ignition (TTI), peak of heat release (pHRR), time to peak HRR (ttpHRR), total heat released (THR) and mass loss percentage. Firstly, it is observed that the sample with the highest curve corresponds to PP+35%Boeh+15%Col, which ignites after 35.73 s of exposure and shows a pHRR of 216.3 kW/m^2 at 67.33 s. Therefore, it is not only the sample with the highest value, but also the first to combust and to reach the maximum. Thus, it is confirmed that boehmite and colemanite do not act as synergistic mixture and therefore, it is discarded from the study. This sample is followed by PP+40%Bruc+10%EG with a time to ignition 10 s longer and a pHRR of 191.5 kW/m^2 at 157 s, which is an improvement over the previous one. The peak time is significantly delayed because the curve of this sample has a different geometry due to the action of the expandable graphite. The beginning is more rounded, so the maximum is reached later and after the peak, the curve

drops because the expandable graphite absorbs the heat to expand. However, although it seems that the expandable graphite acts effectively in the mixture, the curve continues to fall to values below 20 kW/m^2 before the 10 min, so the combustion time of this sample is significantly lower than the others. This is not beneficial in a material that is intended to be fire resistant because it means that there is less time available before the material burns completely. Therefore, due to the results obtained in this test and the manufacturing difficulties of the material, this mixture is discarded for the next stage.

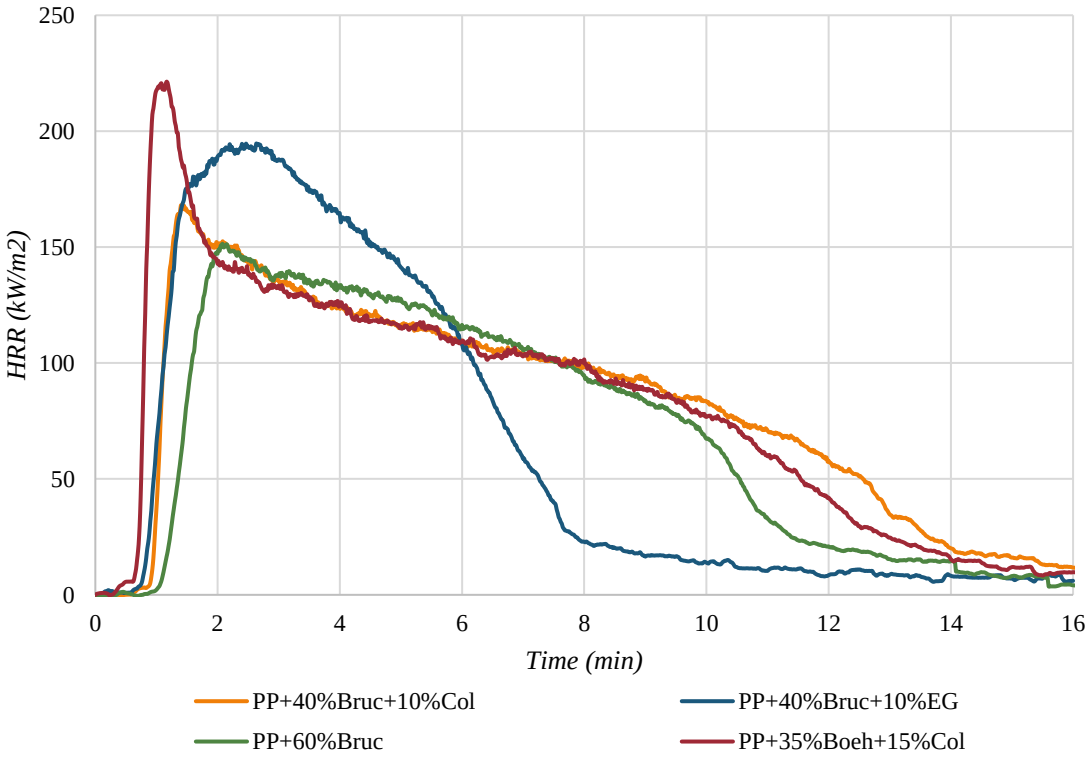

FIGURE 43: HRR VS TIME FOR STAGE 2 SAMPLES IN CONE CALORIMETER

TABLE 25: CONE CALORIMETER RESULTS FOR STAGE 2 SAMPLES

Sample	TTI (s)	pHRR (kW/m^2)	ttpHRR (s)	THR (MJ)	Mass loss (%)
PP+60%Bruc	60.75 ± 3.99	155.70 ± 1.35	127 ± 9.54	66.83 ± 0.60	47.78 ± 0.53
PP+40%Bruc +10%Col	50.79 ± 0.49	169.17 ± 1.03	86.33 ± 2.05	80.63 ± 0.31	53.81 ± 0.64
PP+40%Bruc +10%EG	46.33 ± 0.25	191.50 ± 2.91	157 ± 2.94	63.57 ± 1.52	52.48 ± 0.62
PP+35%Boeh +15%Col	35.73 ± 0.62	216.30 ± 3.91	67.33 ± 2.05	80.33 ± 2.11	52.01 ± 0.97

Next is the PP+40%Bruc+10%Col with a TTI of 50.79 s, a pHRR 11.7% lower than the PP+40%Bruc+10%EG sample and a peak occurring at 86.33 s. Compared to the previous sample, the peak occurs earlier due to the mechanism of action of the additives. The curve at the beginning

is steeper where the peak is reached and then the HRR decreases more steadily, reaching the longest burn time. This geometry indicates the formation of a char layer, the HRR increases until an efficient char layer is formed and, as the layer thickens, the HRR decreases [62]. This is consistent with the mechanism of action of brucite since by its decomposition reaction, it forms a layer of magnesium oxide ash that can act as a protective layer for the polymer [63]. Finally, the PP+60%Bruc sample shows the best results. This sample has the highest TTI, which makes it the material that takes the longest to start burning and has the lowest pHRR value. As for the curve, it presents a similar geometry to the previous one, but the peak occurs at a longer time, at about 40 s more, which is a significant difference, as well as being less abrupt.

Finally, the results of the THR and mass loss percentage are analysed. Regarding the THR, similar values are obtained for the samples PP+35%Boeh+15%Col and PP+40%Bruc+10%Col, which are around 80 MJ, and they are higher than for the other samples. This increase means that these mixtures are not able to trap as much fuel in the condensed phase so their action in this phase is not as effective [41]. On the other hand, the samples PP+60%Bruc and PP+40%Bruc+10%Col have values around 65 MJ, being slightly lower in the mixture with expandable graphite, which means that these mixtures have a greater effect in the condensed phase. In the case of PP+60%Bruc this is because its decomposition reaction is endothermic and therefore absorbs heat from combustion, and for PP+40%Bruc+10%EG it is because in addition to brucite, the expandable graphite also absorbs heat to expand. Regarding to mass loss, no significant differences are observed between mixtures with the same total percentage of additive, so the additives studied do not influence this variable, in this case it depends on the percentage of polymer in the mixture. In conclusion, the sample with the best properties is **PP+60%Bruc** followed by **PP+40%Bruc+10%Col**, therefore, they are the candidates for the next stage.

To summarise, the three tests carried out lead to different conclusions as to which mixture has the best properties. Analysing the results globally, the samples with boehmite are discarded because the results have not been satisfactory in any of the two stages, in addition to the fact that it does not present synergy with colemanite or brucite. On the other hand, with brucite there seems to be a synergistic effect with the two additives. In both the UL94 and 94HB tests, PP+40%Bruc+10%EG showed the best results, while in the MCC and CC tests it was PP+40%Bruc+10%Col. As the sample with EG presented difficulties in the manufacture and in the more specific tests it did not obtain the best results, it was discarded for the next stage. On the other hand, the sample with colemanite showed promising results as a synergistic mixture, so it was selected together with the PP+60%Bruc from Stage 1 for the next stage.

3.8 CONCLUSIONS

The conclusions drawn at this second stage are summarised below:

- During extrusion, the mixtures corresponding to PP+20%EG and PP+40%Bruc+10%EG did not flow properly, so the filament broke and it was not possible to work continuously. Therefore, to obtain the mixtures, the filaments had to be further processed to obtain pellets.

- As the additives used have a higher density with respect to PP, the density of the mixtures increases with the total percentage of additive.

- In DSC test, it was observed that expandable graphite acts as a nucleant in polypropylene because it increases the percentage of crystallinity, improves size homogeneity, and increases the crystallisation curve temperatures, but it does not accelerate the crystal formation.

- In the TGA, no satisfactory results were obtained because all the mixtures showed a thermal stability lower than unfilled PP.

- In the DMTA test, an increase in storage modulus was obtained over the entire temperature range, except for the PP+10%Col sample. Furthermore, comparing the different mixtures, it was observed that those corresponding to brucite had the highest thermo-mechanical stability.

- In oscillatory rheology, it was observed that expandable graphite increases viscosity to a greater extent than colemanite due to the density and typology of its particles. As for the mixtures developed in this stage, the same trend was obtained as in Stage 1 because the mixtures corresponding to brucite have a significantly higher viscosity than those of boehmite.

- Additives significantly influence the mechanical properties. Additives increase the elastic and flexural modulus and decrease the ultimate tensile and impact strength and the higher the percentage the greater the effect. Regarding to the mixtures of additives developed in this stage, it was observed that the mixture of brucite and colemanite shows promising mechanical results because the mechanical properties were better at the same or even higher loading levels.

- In the fire tests, it was observed that boehmite samples do not have a synergistic effect with colemanite and expandable graphite. Therefore, as the results obtained in this stage and in Stage 1 were not satisfactory, the use of boehmite was discarded. In the case of brucite, both colemanite and expandable graphite seem to have a synergistic effect. As in both MCC and CC, the brucite/colemanite mixture had the best results and the brucite/EG mixture presented manufacturing problems, it was decided to use the brucite/colemanite mixture in the next stage.

- Finally, since the mixture of brucite and colemanite seems to have a synergistic effect but the total percentage used is not sufficient to meet the requirements of the UL94 test, it was decided to use this mixture at 60% in total in the next phase and compare it with the PP+60%Bruc mixture, in order to confirm whether they have a synergistic effect.

4. STAGE 3

From the results obtained in the two previous stages, it was concluded that the best mixtures were the 60% brucite and the brucite/colemanite mixture. To confirm that the brucite/colemanite mixture acts as a synergistic mixture, in this stage it was decided to study its effect at different proportions to determine the optimum percentages for each component. For this purpose, a total additive percentage of 60% was established and a level was set every 10% for each of the additive. In addition, to confirm that these additives are acting effectively as retardants, a mixture of 60% calcium carbonate was added. As calcium carbonate is a compound that has no effect, it serves as a reference to compare mixtures with the same proportion of combustible material and thus avoid its influence. Finally, as the additives used are of natural origin, but the matrix is of synthetic origin, it was chosen to add a biopolymer to the study. In this case, it was decided to use PBS because it has similar properties to isotactic polypropylene, and it has not been investigated in depth in terms of fire resistance. In summary, for the two polymeric matrices, it is decided to study the brucite/colemanite mixture at 60% total additive by varying the proportion of each component to determine which mixture is optimal. Table 26 summarises all the mixtures studied, specifying matrix, additive, percentages, and nomenclature of the samples.

TABLE 26: MIXTURES OF PP AND PBS WITH FLAME RETARDANT ADDITIVES TESTED IN STAGE 3

Matrix	Additive 1	Percentage	Additive 2	Percentage	Nomenclature
PP	Brucite	60	Colemanite	-	PP+60%Bruc
		50		10	PP+50%Bruc+10%Col
		40		20	PP+40%Bruc+20%Col
		30		30	PP+30%Bruc+30%Col
		20		40	PP+20%Bruc+40%Col
		10		50	PP+10%Bruc+50%Col
		0		60	PP+60%Col
	$CaCO_3$	60	-	-	PP+60%$CaCO_3$
PBS	-	-	-	-	PBS
	Brucite	60	Colemanite	-	PBS+60%Bruc
		50		10	PBS+50%Bruc+10%Col
		40		20	PBS+40%Bruc+20%Col
		30		30	PBS+30%Bruc+30%Col
		20		40	PBS+20%Bruc+40%Col
		10		50	PBS+10%Bruc+50%Col
		0		60	PBS+60%Col
	$CaCO_3$	60	-	-	PBS+60%$CaCO_3$

4.1 COMPOSITE PREPARATION

At this stage during extrusion, no difficulties were encountered for any of the mixtures despite the high percentage load. The only difference observed was that the feed rate could be increased as the percentage of colemanite increased because the mixture flowed better. Once the mixtures were obtained, the plates were manufactured for characterisation by compression moulding. Figure 44 shows the plates obtained with the PP matrix and it is observed that as the percentage of colemanite increases, the plate acquires a dark khaki green colour. In terms of homogeneity, the PP+60%Bruc and PP+60%$CaCO_3$ samples do not seem to present a uniform distribution of the additives, as the colour of the plate is not homogeneous.

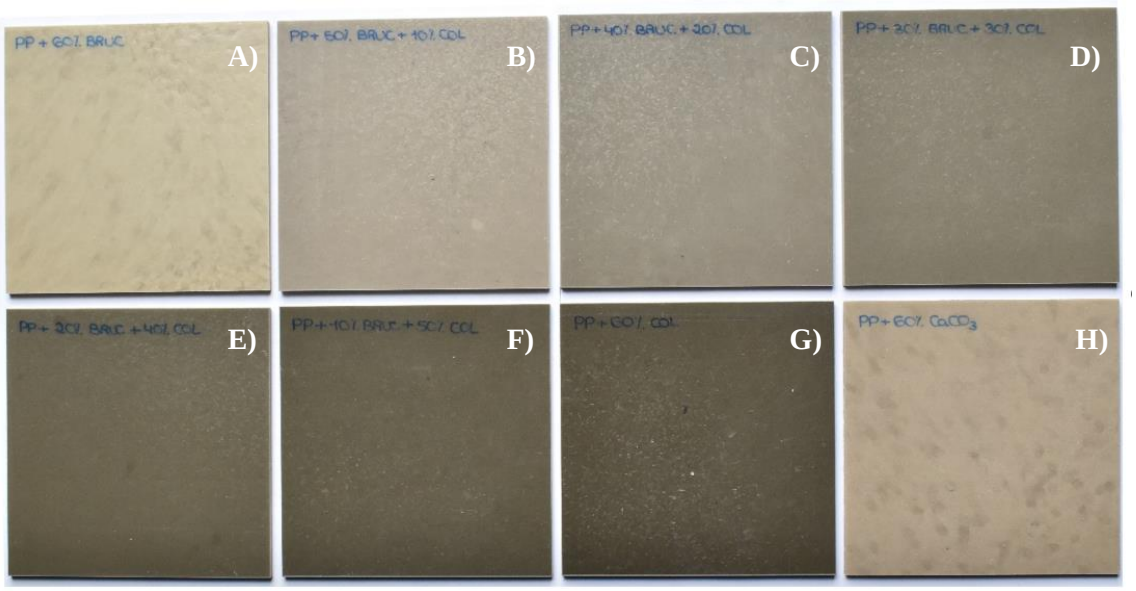

FIGURE 44: PP PLATES MANUFACTURED IN STAGE 3. A) PP+60%BRUC, B) PP+50%BRUC+10%COL, C) PP+40%BRUC+20%COL, D) PP+30%BRUC+30%COL, E) PP+20%BRUC+40%COL, F) PP+10%BRUC+50%COL, G) PP+60%COL, H) PP+60%$CACO_3$

4.2 PRELIMINARY CHARACTERIZATION

Next, Table 27 shows the results for density, ash content and ANOVA analysis of the PP samples. The analysis of each matrix is carried out separately because, in addition to having different origins, the density of the matrices shows significant differences, so the analysis altogether would lead to erroneous conclusions. The statistical analysis showed that the additive has no significant influence on either the density or the ash content. In the case of density, it is observed that, as the mixtures contain 60% total additive and the density of the minerals is much higher than that of PP, the density of the mixtures increase considerably. Comparing the different samples of brucite and colemanite, no significant differences or a clear trend with respect to the percentage are observed because the density of both additives are similar, 2.3-2.4 g/cm^3 for brucite

versus 2.42 g/cm^3 for colemanite [6]. Finally, the sample with $CaCO_3$ has the highest density because its particle density is 2.73 g/cm^3 [64].

TABLE 27: RESULTS OF DENSITY AND ASH CONTENT OF STAGE 3 PP MIXTURES

Sample	Density (g/cm^3)	Ash content (%)
PP	0.895 ± 0.003	0.09 ± 0.10
PP+60%Bruc	1.357 ± 0.005	41.32 ± 0.31
PP+50%Bruc+10%Col	1.385 ± 0.009	42.13 ± 0.38
PP+40%Bruc+20%Col	1.390 ± 0.008	43.45 ± 0.20
PP+30%Bruc+30%Col	1.402 ± 0.008	44.79 ± 0.11
PP+20%Bruc+40%Col	1.388 ± 0.008	44.71 ± 0.20
PP+10%Bruc+50%Col	1.382 ± 0.002	44.98 ± 0.29
PP+60%Col	1.370 ± 0.006	44.30 ± 0.07
PP+60%$CaCO_3$	1.414 ± 0.002	53.13 ± 0.67
p-value	0.9489	0.9576

As for the ash content, it is observed that the increase with respect to the PP is significant because the additives are not completely decomposed, brucite is converted into the corresponding oxide and colemanite releases water, leaving a remnant of ash due to these compounds. As for the trend, it can be observed that the PP+60%Col sample has a higher ash content because the molecular weight of its reaction product is higher than that of the brucite. Finally, as calcium carbonate does not decompose, the sample PP+60%$CaCO_3$ has the highest ash content.

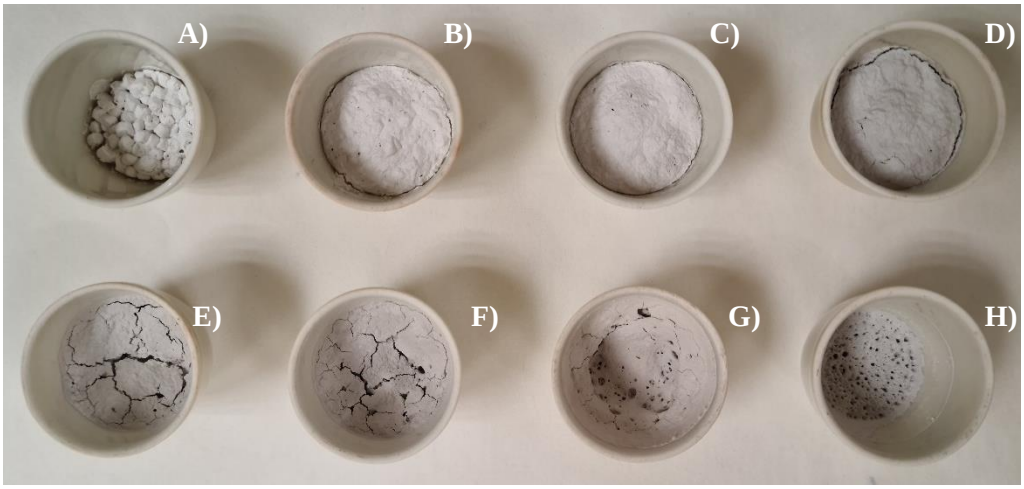

FIGURE 45: IMAGES OF THE ASHES FOR THE PP SAMPLES OF STAGE 3. A) PP+60%BRUC, B) PP+50%BRUC+10%COL, C) PP+40%BRUC+20%COL, D) PP+30%BRUC+30%COL, E) PP+20%BRUC+40%COL, F) PP+10%BRUC+50%COL, G) PP+60%COL, H) PP+60%$CACO_3$

Figure 45 shows the ashes obtained for the PP samples and there are significant differences in the structure. Sample A, which corresponds to the PP+60%Bruc mixture, although it generates the ash layer, maintains the shape of the pellets. Then, mixtures B, C and D show a more uniform and cohesive structure, so that the two additives in these proportions have combined adequately to form a resistant protective layer. However, as the colemanite content increases, the ash loses this cohesion, cracks are formed, and the layer does not hold up because it sinks in the central area as in sample G) PP+60%Col. In the case of sample H) PP+60%$CaCO_3$, a soft, porous ash with low height is observed. Therefore, from the appearance of the ash, samples B, C and D could have the best fire resistance properties due to the protective layer formed.

Table 28 shows the results for density, ash content and ANOVA analysis of the PBS samples. As with the PP blends, the additive has no significant influence on either the density or the ash content. In the case of density, it is observed that as the additives have a higher density than PBS, the density of the mixture increases. As for the trend, it is observed that the highest density corresponds to the PBS+60%$CaCO_3$ sample because calcium carbonate is the densest, followed by PBS+60%Col. As the densities of brucite and colemanite are similar, there is no clear trend with respect to the percentage of additive. On the other hand, in the results of the ash content, there is a clear trend due to the percentage. As the proportion of ash obtained with colemanite is higher than with brucite, because the molecular weight of the decomposition reaction product is higher, therefore, the higher the percentage of colemanite in the mixture, the higher the ash content. Finally, the PBS+60%$CaCO_3$ sample presents the highest percentage because the additive does not undergo any decomposition during the process.

TABLE 28: RESULTS OF DENSITY AND ASH CONTENT OF STAGE 3 PBS MIXTURES

Sample	Density (g/cm^3)	Ash content (%)
PBS	1.260 ± 0.003	0.24 ± 0.06
PBS+60%Bruc	1.679 ± 0.016	40.78 ± 0.11
PBS+50%Bruc+10%Col	1.727 ± 0.009	43.13 ± 0.64
PBS+40%Bruc+20%Col	1.732 ± 0.000	43.60 ± 0.27
PBS+30%Bruc+30%Col	1.730 ± 0.003	44.75 ± 0.18
PBS+20%Bruc+40%Col	1.737 ± 0.003	44.69 ± 0.04
PBS+10%Bruc+50%Col	1.724 ± 0.006	45.30 ± 0.06
PBS+60%Col	1.739 ± 0.014	45.56 ± 0.07
PBS+60%$CaCO_3$	1.827 ± 0.011	54.05 ± 0.41
p-value	0.9391	0.9455

Figure 46 shows the ashes obtained for the PBS samples and shows significant differences in the structure. The samples with higher brucite content have a more cohesive and uniform structure on the surface and as the amount of colemanite increases, holes appear. These holes serve to release the water generated during decomposition, which is beneficial. For this reason and because of the hardness of the ash, sample E) PBS+20%Bruc+40%Col could show the best fire properties. Subsequently, from 50% colemanite (sample F) it is observed that the ash loses cohesion, thus obtaining a granular structure in sample G) PBS+60%Col, which does not benefit the flame retardancy because a firm protective layer is not formed. Finally, in sample H) PBS+60%$CaCO_3$, because the calcium carbonate does not undergo any decomposition reaction, a granulated ash is obtained without any effect as a protective layer.

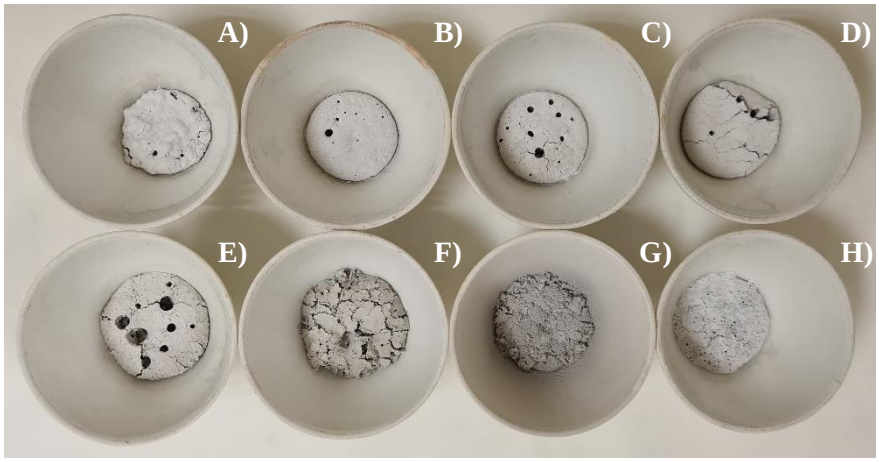

FIGURE 46: IMAGES OF THE ASHES FOR THE PBS SAMPLES OF STAGE 3. A) PBS+60%BRUC, B) PBS+50%BRUC+10%COL, C) PBS+40%BRUC+20%COL, D) PBS+30%BRUC+30%COL, E) PBS+20%BRUC+40%COL, F) PBS+10%BRUC+50%COL, G) PBS+60%COL, H) PBS+60%$CACO_3$

4.3 THERMAL PROPERTIES

4.3.1 DSC

Table 29 shows the results of the second heating curve of the PP samples. The ANOVA analysis shows that the additive has no statistically significant influence on any of the variables analysed. Comparing the $T_{onset,m}$, $T_{end,m}$ and the range, it is observed that all the additive mixtures favour a more homogeneous crystal size because the onset temperature increases, the end temperature decreases and consequently the range of the curve is reduced in comparison with the PP sample. This is because the additives used act as a support for the formation of crystals, thus favouring size homogeneity. In the brucite and colemanite mixtures, it is observed that there is no relationship with respect to the percentage of the components; in fact, the lowest range is obtained for the PP+40%Bruc+20%Col mixture. In the case of calcium carbonate, a decrease in the range is observed, but less significant than for the other additives. In the melting temperature, it is observed that brucite increases the temperature while colemanite decreases it. This means that

brucite improves the thermal stability of the crystalline phase and consequently a higher degree of crystal perfection. In the sample with $CaCO_3$ no significant variation is obtained, which agrees with what has been reported by other authors [65]. Subsequently, a significant decrease in enthalpy is observed in the samples with additives with respect to the unfilled PP, mainly due to the lower percentage of polymer in the samples. In the samples with brucite and colemanite it is observed that the enthalpy is lower with PP+60%Col than with PP+60%Bruc, which means that colemanite absorbs more energy during melting [66]. However, the intermediate samples do not follow this relationship, because the lowest enthalpy is obtained in the PP+30%Bruc+30%Bruc sample, which means that this mixture absorbs more energy and could be related to a better fire resistance. As for PP+60%$CaCO_3$, this sample has the highest enthalpy of all the samples with additives and therefore has the highest percentage of crystallinity. This is because calcium carbonate is an additive that, although it is inert in fire retardancy, has a nucleating effect already reported by other studies [65]. As for the samples with brucite and colemanite, both additives increase the crystallinity and a higher percentage is obtained with the 60% brucite sample, which agrees with what was observed in previous stages. However, the intermediate samples do not follow a linear trend; the PP+30%Bruc+30%Col sample, having the lowest enthalpy, has the lowest percentage of crystallinity of all the samples with additives. The percentage of crystallinity is generally affected by dispersion, percentage, or surface chemistry of the additives [67]. Therefore, the brucite/colemanite combination may be hindering dispersion and consequently the additives may not act properly as a support for crystal formation.

TABLE 29: DSC RESULTS OF SECOND MELTING CURVE OF THE PP SAMPLES OF STAGE 3

Sample	$T_{onset,m}$ (°C)	$T_{end,m}$ (°C)	Range (°C)	T_m (°C)	ΔH_m (J/g)	w_c (%)
PP	153.33	169.85	16.52	163.67	77.41	37.38
PP+60%Bruc	155.56	168.04	12.48	164.85	47.87	57.78
PP+50%Bruc +10%Col	157.27	166.94	9.67	163.95	43.30	52.27
PP+40%Bruc +20%Col	157.11	166.55	9.44	163.36	40.47	48.85
PP+30%Bruc +30%Col	156.57	166.57	9.70	163.05	37.09	44.77
PP+20%Bruc +40%Col	154.89	165.93	11.04	162.55	38.01	45.88
PP+10%Bruc +50%Col	156.59	166.87	10.28	162.91	39.75	47.98
PP+60%Col	155.43	167.40	11.97	162.42	40.30	48.65
PP+60%$CaCO_3$	155.00	167.60	12.60	164.04	48.33	58.34
p-value	0.7384	0.6588	0.7468	0.6649	0.8787	0.9990

Table 30 below shows the results obtained in the cooling curve of the PP samples. As in the heating curve, the additive does not have a significant effect on any of the parameters determined. At a global level, it is observed that all the additives increase both $T_{onset,c}$ and T_c, because their nucleating effect favours the formation of crystals and, consequently, crystallisation occurs at higher temperatures. Among the different additives, it is observed that calcium carbonate has the greatest nucleating effect because it has the highest temperatures, followed by brucite and colemanite. In the intermediate mixtures of brucite and colemanite, it is observed that the lowest temperatures correspond to the proportions 40/20 and 30/30, so the combination of both additives at that proportions hinders their nucleating action. This agrees with what was observed in the crystallinity percentage, so it would be necessary to carry out studies on the dispersion of the particles of these mixtures to determine if there is any problem when they are combined or if it is due to another reason, such as the surface chemistry of both additives. Finally, in the difference between $T_{onset,c}$ and T_c, it is observed that although calcium carbonate favours the formation of crystals, this does not occur at a higher rate. However, brucite improves the homogeneity of the crystals and accelerates their production.

TABLE 30: DSC RESULTS OF COOLING CURVE OF THE PP SAMPLES OF STAGE 3

Sample	$T_{onset,c}$(°C)	T_c (°C)	$T_{onset,c}$-T_c
PP	120.93	116.76	4.17
PP+60%Bruc	128.64	125.34	3.30
PP+50%Bruc+10%Col	126.92	123.29	3.63
PP+40%Bruc+20%Col	126.01	122.63	3.38
PP+30%Bruc+30%Col	126.35	122.78	3.57
PP+20%Bruc+40%Col	127.87	123.70	4.17
PP+10%Bruc+50%Col	127.64	123.60	4.04
PP+60%Col	127.09	122.91	4.18
PP+60%$CaCO_3$	131.66	127.37	4.29
p-value	0.9947	0.9983	0.8991

The effect of additives on the melting curve of samples with PBS is then analysed (Table 31). Firstly, PBS is a polymer with a lower melting point and lower crystallinity percentage than PP. As in the previous matrix, the additive has no statistically significant effect on any of the properties determined. Comparing $T_{onset,m}$, $T_{end,m}$ it is observed that, although the differences are not significant, the additives decrease both temperatures, thus shifting the curves towards lower crystal sizes and consequently less fine structures. Next, in the range of the curve it cannot be determined that the additives have an effect as the differences are less than 1°C. Subsequently, in the melting temperature, it is observed that in all the additive samples a decrease is obtained with respect to the PBS sample, which means that in this matrix the three additives used (brucite,

colemanite and calcium carbonate) reduce the stability of the crystalline phase. On the other hand, the enthalpy of fusion decreases with respect to the unfilled PBS, firstly due to the lower percentage of polymer and secondly due to the absorption of heat by the additives. Comparing the different mixtures, it is observed that colemanite absorbs more heat than brucite, in fact the lowest enthalpy and consequently the lowest crystallinity is obtained in the PBS+60%Col mixture. As for the mixtures of brucite and colemanite, no clear trend is obtained with respect to the percentages of the components. Finally, the same conclusions are obtained for the percentage of crystallinity. The crystallinity increases due to the additives with respect to the PBS sample, but this increase is not as significant as with PP and there is no clear trend with respect to the percentage of the components. In this case, the additive that increases the percentage of crystallinity the most is brucite followed by calcium carbonate. This leads to the conclusion that although PBS may have a similar mechanical behaviour to PP, due to its nature and composition, it is not affected thermally in the same way by the additives used.

TABLE 31: DSC RESULTS OF SECOND MELTING CURVE OF THE PBS SAMPLES OF STAGE 3

Sample	$T_{onset,m}$ (°C)	$T_{end,m}$ (°C)	Range (°C)	T_m (°C)	ΔH_m (J/g)	w_c (%)
PBS	110.37	117.74	7.37	115.67	57.79	28.90
PBS+60%Bruc	109.05	115.83	6.78	113.97	27.60	34.50
PBS+50%Bruc +10%Col	109.10	116.26	7.16	114.20	23.66	29.58
PBS+40%Bruc +20%Col	109.31	115.89	6.58	113.96	27.28	34.10
PBS+30%Bruc +30%Col	109.59	116.07	6.48	114.07	25.57	31.96
PBS+20%Bruc +40%Col	109.52	116.03	6.51	114.08	24.29	30.36
PBS+10%Bruc +50%Col	109.49	115.92	6.43	113.99	24.30	30.37
PBS+60%Col	108.83	115.52	6.69	113.49	23.62	29.52
PBS+60%$CaCO_3$	107.54	115.81	8.27	113.82	25.14	31.42
p-value	0.9683	0.9705	0.7498	0.9526	0.9437	0.9470

Finally, the results obtained in the crystallisation curve of the PBS samples are analysed (Table 32). As in the previous results, the additive does not have a statistically significant effect on $T_{onset,c}$, $T_{c,}$ and the difference between them. It is observed that the additives used do not act as nucleants in the PBS because they decrease both $T_{onset,c}$ and T_c, thus delaying the formation of crystals. Furthermore, for this reason, it was observed that the heating curves were shifted towards smaller crystal sizes. Regarding the temperature difference, it was observed that the additives used also increase the temperature difference, thus not only delays crystallisation but also slows it down. In conclusion, brucite, colemanite and calcium carbonate do not act as nucleants in PBS.

TABLE 32: DSC RESULTS OF COOLING CURVE OF THE PBS SAMPLES OF STAGE 3

Sample	$T_{onset,c}$(°C)	T_c (°C)	$T_{onset,c}$-T_c
PBS	88.39	85.57	2.82
PBS+60%Bruc	87.69	82.89	4.80
PBS+50%Bruc+10%Col	85.99	82.27	3.72
PBS+40%Bruc+20%Col	86.53	82.60	3.93
PBS+30%Bruc+30%Col	87.00	82.93	4.07
PBS+20%Bruc+40%Col	86.30	82.23	4.07
PBS+10%Bruc+50%Col	87.30	82.87	4.43
PBS+60%Col	84.82	80.88	3.94
PBS+60%$CaCO_3$	82.39	78.57	3.82
p-value	0.3081	0.8388	0.9989

4.3.2 DMTA

Next, the effect of the brucite and colemanite mixtures on the thermo-mechanical stability of the material is evaluated. Firstly, the samples corresponding to the polypropylene matrix in Figure 47 are analysed.

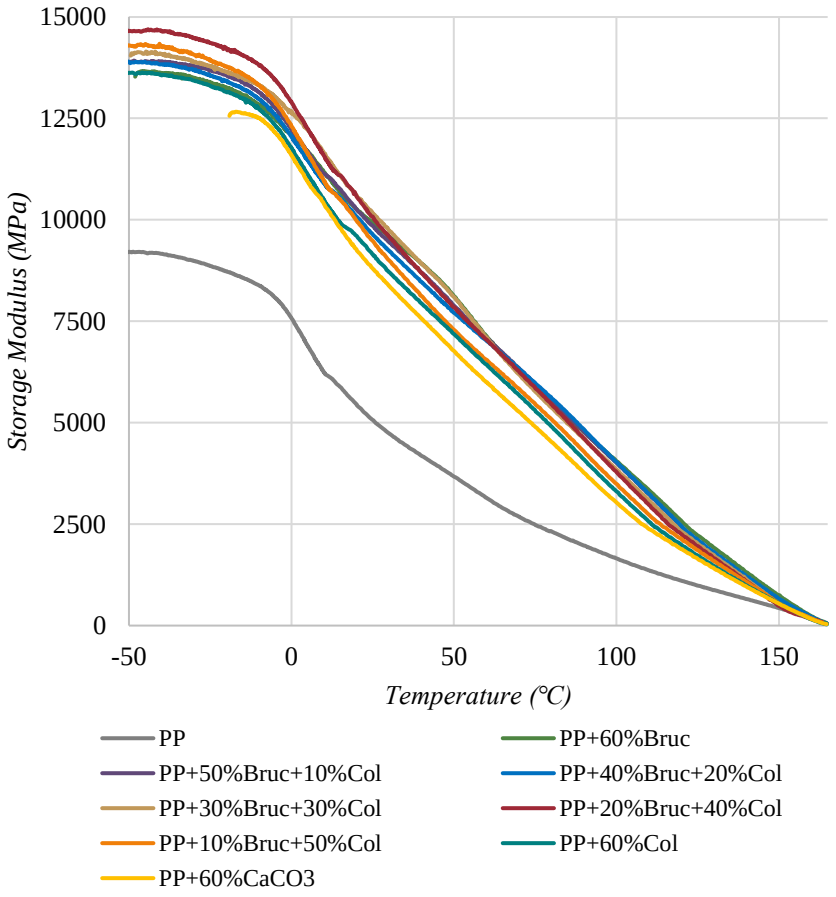

FIGURE 47: STORAGE MODULUS VS TEMPERATURE OF PP SAMPLES OF STAGE 3

As seen in previous stages, the additives used, as being rigid particles, provide rigidity to the composite and consequently the storage modulus increases. At this stage, no significant differences are observed between the curves, which may be because all the mixtures have a total additive content of 60%. Comparing the different mixtures, the one with the lowest stability is the calcium carbonate mixture. This mixture is used as a reference to compare materials with the same proportion of polymeric material. Therefore, the flame retardants used not only improve the flame retardant properties, but also have a slight effect on the thermo-mechanical stability of PP. Regarding the different mixtures with brucite and colemanite, no clear trend is observed with respect to the percentage of each of them. In the initial part, between -50 and 20°C, it is observed that the sample PP+20%Bruc+40%Bruc is the sample with the highest storage modulus, but from this temperature onwards, it becomes equal to other samples. In conclusion, no definite trend is observed due to the percentages of brucite and colemanite used.

Table 33 shows the results of the storage modulus at 20, 100 and 150°C and the value obtained for the glass transition temperature. As observed graphically there are no significant differences due to the additive in the storage modulus for the three temperatures and there is no clear trend with respect to the percentage of brucite or colemanite.

TABLE 33: DMTA RESULTS OF PP SAMPLES OF STAGE 3

Sample	$E'_{20°C}$ (MPa)	$E'_{100°C}$ (MPa)	$E'_{150°C}$ (MPa)	T_g (°C)
PP	5453.7	1654.7	431.3	4.94
PP+60%Bruc	10262.7	4051.5	750.1	10.94
PP+50%Bruc+10%Col	10264.2	4013.6	610.9	5.75
PP+40%Bruc+20%Col	10085.5	4033.6	658.8	5.94
PP+30%Bruc+30%Col	10598.6	3844.9	527.9	14.05
PP+20%Bruc+40%Col	10576.2	3783.0	482.4	8.27
PP+10%Bruc+50%Col	9978.0	3490.5	547.8	7.39
PP+60%Col	9598.8	3305.6	547.8	6.26
PP+60%$CaCO_3$	9271.2	3033.4	537.8	7.79
p-value	0.9689	0.9828	0.9913	0.8104

Apparently, the storage modulus is higher in the mixtures with brucite than with colemanite if only the two samples are compared at 60%, i.e., PP+60%Bruc vs PP+60%Col. However, when these two additives are mixed the same trend is not obtained, in fact the mixtures that present the highest thermal stability at 20°C are PP+30%Bruc+30%Bruc and PP+20%Bruc+40%Bruc, while at 100 and 150 degrees it is PP+60%Bruc. In conclusion, brucite seems to have a greater effect on the thermo-mechanical stability of the material. As for the glass transition temperature, in all the mixtures studied it increases with respect to that obtained for PP, due to the incorporation of

additives restricts the movement of the polymer chains [13]. As in the storage modulus, the mixture with 60% brucite has a higher T_g than the sample corresponding to 60% colemanite, but the intermediate mixtures do not follow the same trend.

Figure 48 below shows the storage modulus curves of the samples with PBS. In this case the test is performed up to 100°C because the melting point of PBS is around 120°C. As seen with PP, the additives add stiffness to the material, so the storage modulus increases significantly with respect to unfilled PBS. In addition, in these samples the difference between the curves is greater than with PP, but still not a significant difference.

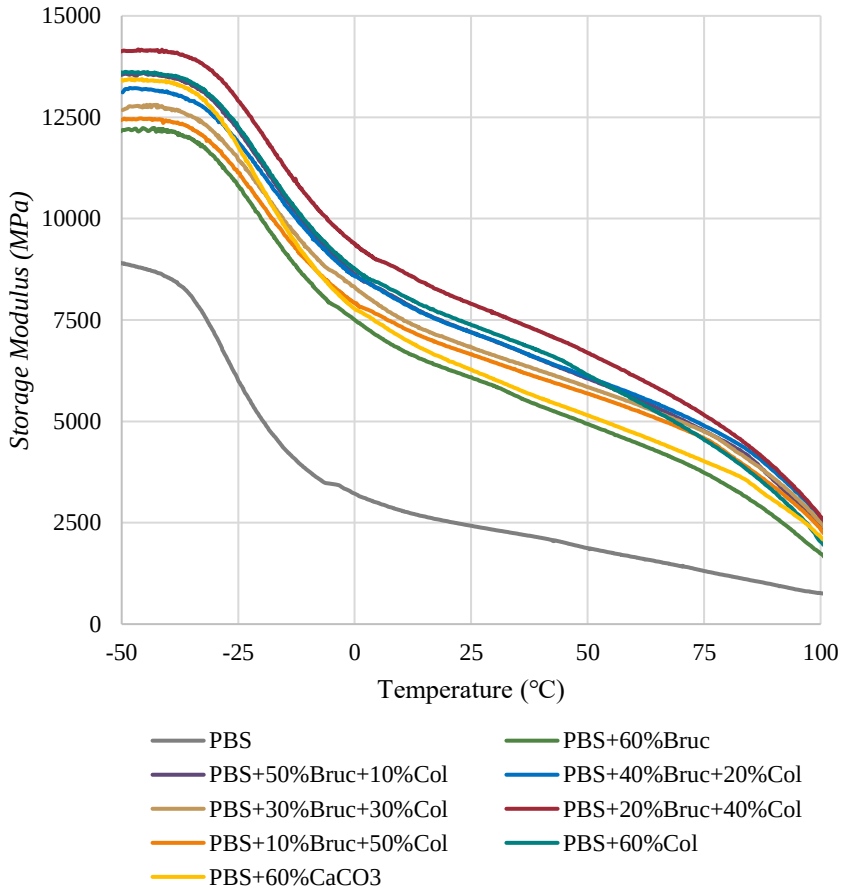

FIGURE 48: STORAGE MODULUS VS TEMPERATURE OF PBS SAMPLES OF STAGE 3

Comparing the different mixtures, the one with the lowest stability over the whole temperature range is the one corresponding to PBS+60%Bruc, which means that this additive does not act in the same way in all polymeric matrices. Next, in the temperature range from 0 to 100°C, which would be the range that includes the normal operating temperatures to which the material could be subjected, is the PBS+60%$CaCO_3$ mixture. This sample, as mentioned above, serves as a comparison with which in the PBS matrix, colemanite and its mixtures with brucite improve the thermo-mechanical stability in the PBS matrix. Subsequently, as with PP, there is no

clear trend with respect to the percentages of the two components and the sample with the highest stability over the whole temperature range is PBS+20%Bruc+40%Col. In conclusion, in general terms, the additives used in this third stage improve the thermo-mechanical stability of both PP and PBS matrices, but there is no clear trend with respect to the percentages used for both components.

Table 34 shows the results of the storage modulus at 20 and 100°C and the value obtained for the glass transition temperature. As observed graphically there are no significant differences due to the additive in the storage modulus for the two temperatures and there is no clear trend with respect to the percentage. With the results at 20°C, it is observed that on average the storage modulus of the mixtures is 182% higher than PBS, which is a very significant improvement. Analysing the different mixtures, it is observed that in the PBS matrix the storage modulus is higher with colemanite than with brucite and in fact the PBS+60%Bruc sample presents the lowest stability over the whole temperature range. Thus, the additives used do not have the same effect on PP and PBS. At 100°C, it is observed that the samples corresponding to the mixtures of brucite and colemanite have a higher E' than those obtained for the additives individually and for $CaCO_3$, which means that these additives complement each other to improve the thermo-mechanical stability of the material. Finally, in the results of the glass transition temperature, it is observed that in all the mixtures studied it increases significantly with respect to that obtained for PBS, because the incorporation of additives restricts the movement of the polymeric chains [12]. Regarding the trend, it is observed that the data describe a negative parabola, i.e., the highest T_g is obtained at equal proportions of colemanite and brucite (30/30), followed by the 40/20 and 20/40 mixtures. Thus, when additives are used in more similar proportions, they restrict more the movement of the polymer chains.

TABLE 34: DMTA RESULTS OF PBS SAMPLES OF STAGE 3

Sample	$E'_{20°C}$(MPa)	$E'_{100°C}$(MPa)	T_g (°C)
PBS	2534.0	761.1	-26.78
PBS+60%Bruc	6283.5	1738.5	-16.90
PBS+50%Bruc+10%Col	7420.0	2356.7	-16.06
PBS+40%Bruc+20%Col	7406.5	2626.4	-15.23
PBS+30%Bruc+30%Col	7034.1	2504.8	-14.51
PBS+20%Bruc+40%Col	8133.4	2639.3	-15.44
PBS+10%Bruc+50%Col	6842.9	2336.5	-17.19
PBS+60%Col	7608.4	2033.7	-17.22
PBS+60%$CaCO_3$	6511.6	2149.3	-18.25
p-value	0.8609	0.6931	0.9339

4.4 RHEOLOGY

Next, the effect of additives on the viscosity of PP is analysed. Figure 49 shows the curves obtained at 190°C and it is observed that the most viscous samples present turbulence from 400 1/s onwards. In order of viscosity, the sample with the lowest viscosity is the unfilled PP because it has no additive. This sample is followed by PP+60%$CaCO_3$ and PP+60%Col, which do not show significant differences. The PP+60%$CaCO_3$ sample has less effect on viscosity than the rest of the samples because, due to the higher density of its particles, there is a higher volumetric proportion of polymer that can favour the flow of the mixture. As for PP+60%Col, considering the density of its particles, it should affect almost as much as brucite, however, of the mixtures with brucite/colemanite, it is the one with the lowest viscosity. This could be because its composition facilitates fluidity. In fact, in stage 2 it was observed that the viscosity did not increase significantly and during the extrusion process it was also observed that the higher the colemanite content, the better the mixture flowed and the higher the feed rate could be increased. This conclusion is also confirmed because the lower the colemanite content, the higher the viscosity and therefore the sample with the highest viscosity is PP+60%Bruc. Therefore, the substitution of part of the brucite by colemanite in PP is beneficial because it facilitates the flow.

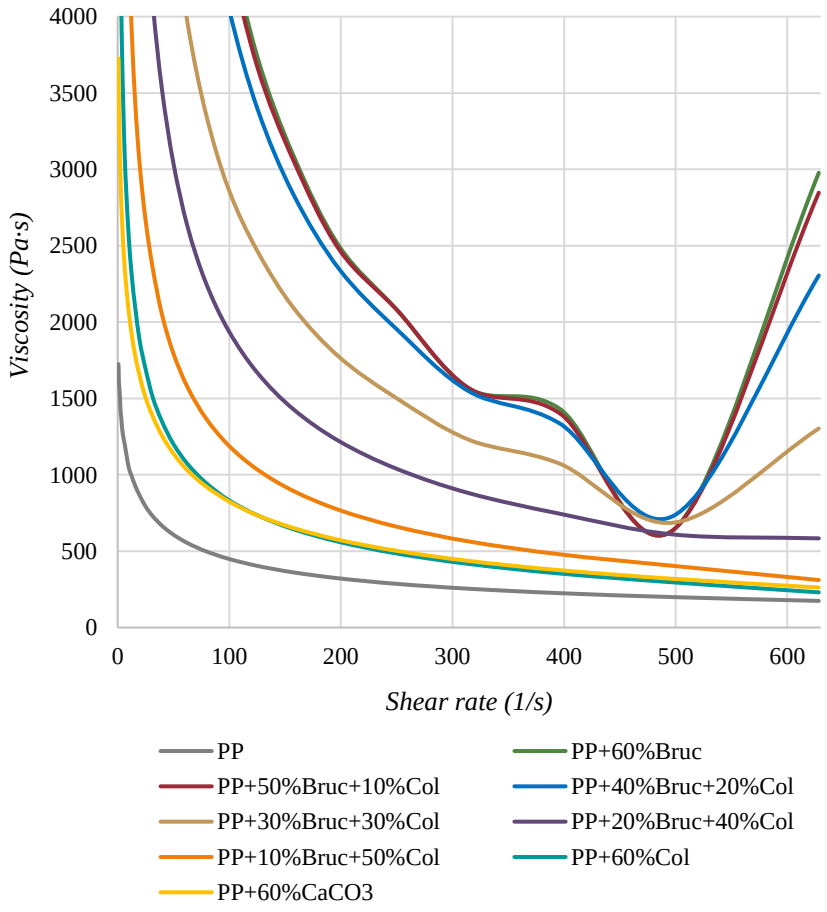

FIGURE 49: VISCOSITY CURVES OF PP SAMPLES OF STAGE 3 AT 190°C

On the other hand, the PBS samples do not show the same trend (Figure 50). Firstly, it is observed that the most viscous curves do not show turbulence and correspond to PBS+10%Bruc+50%Col and PBS+60%Col. Thus, colemanite has the opposite effect to that obtained with PP. Next are the samples PBS+60%$CaCO_3$ and PP+60%Bruc followed by the rest of the brucite/colemanite mixtures. In the case of the mixtures, no differences are obtained between the curves, and they do not follow a clear trend with respect to the percentage, which leads to the conclusion that the substitution of part of the brucite by colemanite favours the creep of the mixture, except for the 10/50 ratio. Finally, the least viscous sample corresponds to the unfilled PBS.

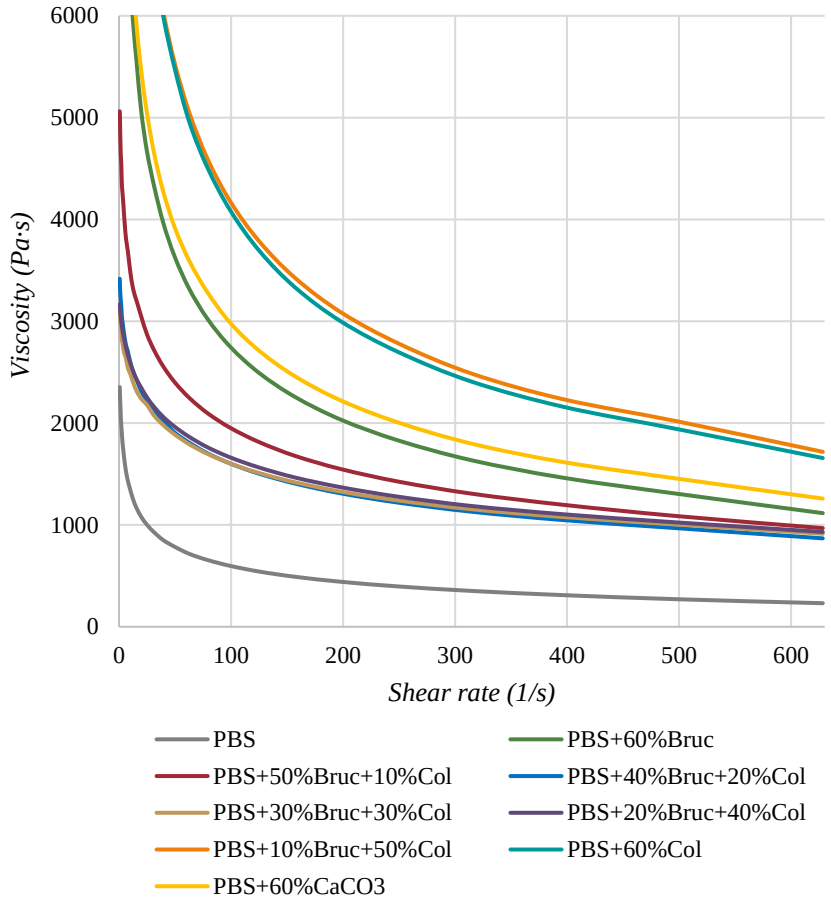

FIGURE 50: VISCOSITY CURVES OF PP SAMPLES OF STAGE 3 AT 140°C

4.5 MECHANICAL TESTS

Regarding the mechanical tests, Table 35 shows the results obtained for the PP samples in the three tests carried out, tensile, flexural and impact. The ANOVA analysis shows that the additive has a statistically significant effect on all parameters. In the case of the tensile test, it is observed that the additives increase the elastic modulus because they provide stiffness to the material and comparing the different mixtures, it is not possible to determine a clear trend with

respect to the percentages of brucite and colemanite. The elastic modulus of the PP+60%Bruc sample is slightly higher than that of PP+60%Col, but the intermediate samples do not follow this trend; in fact, the sample with the highest elastic modulus is the one corresponding to PP+40%Bruc+20%Col. Finally, the PP+60%$CaCO_3$ sample has the lowest elastic modulus of all the additive samples because its particles have a higher density than brucite and colemanite and therefore occupy less volume and affect the stiffness of the material to a lesser extent. Subsequently, the maximum tensile strength does not show a trend with respect to the additives and percentages used. The strength decreases due to the incorporation of the additives because the force is transferred inefficiently to the particles, which means that as there is a lower proportion of plastic in the section of the specimen, the material is less resistant. As for the mixtures, it is observed that the substitution of part of the brucite by colemanite allows obtaining a material with better tensile strength properties because the maximum stress is affected to a lesser extent since 22.44 MPa was obtained in the PP+50%Bruc+10%Col sample with respect to the 19.51 MPa of the PP+60%Bruc. On the other hand, in the flexural modulus, an increase is obtained due to the incorporation of the additives because they increase the stiffness of the material. As in the tensile test, no trend is obtained with respect to the percentages of brucite and colemanite, and the lowest modulus is obtained in the PP+60%$CaCO_3$ sample due to the higher density of its particles. Finally, the additives reduce the impact strength by reducing the effective area. It is observed that colemanite affects the impact strength to a lesser extent because 7.54 kJ/m^2 is obtained compared to 5.32 kJ/m^2 for PP+60%Bruc. In fact, the intermediate mixes follow this trend, except for PP+50%Bruc+10%Col, where a slightly higher value is obtained. In conclusion, the substitution of part of the brucite by colemanite improves the mechanical properties of PP.

TABLE 35: MECHANICAL PROPERTIES OF PP SAMPLES OF STAGE 3

Sample	Elastic Modulus (MPa)	Tensile strength (MPa)	Flexural Modulus (MPa)	Impact strength (kJ/m^2)
PP	1666.6 ± 62.0	33.55 ± 2.19	1484.5 ± 42.55	28.42 ± 0.89
PP+60%Bruc	4433.5 ± 200.5	19.51 ± 2.94	4117.6 ± 67.2	5.32 ± 1.07
PP+50%Bruc+10%Col	4715.4 ± 106.7	22.44 ± 0.39	4237.4 ± 146.4	5.91 ± 0.58
PP+40%Bruc+20%Col	4889.5 ± 92.8	22.18 ± 0.56	4583.1 ± 110.5	5.89 ± 0.51
PP+30%Bruc+30%Col	4694.2 ± 172.2	21.75 ± 1.58	4114.0 ± 128.7	5.91 ± 0.27
PP+20%Bruc+40%Col	4512.7 ± 26.2	22.32 ± 0.29	4263.5 ± 44.1	6.24 ± 0.64
PP+10%Bruc+50%Col	4373.4 ± 58.7	21.08 ± 0.28	4263.5 ± 44.1	6.31 ± 1.01
PP+60%Col	4319.5 ± 44.1	20.05 ± 0.31	4129.9 ± 110.5	7.54 ± 1.57
PP+60%$CaCO_3$	3801.1 ± 103.1	19.33 ± 0.09	3699.9 ± 121.9	6.67 ± 0.38
p-value	0.0000	0.0059	0.0000	0.0252

Table 36 shows the results obtained for the PBS samples in the three tests carried out. The ANOVA analysis shows that the additive has a statistically significant effect in the tensile and flexural tests. In tensile test, it is observed that the additives increase the elastic modulus considerably because they provide stiffness to the material. Comparing the different mixtures, no clear trend can be determined with respect to the percentages of brucite and colemanite. The elastic modulus of the PP+60%Bruc sample is slightly higher than that of PP+60%Col, but the intermediate samples do not follow this trend, in fact, the sample with the highest elastic modulus is the one corresponding to PBS+30%Bruc+30%Col. Finally, the sample PBS+60%$CaCO_3$ present the lowest modulus because its particles occupy less volume and affect the stiffness of the material to a lesser extent. Subsequently, in the maximum tensile strength, no trend is obtained with respect to the additives and percentages used, in fact the highest maximum stress of the samples with additives is obtained in the sample PBS+30%Bruc+30%Col. The strength decreases due to the incorporation of the additives from 38.47 MPa to 20.59 MPa (on average) because the force is transferred inefficiently to the particles. In the flexural test, the modulus increases because the additives increase the stiffness of the material. As in the flexural test, no trend is obtained with respect to the percentages of brucite and colemanite, and the lowest modulus is obtained in the PP+60%$CaCO_3$ sample due to the higher density of its particles. Finally, the additives reduce the impact strength by reducing the effective area. In this case, no significant differences are observed in the samples with brucite and colemanite, so that the substitution of part of the brucite by colemanite does not seem to improve the mechanical properties of PBS.

TABLE 36:MECHANICAL PROPERTIES OF PBS SAMPLES OF STAGE 3

Sample	Elastic Modulus (MPa)	Tensile strength (MPa)	Flexural Modulus (MPa)	Impact strength (kJ/m^2)
PBS	653.3 ± 71.8	38.47 ± 0.56	745.4 ± 17.5	16.09 ± 0.56
PBS+60%Bruc	3138.7 ± 51.2	20.84 ± 2.01	3165.1 ± 159.9	9.51 ± 1.22
PBS+50%Bruc+10%Col	3220.9 ± 48.0	21.97 ± 2.11	3320.7 ± 138.4	9.09 ± 1.35
PBS+40%Bruc+20%Col	3107.3 ± 73.3	21.11 ± 0.84	3192.4 ± 65.9	8.53 ± 0.82
PBS+30%Bruc+30%Col	3511.5 ± 125.3	22.73 ± 1.40	3055.6 ± 107.9	8.61 ± 0.41
PBS+20%Bruc+40%Col	3374.4 ± 42.2	20.87 ± 0.85	2797.9 ± 146.3	8.30 ± 0.84
PBS+10%Bruc+50%Col	2898.6 ± 144.9	18.74 ± 0.73	2656.5 ± 49.1	9.90 ± 0.74
PBS+60%Col	3010.3 ± 61.4	17.87 ± 0.49	2632.3 ± 98.8	9.31 ± 0.55
PBS+60%$CaCO_3$	2532.4 ± 47.6	20.62 ± 0.29	2058.9 ± 129.6	11.48 ± 0.31
p-value	0.0000	0.0000	0.0000	0.0790

4.6 FIRE TESTS

At this stage, both the UL94 test and the cone calorimetric test are carried out to determine whether brucite and colemanite have a synergistic effect and which are the best percentages.

4.6.1 UL94

First, the results obtained on the PP samples in both the 94HB and 94V tests are analysed (Table 37). In the horizontal propagation test, it is observed that the additive has a statistically significant effect on the propagation velocity. Comparing the different mixtures of brucite and colemanite, it is observed that 60% brucite considerably improves the material properties, while with 60% colemanite the reduction is only 11.6% with respect to the PP sample, which would not justify its use. However, when both additives are combined, satisfactory results are obtained as the material does not propagate flame. Due to the difference in behaviour between brucite and colemanite, it is observed that higher proportions of brucite lead to a higher reduction of the propagation velocity. Therefore, the partial substitution of brucite by colemanite achieves zero propagation velocity, whereby both additives in such proportions clearly act as synergistic mixtures. Among the mixtures, the best results are obtained with the samples PP+50%Bruc+10%Col and PP+30%Bruc+30%Bruc, although for the samples PP+60%Bruc and PP+40%Bruc+20%Col the results are also satisfactory because the speed obtained is lower than 5 mm/min. In terms of classification, the samples with brucite and their mixtures with colemanite meet the requirements of the HB classification. Finally, the PP+60%$CaCO_3$ mixture has an even higher speed than unfilled PP because it has less polymer, i.e., less material to burn, so it burns faster. Therefore, the mixtures developed not only improve the properties of unfilled PP significantly but compared to a blend with the same proportion of combustible material, the improvement is even greater.

TABLE 37: RESULTS OF UL94 TEST OF PP SAMPLES OF STAGE 3

	Horizontal test 94 HB		**Vertical test 94V**		
Sample	**Propagation speed (mm/min)**	**Class**	**Flame time (s)**	**Propagation speed (mm/min)**	**Class**
PP	46.00 ± 1.89	-	148.84 ± 6.12	86.44 ± 3.40	-
PP+60%Bruc	3.34 ± 5.78	HB	155.19 ± 87.74	46.00 ± 26.24	-
PP+50%Bruc +10%Col	0.00 ± 0.00	HB	140.76 ± 119.02	42.86 ± 39.21	-
PP+40%Bruc +20%Col	1.01 ± 1.76	HB	90.26 ± 103.86	37.86 ± 34.95	-
PP+30%Bruc +30%Col	0.00 ± 0.00	HB	189.80 ± 86.07	59.74 ± 1.75	-
PP+20%Bruc +40%Col	32.28 ± 0.51	HB	159.92 ± 46.37	65.35 ± 2.01	-
PP+10%Bruc +50%Col	34.41 ± 1.79	HB	109.28 ± 29.77	83.12 ± 5.22	-
PP+60%Col	40.64 ± 2.63	-	87.43 ± 21.48	119.24 ± 4.21	-
PP+60%$CaCO_3$	50.27 ± 2.16	-	131.21 ± 7.07	109.40 ± 4.04	-
p-value	0.0000		0.3348	0.0000	

In the vertical test the conclusions obtained are similar. As the samples do not meet the requirements of UL94V, the analysis is carried out by comparing the results of the vertical propagation velocity. As in the previous test, it is found that the additive has a statistically significant effect on the vertical propagation velocity. Comparing the different mixtures, it is observed that PP+60%$CaCO_3$ and PP+60%Col show a speed even higher than that obtained with unfilled PP, which is not a satisfactory result. Then, when colemanite is mixed with brucite, it is observed that the speed is lower at higher brucite percentages, and the lowest propagation speed is obtained in the sample PP+40%Bruc+20%Col. Therefore, the best results are obtained when the brucite content is higher than the colemanite content, as in the horizontal test. In conclusion, brucite and colemanite act as synergistic additives since the results obtained in their mixtures are better than when they are used separately. Moreover, in the PP matrix, better results are obtained at higher proportions of brucite.

TABLE 38: RESULTS OF UL94 TEST OF PBS SAMPLES OF STAGE 3

	Horizontal test 94 HB		**Vertical test 94V**		
Sample	**Propagation speed (mm/min)**	**Class**	**Flame time (s)**	**Propagation speed (mm/min)**	**Class**
PBS	14.41 ± 13.13	-	20.27 ± 6.21	41.55 ± 25.53	V-2
PBS+60%Bruc	8.13 ± 14.09	HB	20.05 ± 14.56	41.71 ± 28.22	-
PBS+50%Bruc +10%Col	0.00 ± 0.00	HB	15.76 ± 8.46	39.25 ± 25.66	V-1
PBS+40%Bruc +20%Col	0.00 ± 0.00	HB	7.03 ± 5.07	25.44 ± 35.51	V-1
PBS+30%Bruc +30%Col	0.00 ± 0.00	HB	0.46 ± 0.79	0.00 ± 0.00	V-0
PBS+20%Bruc +40%Col	0.00 ± 0.00	HB	0.53 ± 0.85	0.00 ± 0.00	V-0
PBS+10%Bruc +50%Col	0.00 ± 0.00	HB	0.41 ± 0.59	0.00 ± 0.00	V-0
PBS+60%Col	9.17 ± 15.89	-	27.84 ± 11.07	33.62 ± 19.87	-
PBS+60%$CaCO_3$	37.91 ± 2.83	-	104.56 ± 59.03	49.81 ± 5.32	-
p-value	0.5630		0.0000	0.0000	

The results obtained for the PBS matrix are analysed below (Table 38). For this matrix, it is observed that the additive has a statistically significant effect on the vertical propagation speed and the flame time. In the horizontal test, it is observed that the PBS matrix per se has better fire resistance properties because its flame spread speed is significantly lower than that obtained for PP, 14.41 mm/min compared to 46 mm/min for PP. When 60%$CaCO_3$ is added to this matrix, a considerable deterioration is observed because the velocity increases to 38 mm/min, which is associated with the lower amount of combustible material to burn. As for the mixtures of brucite and colemanite, it is observed that when both additives are used individually, the velocity is

reduced by 5 to 6 mm/min, the reduction being greater with brucite. However, when both additives are combined, the material does not propagate the flame regardless of the proportion used for both additives. Thus, in the PBS matrix, the additives also act as a synergistic mixture. Subsequently, in the vertical test, it is observed that brucite does not improve the propagation speed while colemanite reduces it by almost 8 mm/min. Therefore, in the PBS matrix, colemanite has a better effect. This trend is confirmed in the mixtures of both additives because it is observed that when acting together, brucite and colemanite decrease the propagation speed and the best results are obtained at higher colemanite contents. This difference with respect to the results obtained in the PP matrix may be due to the temperature or mechanism of action of the additives. The additives must act before or during the degradation of the matrix [2], so as colemanite starts to degrade about 40°C later than brucite and its mechanism of action is mainly the release of water, it may present a higher compatibility with the PBS matrix. To confirm this, it would be necessary to perform a TGA test with a coupled FTIR that would allow us to determine the decomposition mechanism of each component individually and of the mixtures. In terms of classification, the mixtures PBS+30%Bruc+30%Col, PBS+20%Bruc+40%Col and PBS+10%Bruc+50%Col meet the requirements of the most demanding level V-0. In conclusion, brucite and colemanite have a synergistic effect in the PBS matrix because better properties are obtained with the combination than if they were used individually. In addition, the materials do not spread fire both vertically and horizontally when equal proportions of both additives are used or when the colemanite content is higher.

4.6.2 Cone Calorimeter

To determine which mixtures are the best, the cone calorimetric test was also performed because it is the most effective and widely used test to study the mechanism of action of flame retardants. Firstly, the heat release rates (HRR) vs time curves of PP samples are presented in Figure 51. At the beginning of the curve, the mixture that combusts the fastest is PP+60%Col because the HRR starts to increase before the rest of the samples, and therefore presents the lowest TTI (time to ignition). On the other hand, PP+50%Bruc+10%Col is the latest, and in the intermediate samples it is observed that the higher the brucite content, the more the combustion is delayed. Thus, the mixture of both additives, brucite and colemanite, hinders the ignition of the material, and the effect is better when the brucite content is higher, which is consistent with the trend observed in the UL94 test. Subsequently, the HRR rises rapidly, especially in the samples with the shortest ignition time, until the maximum HRR (pHRR) is reached and then falls steadily in all samples due to the mechanism of action of the flame retardants. This geometry indicates that a thick ash layer is formed, because an initial increase in HRR is obtained until the protective ash layer is formed and as this layer thickens the HRR decreases [62]. The only sample with a different geometry is PP+60%$CaCO_3$, which also has the highest pHRR. The curve shows that

the HRR peak is around 115 s, then decreases more abruptly than in the other samples until a sort of plateau is reached from 215 to 340 s. Subsequently, the curve drops rapidly, so the test ends earlier than for the other mixtures studied. This difference in geometry and test time is because, as calcium carbonate has no effect as a retardant, does not form a protective layer, does not absorb heat, etc., the sample releases more heat and burns more quickly. As for the mixtures with brucite and colemanite, there is no clear trend in the pHRR with respect to the percentage of the components and apparently the higher the colemanite content, the longer it takes to finish the test. However, with these curves it is not possible to deduce which are the best mixtures, therefore, the results of this test are analysed in detail below.

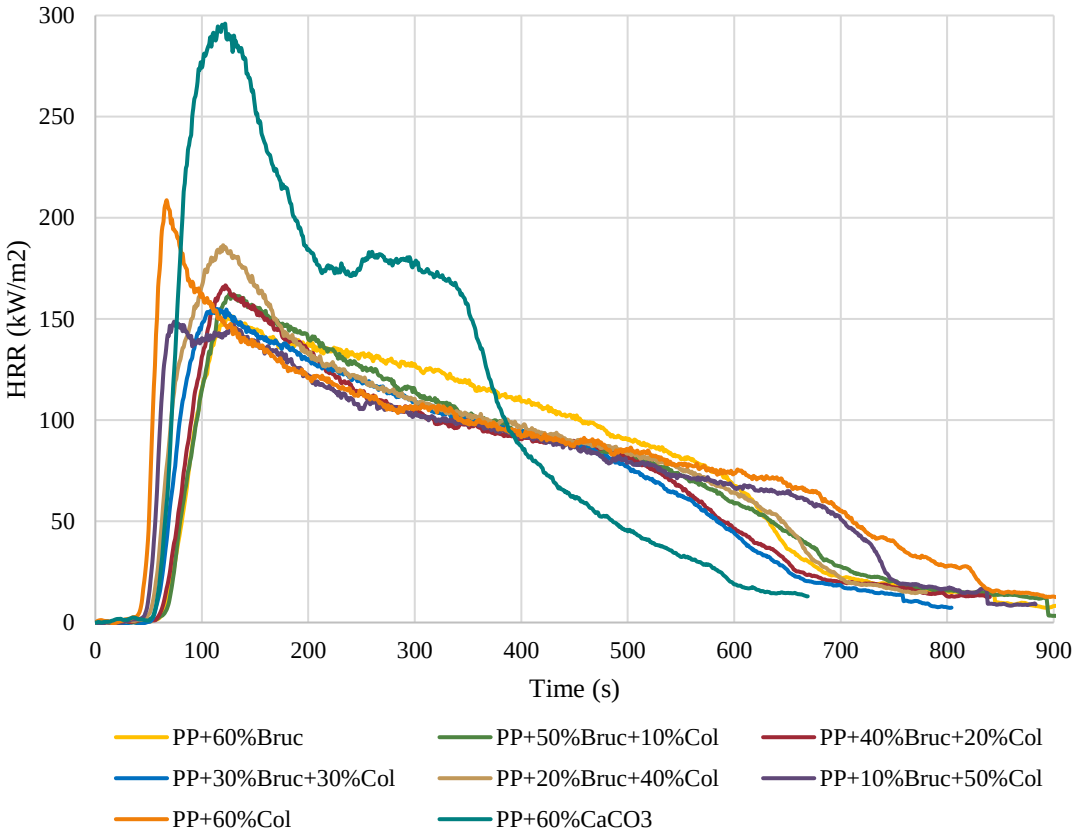

FIGURE 51: HRR CURVES VS TIME OF PP SAMPLES OF STAGE 3

Table 39 shows the results obtained for the PP samples in the calorimetric cone test and the additive has a statistically significant effect on all the variables. Furthermore, in the table the best values for each of the variables determined have been marked and as can be seen, they do not coincide, so it is necessary to analyse each of them individually to determine which of these variables are the most important and, consequently, which are the best additive proportions. Firstly, the results of the time to ignition (TTI) show that the samples with higher colemanite than brucite content (60%Col, 10/50 and 20/40) present low ignition times and even lower than the reference sample (PP+60%$CaCO_3$), which results in a worsening of the material properties in

these samples. Subsequently, as the brucite content in the mixtures increases, the ignition time increases, reaching a maximum in the PP+50%Bruc+10%Col sample. In conclusion, brucite and colemanite act as a synergistic mixture because better results are obtained when they are used in combination and better results are obtained in the PP matrix at higher brucite proportions.

TABLE 39: CONE CALORIMETER RESULTS OF PP SAMPLES OF STAGE 3

Sample	TTI (s)	pHRR (kW/m2)	ttpHRR (s)	THR (MJ)	EHC (MJ/kg)	Mass Loss (%)
PP+60%Bruc	60.75 ± 3.99	155.7 ± 1.4	127.0 ± 9.5	66.83 ± 0.60	30.37 ± 0.14	47.78 ± 0.53
PP+50%Bruc +10%Col	68.50 ± 4.24	163.5 ± 4.5	132.3 ± 5.9	64.73 ± 0.85	29.80 ± 1.04	46.85 ± 1.32
PP+40%Bruc +20%Col	60.50 ± 3.75	167.2 ± 14.4	122.3 ± 2.5	59.70 ± 1.59	28.33 ± 0.63	44.85 ± 0.26
PP+30%Bruc +30%Col	54.79 ± 1.60	158.1 ± 2.2	109.7 ± 4.5	59.23 ± 3.78	27.92 ± 0.97	44.82 ± 0.32
PP+20%Bruc +40%Col	49.29 ± 1.53	188.5 ± 11.2	122.3 ± 4.0	66.57 ± 1.17	30.96 ± 0.19	46.29 ± 0.84
PP+10%Bruc +50%Col	44.59 ± 0.22	150.4 ± 3.4	75.5 ± 3.5	66.45 ± 1.77	31.11 ± 1.19	46.14 ± 1.07
PP+60%Col	41.41 ± 1.37	209.2 ± 8.8	66.5 ± 2.1	73.65 ± 1.63	33.85 ± 0.20	47.71 ± 0.69
PP+60%$CaCO_3$	53.23 ± 3.13	299.8 ± 17.7	116.0 ± 5.6	74.73 ± 3.55	38.84 ± 1.60	40.56 ± 0.20
p-value	0.0000	0.0000	0.0000	0.0000	0.0000	0.0000

The results obtained for pHRR are then analysed and, on average, the values are lower when the brucite content is higher than the colemanite content, but there is no clear trend with respect to the percentage. For this reason, pHRR and ttpHRR are analysed together because it is important to know the amount of heat released by the material, but also at what point in the test this peak occurs. Comparing both variables together, it is of interest that the peak is as low as possible and that it occurs as late as possible, and in this case a disparity in the results of the two variables is observed. In the pHRR the lowest values are obtained in the samples PP+60%Bruc and PP+10%Bruc+50%Col and in the ttpHRR the highest values are obtained in PP+60%Bruc and PP+50%Bruc+10%Col. Therefore, the sample PP+60%Bruc fulfils the criteria for both variables, but not PP+10%Bruc+50%Col. PP+10%Bruc+50%Col has the lowest pHRR of all the samples studied, but the peak occurs almost one minute earlier than PP+60%Bruc, in fact, it is the second lowest ttpHRR value. Therefore, compared to the other mixtures, it has received less energy from the conical heater before reaching the peak and therefore has a lower pHRR value. Discarding this sample for this reason, the next one by pHRR values is the mixture PP+30%Bruc+30%Col which presents a ttpHRR of 110 s, so it could be one of the mixtures for the next stage. The table then shows the results of the total heat release (THR) and effective heat of combustion (EHC) and for both variables it is of interest that the value is as low as possible. In this case, the best values for both parameters are PP+40%Bruc+20%Col and PP+30%Bruc+30%Col, which means that in

both mixtures the material releases less heat/energy, which is beneficial for flame retardancy. Furthermore, compared to the reference sample, a reduction of approximately 20% in THR and 28% in EHC has been obtained. It should also be noted that the reduction with respect to the other samples of brucite and colemanite is significant, especially in THR, which means that the mixtures in these proportions may have prevented the polymer from burning completely or absorbed more heat. Finally, in the mass loss percentage, it is also important to keep it as low as possible, and this corresponds to the PP+60%$CaCO_3$ sample. However, this result has not been marked because it is the reference sample and because the calcium carbonate, as it does not undergo any modification or alteration during the process, only the proportion of plastic, which is 40%, is burnt. As for the brucite and colemanite mixtures, the best results correspond to the mixtures PP+40%Bruc+20%Col and PP+30%Bruc+30%Col, coinciding with the THR and EHC, so they could be the mixtures chosen for the next stage.

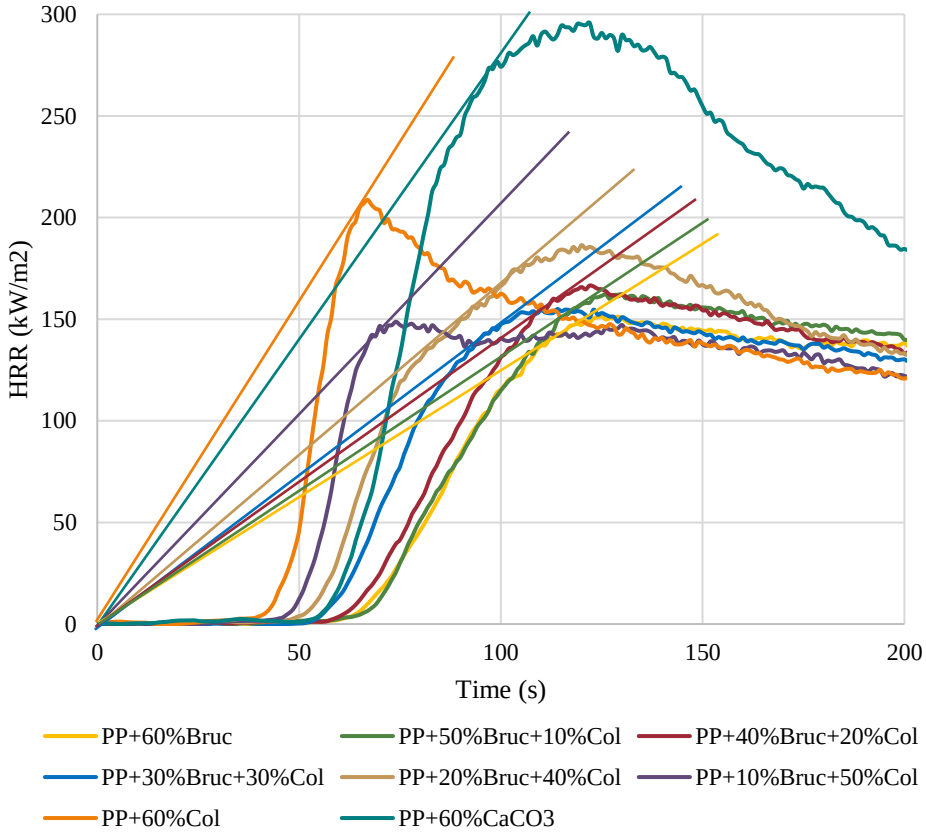

FIGURE 52: FIGRA REPRESENTATION IN THE RESULTS OF THE CONE CALORIMETER OF PP SAMPLES

To obtain more information from the results obtained, the derived parameters FIGRA and MARHE have also been calculated. Both parameters, what they represent and how they are determined are explained in Chapter 2. In the case of FIGRA it is determined numerically, but it can also be represented graphically by joining the beginning of the test with the highest part of the curve, as shown in Figure 52. FIGRA would be the slope of this curve and represents the

growth of the burning intensity, so the higher the slope, the higher the fire risk [68]. This representation clearly shows that the lines with the highest slope are those corresponding to the highest colemanite values and that the slope decreases as the brucite content increases, so the mixtures for the next stage should be those with equal or higher brucite content. In addition, MARHE results (Table 40) also shows that brucite has a better effect on flame retardancy than colemanite, which leads to the conclusion that the best results in the PP matrix are obtained in mixtures with higher proportions of brucite.

TABLE 40: FIGRA AND MAHRE RESULTS OF PP SAMPLES OF STAGE 3

Sample	FIGRA (kW/m^2 s)	MARHE (kW/m^2)
PP+60%Bruc	1.2525	103.16
PP+50%Bruc+10%Col	1.3148	100.25
PP+40%Bruc+20%Col	1.4167	97.42
PP+30%Bruc+30%Col	1.4892	100.42
PP+20%Bruc+40%Col	1.692	110.91
PP+10%Bruc+50%Col	2.096	102.28
PP+60%Col	3.1511	113.5
PP+60%$CaCO_3$	2.8202	165.85

Figure 53 below shows the curves obtained for PBS samples. In comparison with the curves obtained with the PP matrix, the PBS matrix has lower HRR values, which agrees with the results obtained in the UL94 test. Therefore, the PBS matrix has better fire properties despite its lower melting point. In this case, at the beginning of the curve there are no significant differences between the different samples so graphically it cannot be determined which is more easily flammable. However, differences are observed at the peak of the HRR. The highest value corresponds to the PBS+60$CaCO_3$ sample because the additive used does not act as a retardant and once the peak is reached, the HRR drops more sharply. As for the samples with additives, apparently the highest values are obtained with the samples PP+60%Col followed by PP+60%Bruc, therefore the mixtures of both additives act in a synergic way since the results obtained are better when they are used together. As for the geometry, this indicates that a protective ash layer is formed because the HRR increases until this layer is formed and as it thickens the HRR decreases. Finally, in the final part of the test, similar behaviour is observed between the different mixtures except for PBS+60%$CaCO_3$, which ends earlier because the plastic burns earlier due to the fact that the calcium carbonate does not act as a retardant.

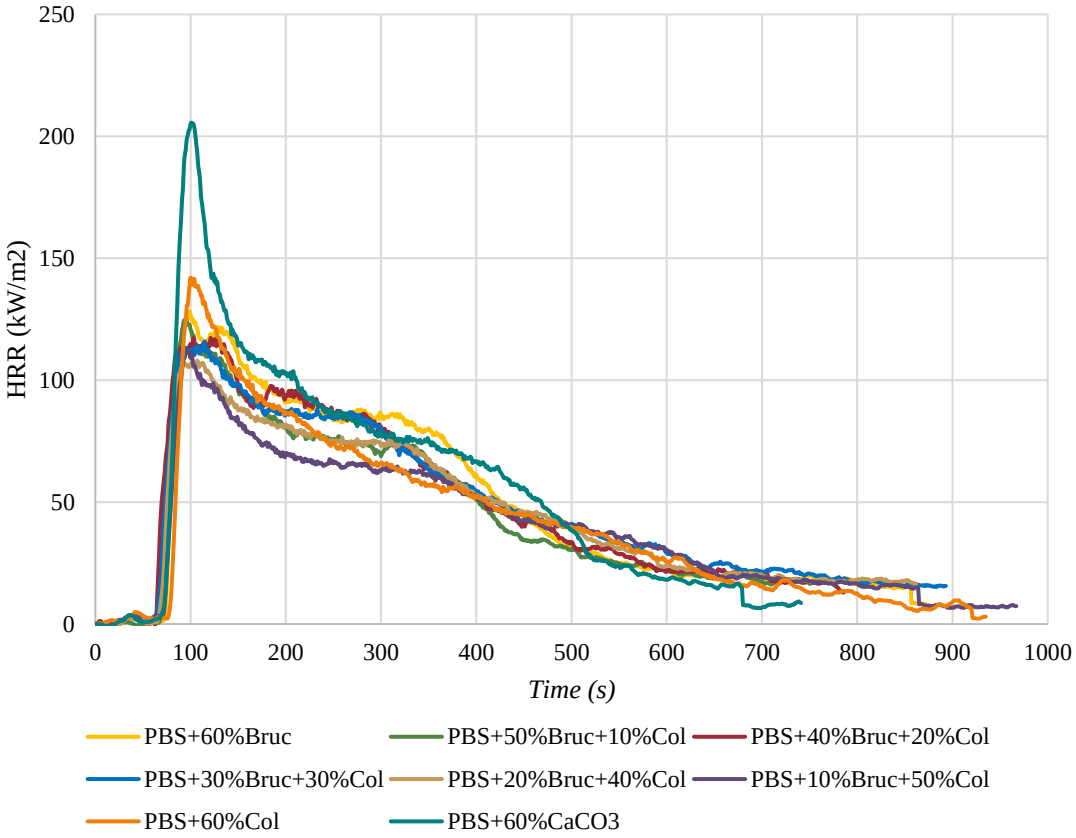

FIGURE 53: HRR CURVES VS TIME OF PBS SAMPLES OF STAGE 3

Table 41 below shows the results obtained for the PBS samples and, in this case, the additive has a statistically significant effect on all variables except THR. As in PP samples, the best results have been marked for each of the variables determined. Firstly, in the TTI results, colemanite delays ignition more and the best results are obtained in the samples PP+60%Col and PP+60%Bruc. As for the mixtures, the TTI is slightly lower than the reference sample PBS+60%$CaCO_3$, therefore in the PBS matrix no improvement in TTI is observed for the use of the brucite/colemanite combination. On the other hand, in the pHRR, the highest values are obtained with the samples PBS+60%$CaCO_3$, PBS+60%Col and PBS+60%Bruc, so in this property, the use of the additives together does have a satisfactory effect. Furthermore, better results are obtained with higher colemanite contents, which agrees with the results obtained in the UL94 test. Subsequently, in the ttpHRR test, a difference of less than 20 s is obtained between all the samples, so it is not possible to draw conclusions on this variable. In the case of THR, although the differences are not statistically significant, a small improvement is obtained with respect to the reference sample and the most satisfactory results correspond to the samples PBS+10%Bruc+50%Col and PBS+60%Col. Since the sample PBS+10%Bruc+50%Col presents the lowest THR value and the second lowest pHRR, it can be concluded that the additives in these proportions present good retardation results and therefore could be one of the candidate mixtures for the next stage. Subsequently, in the EHC results, significant differences are obtained due to

the additive, mainly because the improvement with respect to the PBS+60%$CaCO_3$ sample is greater than in the previous case. In this variable, it is observed that the results obtained with the brucite/colemanite mixture are lower than when they are used individually, which ratifies that these additives act as a synergistic mixture also in the PBS. Finally, in the mass loss percentages, better results are also obtained with higher percentages of colemanite, therefore it is concluded that colemanite has better results on the properties of PBS than brucite.

TABLE 41: CONE CALORIMETER RESULTS OF PBS SAMPLES OF STAGE 3

Sample	TTI (s)	pHRR (kW/m2)	ttpHRR (s)	THR (MJ)	EHC (MJ/kg)	Mass Loss (%)
PBS+60%Bruc	71.63 ± 0.88	128.15 ± 12.52	99.00 ± 0.00	41.60 ± 3.54	15.76 ± 1.32	43.63 ± 0.52
PBS+50%Bruc +10%Col	66.72 ± 1.28	125.75 ± 0.07	94.00 ± 1.41	38.45 ± 5.59	13.97 ± 0.50	45.47 ± 3.32
PBS+40%Bruc +20%Col	62.56 ± 1.77	117.3 ± 0.30	103.00 ± 0.30	39.40 ± 0.50	12.88 ± 0.70	48.54 ± 3.68
PBS+30%Bruc +30%Col	63.59 ± 1.28	115.75 ± 1.06	106.50 ± 12.02	42.05 ± 2.47	13.28 ± 0.26	52.02 ± 0.24
PBS+20%Bruc +40%Col	65.13 ± 3.01	110.25 ± 3.61	100.00 ± 9.90	39.90 ± 2.40	13.21 ± 0.11	49.43 ± 3.35
PBS+10%Bruc +50%Col	69.03 ± 0.40	113.65 ± 1.63	96.50 ± 2.12	37.20 ± 2.12	14.49 ± 0.11	43.42 ± 1.68
PBS+60%Col	75.15 ± 0.44	142.30 ± 4.10	102.00 ± 2.83	38.30 ± 0.28	16.51 ± 0.37	38.15 ± 2.07
PBS+60%$CaCO_3$	68.84 ± 1.37	207.85 ± 0.35	101.50 ± 2.12	42.10 ± 1.70	19.21 ± 0.23	36.22 ± 0.67
p-value	0.0000	0.0000	0.0001	0.1660	0.0000	0.0000

To obtain more information from the results obtained, the derived parameters FIGRA and MARHE have been calculated. Table 42 shows the results and it is observed that in both parameters the samples PBS+20%Bruc+40%Col and PBS+10%Bruc+50%Col present the best values, therefore, together with the results obtained previously in the pHRR it is concluded that these mixtures present the best flame retardancy results in the PBS matrix.

TABLE 42: FIGRA AND MAHRE RESULTS OF PBS SAMPLES OF STAGE 3

Sample	FIGRA (kW/m^2 s)	MARHE (kW/m^2)
PBS+60%Bruc	1.315	74.94
PBS+50%Bruc+10%Col	1.338	67.80
PBS+40%Bruc+20%Col	1.311	73.51
PBS+30%Bruc+30%Col	1.239	70.95
PBS+20%Bruc+40%Col	1.165	65.41
PBS+10%Bruc+50%Col	1.183	58.58
PBS+60%Col	1.421	67.53
PBS+60%$CaCO_3$	2.072	84.13

4.7 SELECTION OF THE BEST MIXTURES

Due to the different results obtained for the different parameters, it is difficult to determine which mixtures are suitable for the next phase. For this reason, it is necessary to develop a method that allows all the variables to be considered in order to decide which are the best mixtures for each matrix. Since the procedure used in step 1 is not feasible in this case, for each of the variables studied above, a value from 1 to 8 was established for each sample according to the results obtained, with 1 being the best and 8 the worst. In the event of a tie, the same value was established for the different samples. Once the order was established for each variable, it was determined which variables were the most important, since they are not all equally important. In this case, it was determined that the most important variables should be pHRR, THR, EHC and mass loss, and once chosen, the result of these variables was multiplied by two to give more importance to the final result. Finally, all the columns were added together to obtain a total value for each sample and the best mixtures were those with the lowest values.

Table 43 below shows the results obtained following this methodology for the PP samples. Firstly, brucite has a better effect on flame retardancy than colemanite, since the samples with higher percentages of this additive have lower values in the last column, which agrees with the conclusions obtained in both the UL94 test and the cone calorimeter tests. As for the mixtures, this methodology showed that **PP+40%Bruc+20%Col and PP+30%Bruc+30%Col** had the best results, therefore, they are the mixtures selected as optimal and the ones used in composites reinforced with natural fibre.

TABLE 43: SELECTION OF THE BEST MIXTURES OF PP SAMPLES

Sample	TTI	pHRR	ttpHRR	THR	EHC	Mass Loss	FIGRA	MAHRE	Horiz speed	Vert speed	TOTAL
PP+60%Br	2	2	2	6	4	7	1	5	3	3	55
PP+50/10	1	4	1	3	3	5	2	2	1	2	41
PP+40/20	3	5	3	2	2	2	3	1	2	1	38
PP+30/30	4	3	5	1	1	1	4	3	1	4	37
PP+20/40	6	6	3	5	5	4	5	6	4	5	74
PP+10/50	7	1	6	5	6	3	6	7	5	6	73
PP+60%Cl	8	7	7	7	7	6	8	8	6	8	107
PP+60%CC	5	8	4	8	8	8	7	9	7	7	110
		x2		**x2**	**x2**	**x2**					

Following this methodology also for the determination of the best mixtures with the PBS matrix, it is observed that colemanite has a better effect on flame retardancy and it is confirmed that the optimum samples are **PBS+20%Bruc+40%Col and PBS+10%Bruc+50%Col**.

TABLE 44: SELECTION OF THE BEST MIXTURES OF PBS SAMPLES

Sample	TTI	pHRR	ttpHRR	THR	EHC	Mass Loss	FIGRA	MAHRE	Horiz speed	Vert speed	TOTAL
PBS+60%Br	2	6	6	6	6	3	5	7	2	5	74
PBS+50/10	5	5	8	3	4	4	6	4	1	4	66
PBS+40/20	8	4	2	4	1	5	4	6	1	2	55
PBS+30/30	7	3	1	7	3	7	3	5	1	1	61
PBS+20/40	6	1	5	5	2	6	1	2	1	1	45
PBS+10/50	3	2	7	1	5	2	2	1	1	1	37
PBS+60%Cl	1	7	3	2	7	1	7	3	3	3	61
PBS+60%CC	4	8	5	8	8	8	8	8	4	6	107
		x2		**x2**	**x2**	**x2**					

4.8 CONCLUSIONS

The following is the summary of the conclusions of this third phase:

- No extrusion difficulties occurred despite the high additive load and colemanite facilitated feeding.

- As the additives used have a higher density with respect to PP, the density of the mixtures increases, and no trend is obtained with respect to the percentages because the density of brucite and colemanite are similar.

- In the ash determination, the percentage increased as the percentage of colemanite increased due to the higher molecular weight of its decomposition product. In terms of structure, in the PP matrix a more compact ash was obtained at higher percentages of brucite than colemanite, while in the PBS matrix it corresponded to the PBS+20%Bruc+40%Col sample.

- In DSC test, no statistically significant effect was obtained due to the additive on any of the variables determined, both in the PP and PBS matrix. Furthermore, in the PP matrix, the three additives used, brucite, colemanite and calcium carbonate, act as nucleating agents, while in the PBS matrix, the same effect could not be concluded.

- In DMTA test, the additives used in this second stage improve the thermo-mechanical stability of both PP and PBS matrices, but there is no clear trend with respect to the percentages used for both components.

- In oscillatory rheology, it was observed that due to the high additive loading the viscosity of the mixture increases significantly. Despite this, in both matrices it was observed that the partial substitution of the brucite by colemanite is beneficial because it facilitates the flow reducing the viscosity of the mixture.

- In the mechanical test it was obtained that the additive has a significant influence in the mechanical properties because they increase the elastic and flexural modulus and decrease the ultimate tensile and impact strength. On one hand in the PP mixtures, it was observed that the substitution of part of the brucite by colemanite improves the mechanical properties, while in PBS matrix no improvement was observed.

- In the UL94 test it was confirmed that brucite and colemanite act as synergistic additives since the results obtained in their mixtures are better than when they are used separately. Moreover, in the PP matrix, better results are obtained at higher proportions of brucite, while in the PBS matrix, better results are obtained at higher percentages of colemanite.

- The cone calorimeter test confirms the conclusions of the UL94 test. Analysing the results of both tests together, it was obtained that the optimum samples in the PP matrix are PP+40%Bruc+20%Col and PP+30%Bruc+30%Col, and in the PBS matrix PBS+20%Bruc+40%Col and PP+10%Bruc+50%Col. Therefore, these mixtures are the ones that will be used as matrices in the manufacture of natural fibre reinforced composites.

5. INDEX OF TABLES AND FIGURES

6. REFERENCES

1. Morgan AB, Gilman JW. An overview of flame retardancy of polymeric materials: application, technology, and future directions. Fire Mater [Internet] 2013;37:259–79. Available from: https://onlinelibrary.wiley.com/doi/10.1002/fam.2128
2. Hull TR, Witkowski A, Hollingbery L. Fire retardant action of mineral fillers. Polym Degrad Stab 2011;96:1462–9.
3. Rothon R, Hornsby P. Fire Retardant Fillers for Polymers. In: Polymer Green Flame Retardants. Elsevier; 2014. page 289–321.
4. de Chirico A, Armanini M, Chini P, Cioccolo G, Provasoli F, Audisio G. Flame retardants for polypropylene based on lignin. Polym Degrad Stab 2003;79:139–45.
5. Gallina G, Bravin E, Badalucco C, Audisio G, Armanini M, de Chirico A, et al. Application of cone calorimeter for the assessment of class of flame retardants for polypropylene. Fire Mater 1998;22:15–8.
6. Roberts WL, Campbell TJ, Rapp Jr. GR. Encyclopedia of Minerals. Van Nostrand Reinhold; 1990.
7. Wypych A. Lignin. In: Databook of Adhesion Promoters. Elsevier; 2018. page 161.
8. Sauerwein R. Mineral Filler Flame Retardants. In: Non-Halogenated Flame Retardant Handbook. Hoboken, NJ, USA: John Wiley & Sons, Inc.; 2014. page 75–141.
9. Hai C, Zhang L, Zhou Y, Ren X, Liu J, Zeng J, et al. Phase Transformation and Morphology Evolution Characteristics of Hydrothermally Prepared Boehmite Particles. J Inorg Organomet Polym Mater 2018;28:643–50.
10. Pang H, Ning G, Gong W, Ye J, Lin Y. Direct synthesis of hexagonal Mg(OH)2 nanoplates from natural brucite without dissolution procedure. Chemical Communications 2011;47:6317.
11. Hararak B, Winotapun C, Inyai J, Wannid P, Prahsarn C. Production of UV-shielded spherical lignin particles as multifunctional bio-additives for polyvinyl alcohol composite films. Journal of Nanoparticle Research 2021;23:193.
12. Ehrenstein GW, Riedel G, Trawiel P. Differential Scanning Calorimetry (DSC). In: Thermal Analysis of Plastics. München: Carl Hanser Verlag GmbH & Co. KG; 2004. page 1–110.
13. Pedrazzoli D, Khumalo VM, Karger-Kocsis J, Pegoretti A. Thermal, viscoelastic and mechanical behavior of polypropylene with synthetic boehmite alumina nanoparticles. Polym Test 2014;35:92–100.
14. Streller RC, Thomann R, Torno O, Mülhaupt R. Isotactic Poly(propylene) Nanocomposites Based upon Boehmite Nanofillers. Macromol Mater Eng 2008;293:218–27.

15. Streller RC, Thomann R, Torno O, Mülhaupt R. Morphology, Crystallization Behavior, and Mechanical Properties of Isotactic Poly(propylene) Nanocomposites based on Organophilic Boehmites. Macromol Mater Eng 2009;294:380–8.
16. Cook M, Harper JF. The influence of magnesium hydroxide morphology on the crystallinity and properties of filled polypropylene. Advances in Polymer Technology 1998;17:53–62.
17. Chen X, Yu J, Guo S, Luo Z, He M. Effects of magnesium hydroxide and its surface modification on crystallization and rheological behaviors of polypropylene. Polym Compos 2009;30:941–7.
18. Tahir I, Rapinac J, Abutunis A, Menta VG. Investigating the Effects of Tobacco Lignin on Polypropylene. Polymers (Basel) 2022;14:706.
19. Fujiyama M. Structures and Properties of Injection Moldings of Flaky Filler-filled Polypropylenes. International Polymer Processing 1992;7:358–73.
20. An Y, Wang S, Li R, Shi D, Gao Y, Song L. Effect of different nucleating agent on crystallization kinetics and morphology of polypropylene. e-Polymers 2019;19:32–9.
21. Ehrenstein GW, Riedel G, Trawiel P. Thermogravimetry (TG). In: Thermal Analysis of Plastics. München: Carl Hanser Verlag GmbH & Co. KG; 2004. page 139–71.
22. Brebu M, Vasile C. Thermal degradation of lignin - A Review. Cellulose Chemistry and Technology 2010;44:353–63.
23. Costes L, Laoutid F, Brohez S, Dubois P. Bio-based flame retardants: When nature meets fire protection. Materials Science and Engineering R: Reports [Internet] 2017;117:1–25. Available from: http://dx.doi.org/10.1016/j.mser.2017.04.001
24. Liu SP, Ying JR, Zhou XP, Xie XL, Mai YW. Dispersion, thermal and mechanical properties of polypropylene/magnesium hydroxide nanocomposites compatibilized by SEBS-g-MA. Compos Sci Technol 2009;69:1873–9.
25. Larcey PA, Redfern JP, Bell GM. Studies on magnesium hydroxide in polypropylene using simultaneous TG-DSC. Fire Mater 1995;19:283–5.
26. Menard KP. Dynamic mechanical analysis : a practical introduction. CRC Press; 1999.
27. Bai H, Wang Y, Zhang Z, Han L, Li Y, Liu L, et al. Influence of Annealing on Microstructure and Mechanical Properties of Isotactic Polypropylene with β-Phase Nucleating Agent. Macromolecules 2009;42:6647–55.
28. Ebeid EZM, Zakaria MB. State of the art and definitions of various thermal analysis techniques. In: Thermal Analysis. Elsevier; 2021. page 1–39.
29. Pedrazzoli D, Khumalo VM, Karger-Kocsis J, Pegoretti A. Thermal, viscoelastic and mechanical behavior of polypropylene with synthetic boehmite alumina nanoparticles. Polym Test 2014;35:92–100.

30. Rosato D v, Rosato D v, Rosato M v. Plastic Product Material and Process Selection Handbook. Elsevier; 2004.
31. NETZSCH Analyzing & Testing. Introducción a la reometría rotacional [Internet]. 2020;Available from: https://vimeo.com/458910953
32. Toriz G, Denes F, Young RA. Lignin-polypropylene composites. Part 1: Composites from unmodified lignin and polypropylene. Polym Compos 2002;23:806–13.
33. Chen F, Dai H, Dong X, Yang J, Zhong M. Physical properties of lignin-based polypropylene blends. Polym Compos 2011;32:1019–25.
34. Sameni J, Jaffer SA, Sain M. Thermal and mechanical properties of soda lignin/HDPE blends. Compos Part A Appl Sci Manuf 2018;115:104–11.
35. Hohenwarter D, Mattausch H, Fischer C, Berger M, Haar B. Analysis of the Fire Behavior of Polymers (PP, PA 6 and PE-LD) and Their Improvement Using Various Flame Retardants. Materials 2020;13:5756.
36. Meng Q xuan, Zhu G qing, Yu M miao, Pan R liang. The Effect of Thickness on Plywood Vertical Fire Spread. Procedia Eng 2018;211:555–64.
37. Pi H, Guo S, Ning Y. Mechanochemical improvement of the flame-retardant and mechanical properties of zinc borate and zinc borate-aluminum trihydrate-filled poly(vinyl chloride). J Appl Polym Sci 2003;89:753–62.
38. Ning Y, Guo S. Flame-retardant and smoke-suppressant properties of zinc borate and aluminum trihydrate-filled rigid PVC. J Appl Polym Sci 2000;77:3119–27.
39. Genovese A, Shanks RA. Structural and thermal interpretation of the synergy and interactions between the fire retardants magnesium hydroxide and zinc borate. Polym Degrad Stab 2007;92:2–13.
40. Cavodeau F, Viretto A, Otazaghine B, Lopez-Cuesta JM, Delaite C. Influence of colemanite on the fire retardancy of ethylene-vinyl acetate and ethylene-methyl acrylate copolymers. Polym Degrad Stab 2017;144:401–10.
41. Isitman NA, Kaynak C. Effect of partial substitution of aluminum hydroxide with colemanite in fire retarded low-density polyethylene. J Fire Sci 2013;31:73–84.
42. Kaynak C, Isitman NA. Synergistic fire retardancy of colemanite, a natural hydrated calcium borate, in high-impact polystyrene containing brominated epoxy and antimony oxide. Polym Degrad Stab 2011;96:798–807.
43. Wang X, Kalali EN, Wan JT, Wang DY. Carbon-family materials for flame retardant polymeric materials. Prog Polym Sci 2017;69:22–46.
44. Xie R, Qu B. Synergistic effects of expandable graphite with some halogen-free flame retardants in polyolefin blends. Polym Degrad Stab 2001;71:375–80.
45. Laachachi A, Burger N, Apaydin K, Sonnier R, Ferriol M. Is expanded graphite acting as flame retardant in epoxy resin? Polym Degrad Stab 2015;117:22–9.

46. Sever K, Tavman İH, Seki Y, Turgut A, Omastova M, Ozdemir I. Electrical and mechanical properties of expanded graphite/high density polyethylene nanocomposites. Compos B Eng 2013;53:226–33.
47. American Elements. Expandable Graphite Product Datasheet [Internet]. Available from: https://www.americanelements.com/graphite-expandable-12777-87-6
48. Frost RL, Scholz R, Ruan X, Lima RMF. Thermal analysis and infrared emission spectroscopy of the borate mineral colemanite (CaB3O4(OH)3·H2O). J Therm Anal Calorim 2016;124:131–5.
49. Oulmou F, Benhamida A, Dorigato A, Sola A, Messori M, Pegoretti A. Effect of expandable and expanded graphites on the thermo-mechanical properties of polyamide 11. Journal of Elastomers & Plastics 2019;51:175–90.
50. Şahin T. Mechanical and Thermal Properties of Colemanite Filled Polypropylene. KGK rubberpoint [Internet] 2011;64:16–21. Available from: www.kgk-rubberpoint.de
51. Waclawska I, Stoch L, Paulik J, Paulik F. Thermal decomposition of colemanite. Thermochim Acta 1988;126:307–18.
52. Galwey AK. Structure and order in thermal dehydrations of crystalline solids. Thermochim Acta 2000;355:181–238.
53. Güldaş A, Güllü A, Çankaya A. Determination of the Rheological Properties of Polypropylene Filled with Colemanite. Polym Adv Technol 2017;28:1179–84.
54. Schirp A, Su S. Effectiveness of pre-treated wood particles and halogen-free flame retardants used in wood-plastic composites. Polym Degrad Stab 2016;126:81–92.
55. Cosansu G, Cogun C. An investigation on use of colemanite powder as abrasive in abrasive waterjet cutting (AWJC). Journal of Mechanical Science and Technology 2012;26:2371–80.
56. Cho N, Lee B, Choi S, Kim J, Kim J, Yu J, et al. Brucite shows antibacterial activity via establishment of alkaline conditions. RSC Adv 2021;11:18003–8.
57. Chen X, Yu J, Lu S, Wu H, Guo S, Luo Z. Combustion Characteristics of Polypropylene/Magnesium Hydroxide/Expandable Graphite Composites. Journal of Macromolecular Science, Part B 2009;48:1081–92.
58. Chen X, Wu H, Luo Z, Yang B, Guo S, Yu J. Synergistic effects of expandable graphite with magnesium hydroxide on the flame retardancy and thermal properties of polypropylene. Polym Eng Sci 2007;47:1756–60.
59. Bilici İ. The Effect of Colemanite on Thermal Properties of Recycled Polyethylene. Acta Phys Pol A 2019;135:922–4.
60. Terzi E, Kartal SN, Pişkin S, Stark N, Kantürk Figen A, White RH. Colemanite: A Fire Retardant Candidate for Wood Plastic Composites. Bioresources 2018;13.

61. Sonnier R, Ferry L, Longuet C, Laoutid F, Friederich B, Laachachi A, et al. Combining cone calorimeter and PCFC to determine the mode of action of flame-retardant additives. Polym Adv Technol 2011;22:1091–9.
62. Schartel B, Hull TR. Development of fire-retarded materials - Interpretation of cone calorimeter data. Fire Mater 2007;31:327–54.
63. Molefe DM, Labuschagne J, Focke WW, van der Westhuizen I, Ofosu O. The effect of magnesium hydroxide, hydromagnesite and layered double hydroxide on the heat stability and fire performance of plasticized poly(vinyl chloride). J Fire Sci 2015;33:493–510.
64. Tangboriboon N, Rortchanakarn S, Petcharoen K, Sirivat A. Effects of foaming agents and calcium carbonate on thermo-mechanical properties of natural rubber foams. Polimeri 2015;35:10–7.
65. Eiras D, Pessan A. Influence of Calcium Carbonate Nanoparticles on the Crystallization of Olypropylene. 2009.
66. Lee SY, Kang IA, Doh GH, Kim WJ, Kim JS, Yoon HG, et al. Thermal, mechanical and morphological properties of polypropylene/clay/wood flour nanocomposites. Express Polym Lett 2008;2:78–87.
67. Altay L, Sarikanat M, Sağlam M, Uysalman T, Seki Y. The effect of various mineral fillers on thermal, mechanical, and rheological properties of polypropylene. Research on Engineering Structures and Materials 2021;
68. Sundström B. The development of a European fire classification system for building products - test methods and mathematical modelling. Fire Safety Engineering and Systems Safety; 2007.

CHAPTER 5

CHEMICAL TREATMENTS APPLIED TO NATURAL FIBRES

TABLE OF CONTENTS

This chapter shows the different treatments carried out on the natural fibre fabric. Firstly, the materials and the methodology used in the treatments, followed by the explanation of the characterization tests carried out and the results obtained. Finally, it concludes with identification of the optimal treatment.

1. INTRODUCTION

The use of natural fibres as reinforcement in composites is a topic of great interest, but due to their combustible nature, some modifications are necessary to improve their fire properties. Treatments are generally focused on improving the mechanical properties by reducing the hydrophilic nature of the fibre and improving the fibre-matrix adhesion, but in this case, we have focused on selecting a treatment that improves the fire resistance.

Chapter 3, section 3.2 reviewed many treatments that can be applied to natural fibres to improve their fire resistance properties. In this thesis a synthetic and a natural treatment have been selected considering their effect and availability. From the synthetic options, silane treatment was selected because it has been shown to improve mechanical and fire properties, as silanol forms hydrogen bonds with fibre and matrix contributing to better adhesion, increasing thermal stability [1,2]. The treatment was carried out with (3-Aminopropyl)triethoxysilane (APTES) according to the method used by Sajna et al.[2], because they applied the treatment to banana fibres, and observed that APTES decreases the burning rate and the dripping, in addition to reduce the pHRR by 26%.

On other hand, from the natural treatments, banana pseudostem sap (BPS) was selected due to its high availability in the Canary Islands and its observed effect in different natural fibres. Banana is the first crop in terms of production in this region and they are also the main producers in Europe [3,4]. During cultivation, each pseudostem bears fruit only once, so when it is harvested, the pseudostem is cut, generating a large amount of waste. The pseudostems are usually left in the plantation to nourish the soil for their mineral content, but one of the options for their revaluation is the extraction of the fibre. The pseudostem is composed of 90% water, 0.6% fibre and 9.4% pulp [5], and the fibre is extracted by a mechanical process. During the process two different raw materials are obtained, high quality natural fibre and residual pulp. The pulp has a high-water content which can be extracted by pressing, thus obtaining the BPS (Figure 1). BPS can also be extracted directly from the pseudostem, but in this way the pseudostem can be used in its entirety, thus minimising waste production.

FIGURE 1: BANANA PSEUDOSTEM SAP EXTRACTION

2. MATERIALS AND METHODS

2.1 MATERIALS

As previously mentioned, the reinforcing material used in the composites is a technical linen fabric FlaxDry BL with a density of 200g/m^2 and 2x2 twill structure. This fabric has good mechanical properties, vibration absorption, electrical insulation, and near-zero thermal coefficient of expansion. In addition, it allows the manufacture of more ecological pieces as it is made entirely from natural fibres and provides a unique aesthetic appearance.

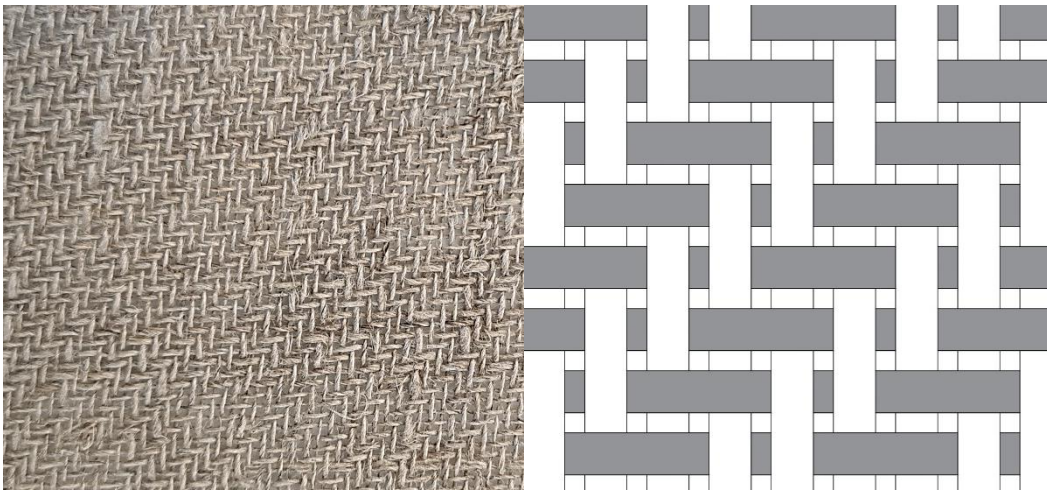

FIGURE 2: LINEN FABRIC 2X2 TWILL STRUCTURE

The chemicals used for the treatments were sodium hydroxide (NaOH) in pellets from Honeywell with 98% assay, 3-Aminopropyltriethoxysilane (APTES) 99% from Thermo Scientific Acros, boric acid (H_3BO_3) analytical grade from Labkem and ethanol absolute for analysis from Merck. For the extraction of BPS, the banana fibre was first extracted mechanically from the leaves of the pseudostem using a system patented by the University of Las Palmas de Gran Canaria [6]. Once extracted, the pulp is collected and pressed to obtain the sap. Due to the liquid still contains solid matter, it is necessary to do a double filtration, first with a 500µm sieve and then with filter paper (Figure 3).

FIGURE 3: BPS FILTRATION

2.2 FIBRE TREATMENTS

For silane treatment, a solution of APTES at 0.6% was prepared by dissolving it in an ethanol/water solution in the ratio of 6:4. Subsequently, the linen fabric was immersed in the solution for 30 min at a fibre/solution ratio of 1:15. Then, the fibres were dried in air for 1 day.

As previously reviewed in Chapter 2, BPS has been applied in diverse types of fibre and conditions, and it has been concluded that the best results are obtained with concentrated BPS solutions at alkaline pH and with a smoke and afterglow suppressant. For this reason, in this case, the influence of the concentration and the addition of boric acid in linen fabric was studied according to the method of Basak et al. [7–9]. The concentrations studied were pure BPS (1:1), concentrated to a half (2:1) and concentrated to a quarter (4:1). The concentrate was prepared by evaporation of the water until the desired volume was reached. In addition, the effect of boric acid was studied by treating the fabric with only 3% boric acid and adding 3% boric acid to the solution concentrated to a quarter (4:1+3%BA). In all the formulations, the solutions were alkalinised by adding sodium hydroxide to pH 10 and then the linen fabric was treated for 30 min maintaining the fibre-solution ratio of 1:15. Lastly, the fibres were dried in air for 1 day.

2.3 CHARACTERIZATION TESTS

First, the macro- and microelements and organic matter of the filtered BPS were analysed by Laboratorio Agroalimentario y Fitopatológico of Cabildo de Gran Canaria to determine its composition, compare it with the literature and thus justify the mechanism of the observed self-extinguishing effect. The techniques used were dry combustion, electrometry and microwave digestion followed by ICP-OES.

The treatments increase the weight of the fabric due to their reaction with the fibre or by deposition of elements on the surface, so before any characterization, it was determined the percentage of add-on of each treatment. For this purpose, samples were weighed before and after treatment, previously conditioned at room temperature and humidity. The results are expressed in percentage as shown below, where M_1 and M_2 are the weight of the sample before and after treatment, respectively. The results reported are the average of four determinations.

$$\% \, add - on = \frac{M_2 - M_1}{M_1} \cdot 100$$

Then, optical microscopy has been used to study the natural fibre textile and the effects of the treatments. The microscope used was the Olympus BX51 optical microscope with objectives from 2x to 100x.

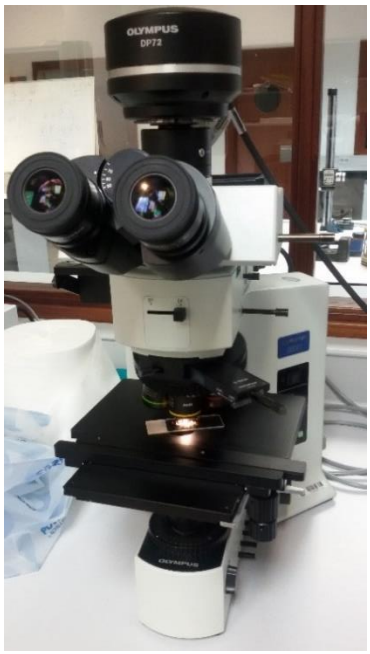

FIGURE 4: OLYMPUS BX51 MICROSCOPE

For thermal and fire characterization, thermogravimetry (TGA), micro-scale combustion calorimetry (MCC) and vertical flammability tests were carried out. TGA tests were performed by Aiju Technological Institute on a TA Instruments TGA Q500 following UNE-EN ISO 11358-1 standard. The samples were heated from 30℃ to 600℃ at 20℃/min under nitrogen atmosphere and then from 600℃ to 1000℃ at 20℃/min under oxygen and the flux for both gases was 50 mL/min. The tests were performed three times to ensure the repeatability. The micro-scale combustion calorimetry test, which is described in Chapter 2 Section 4.4, was performed by the IMDEA Materials Institute. The samples were tested according to method B of ASTM D7309, which consists in an aerobic pyrolysis in 80/20 nitrogen/oxygen flow. The samples were heated from 100 to 700℃ at 1℃/s and the combustor was maintained at 900℃. Finally, the vertical flammability tests were carried out in accordance with UNE-EN ISO 11925-2:2020 (Chapter 2 Section 4.5). To perform the tests, it was used the lab-made equipment used for UL94 test with a fabric holder (Figure 1Figure 5). The specimens of dimension 250x90 mm were tested with the Bunsen burner at 45º with an application time of 15 s. In the test it is recorded whether ignition occurs, when the flame front exceeds 150 mm above the point of application, the presence of ignited particles or droplets and any physical observations. At least 4 specimens were tested for each treatment.

FIGURE 5: FABRIC HOLDER FOR VERTICAL FLAMMABILITY TESTS

3. RESULTS AND DISCUSSION

Firstly, the results of the analysis of the composition of filtered BPS are shown in Table 1. Of the macroelements, it showed the presence of potassium and magnesium in higher amounts,

followed by nitrogen, phosphorus, and sodium. The elements can be found in the form of salts like potassium chloride, potassium fluoride, magnesium nitrate and potassium nitrate, among others, as reported in the literature [7,10]. Of the microelements, manganese stands out with 4 mg/L. Therefore, flame retardancy could be attributed to the presence of free metal ions, salts, phosphates, etc. that form an intumescent coating on the fibre surface that restricts the rise of heat, the release of flammable gases and favours the char formation [11]. Lastly, despite the double filtration, trace of suspended organic matter remain in the BPS and the pH of the solution is slightly acid. In addition, it is confirmed that the solution has a large amount of dissolved ions, as reported in literature, since a conductivity of 14 dS/m is obtained, corresponding to the brackish water range.

TABLE 1: COMPOSITION OF BPS

Determination	Result	Method
	Macroelements	
Nitrogen	0.03 g/100 mL	Dry combustion
P_2O_5	0.02 g/100 mL	Microwave+ICP-OES
K_2O	0.39 g/100 mL	Microwave+ICP-OES
CaO	<0.01 g/100 mL	Microwave+ICP-OES
MgO	0.12 g/100 mL	Microwave+ICP-OES
Na	0.01 g/100 mL	Microwave+ICP-OES
	Microelements	
B	0.2 mg/L	Microwave+ICP-OES
Cu	<0.3 mg/L	Microwave+ICP-OES
Fe	<0.2 mg/L	Microwave+ICP-OES
Mn	4 mg/L	Microwave+ICP-OES
Zn	<0.2 mg/L	Microwave+ICP-OES
Organic matter	0.45 g/100 mL	Calculated
pH	5.1	Electrometry
Conductivity	14 dS/m	Electrometry

In silane treatment, it was observed that after one hour the solution showed a light yellow-green colour, without bubbles or precipitates (Figure 6). Silanes have two different functional groups, one end interacts with the polymeric matrix, while the other interacts with the fibre. On the fibre side, the alkoxy silane group is hydrolysed by water to form silanol, which reacts with the hydroxyl groups on the fibre surface [12]. No residues are formed after the reaction, only water, so the colour of the solution can be attributed to the fact that the treatment was applied with a solution containing ethanol and water as a solvent, which may have removed some colour or impurities from the surface of the fibre, although the fabric does not show a noticeable visual difference. To confirm, the linen fabric was immersed in the ethanol/water solution following the

same criteria of concentration, proportion, and application time, and it was found that the solution turned a greenish-yellow colour, confirming that the colour change is due to the solvent.

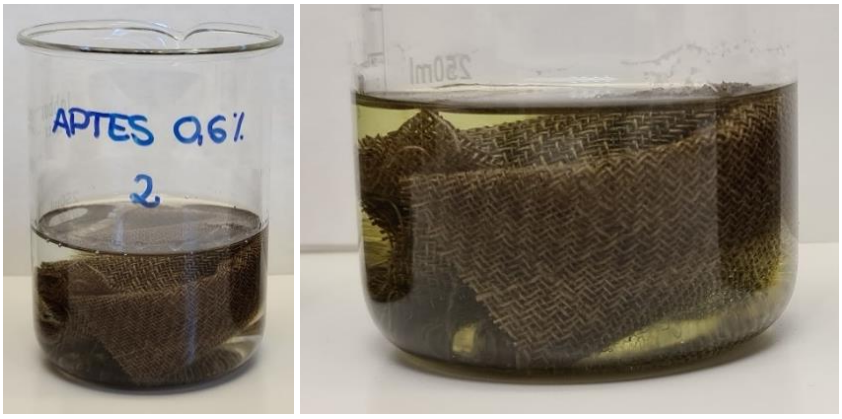

FIGURE 6: SILANE TREATMENT BEFORE AND AFTER

On the other hand, in BPS treatment after the concentrate process, a noticeable change in the colour of the solution was observed, from a lighter and more transparent colour to a dark and opaque brown (Figure 7). In addition, the formation of a precipitate was perceived, being more noticeable in the more concentrated solutions and it increased with the addition of NaOH**¡Error! No se encuentra el origen de la referencia.**. These observations lead to the conclusion that the alkaline pH favours the deposition of the elements dissolved in the solution on the fibre surface because it causes them to precipitate. In fact, Basak et. al. [13] treated cotton fabric at different pH and confirmed that alkali increased the uptake.

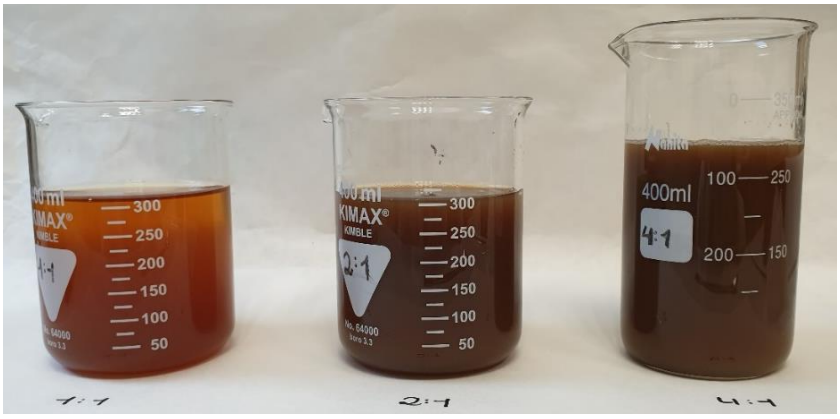

FIGURE 7: BPS SOLUTION TREATMENTS

In addition, comparing the fibre before and after treatment, it was observed that the fibre shrinks a little and becomes stiffer and rougher, as well as it turns a browner colour and there are darker areas where the BPS precipitate has accumulated (Figure 8). In the case of 3% boric acid treatment, no change in solution or fibre was observed after treatment.

FIGURE 8: LINEN FABRIC BEFORE AND AFTER TREATMENT WITH BPS

After the treatment, the add-on percentage was determined (Table 2). In silane treatment, low uptake is observed due to the low concentration of the solution. On the other hand, in the BPS treatment the uptake increases with the solution concentration reaching 17% for BPS 4:1 and up to about 19% when 3% BA is added. However, when treated with boric acid only, the uptake is almost zero. Comparing the results with other authors, it is observed that for BPS the results obtained for the 1:1 solution is similar with other fibres, 5 for cotton [9] and 4.5 for corn fibre [8]. Nevertheless, when the concentration is increased, the values obtained for linen fabric are higher, reaching more than double for the 4:1 solution despite not having mordanted the fibre. This fact can be justified because BPS is a solution that comes from a natural resource, so depending on its origin, extraction process, plant species, even in different plants of the same crop, the properties, composition, and effect may vary. In fact, as the concentration increases, a larger deviation in the percentage is observed because different BPS samples were used. If the starting solutions have differences in concentration, this fact is magnified when they are concentrated, so using different BPS samples allow us to observe whether these differences significantly affect the retarding effect. Furthermore, the analyses available in the literature have not determined the same elements or the conductivity, so it is not possible to determine to which factor justifies the difference in add on%.

TABLE 2: ADD-ON PERCENTAGE OF THE TREATMENTS

Sample	Add-on %
APTES 0.6%	1.05 ± 0.22
BPS 1:1	4.75 ± 0.74
BPS 2:1	7.56 ± 0.61
BPS 4:1	17.09 ± 3.99
BPS 4:1+3%BA	18.80 ± 4.30
3%BA	0.30 ± 0.11

Subsequently, optical microscopy was used to study the effect of the treatments. Firstly, the APTES-treated fabric was analysed. As shown in Figure 9, despite the low percentage of add-on, the treated fibre shows differences, with respect to the untreated fibre, a swelling is observed as the size of the yarns increased and, consequently, the voids are reduced, as well as a more irregular surface. This fact would justify the results obtained in other articles in which it is observed that silane treatment improves adhesion with the polymeric matrix and, as a consequence, the mechanical properties, not only due to the chemical bonding with both phases, but also because the more irregular and rougher surface favours physical bonding with the polymer [14,15].

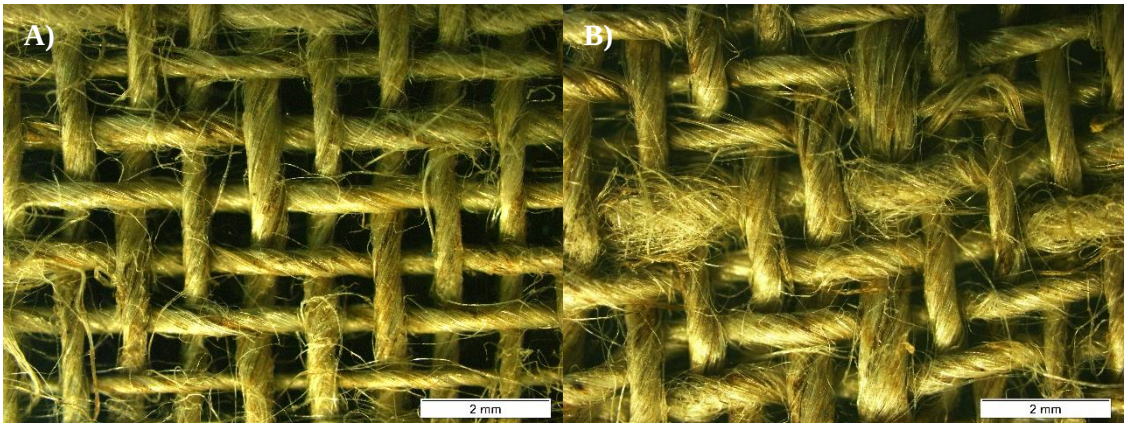

FIGURE 9: MICROSCOPIC IMAGES OF LINEN TREATED WITH APTES. A) LINEN B) LINEN TREATED WITH APTES AT 0.6%

Regarding to BPS treatment, Figure 10 shows the images of the linen fabric treated at the different concentrations, 1:1, 2:1, 4:1 and 4:1+3%BA. Compared to the control fabric, deposition of small particles on the surface is observed, which increases with the concentration. In addition, a slight swelling and increase in roughness is observed, but not as noticeable as in the case of silane. Finally, in the linen fabric treated at 4:1 with 3% of boric acid (Figure 10), the formation of clusters is observed on the surface of the fibre and between yarns, which leads to the conclusion that boric acid in the BPS solution favours the deposition of the salts dissolved in the extract and for this reason increases the add-on with respect to the BPS 4:1 treatment. Since this deposition is not homogeneous and, consequently, a greater dispersion in the mechanical and fire characteristics could be obtained, a pre-treatment process of mordanting could be added.

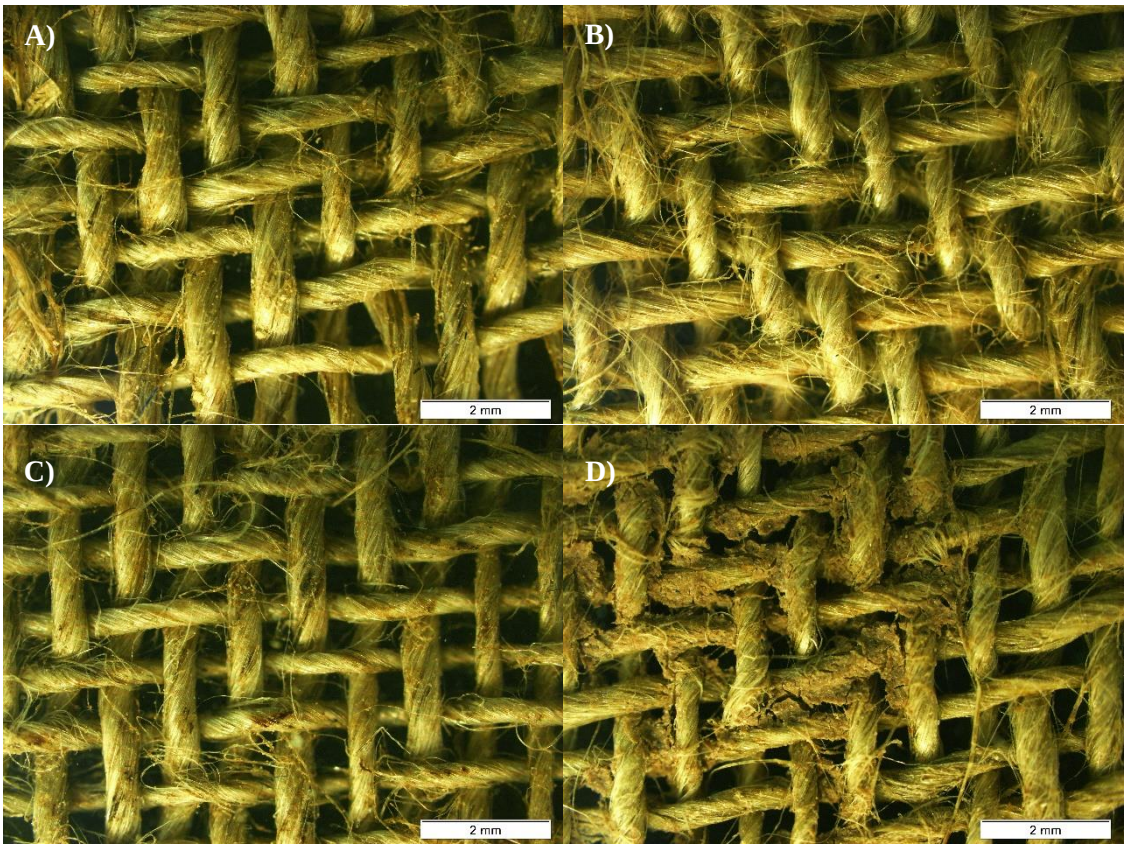

FIGURE 10: MICROSCOPIC IMAGES OF LINEN TREATED WITH BPS. A) 1:1 B) 2:1 C) 4:1 D) 4:1+3%BA

Once the fabric had been analysed the thermal characterization was performed. Firstly, the vertical ignitability test was carried out in accordance with the standard UNE-EN ISO 11925-2:2020, which results are summarised in Table 3. In the test, it was observed that the linen sample ignites easily, the entire sample burnt, and the char is very weak. However, when the fabric is treated with 0.6% APTES, it catches the flame, but the propagation is slower, and the char has a black colour and a firmer structure than the control sample. On the other hand, when the fabric is treated with BPS, it is observed that the flame time decreases with the concentration, reaching zero in the samples treated with BPS 4:1, making the fabric self-extinguishable. Furthermore, as the concentration of BPS increases, not only does the flame not completely burn the sample, but it is followed by a longer afterglow combustion, which is beneficial because it is slower and at less temperature, thus providing more evacuation time in a less hazardous environment. Lastly, the boric acid treatment shows comparable results to the silane treatment, the sample ignites and burns completely but at a lower rate than the control sample.

The effect of the treatments can also be observed visually by comparing their behaviour over the test time. Figure 11: shows the samples of each treatment 30 seconds after the start of the flame application. First, the treatments with APTES, BA, and BPS 1:1 slightly improve the fire properties compared to the control sample, but the flame time and propagation speed remain high.

However, when the BPS concentration is increased to 2:1 a noticeable change in behaviour is observed, since at the same test time the sample has no flame, and the affected area is halved. Lastly, the treatments concentrated to a quarter (BPS 4:1 and BPS 4:1+3%BA) have a significant effect on the fire properties of the linen fabric, because they do not catch up flame and after 30 seconds the progression of the afterglow is slow and the char is reduced in comparison with the other samples, so it is concluded that it has the best properties compared to the other treatments.

TABLE 3: RESULTS OF THE VERTICAL FLAMMABILITY TESTS

Sample	Control linen	APTES 0.6%	BPS 1:1	BPS 2:1	BPS 4:1	BPS 4:1 +3%BA	3%BA
Ignition occurs	Yes	Yes	Yes	Yes	No	No	Yes
Flame front exceed 150 mm	Yes	Yes	Yes	Yes	No	No	Yes
Time to 150 mm (s)	18.87	23.58	18.02	17.23	-	-	22.27
Time to 250 mm (s)	21.62	28.04	23.56	-	-	-	28.44
Flame time (s)	21.97	29.03	20.95	19.36	-	-	27.41
State of the fabric	Completely burnt with flame	Completely burnt with flame	Burnt initially with flame followed by afterglow	Burnt initially with flame followed by afterglow	Partially burnt with afterglow	Partially burnt with afterglow	Completely burnt with flame

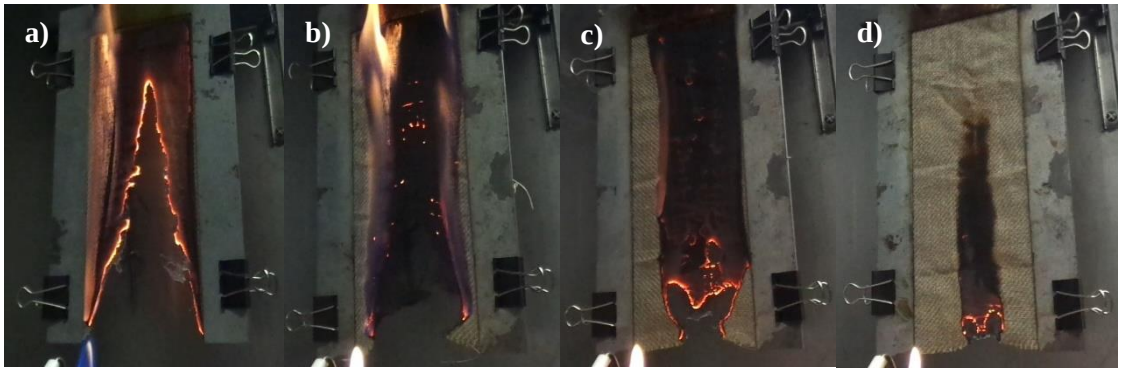

Control APTES 0.6% BPS 1:1 BPS 2:1

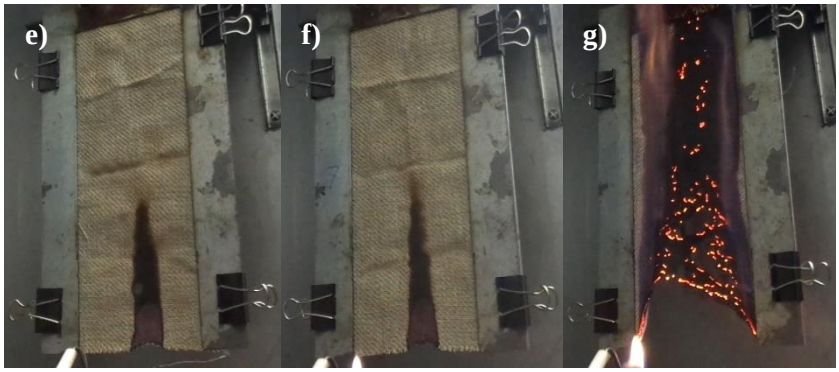

BPS 4:1 BPS 4:1+3%BA 3%BA

FIGURE 11: COMPARISON OF BURNING BEHAVIOUR OF LINEN TREATED SAMPLES AT 30 SECONDS

Subsequently, the MCC test of the BPS-treated fabric was carried out to assess the flammability, determine the heat release rate, and thus confirming the best treatment for linen fabric. A minimum of 3 tests were performed on each sample to ensure repeatability, as only a few milligrams of the sample were used and the peak of Heat Release Rate (pHRR), temperature of the peak (T_{peak}) and Total Heat Released (THR) values were determined. Table 4 shows the mean of the tested replicates, the standard deviation and the reduction compared to the control sample and Figure 12 the curves obtained. It should be noted that in both the MCC and the vertical ignition test show that despite the use of different solutions, the results show small deviations; in fact, the highest values correspond to the control fibre, which leads to the conclusion that the differences in concentration of the initial solutions have not significantly affected the retardant effect. As in the vertical flammability test, the BPS solution significantly improves the flammability of linen. Firstly, it is observed that the pHRR decreases as the concentration of the BPS solution increases. When the treatment is applied as it is (BPS 1:1), a reduction of almost 25% is obtained, and when the concentration is increased to one quarter (BPS 4:1), a reduction of 62% is achieved compared to the control linen. Subsequently, when 3% boric acid is applied, a reduction of 78% is obtained, so it is concluded that in addition to reducing afterglow and smoke generation, it helps to reduce the heat release rate. In the case of peak temperature, no trend is observed with respect to concentration, however, they are significantly lower with respect to the control fabric, with the BPS 4:1+3%BA treatment being the lowest (difference of about 63°C). This confirms the mechanism of action of BPS, as the earlier pyrolysis means that the treatment dehydrates the cellulose earlier, so fewer flammable gases are released and the char mass remaining at higher temperature is bigger. Finally, the THR of linen is in the range of 11-13 kJ/g, which corresponds to complete degradation of the fibres. However, the THR of BPS-treated fibres is reduced to 9.5 kJ/g in the case of BPS 1:1 and 5.54 kJ/g in the case of BPS 4:1+3%BA, which means that the char is not completely degraded, as well as it helps to absorb the heat generated. This can also be confirmed by the fact that heat is still released at the end of the pyrolysis ramp, HRR close to 4-5 W/g (Figure 12).

TABLE 4: MICRO CONE CALORIMETRY RESULTS OF BPS-TREATED LINEN FABRICS

Sample	pHRR (W/g)	Reduction in pHRR (%)	T_{peak} (°C)	THR (kJ/g)	Reduction in THR (%)
Linen	180.10 ± 8.13	-	363.85 ± 1.17	11.89 ± 0.84	-
BPS 1:1	135.58 ± 1.44	24.72%	324.78 ± 0.99	9.55 ± 0.27	19.68%
BPS 2:1	107.68 ± 5.24	40.21%	316.62 ± 1.48	8.70 ± 0.29	26.83%
BPS 4:1	67.50 ± 2.43	62.52%	327.75 ± 2.68	7.53 ± 0.11	36.67%
BPS 4:1+3%BA	38.41 ± 3.54	78.67%	301.26 ± 5.22	5.54 ± 0.26	53.41%

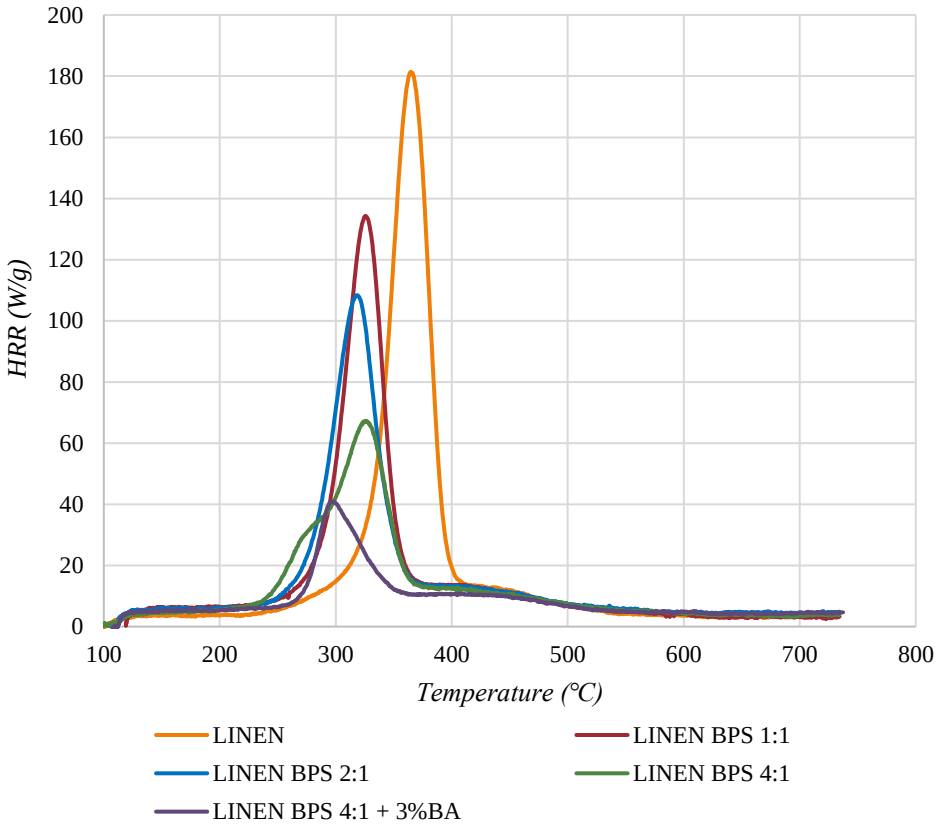

FIGURE 12: HEAT RELEASE RATE CURVES OF LINEN FABRIC TREATED WITH BPS

To confirm the mechanism of action of BPS, the TGA test of untreated and BPS 4:1 treated fibre was performed (Figure 13). The TG curve of the control linen sample shows at the beginning of the curve a weight loss up to 200°C of 4.4% due to the moisture contained in the fibre. Next, it is observed the main pyrolysis step with a degradation temperature or left limit temperature (T_L) around 188.5°C and onset of 328-329°C. In the first part of this stage, from 200 to 275°C, depolymerisation of hemicellulose and pectin occurs with a weight loss of 4%. Subsequently, in the range between 275 and 375°C, it is produced the pyrolysis of cellulose with a maximum weight loss rate of 1.49%/°C at 360°C and a total weight loss of 61.4%. Then, between 375 and 580°C, lignin decomposition occurs at a slower rate, as it is the most difficult compound to thermally degrade. In this last stage, the loss is 19.3%, but it must be considered that lignin degradation occurs throughout the temperature range, so the approximate composition of the fibre cannot be determined with the above percentages. Finally, from 580°C due to the gas change from nitrogen to oxygen, there is a complete decomposition of the carbonaceous residues or compounds that have not been completely degraded to finally obtain a residue of 0.6%.

In the BPS-treated linen fabric, it is observed a higher weight loss (8.3%) in the initial stage (20-200°C) due to the presence of more moisture in the fabric because of the inorganic salts and their hydrates. Then, the main pyrolysis step is observed with a left limit temperature of 190°C,

similar to the control fabric, however, the onset temperature is 291℃, which is about 40℃ lower. This fact confirms that BPS treatment catalyses the dehydration of the cellulosic material and, consequently, reduces the release of flammable gases as levoglucosan and pyroglucosan, and generates more char. Furthermore, the mass loss in this stage is 40% with the maximum mass rate of 0.81%/℃ at 333.7℃, so the treatment reduced the amount of mass loss in the pyrolysis, in addition to the combustion temperature due to the dilution of flammable volatiles by the generation of non-oxidisable CO_2 and H_2O. As a result, the treated fabric generated more char at higher temperature and at 580℃, it increased from 10.8% to 22% due to the presence of inorganics. Finally, because of the gas change, the carbonaceous residues decompose until 800℃.

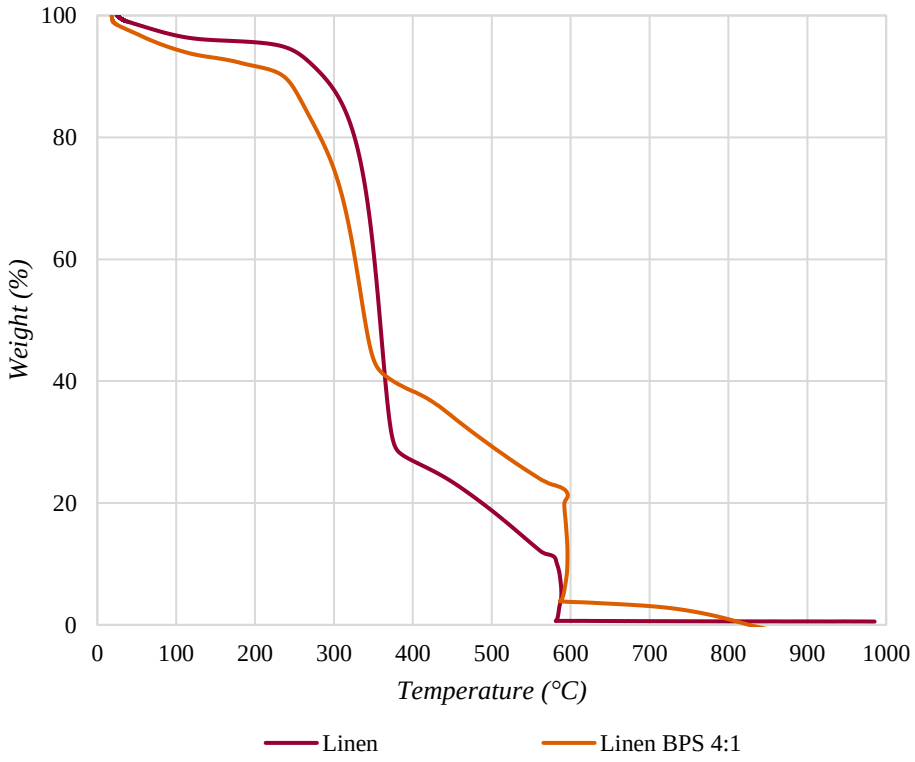

FIGURE 13: TGA CURVES OF THE CONTROL LINEN AND BPS 4:1

4. CONCLUSIONS

The present study has shown the effect of a synthetic treatment with APTES and a natural treatment with BPS on linen fabric. On the one hand, the silane treatment slightly improves the fire properties. It delays the propagation speed, increasing the flame time by 7 seconds, but not enough to be used as a composite reinforcement. However, the treatment with BPS significantly improved the thermal stability by inhibiting ignition completely. The BPS treatment was applied at different concentrations, at alkaline pH and in combination with a smoke suppressant, and the mixed formulation of BPS 4:1 and 3%BA was found to be the most suitable for imparting flame retardancy to the linen fabric. This treatment reduced the heat release rate (HRR) by 78%, the total heat release (THR) by 53% and hinder the flame catch-up in the vertical flammability test, making the fabric self-extinguishable. In addition to its retardant effect, the treatment with BPS has other advantages, such as the fact that the application process is simple and that it is a residue present in large quantities in the Canary Islands that is currently not used, which makes it a promising residue for improving the fire-resistant properties of natural fibres.

5. INDEX OF TABLES AND FIGURES

6. REFERENCES

1. Członka S, Strąkowska A, Pospiech P, Strzelec K. Effects of Chemically Treated Eucalyptus Fibers on Mechanical, Thermal and Insulating Properties of Polyurethane Composite Foams. Materials 2020;13:1781.
2. Sajna VP, Mohanty S, Nayak SK. A study on thermal degradation kinetics and flammability properties of poly(lactic acid)/banana fiber/nanoclay hybrid bionanocomposites. Polym Compos 2017;38:2067–79.
3. Consejería de Agricultura Ganadería y Pesca. Mapa de cultivos de Canarias (Campañas 2015-2021) [Internet]. 2021 [cited 2022 Oct 3]. Available from: https://www.gobiernodecanarias.org/agricultura/temas/mapa_cultivos/
4. Eurostat. Crop production in EU standard humidity: Banana, harvested production in EU standard humidity [Internet]. 2022 [cited 2022 Oct 3];Available from: https://ec.europa.eu/eurostat/databrowser/bookmark/1372602c-caf0-4de1-a8c1-95b5ac61343a?lang=en
5. Ortega Z, Benítez AN, Monzón MD, Hernández PM, Angulo I, Marrero MD. Study of Banana Fiber as Reinforcement of Polyethylene Samples Made by Compression and Injection Molding. J Biobased Mater Bioenergy 2010;4:114–20.
6. Monzón Verona MD, Suárez García LA, Pestana Guillén JD, Ortega García F, Benítez Vega AN, Ortega Medina Z, et al. Procedimiento y máquina para la obtención de fibra a partir de hojas. 2013;
7. Basak S, Samanta KK, Chattopadhyay SK, Narkar R. Self-extinguishable ligno-cellulosic fabric using banana pseudostem sap. 2015.
8. Kambli ND, Samanta KK, Basak S, Chattopadhyay SK, Patil PG, Deshmukh RR. Characterization of the corn husk fibre and improvement in its thermal stability by banana pseudostem sap. Cellulose 2018;25:5241–57.
9. Basak S, Samanta KK, Chattopadhyay SK, Saxena S, Narkar & R. Banana pseudostem sap and boric acid-A new green intumescent for making self-extinguishing cotton fabric. 2018.
10. Basak S, Samanta KK, Chattopadhyay SK, Narkar RS, Mahangade R. Flame retardant cellulosic textile using banana pseudostem sap. International Journal of Clothing Science and Technology 2015;27:247–61.
11. Basak S, Samanta KartickK, Saxena S, Chattopadhyay SK, Narkar R, Mahangade R, et al. Flame resistant cellulosic substrate using banana pseudostem sap. Polish Journal of Chemical Technology 2015;17:123–33.
12. Xie Y, Hill CAS, Xiao Z, Militz H, Mai C. Silane coupling agents used for natural fiber/polymer composites: A review. Compos Part A Appl Sci Manuf 2010;41:806–19.

13. Basak S, Saxena S, Chattopadhyay S, Narkar R, Mahangade R. Banana pseudostem sap: A waste plant resource for making thermally stable cellulosic substrate. Journal of Industrial Textiles 2016;46:1003–23.
14. Fang C cui, Song X, Zou T, Li Y yuan, Wang P, Zhang Y. Natural jute fiber treated with silane coupling agent KH570 reinforced polylactic acid composites: mechanical and thermal properties. Textile Research Journal 2022;004051752210971.
15. Liu Y, Lv X, Bao J, Xie J, Tang X, Che J, et al. Characterization of silane treated and untreated natural cellulosic fibre from corn stalk waste as potential reinforcement in polymer composites. Carbohydr Polym 2019;218:179–87.

CHAPTER 6

COMPOSITES REINFORCED WITH NATURAL FIBRES

TABLE OF CONTENTS

During the development of this thesis, the fire properties of the polymeric matrix and the fabric have been improved separately to then be combined to produce the composite. This chapter describes the methodology used to manufacture the natural fibre reinforced composites and their subsequent characterization. The results obtained for each polymeric matrix and their discussion are then shown, concluding with formulations for the composite optimised for polypropylene and polybutylene succinate.

1. INTRODUCTION

Composite is defined as the combination of two or more materials that have quite different properties, do not dissolve or blend with each other and work together to give the composite unique properties [1]. The aim is to obtain materials with physico-mechanical properties superior to those of the individual constituent materials and at a lower cost. In general, a composite consists of a matrix and a reinforcement (or filler) and can be classified according to the nature of the matrix and the type of reinforcement [2]. In terms of the matrix, there are ceramic, polymeric or metallic matrix composites, with most of those available on the market being polymeric [1]. In terms of reinforcement, there are fibre, particulate and structural composites. In this case, it is a polymeric composite with structural reinforcement, specifically the sandwich type. This consists of a core material bonded between two natural fibre skins, where the core material brings stability, fire resistance and provides rigidity [3]. This geometry results in a strong, rigid, and lightweight structure, which is a particularly important feature in vehicle design [4]. One of the important things to bear in mind when manufacturing a sandwich or laminate polymer composite is that it must be symmetrical, as the core layers and the outer layers do not have the same degree of shrinkage, so warping could occur if this is not considered.

Natural fibres as reinforcement for polymeric composites have received increasing attention due to the growing concern for plastic waste generation and the search for environmentally friendly raw materials. These composites have received interest from academia and industry due to their good properties and superior advantages over synthetic fibres in terms of relatively low weight, low cost, less damage to processing equipment, good specific mechanical properties, and biodegradability, among others [5]. In addition, the use of the natural fibre fabric provides a decorative effect to the composite. Consequently, natural fibre reinforced composites (NFPC) have received significant attention in automotive, aerospace, construction, electrical and electronic, sports, recreational, and medical applications [6]. Of these, the applications with the largest market share are in the construction and automotive sectors [7], where fire resistance is a key requirement to accomplish.

As previously mentioned, the options available to reduce the flammability of the composites are to improve the properties of the matrix, the fibre and/or the composite as a whole. Throughout this thesis, the properties of the polymeric matrices on the one hand and the fabric on the other hand have been improved, so this chapter unifies the conclusions obtained in chapters 4 and 5, the mixtures and the treatment determined as optimal. For PP, the mixtures with 40% brucite plus 20% colemanite and 30% brucite plus 30% colemanite, and for PBS 20% brucite plus 40% colemanite, and 10% brucite plus 50% colemanite. For the treatment, the BPS concentrated to a quarter with 3% boric acid at pH 10. For this purpose, the polymeric matrices without additive, with the optimal mixtures and with calcium carbonate, will be reinforced with the treated and untreated linen fabric to determine which formulation is best for each matrix and whether fibre treatment is necessary.

2. MATERIALS AND METHODS

In this chapter the materials used are polypropylene Luban HP5101R and polybutylene succinate BioPBS FZ91 as polymers, brucite HQ-1250, colemanite and calcium carbonate as additives, and linen fabric FlaxDry BL as reinforcement. Regarding to the treatment, BPS filtered and concentrated to a quarter, sodium hydroxide from Honeywell and boric acid from Labkem.

The methodology used for extrusion and for fibre treatment is the same as explained in Chapters 3 and 5. For extrusion, the dried ground polymers are mixed with the corresponding proportions of additive and extruded in a twin-screw extruder. Once the pellets are obtained, they must be dried before proceeding with compression moulding at 105 ℃ for PP and at 80℃ for PBS for 24 h. The composites manufactured have three layers, two of fibre and one of plastic in the middle, therefore, the procedure consists of manufacture the plastic layer first. For this purpose, an aluminium mould with male and female parts and a 190x190mm cavity (Figure 1) was used to manufacture a 3mm thick plate. The equipment used was a Collin hot plate press model P200P/M.

FIGURE 1: ALUMINIUM MOULD WITH MALE AND FEMALE PARTS

Then, the linen fabric is cut to the same size of the mould, treated with the BPS 4:1+3%BA solution at pH 10 and dried in an oven at 105℃ for 24 h. Once dried, the layers of fabric and polymer are alternated inside the mould and processed in the platen press. During the trials, it was observed that additives and fibre affect the compression moulding process parameters, so they vary depending on the part to be manufactured as shown in **¡Error! No se encuentra el origen de la referencia.**. It is necessary to increase the pressure with the addition of additive because it increases the viscosity of the mixture, and the pressure ensures that the material is evenly distributed throughout the mould. In addition, when reinforcement is added, the pressure is increased by five bar to facilitate adhesion with the plastic matrix and ensure that the polymer passes through the voids in the fabric.

TABLE 1: COMPRESSION MOULDING PROCESS PARAMETERS

Composite	Temperature (℃)	Pressure (bar)
PP without additive	200	10
PP with additive	200	30
PP composite	190	35
PBS without additive	150	10
PBS with additive	150	30
PBS composite	140	35

For the thermal characterisation of the composites, DSC test was carried out in a Perkin Elmer DSC 4000 with the same temperature programs and sample weight between 11.5 and 12.5 mg. It was necessary to increase the sample weight to obtain a clear signal due to the composite has a lower percentage of polymer.

Regarding mechanical tests, the equipment used to perform the tensile and flexural tests was a testing machine model LY-1065 from Dongguan Liyi Test Equipment. The tensile test was performed according to the standards UNE-EN ISO 527-1 and UNE-EN ISO 527-2 with a load cell of 500 kg and a constant crosshead speed of 10 mm/min. At least five replicates of 1A specimens were tested for each mixture. For flexural test, a load cell of 50 kg was used, a speed of 10 mm/min and a three-point test fixture with a span of 64mm. The test was performed based on the UNE-EN ISO 178 standard until breakage or decrease of the strength and at least five replicates 80x10x3mm per group were tested. Finally, Izod impact tests were conducted based on UNE-EN ISO 190 using an Izod&Charpy Impact tester model LY-XJJD 50 from Liyi Test Equipment Co. The pendulum force used was 5.5J and five un-notched samples with dimensions 80x10x3mm per group were tested.

In the case of fire properties, UL94 tests were performed according to the procedure developed by Underwriters Laboratories in a flammability cabinet UL94 of Noselab Ats. In this case, the gas used was methane with a flame 2cm high and the application time was 10 seconds for 94V and 30 seconds for 94HB. The test procedure was the same as for the unreinforced materials, excepts for the gas change (Chapter 3, section 2.7.1).

3. RESULTS AND DISCUSSION

During manufacturing, the composites obtained showed good visual characteristics because the mixture of the polymer with the additives was able to penetrate the fabric, thus achieving good adhesion between the matrix and the reinforcement. However, when the fabric is treated with the BPS adhesion worsens. A noticeable effect was observed as the fibre does not remain as deep into the plastic, so the treatment hinders the adhesion and consequently the mechanical properties may be lower (Figure 2).

FIGURE 2: COMPARISON OF COMPOSITES WITH UNTREATED (LEFT) AND TREATED (RIGHT) LINEN FABRIC

Table 2 below shows all the composites manufactured, specifying the matrix used, treatment, nomenclature, and fibre percentage. It is observed that the matrices without additives have a higher fibre percentage due to the lower density of the polymeric matrix compared to the samples with additives. In fact, the samples with the highest density are those with calcium carbonate and for this reason have the lowest percentage of fibre. Composites have been manufactured without the same percentage of fibre, firstly because when a part is manufactured at an industrial level, it must have a certain volume and the mass of material required is determined on this basis. For this reason, the necessary amount of material has been calculated based on the 3mm thickness of the plastic plate. Secondly, as it is a woven reinforcement, it is not possible to modify the fibre

percentage unless more layers are added, and this would modify the structure of the composite, which would not allow it to be compared with other matrices. Another aspect to note is the percentage increase in the case of treated fibre. As explained in the previous chapter, the treatment increases the weight of the fibre due to their reaction with it or by deposition of elements on the surface, and for this reason the percentage of fibre is higher in treated samples.

TABLE 2: COMPOSITES MANUFACTURED

Polymeric Matrix	Treatment	Sample code	% Fibre (w/w)
PP	No	PP/LN-NT	14.72 ± 0.21
	Yes	PP/LN-T	17.68 ± 0.17
PP+40%Bruc +20%Col	No	PP+40-20/LN-NT	9.15 ± 0.15
	Yes	PP+40-20/LN-T	10.59 ± 0.08
PP+30%Bruc +30%Col	No	PP+30-30/LN-NT	9.25 ± 0.14
	Yes	PP+30-30/LN-T	11.07 ± 0.52
PP+60%$CaCO_3$	No	PP+60CC/LN-NT	8.97 ± 0.15
	Yes	PP+60CC/LN-T	10.57 ± 0.26
PBS	No	PBS/LN-NT	10.31 ± 0.28
	Yes	PBS/LN-T	12.31 ± 0.48
PBS+20%Bruc +40%Col	No	PBS+20-40/LN-NT	8.07 ± 0.11
	Yes	PBS+20-40/LN-T	10.13 ± 0.17
PBS+10%Bruc +50%Col	No	PBS+10-50/LN-NT	7.94 ± 0.04
	Yes	PBS+10-50/LN-T	9.95 ± 0.09
PBS+60%$CaCO_3$	No	PBS+60CC/LN-NT	7.09 ± 0.05
	Yes	PBS+60CC/LN-T	8.53 ± 0.46

The results and discussion of the tests for the PP and PBS matrix are shown separately below. For the discussion of the results, a multifactorial ANOVA analysis was carried out to study the effect of the different materials used as matrix and the treatment of the fibre.

3.1 PP MATRIX

DSC tests were performed to study the effect of the fabric and the treatment on the thermal properties of the material. Table 3 shows the results of the second melting curve for PP composites, onset ($T_{onset,m}$), end ($T_{end,m}$) and melting (T_m) temperatures, enthalpy (ΔH_m), and percentage of crystallinity (w_c). In this case, the values of the partial areas are not reported since no significant differences were obtained (p-value>0.05), but the totality of the results together with the p-values of the matrix and the treatment are shown in Annex. As far as crystallinity is concerned, it is necessary to emphasise that the samples are not entirely polymeric but have additives and fibre, so a correction of the formula is necessary. It is not possible to ensure that the

percentage of polymer calculated is correct since a small sample of the composite was extracted, so it should be taken as an approximation based on levels that were added to the whole, and it should be used for comparative purposes only. In this regard, the formula for the percentage of crystallinity is as follows:

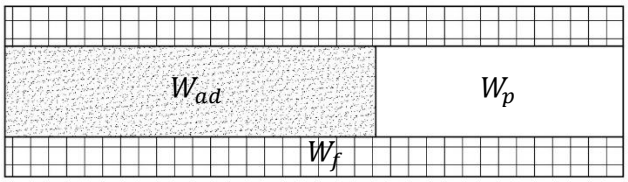

$$W_p = (1 - W_f) \cdot (1 - X_{ad})$$

$$w_c = \frac{\Delta H_m}{\Delta H_m^0} \cdot \frac{100}{W_p}$$

ΔH_m: Heat of fusion sample (J/g)

ΔH_m^0: Heat of fusion of 100% crystalline material (J/g). 207.1 J/g for PP and 200 J/g for PBS

W_p: Percentage of polymer in the composite in parts per unit

W_{ad}: Percentage of additive in the composite in parts per unit

W_f: Percentage of fibre in the composite in parts per unit

X_{ad}: Percentage of additive in the extrusion or plastic plate in parts per unit

TABLE 3: DSC RESULTS OF SECOND MELTING CURVE FOR PP COMPOSITES

Sample		$T_{onset,m}$(°C)	$T_{end,m}$(°C)	Range (°C)	ΔH_m (J/g)	T_m (°C)	w_c (%)
PP/LN-NT		154.99	169.76	14.77	77.48	163.24	43.87
PP/LN-T		155.20	170.06	14.86	77.87	163.59	45.67
PP+40-20/LN-NT		155.57	168.19	12.62	36.35	163.90	48.29
PP+40-20/LN-T		153.85	167.82	13.97	40.15	164.03	54.20
PP+30-30/LN-NT		155.42	168.68	13.26	38.18	164.52	50.79
PP+30-30/LN-T		153.55	168.48	14.93	35.73	162.90	48.50
PP+60CC/LN-NT		155.53	168.26	12.73	34.65	162.57	45.95
PP+60CC/LN-T		155.58	168.79	13.21	37.56	163.18	50.70
p-value	**Matrix**	0.6082	0.0262	0.1079	0.0006	0.5485	0.2585
	Treatm	0.2322	0.7775	0.0928	0.4693	0.8102	0.2585

Firstly, it is observed that the onset temperature is not affected by the different matrices or the treatment, however, there is a significant difference in the end temperature (p-value<0.05). It is observed a decrease in this temperature with the additives and consequently a decrease in the range of the curve. This is justified by the fact that the additives used act as support for the formation of crystals, thus obtaining a more homogeneous distribution. On the other hand, it is

observed that the treatment, although it does not have a significant effect, increases the range of the curve compared to the untreated samples. This means that the particles and compounds adhered to the fibre surface increase the size range of the polymer crystals, so the crystalline structure is less fine when using BPS 4:1+3%BA treated fibre. Next, a significant effect of the matrix on the enthalpy of fusion is obtained. This is due to the difference in the amount of polymer present in the samples, the higher the percentage of PP, the higher the enthalpy. For this reason, the enthalpy is much higher in the samples without additives, whereas no significant differences are observed between the samples with colemanite, brucite and calcium carbonate. In the case of the treatment, an increase is observed, except in the PP+30-30/LN-T sample, so it is not possible to confirm the trend with respect to the treatment. In fact, the multifactorial ANOVA analysis shows that the treatment has no significant difference. Then, the melting temperature is not affected by either the type of matrix or the treatment and is in the range of 162.5 to 164.5ºC. Finally, the percentage of crystallinity, although it does not have a significant difference for either of the two factors, shows an upward trend when additives are used, especially with flame retardants, since they act as a nucleant in PP matrix, as reported in this thesis and in the literature [8–10]. As for the treatment, it seems to increase the percentage of crystallinity, except in PP+30-30/LN-T sample, which would justify the increase in the range of the curve. The compounds adhered to the fibre due to the treatment act as support for the formation of crystals because they increase in quantity, but in a less homogeneous distribution due to their size range increases.

Table 4 below shows the results of the crystallisation curve. As in the melting curve, no significant differences are observed in the onset temperature with respect to matrix and treatment. However, although the difference is not noticeable, an upward trend is observed, especially with flame retardant additives. This trend is also observed in the crystallisation temperature and as previously mentioned in the study of the unreinforced materials, this is because the additives used act as a nucleants. The fact that this is more noticeable in the cooling curve is because the nucleating agents do not usually influence the melting temperature, but they do affect the crystallization temperature [11]. Again, in the case of treatment it is not possible to draw conclusions on whether it shows a trend as it does not have the same effect for all samples. Regarding the enthalpy of crystallisation, it shows a significant difference with respect to the type of matrix due to the difference in the amount of polymer present in the sample, whereas no significant differences are observed between the samples with additives. The treatment does not significantly affect this property, but an upward trend is observed, as in the enthalpy of fusion, except for sample PP+30-30/LN-T. Finally, the difference between the onset and peak temperature has been calculated because it shows the increase or decrease of the crystallisation rate and consequently the nucleating effect of the compounds. It is observed that smaller differences are obtained in the samples with flame retardants, which means that the crystallisation

is faster and therefore these additives have a nucleating effect on the polypropylene. Furthermore, this confirms the conclusions obtained in the melting curve about the increase in the percentage of crystallinity due to the flame retardant additives (Table 3).

TABLE 4: DSC RESULTS OF COOLING CURVE FOR PP COMPOSITES

Sample		$T_{onset,c}$(°C)	ΔH_c (J/g)	T_c (°C)	$T_{onset,c}$-T_c
PP/LN-NT		121.45	76.93	116.19	5.26
PP/LN-T		121.38	78.01	116.18	5.2
PP+40-20/LN-NT		126.34	35.62	122.25	4.09
PP+40-20/LN-T		131.90	39.71	127.74	4.16
PP+30-30/LN-NT		127.51	38.09	123.15	4.36
PP+30-30/LN-T		123.35	36.26	119.12	4.23
PP+60CC/LN-NT		123.19	34.65	117.90	5.29
PP+60CC/LN-T		124.36	37.44	117.95	6.41
p-value	**Matrix**	0.2247	0.0004	0.1450	0.0641
	Treatm	0.7752	0.3168	0.8601	0.4562

Regarding to the mechanical tests, the results of the tensile test are analysed first. Figure 3 shows the elastic modulus and tensile strength of PP composites together with their standard deviation. As observed in the unreinforced materials, the additives increase the elastic modulus due to the increased stiffness of the particles. However, they also increase the brittleness and consequently the maximum tensile strength decreases considerably. This is due to the poor adhesion between the particles and the matrix, the effective cross-section is reduced, which leads to the debonding of the cross-section and thus the tensile strength decreases. In fact, particle density plays a key role in this case. The density of the particles used from the highest to the lowest are $CaCO_3$>colemanite>brucite, so the higher the density, the higher the effective cross-section and therefore the lower the effect of the additive on the mechanical properties. For this reason, the composite with virgin polypropylene is followed by the composite with calcium carbonate, then the samples PP+30-30 due to their higher content of colemanite, and finally the sample PP+40-20. The difference in these last two samples is not significant because the difference in density between the two additives is small, 2.39 g/cm^3 for brucite versus 2.42 g/cm^3 for colemanite [12]. On the other hand, no significant differences in elastic modulus were observed for the treatment, but a p-value of 0 was obtained for the maximum tensile strength. As expected, the strength decreases when the treatment is applied because the fibre had a worse adhesion to the plastic layer due to the shrinkage, roughness, and stiffness of the fibre caused by the treatment, as well the accumulations of BPS solution that the plastic cannot cover well. Therefore, it is confirmed that the treatment decreases the mechanical properties.

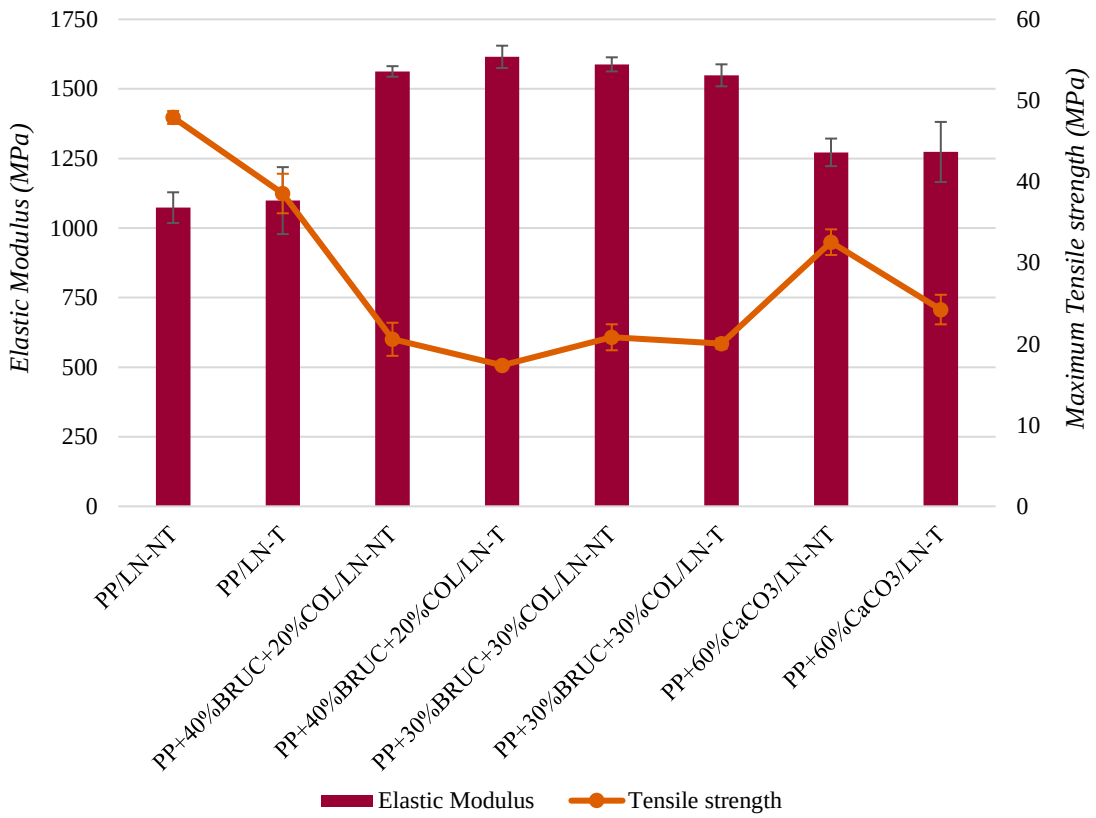

FIGURE 3: TENSILE TEST RESULTS OF PP COMPOSITES

It should be noted that the specimens with fabric and flame retardant additives show multiple fractures until the specimen breaks completely because the additive increases the fragility of the sample, however the fabric maintains the strength until it breaks. This can be seen in the stress-strain graph by the presence of multiple peaks in the upper zone (Figure 4) and by the appearance of cracks in the specimen during the tests (Figure 4).

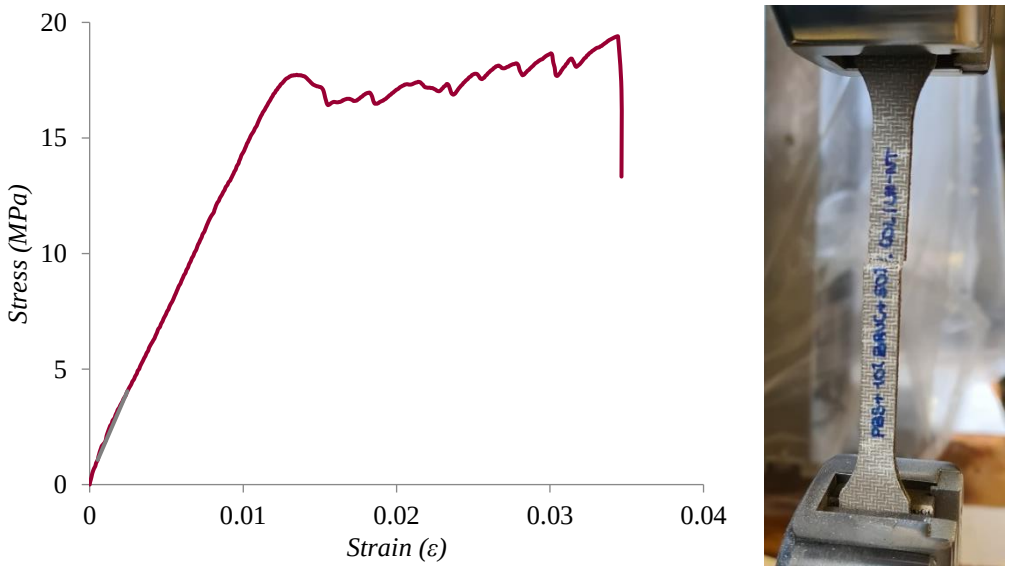

FIGURE 4 AND 5: STRESS-STRAIN GRAPH OF POLYPROPYLENE COMPOSITE WITH FLAME RETARDANT ADDITIVES AND SPECIMEN WITH MULTIPLE CRACKS

In the case of the flexural and impact test both the type of matrix and the treatment have a significant effect (Table 5). On the one hand, due to the stiffness of the additives, the composites require more force to be bent and consequently the flexural modulus increases. To justify their effect, the hardness of the minerals must be considered. In order of hardness on the Mohs scale, colemanite has a hardness of 4.5 [13], followed by calcium carbonate with 3 [14] and finally brucite which is between 2.5 and 3 [15]. Considering that brucite and colemanite are mixed in the composite, the stiffest mixture is expected to be PP+30-30 due to its higher content of colemanite, followed by PP+40-20 and finally PP+60CC. Comparing this expected trend with the flexural modulus, it is confirmed that both follow the same trend, so the increase in the flexural modulus and its tendency is due to the stiffness of the additives used. On the other hand, the impact resistance is considerably reduced with the addition of the additives due to the reduction of the effective cross-section. The particles do not have a good adhesion to the plastic matrix, so they do not act as a whole, and it is only the polymeric particles that resist the impact. For this reason, the density of the additives is a key variable, since the higher the density, the greater the plastic surface area in the cross-section and the greater the resistance. Because of this, the impact resistance is higher in the virgin polypropylene composites, followed by the PP+60CC, then PP+30-30 and finally the PP+40-20 sample. Finally, the treatment has a significant effect (p-value<0.05) on the flexural modulus and impact resistance since it reduces their strength. This is justified by the fact that the treatment hinders the fibre to adhere to the polymeric matrix, which reduces the effectiveness of the fabric that must act as reinforcement.

TABLE 5: FLEXURAL AND IMPACT TEST RESULTS OF PP COMPOSITES

Sample		Flexural Modulus (MPa)	Impact Resistance (kJ/m^2)
PP/LN-NT		3169.2 ± 56.3	15.48 ± 0.77
PP/LN-T		2948.5 ± 70.4	8.51 ± 1.12
PP+40-20/LN-NT		4885.9 ± 105	6.60 ± 0.42
PP+40-20/LN-T		3964.8 ± 107.2	4.37 ± 0.92
PP+30-30/LN-NT		4645.6 ± 129.7	6.55 ± 0.39
PP+30-30/LN-T		4808.0 ± 442.0	5.77 ± 0.82
PP+60CC/LN-NT		4116.0 ± 336.9	11.28 ± 0.78
PP+60CC/LN-T		4031.7 ± 184.1	6.85 ± 0.58
p-value	**Matrix**	0.0000	0.0000
	Treatm	0.0096	0.0000

The results and discussion of the UL94 test on PP composites are shown below. Table 6 shows first the results of the horizontal propagation tests 94 HB followed by the vertical test 94V. Firstly, the results of the composites without additives, with flame retardants and with calcium carbonate are compared. It should be noted that the purpose of using calcium carbonate is to

compare samples with the same proportion of combustible material to verify that the additives used improve the fire properties. In the horizontal test it is observed that colemanite and brucite have a significant effect because the flame propagation is completely prevented as the flame is extinguished before reaching the first mark. Regarding to the treatment, it also has a significant effect because it reduces the propagation speed. In this test, all the samples meet the criteria of the method as it is generally considered the easiest test to pass because it is the least stringent but is useful for comparing samples.

TABLE 6: UL94 RESULTS OF PP COMPOSITES

		Horizontal test 94 HB		Vertical test 94V		
Sample		**Propagation speed (mm/min)**	**Class**	**Flame time (s)**	**Propagation speed (mm/min)**	**Class**
PP/LN-NT		21.16 ± 0.59	HB	123.1 ± 36.8	108.52 ± 12.10	-
PP/LN-T		18.95 ± 0.42	HB	146.4 ± 47.3	104.30 ± 4.29	-
PP+40-20/LN-NT		0.00 ± 0.00	HB	266.3 ± 58.6	51.18 ± 5.68	-
PP+40-20/LN-T		0.00 ± 0.00	HB	16.6 ± 4.2	0.00 ± 0.00	V-1
PP+30-30/LN-NT		0.00 ± 0.00	HB	205 ± 163.4	33.63 ± 20.08	-
PP+30-30/LN-T		0.00 ± 0.00	HB	21.7 ± 22.2	0.00 ± 0.00	-
PP+60CC/LN-NT		21.88 ± 1.38	HB	127.0 ± 13.8	87.57 ± 3.68	-
PP+60CC/LN-T		19.76 ± 0.90	HB	131.9 ± 6.8	84.22 ± 4.21	-
p-value	**Matrix**	0.0000		0.9078	0.0000	
	Treat	0.0053		0.0010	0.0000	

In the case of the vertical test, a significant effect of the matrix and the treatment on the propagation speed is also obtained. When comparing the speed results of the samples with untreated fabrics, the PP+40-20 mixture reduced the speed by 53% and 41.6% compared to the sample without additives and with calcium carbonate, respectively. Furthermore, in the case of sample PP+30-30, the reduction is even greater, 69% and 61.6% respectively. This confirms that the additives used reduce the vertical propagation speed, but not enough to meet the test criteria. However, the treatment applied to the fibre ensures that the samples do not spread the flame, that the flame is extinguished itself and significantly reduces the flame time. This treatment has no significant effect on virgin and carbonate samples, but in the case of flame retardant additives it allows the PP+40-20/LN-T sample to be classifies as V-1 because the flame takes less than 30s to extinguish. In the case of PP+30-30/LN-T sample, the dispersion in the residual flame time is exceptionally large since in some specimens the flame takes more than 30s to extinguish, while in others it takes less than 10s. For this reason, although its propagation speed is lower than the PP+40-20/LN-T sample, it does not meet the criteria for the vertical test because the required time is not met in all tested specimens. This difference in results may be justified by the low

homogeneity of the treatment, since agglomerations were observed in certain areas of the fabric, which does not allow all the same retardant effects to be obtained in all test specimens. This fact could be solved by applying the treatment with a previous mordanting or by improving the application methodology of the treatment. However, it can be confirmed that the treatment of the fabric is key in the case of polypropylene composites because it considerably improves the fire properties by preventing flame propagation.

In summary, considering the results of DSC, mechanical and UL94 tests, **the best mixture for PP composite is 40% brucite plus 20% colemanite with linen fabric treated with BPS4:1+3%BA.**

3.2 PBS MATRIX

The main results for the DSC test of the PBS composites are shown below, in Table 7 for the second melting curve and in the Table 8 for the crystallisation curve. All the results together with the values of the statistical analysis can be found in Annex.

TABLE 7: DSC RESULTS OF SECOND MELTING CURVE FOR PBS COMPOSITES

Sample		$T_{onset,m}$(°C)	$T_{end,m}$(°C)	Range (°C)	ΔH_m (J/g)	T_m (°C)	w_c (%)
PBS/LN-NT		107.73	120.6	12.87	57.19	115.43	31.88
PBS/LN-T		106.16	119.72	13.56	55.86	114.59	31.85
PBS+20-40/LN-NT		107.36	115.20	7.84	22.04	112.71	29.97
PBS+20-40/LN-T		108.43	117.91	9.48	24.53	115.02	34.12
PBS+10-50/LN-NT		106.93	116.9	9.97	21.95	114.55	29.81
PBS+10-50/LN-T		107.28	115.64	8.36	25.12	112.55	34.87
PBS+60CC/LN-NT		105.99	116.65	10.66	25.74	113.69	34.63
PBS+60CC/LN-T		103.54	115.45	11.91	28.03	112.68	38.30
p-value	**Matrix**	0.2196	0.1380	0.0582	0.0004	0.6060	0.1486
	Treatm	0.4853	0.8800	0.5469	0.2019	0.7079	0.0642

Firstly, it is observed that the onset and end temperatures and the range of the curve are not significantly affected by the different matrices or the treatment. However, as with PP composites, the range of the curve is reduced by additives, especially with colemanite and brucite. This is justified because the additives also act as support for the formation of PBS crystals, resulting in a more homogeneous distribution. In this case there are no references in the literature on the effect of brucite and colemanite on crystallinity, but in Chapter 4 it was also observed that these additives reduce the range of the melting curve of PBS matrix, although less than in polypropylene. As for the treatment, it apparently increases the range of the curve, except for

PBS+10-50/LN-T sample, which coincides with the results observed previously with polypropylene, thus concluding that the BPS treatment compounds increase the size range of the polymer crystals. Next, a significant effect of the matrix on the enthalpy of fusion is obtained due to the difference in the amount of polymer present in the samples. The enthalpy is much higher in the samples without additives, whereas no significant differences are observed between the samples with colemanite, brucite and calcium carbonate. Again, the treatment does not have a significant effect, but it seems to increase the enthalpy and thus the percentage of crystallinity, however, it is not possible to confirm this fact, as the virgin PBS samples do not follow this trend. Next, the melting temperature is not affected by the two factors and is in the range of 112.5 to 115.5°C, and if compared with the values obtained for the unreinforced materials, it is observed that there is not much difference after applying linen fabric as reinforcement. Finally, the percentage of crystallinity is affected by the treatment, while for the different matrices no significant effect is obtained. It is observed that the samples with colemanite and brucite and untreated fabric show a small decrease in crystallinity, while with calcium carbonate it increases. Comparing these results with those obtained for the unreinforced matrix (Chapter 4, Section 4), it was found that all three additives have a nucleating effect on PBS, being higher for brucite, but as it is the additive with the lowest proportion its influence is not significant. So, the small decrease in the composites with colemanite and brucite can be justified by the error associated with the percentage of polymer used to correct the formula, but it can be confirmed that calcium carbonate has a nucleating effect on the PBS matrix. On the other hand, when treatment is applied, an increase in crystallinity is observed for all samples with additives because the compounds present in the BPS solution, salts, oxides, phosphates, etc, act as a support for the formation of crystals. For this reason, the sample with the highest crystallinity corresponds to the PBS+60CC/LN-T, because the effect of the additive is added to the treatment.

Table 8Table 4 below shows the results of the crystallisation curve. First, no significant differences are obtained in the onset or crystallisation temperature due to matrix or treatment, and in fact no trend was observed for both factors. Therefore, it is concluded that the additives used have no influence on the crystallisation temperatures, onset and peak, of PBS composites. Regarding the enthalpy of crystallisation, it shows a significant difference with respect to the type of matrix due to the difference in the amount of polymer present in the sample, whereas no significant differences are observed between the samples with additives. Only the value for the calcium carbonate samples is slightly higher due to their higher percentage of crystallinity. The treatment does not significantly affect this property, but an upward trend is observed except for sample PBS/LN-T. Finally, the difference between the onset and peak temperature has been calculated because it shows the influence on the crystallisation rate and a significant effect has been obtained due to the matrix. It is observed that smaller differences are obtained in the samples

with PBS+20-40, which means that the crystallisation is faster and therefore these additives in that proportion favour the formation of crystals. This is justified because brucite has a greater effect on crystallinity (Chapter 4, section 4), and this mixture is the one with the highest proportion of this additive. Next, no differences are observed between the virgin PBS and the PBS+10-50 sample, and the greatest difference is observed in the PBS+60CC sample. This is because calcium carbonate increases the crystallinity, but does not increase the rate of crystals formation, so the range of the curve is greater.

TABLE 8: DSC RESULTS OF COOLING CURVE FOR PBS COMPOSITES

Sample		$T_{onset,c}$(°C)	ΔH_c (J/g)	T_c (°C)	$T_{onset,c}$-T_c
PBS/LN-NT		88.82	57.96	83.53	5.29
PBS/LN-T		87.81	56.66	82.65	5.16
PBS+20-40/LN-NT		87.56	22.96	83.01	4.55
PBS+20-40/LN-T		89.5	24.89	84.87	4.63
PBS+10-50/LN-NT		87.69	22.09	82.33	5.36
PBS+10-50/LN-T		85.51	24.96	80.32	5.19
PBS+60CC/LN-NT		86.59	26.22	80.87	5.72
PBS+60CC/LN-T		84.49	27.61	78.87	5.62
p-value	**Matrix**	0.2673	0.0003	0.1432	0.0031
	Treatm	0.4487	0.2648	0.4671	0.2433

As for the mechanical test results, Figure 6 shows the tensile properties of the PBS composites. As observed in the unreinforced materials and PP composites, the additives used increase the elastic modulus due to the increased stiffness of the particles. Considering the hardness of the additives used, colemanite is the highest on the Mohs sale and consequently mixtures containing this additive have the highest elastic modulus. These are followed by calcium carbonate composites and finally virgin PBS composites. Regarding to the treatment, no significant differences were observed (p-value 0.57), however it has a significant effect in the maximum tensile strength. The strength decreases when the treatment is applied because the fibre had a worse adhesion to the plastic layer due to shrinkage, stiffness and accumulations of the BPS solutions that hinder the plastic to cover the fabric. As for the additives, these also have a significant effect on the maximum tensile strength. The additives increase the brittleness of the composites and consequently the strength decreases. This is due to the poor adhesion between the particles and the matrix; therefore, the effective cross-section is reduced. As explained before, the tendency obtained with respect to the additives is due to the density of the particles. The higher the density of the particles, the higher the effective cross-section and therefore the strength is less affected. For this reason, the composite with the highest strength value is the virgin PBS followed

by the composite with calcium carbonate, the PBS+10-50 samples and finally the PBS+20-40 composites.

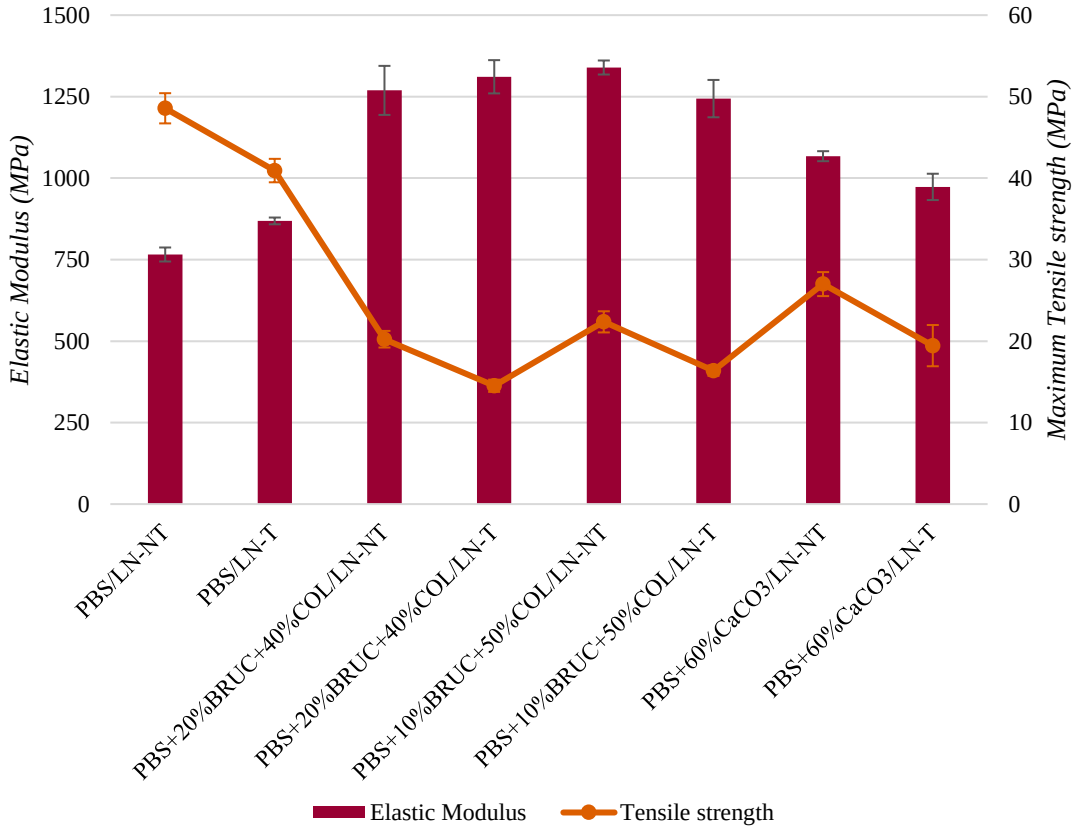

FIGURE 6: TENSILE TEST RESULTS OF PBS COMPOSITES

In the case of the flexural and impact tests, the type of matrix and the treatment have a significant effect (Table 9). On the one hand, the stiffness of the additives increases the flexural modulus and, consequently, the composites require more force to be bent. Due to the higher hardness of colemanite and brucite mixtures, these samples have the highest values of flexural modulus followed by calcium carbonate and finally virgin PBS. In terms of impact strength, it is observed that calcium carbonate does not decrease the properties of the composite despite being at 60%, however, with flame retardants this strength is reduced by half in the PBS+20-40/LN-NT sample. As with the maximum tensile strength, the key aspect in this case is the particle density, because without good adhesion, only the polymeric particles resist the impact. Therefore, the impact resistance is highest for virgin PBS and PBS+60CC, followed by PBS+10-50 and finally PBS+20-40. The difference in density between colemanite and brucite is small, but this difference justifies the lower impact strength of the mixture with higher brucite content. Finally, the treatment has a significant effect on the flexural modulus and impact resistance, as it reduces their strength by worsening the adhesion of the fibre to the polymeric matrix, which reduces the effectiveness of the fabric that must act as reinforcement.

TABLE 9: FLEXURAL AND IMPACT TEST RESULTS OF PBS COMPOSITES

Sample		Flexural Modulus (MPa)	Impact Resistance (kJ/m^2)
PBS/LN-NT		2321.3 ± 46.6	18.44 ± 1.45
PBS/LN-T		2238.3 ± 55.3	9.92 ± 1.83
PBS+20-40/LN-NT		3641.2 ± 176	9.51 ± 0.75
PBS+20-40/LN-T		3446.9 ± 207	6.19 ± 0.54
PBS+10-50/LN-NT		3507.2 ± 139.7	12.66 ± 1.48
PBS+10-50/LN-T		3026.1 ± 115.6	7.20 ± 0.43
PBS+60CC/LN-NT		2650.7 ± 342.6	17.86 ± 1.29
PBS+60CC/LN-T		2119.2 ± 165.7	10.50 ± 1.69
p-value	**Matrix**	0.0000	0.0000
	Treatm	0.0000	0.0000

The results of the fire test of the PBS composites are shown below. Table 10 shows first the results of the horizontal propagation tests 94 HB followed by the vertical test 94V. In the horizontal test it is observed that all additives have a significant effect because the flame extinguishes before reaching the first mark, so the propagation speed is zero. With this test it is not possible to determine whether the flame retardant additives improve the properties of the composite because the sample used for comparison with the same amount of combustible material (PBS+60CC) also shows the same effect of no flame propagation. When compared to the sample without additive, the improvement is indeed considerable, but it is necessary to perform the vertical test to verify which sample is better. Regarding to the treatment, it has a significant effect because it reduces the propagation speed of the virgin sample. Again, all samples are classified within the requirements of the method.

TABLE 10: UL94 RESULTS OF PBS COMPOSITES

		Horizontal test 94 HB		Vertical test 94V		
Sample		**Propagation speed (mm/min)**	**Class**	**Flame time (s)**	**Propagation speed (mm/min)**	**Class**
PBS/LN-NT		28.94 ± 2.15	HB	119.2 ± 24.4	99.84 ± 5.73	-
PBS/LN-T		16.22 ± 2.75	HB	94.8 ± 6.7	98.35 ± 4.76	-
PBS+20-40/LN-NT		0.00 ± 0.00	HB	1.8 ± 1.1	0.00 ± 0.00	V-0
PBS+20-40/LN-T		0.00 ± 0.00	HB	0.5 ± 0.1	0.00 ± 0.00	V-0
PBS+10-50/LN-NT		0.00 ± 0.00	HB	3.0 ± 1.8	0.00 ± 0.00	V-0
PBS+10-50/LN-T		0.00 ± 0.00	HB	1.0 ± 0.4	0.00 ± 0.00	V-0
PBS+60CC/LN-NT		0.00 ± 0.00	HB	84.1 ± 5.8	82.76 ± 5.93	-
PBS+60CC/LN-T		0.00 ± 0.00	HB	103.4 ± 6.6	72.41 ± 6.00	-
p-value	**Matrix**	0.0000		0.0000	0.0000	
	Treat	0.0289		0.5961	0.0427	

In the case of the vertical test, a significant effect of the matrix and the treatment on the propagation speed is also obtained. The additives used improve the fire properties of the composite, as they do not allow flame propagation. In fact, the flame is extinguished within 10 seconds, so all composites with colemanite and brucite pass the test and achieve the V-0 classification. Comparing the samples, the flame time is slightly shorter for the PBS+20-40 composites, but the difference is not incredibly significant. As for the treatment, it has a significant effect on the propagation speed because it decreases the value in the virgin PBS and PBS+60CC samples, but in this case, it is not necessary to treat the fibre since only with the flame retardant additives the composites pass the test, and this reduces the mechanical properties.

In summary, considering the results of DSC, mechanical and UL94 tests, both the PP+20-40/LN-NT and P+10-50/LN-NT composites are suitable for PBS composites, but the **best mixture is 10% brucite plus 50% colemanite with untreated linen fabric** due its better mechanical properties.

4. CONCLUSIONS

In this chapter, the conclusions obtained on the improvement of the fire properties of polymeric matrices and natural fibre have been unified to manufacture a composite. The composites have been manufactured with the different additives and with untreated and treated with banana pseudostem sap (BPS) fabric to determine which formulation is best for each matrix and whether fibre treatment is necessary. After characterization and discussion of the results, the following conclusions were drawn:

- The treatment worsens the adhesion with the plastic matrix due to shrinkage, stiffening and increased roughness of the fibre, as well as forming accumulations of the BPS solution that hinder the pass of the plastic through the holes in the fabric. In addition, the percentage of fibre in the composites increases because the treatment increases the weight of the fibre by reacting with it or by deposition of elements on the surface.

- In PP and PBS composites it is observed that the flame retardant additives, brucite and colemanite, decrease the range of the melting curve because they act as a support for the formation of crystals, thus obtaining a more homogeneous distribution. In addition, the treatment seems to increase the crystallinity of the polymers due to the compounds adhered to the surface of the fibre also act as support.

- In DSC curves no significant differences in the melting and crystallization temperatures are obtained with respect to the two factors, matrix and treatment.

- In the study of the mechanical properties, both additives and treatment have a significant effect. The additives are at 60% and decrease the mechanical properties considerably because they do not have a good adhesion with the plastic matrix. In the case of treatment, it worsens the mechanical properties because it hinders the adhesion of the fibre to the plastic matrix.

- In the tensile test, the additives increase the elastic modulus because they increase the stiffness of the material, but also make it more brittle by decreasing the maximum tensile strength. The key variable in the elastic modulus is the hardness of the particles, since the harder the particles, the higher the modulus. However, in the case of the maximum strength, the key variable is the density, since the less dense the additive, the smaller the effective cross-section and therefore the lower the maximum stress.

- In the flexural and impact tests, the same conclusions are drawn. The flexural modulus increases as the hardness of the additives increases and the impact strength decreases due to the density of the particles because they reduce the effective cross-section.

- In the UL94 test of PP composites, a significant effect of the additives and the treatment is obtained. The mixtures with brucite and colemanite inhibit the horizontal flame propagation and decrease the vertical flame speed, but not enough to meet the test criteria. However, the treatment

improves the fire properties by preventing vertical flame propagation and significantly reducing the flame time to achieve a V-1 rating for the PP+40-20/LN-T composite. Therefore, the treatment of linen with BPS is key in PP composites.

- In the UL94 test of PBS composites, a significant effect of additives and treatment is also obtained. The mixtures of brucite and colemanite succeed in inhibiting the flame both vertically and horizontally and the flame extinguishes itself in less than 10s, therefore, all composites with these mixtures are classified as V-0. The treatment reduces the propagation speed, but it is not necessary to apply it due to the flame retardants allow to the composites to pass the test and has the disadvantage of reducing mechanical properties.

- In summary, the best mixture for PP composite is 40% brucite plus 20% colemanite with linen fabric treated with BPS 4:1+3%BA and for PBS composite is 10% brucite plus 50% colemanite with untreated linen fabric. In addition, between the two polymeric matrices, PBS is selected for its better fire properties and its more sustainable character.

5. INDEX OF TABLES AND FIGURES

6. REFERENCES

1. Ngo TD. Introduction to Composite Materials. In: Composite and Nanocomposite Materials - From Knowledge to Industrial Applications. IntechOpen; 2020.
2. Vijay N, Rajkumara V, Bhattacharjee P. Assessment of Composite Waste Disposal in Aerospace Industries. Procedia Environ Sci 2016;35:563–70.
3. Youngquist JA, Youngs R. SOLID WOOD PRODUCTS | Glued Structural Members. In: Encyclopedia of Forest Sciences. Elsevier; 2004. page 1313–8.
4. Ueng CES. Sandwich Composites. In: Encyclopedia of Physical Science and Technology. Elsevier; 2003. page 407–12.
5. Mohammed L, Ansari MNM, Pua G, Jawaid M, Islam MS. A Review on Natural Fiber Reinforced Polymer Composite and Its Applications. Int J Polym Sci 2015;2015:1–15.
6. E. Njoku C, K. Alaneme K, A. Omotoyinbo J, O. Daramola M. Natural Fibers as Viable Sources for the Development of Structural, Semi-Structural, and Technological Materials – A Review. Adv Mater Lett 2019;10:682–94.
7. Grand View Research. Natural Fiber Composites (NFC) Market Size, Share & Trends Analysis Report 2018-2024 [Internet]. Available from: https://www.grandviewresearch.com/industry-analysis/natural-fiber-composites-market
8. Cook M, Harper JF. The influence of magnesium hydroxide morphology on the crystallinity and properties of filled polypropylene. Advances in Polymer Technology 1998;17:53–62.
9. Chen X, Yu J, Guo S, Luo Z, He M. Effects of magnesium hydroxide and its surface modification on crystallization and rheological behaviors of polypropylene. Polym Compos 2009;30:941–7.
10. Altay L, Sarikanat M, Sağlam M, Uysalman T, Seki Y. The effect of various mineral fillers on thermal, mechanical, and rheological properties of polypropylene. Research on Engineering Structures and Materials 2021
11. Wypych G, editor. Effect of nucleating agents on physical-mechanical properties. In: Handbook of Nucleating Agents. ChemTec Publishing; 2016. page 205–15.
12. Roberts WL, Campbell TJ, Rapp Jr. GR. Encyclopedia of Minerals. Van Nostrand Reinhold; 1990.
13. Cosansu G, Cogun C. An investigation on use of colemanite powder as abrasive in abrasive waterjet cutting (AWJC). Journal of Mechanical Science and Technology 2012;26:2371–80.
14. Ersoy O, Fidan S, Köse H, Güler D, Özdöver Ö. Effect of Calcium Carbonate Particle Size on the Scratch Resistance of Rapid Alkyd-Based Wood Coatings. Coatings 2021;11:340.
15. Cho N, Lee B, Choi S, Kim J, Kim J, Yu J, et al. Brucite shows antibacterial activity via establishment of alkaline conditions. RSC Adv 2021;11:18003–8.

CHAPTER 7

CONCLUSIONS AND FUTURE LINES

This chapter presents the main conclusions drawn during the experimental development of this doctoral thesis, which have been detailed in the previous chapters. In view of these conclusions, a series of potential research lines that emerged from the development of this research are presented.

1. CONCLUSIONS

CHAPTER 4: FLAME RETARDANCY OF POLYMERS

- In the extrusion process, it was observed that blends with additive percentages up to 60% can be obtained without difficulties and with good homogeneity, with the exception of those with expandable graphite.

- As the additives used have a higher density compared to PP and PBS matrices, the density of the blends increases with the total percentage of additive and it must be considered in applications where the weight of the composite is an important requirement.

- Brucite, boehmite, colemanite, expandable graphite and calcium carbonate act as nucleating agents for polypropylene because they increase the percentage of crystallinity, favour the formation of crystals and improve the homogeneity of the crystalline structure. As for the PBS matrix, brucite, colemanite and calcium carbonate also act as nucleating agents.

- All the additives used in this thesis, except for lignin, increase the storage modulus with respect to the virgin polymer over the temperature range tested in DMTA test, therefore, they improve the thermo-mechanical stability of the material.

- In oscillatory rheology, it was observed that the viscosity of the mixtures increases with respect to the percentage, being highest for brucite. In addition, PP1151K matrix is discarded due to its high viscosity could hinder the manufacturing of the composites with the natural fibre fabric.

- Additives significantly influence the mechanical properties. They increase the elastic and flexural modulus and decrease the maximum tensile and impact strength with respect to the percentage. Therefore, the additives used stiffen the material and make it less resistant.

- Regarding fire properties, lignin accelerates the flame propagation speed and was therefore discarded as it worsens the fire properties of polypropylene.

- As the results obtained for brucite and boehmite in Stage 1 were not satisfactory in terms of fire resistance, their synergy with colemanite and expandable graphite was studied in order to obtain mixtures with better properties at lower additive percentages.

- In Stage 2, it was observed that the colemanite brucite mixture showed promising results because it presented better fire resistance with a lower affection in the mechanical properties, so it was selected for the next stage.

- Finally, in the study of the brucite and colemanite mixture, the percentages of each component were varied in order to decide on the basis of the fire resistance results which were the best proportions of each component. In the case of the PP matrix, the mixtures determined as optimal were PP+40%Bruc+20%Col and PP+30%Bruc+30%Col, and in the PBS matrix PBS+20%Bruc+40%Col and PP+10%Bruc+50%Col. Therefore, these mixtures were selected as matrices in the manufacture of natural fibre reinforced composites.

CHAPTER 5: CHEMICAL TREATMENTS APPLIED TO NATURAL FIBRES

- The silane treatment with 3-Aminopropyltriethoxysilane (APTES) slightly improves the fire properties of the linen fabric, but not enough to justify its use.

- The banana pseudostem sap (BPS) concentrated to a quarter applied at alkaline pH with a smoke suppressant, boric acid at 3%, proved to be the most suitable treatment to impart flame retardancy to the linen fabric.

CHAPTER 6: COMPOSITES REINFORCED WITH NATURAL FIBRES

- The BPS treatment worsens the adhesion of the fabric with the plastic matrix due to shrinkage, stiffening and increased roughness of the fibre.

- The additives and treatment have a statistically significant effect on the mechanical properties. On one hand, the additives increase the stiffness and decrease the strength of the composites and on the other hand, the treatment worsens the mechanical properties because it hinders the adhesion of the fibre to the plastic matrix.

- Regarding to PP composites, the mixtures with brucite and colemanite inhibit the horizontal flame propagation and decrease the vertical flame speed, but not enough to meet the test criteria of UL94 test. However, the treatment improves the fire properties by preventing vertical flame propagation and significantly reducing the flame time to achieve a V-1 rating for the PP+40-20/LN-T composite. Therefore, the treatment of linen with BPS is key in PP composites.

- Regarding to PBS composites, the mixtures of brucite and colemanite succeed in inhibiting the flame both vertically and horizontally and the flame extinguishes itself in less than 10s, therefore, all composites with these mixtures are classified as V-0. The treatment reduces the propagation speed, but it is not necessary to apply it since the flame retardants allow to the composites to pass the test.

- In summary, the best mixture for PP composite is 40% brucite plus 20% colemanite with linen fabric treated with BPS 4:1+3%BA and for PBS composite is 10% brucite plus 50%

colemanite with untreated linen fabric. In addition, between the two polymeric matrices, PBS is selected for its better fire properties and its more sustainable character.

2. FUTURE RESEARCH LINES

From the results obtained in this thesis it has been possible to determine that brucite and colemanite act as a synergistic mixture in both the polypropylene matrix and the polybutylene succinate and composites have been obtained that meet the criteria of the UL94 test. However, to verify these results, the cone calorimetric test could be performed, which is more widely used in research, is more complete to determine the fire resistance properties of the materials, and would also serve to determine the mechanisms of action of the synergic mixture used. In addition, the composition of the ashes could be analysed because it would provide us with more information about the mechanism of action of the synergic mixture used.

Furthermore, the TGA test could be carried out with a coupled FTIR of the mixtures of brucite and colemanite with both polypropylene and polybutylene succinate in order to obtain more information on the mechanism of action of the synergistic mixture and thus justify why the optimal proportions for the two matrices are different.

Since the main fields of application of these composites are the construction and transport sectors, an analysis of the toxicity of the fumes could be made as this is a key aspect to take into account.

In order to reduce the total percentage of additive and thus have less impact on the mechanical properties, coupling agents could be used to obtain a better particle-matrix adhesion and thus improve their efficiency.

In the case of the treatment applied to the natural fibre fabric, a mordant could be applied beforehand in order to improve the homogeneity of the treatment and thus favour fibre-polymeric matrix adhesion.

Finally, the methodology used in this thesis could be applied to other polymeric matrices and natural fibres since one of the problems with this type of retardants is that they do not act in the same way on different materials.

ANNEX

TABLE OF CONTENTS

1. ANNEX OF CHAPTER 4

1.1 DSC

1.1.1 STAGE 1

TABLE 1: DSC RESULTS OF SECOND MELTING CURVE FOR STAGE 1

Sample		$T_{onset,m}$ (℃)	$T_{end,m}$ (℃)	Range (℃)	X_1 (%)	X_2 (%)	X_3 (%)	ΔH_m (J/g)	T_m (℃)	w_c (%)
PP1101S		153.33	169.85	16.52	31.71	42.68	24.63	77.4109	163.67	37.38
PP1101S+45%Boehmite		152.30	166.79	14.49	30.06	48.95	19.99	54.3516	164.50	47.42
PP1101S+60%Boehmite		151.83	167.74	15.91	23.68	61.64	13.59	42.3283	164.87	51.10
PP1101S+45%Brucite		156.15	168.01	11.86	36.55	47.73	14.30	53.8268	165.00	47.26
PP1101S+60%Brucite		155.44	167.73	12.29	34.66	49.73	14.32	41.4426	164.70	50.03
PP1101S+10%Lignin		154.62	169.94	15.32	30.88	40.43	27.67	77.6343	163.50	41.65
PP1101S+20%Lignin		155.04	169.96	14.92	30.57	51.20	17.14	65.9868	165.66	39.83
PP1151K		161.05	168.49	7.44	57.64	27.60	13.36	87.5702	165.57	42.28
PP1151K+45%Boehmite		155.50	167.06	11.56	40.49	45.71	12.64	51.9252	164.35	45.59
PP1151K+60%Boehmite		152.94	167.37	14.43	29.24	57.29	12.42	39.2771	164.72	47.41
PP1151K+45%Brucite		156.95	167.50	10.55	43.86	39.73	15.05	49.2163	164.33	43.21
PP1151K+60%Brucite		156.10	166.92	10.82	42.86	42.48	13.49	40.2626	164.04	48.60
PP1151K+10%Lignin		156.43	168.69	12.26	39.00	44.84	14.86	85.9845	165.40	46.13
PP1151K+20%Lignin		156.59	167.83	11.24	40.21	38.05	20.60	72.9638	163.60	44.04
p-value	**Matrix**	0.0432	0.0245	0.0186	0.0061	0.0353	0.1299	0.5048	0.9779	0.9930
	Additive	0.2607	0.0217	0.4836	0.1261	0.0356	0.5235	0.0003	0.9992	0.1760

TABLE 2: DSC RESULTS OF COOLING CURVE FOR STAGE 1

Sample		$T_{onset,c}$ (°C)	ΔH_c (J/g)	T_c (°C)	$T_{onset,c}$-T_c
PP1101S		120.93	77.6115	116.76	4.17
PP1101S+45%Boehmite		128.89	54.5999	125.62	3.27
PP1101S+60%Boehmite		131.56	41.6143	128.32	3.24
PP1101S+45%Brucite		127.65	53.7462	124.20	3.45
PP1101S+60%Brucite		128.97	41.1485	124.59	4.38
PP1101S+10%Lignin		119.11	77.3954	113.76	5.35
PP1101S+20%Lignin		114.98	65.9162	110.07	4.91
PP1151K		127.78	86.7367	123.71	4.07
PP1151K+45%Boehmite		128.41	51.5403	125.06	3.35
PP1151K+60%Boehmite		129.94	36.7605	126.80	3.14
PP1151K+45%Brucite		127.21	48.5882	122.97	4.24
PP1151K+60%Brucite		126.78	39.7751	123.44	3.34
PP1151K+10%Lignin		121.63	85.8967	119.02	2.61
PP1151K+20%Lignin		119.17	72.9415	116.23	2.94
p-value	**Matrix**	0.3583	0.5730	0.9933	0.1766
	Additive	0.0097	0.0003	0.1759	0.9058

1.1.2 STAGE 2

TABLE 3: DSC RESULTS OF SECOND MELTING CURVE FOR STAGE 2

Sample		$T_{onset,m}$ (°C)	$T_{end,m}$ (°C)	Range (°C)	X_1 (%)	X_2 (%)	X_3 (%)	ΔH_m (J/g)	T_m (°C)	w_c (%)
PP+30%Boeh		154.51	167.69	13.18	35.79	40.57	22.48	67.1074	162.82	46.29
PP+35%Boeh		153.28	167.87	14.59	33.74	40.78	24.49	62.1547	162.19	46.17
PP+35%Boeh+10%Col		157.09	167.12	10.03	42.34	40.04	16.28	55.5413	163.99	48.76
PP+35%Boeh 15%Col		156.65	166.85	10.20	43.25	38.16	17.39	51.7767	163.43	50.00
PP+35%Boeh 10%EG		157.07	167.03	9.96	43.16	40.53	15.26	59.2063	163.98	51.98
PP+40%Bruc		156.47	166.83	10.36	32.98	44.37	21.53	57.3203	163.48	46.13
PP+40%Bruc+10%Col		158.12	166.85	8.73	47.38	32.43	18.90	46.4950	163.33	44.90
PP+40%Bruc+15%Col		157.43	167.00	9.57	45.78	35.80	17.21	43.9132	163.57	47.12
PP+40%Bruc+10%EG		157.66	166.91	9.25	46.00	37.03	15.80	52.9847	163.84	51.17
PP+10%Col		156.69	168.46	11.77	38.83	31.40	29.03	89.9377	162.54	48.25
PP+20%Col		156.35	168.33	11.98	37.70	38.27	23.10	80.9137	163.58	48.84
PP+10%EG		157.51	167.37	9.86	43.07	37.37	18.43	90.3092	163.77	48.45
PP+20%EG		157.39	167.65	10.26	43.24	38.01	17.62	80.8824	164.08	48.82
p-value	**Additive**	0.0244	0.1520	0.0535	0.0472	0.2073	0.4639	0.0003	0.2125	0.8627

TABLE 4: DSC RESULTS OF COOLING CURVE FOR STAGE 2

Sample		$T_{onset,c}$ (°C)	ΔH_c (J/g)	T_c (°C)	$T_{onset,c}$-T_c
PP+30%Boeh		125.13	66.8004	121.08	4.05
PP+35%Boeh		126.19	61.7566	123.29	2.90
PP+35%Boeh+10%Col		125.55	55.0060	122.22	3.33
PP+35%Boeh 15%Col		126.10	51.0689	122.06	4.04
PP+35%Boeh 10%EG		128.61	58.7949	124.20	4.41
PP+40%Bruc		125.76	56.9329	122.50	3.26
PP+40%Bruc+10%Col		123.88	46.1422	120.73	3.15
PP+40%Bruc+15%Col		124.64	43.2344	121.26	3.38
PP+40%Bruc+10%EG		127.48	52.3577	123.35	4.13
PP+10%Col		119.06	89.3337	115.32	3.74
PP+20%Col		120.93	80.3576	115.63	5.30
PP+10%EG		125.52	90.1851	121.17	4.35
PP+20%EG		126.55	80.7954	121.10	5.45
p-value	**Additive**	0.8321	0.0003	0.5442	0.1103

1.1.3 STAGE 3

TABLE 5: DSC RESULTS OF SECOND MELTING CURVE FOR STAGE 3

Sample		$T_{onset,m}$ (°C)	$T_{end,m}$ (°C)	Range (°C)	X_1 (%)	X_2 (%)	X_3 (%)	ΔH_m (J/g)	T_m (°C)	w_c (%)
PP+60%Bruc		155.56	168.04	12.48	35.43	42.68	24.63	47.8674	164.85	57.78
PP+50%Bruc+10%Col		157.27	166.94	9.67	42.54	48.38	15.02	43.2964	163.95	52.27
PP+40%Bruc+20%Col		157.11	166.55	9.44	45.07	40.31	15.79	40.4655	163.36	48.85
PP+30%Bruc+30%Col		156.57	166.27	9.70	44.03	37.10	16.57	37.0900	163.05	44.77
PP+20%Bruc+40%Col		154.89	165.93	11.04	38.66	38.03	16.57	38.0075	162.55	45.88
PP+10%Bruc+50%Col		156.59	166.87	10.28	43.96	42.91	17.25	39.7480	162.91	47.98
PP+60%Col		155.43	167.40	11.97	40.14	35.37	19.41	40.3007	162.42	48.65
PP+60%$CaCO_3$		155.00	167.60	12.60	37.37	35.99	22.91	48.3299	164.04	58.34
p-value	**Additive**	0.7384	0.6588	0.7468	0.3789	0.5896	0.6080	0.8787	0.6649	0.9990
PBS		110.37	117.74	7.37	34.87	45.16	17.07	57.7915	115.67	28.90
PBS+60%Bruc		109.05	115.83	6.78	18.16	56.68	22.16	27.5997	113.97	34.50
PBS+50%Bruc+10%Col		109.1	116.26	7.16	18.33	56.14	22.56	23.6612	114.20	29.58
PBS+40%Bruc+20%Col		109.31	115.89	6.58	24.96	50.53	21.47	27.2804	113.96	34.10
PBS+30%Bruc+30%Col		109.59	116.07	6.48	30.12	46.41	20.58	25.5673	114.07	31.96
PBS+20%Bruc+40%Col		109.52	116.03	6.51	29.04	47.25	20.55	24.2914	114.08	30.36
PBS+10%Bruc+50%Col		109.49	115.92	6.43	26.67	48.79	21.64	24.2962	113.99	30.37
PBS+60%Col		108.83	115.52	6.69	22.05	52.76	22.57	23.6198	113.49	29.53
PBS+60%$CaCO_3$		107.54	115.81	8.27	4.15	69.20	23.47	25.1387	113.82	31.42
p-value	**Additive**	0.9683	0.9705	0.7498	0.9720	0.9488	0.9524	0.9437	0.9526	0.9470

TABLE 6: DSC RESULTS OF COOLING CURVE FOR STAGE 3

Sample		$T_{onset,c}$ (°C)	ΔH_c (J/g)	T_c (°C)	$T_{onset,c}$-T_c
PP+60%Bruc		128.64	48.0637	125.34	3.30
PP+50%Bruc+10%Col		126.92	43.7532	123.29	3.63
PP+40%Bruc+20%Col		126.01	39.6933	122.63	3.38
PP+30%Bruc+30%Col		126.35	37.0018	122.78	3.57
PP+20%Bruc+40%Col		127.87	37.3749	123.70	4.17
PP+10%Bruc+50%Col		127.64	39.8739	123.60	4.04
PP+60%Col		127.09	39.8949	122.91	4.18
PP+60%$CaCO_3$		131.66	47.5605	127.37	4.29
p-value	**Additive**	0.9947	0.9827	0.9983	0.8991
PBS		88.39	58.5346	85.57	2.82
PBS+60%Bruc		87.69	28.4960	82.89	4.80
PBS+50%Bruc+10%Col		85.99	24.0833	82.27	3.72
PBS+40%Bruc+20%Col		86.53	27.1904	82.60	3.93
PBS+30%Bruc+30%Col		87.00	24.7401	82.93	4.07
PBS+20%Bruc+40%Col		86.30	24.2793	82.23	4.07
PBS+10%Bruc+50%Col		87.30	24.9829	82.87	4.43
PBS+60%Col		84.82	23.6493	80.88	3.94
PBS+60%$CaCO_3$		82.39	25.2256	78.57	3.82
p-value	**Additive**	0.3081	0.9351	0.8388	0.9989

1.2 OSCILLATORY RHEOLOGY

1.2.1 STAGE 1

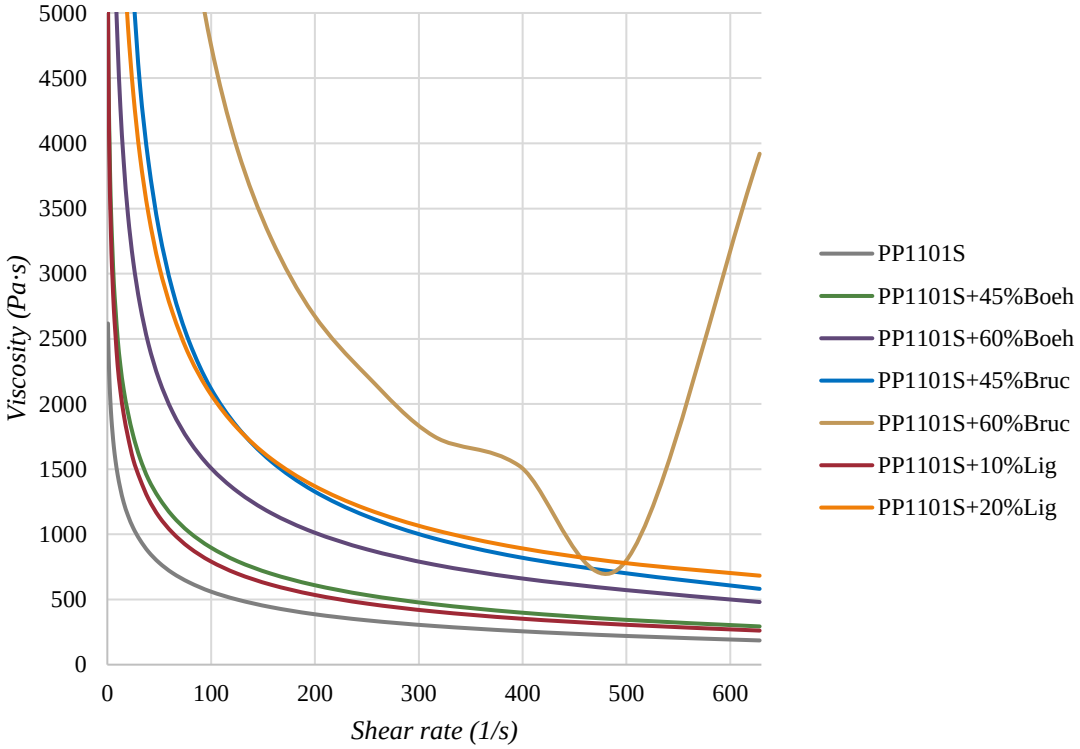

FIGURE 1: VISCOSITY CURVES OF PP1101S SAMPLES OF STAGE 1 AT 170°C

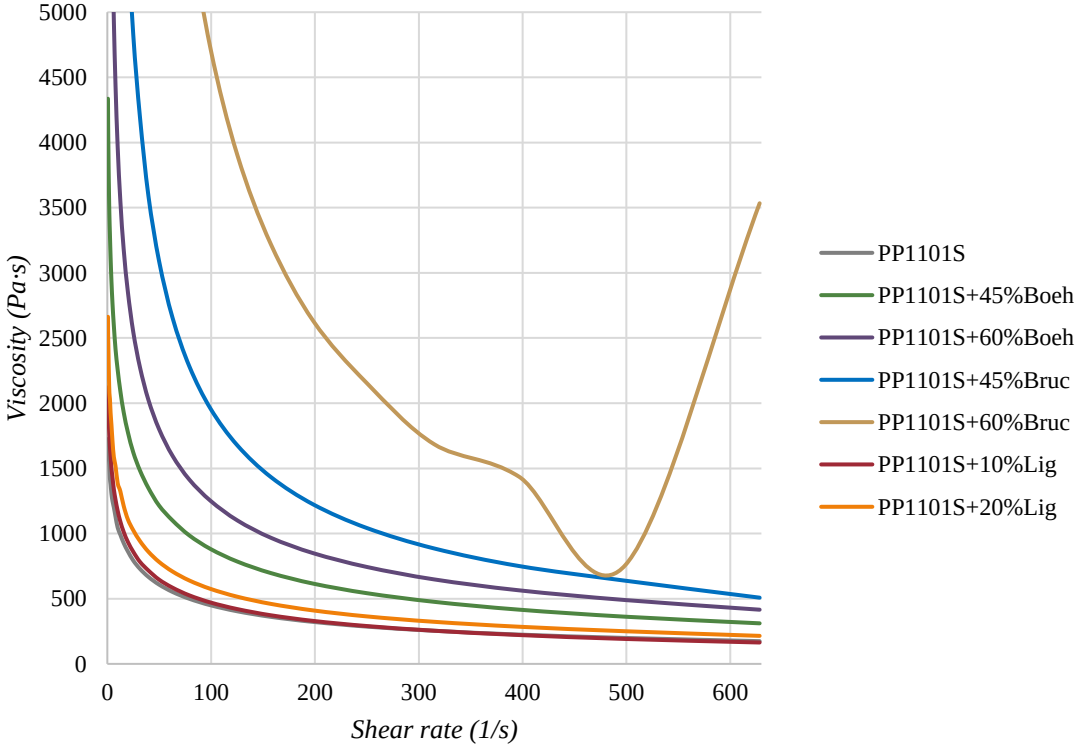

FIGURE 2: VISCOSITY CURVES OF PP1101S SAMPLES OF STAGE 1 AT 190 °C

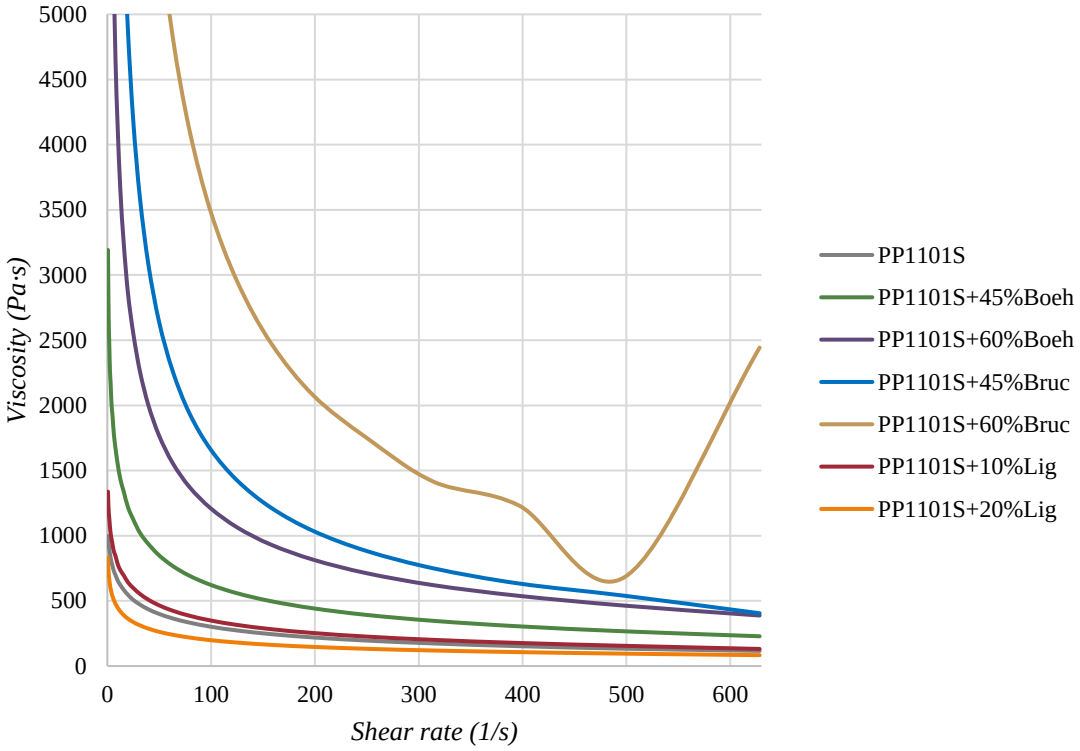

FIGURE 3: VISCOSITY CURVES OF PP1101S SAMPLES OF STAGE 1 AT 210 °C

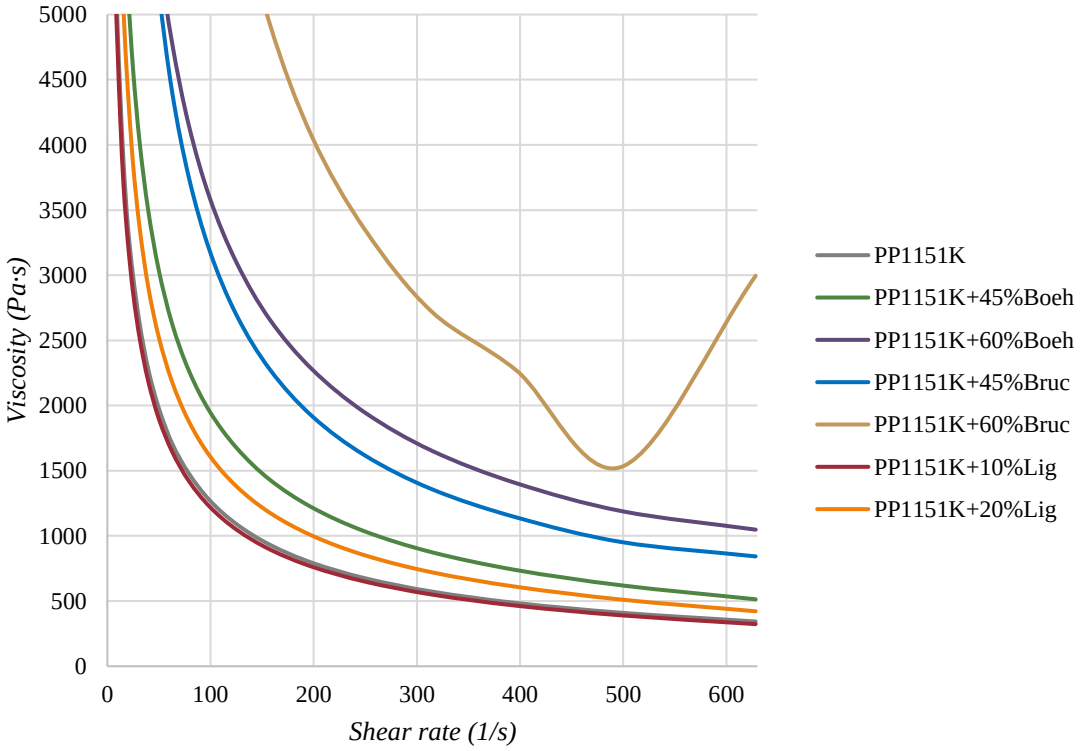

FIGURE 4: 1 VISCOSITY CURVES OF PP1151K SAMPLES OF STAGE 1 AT 170 °C

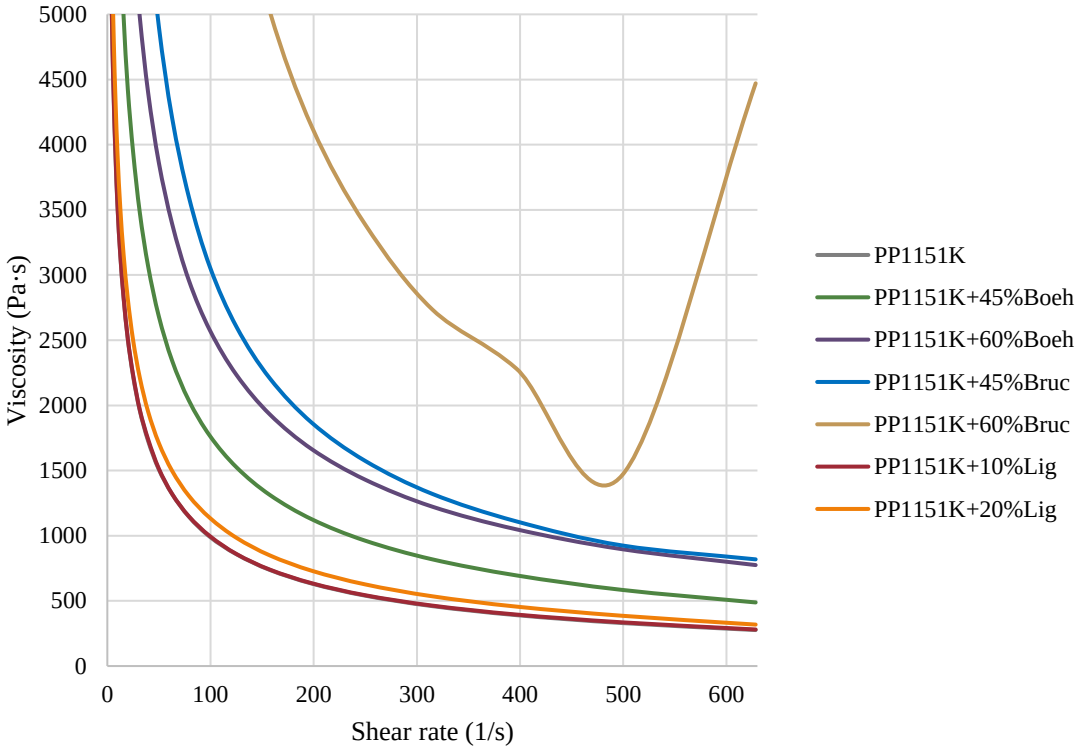

FIGURE 5: VISCOSITY CURVES OF PP1151K SAMPLES OF STAGE 1 AT 190 °C

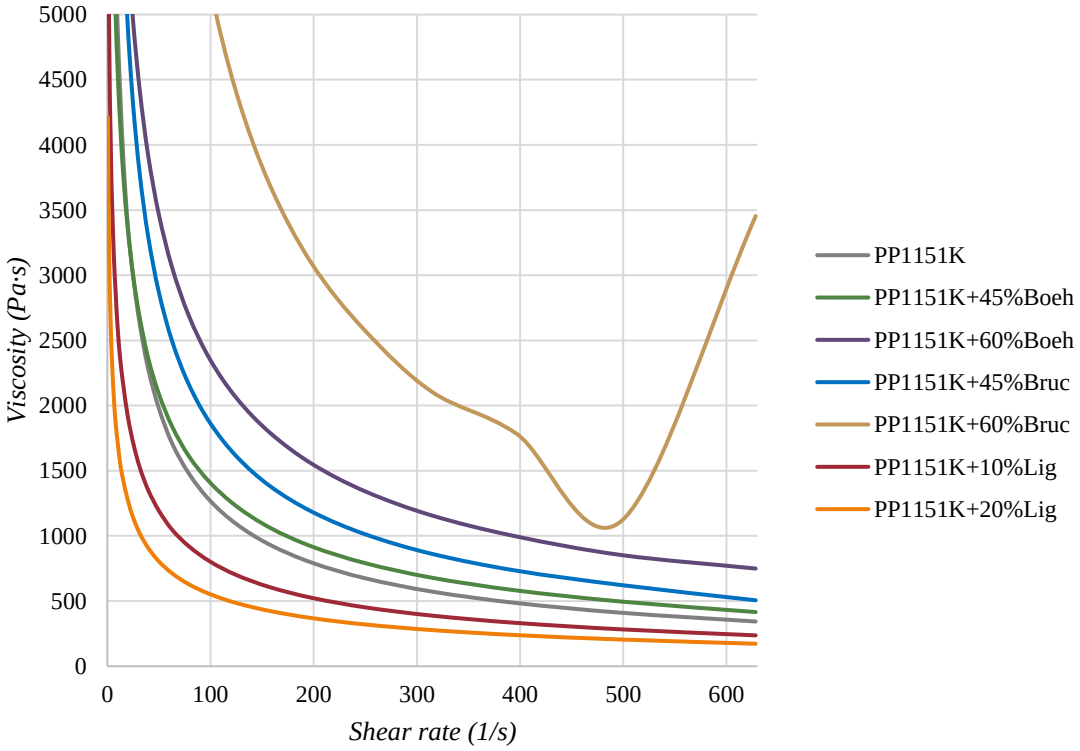

FIGURE 6: VISCOSITY CURVES OF PP1151K SAMPLES OF STAGE 1 AT 210 °C

1.2.2 STAGE 2

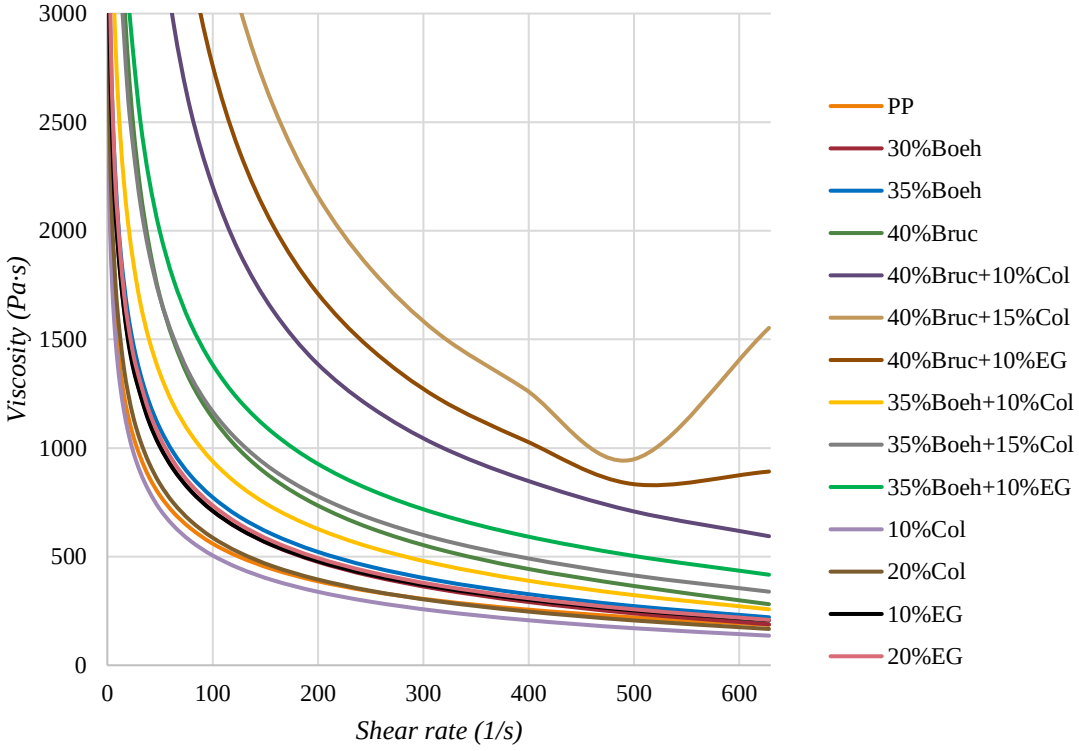

FIGURE 7: VISCOSITY CURVES OF PP SAMPLES OF STAGE 2 AT 170 °C

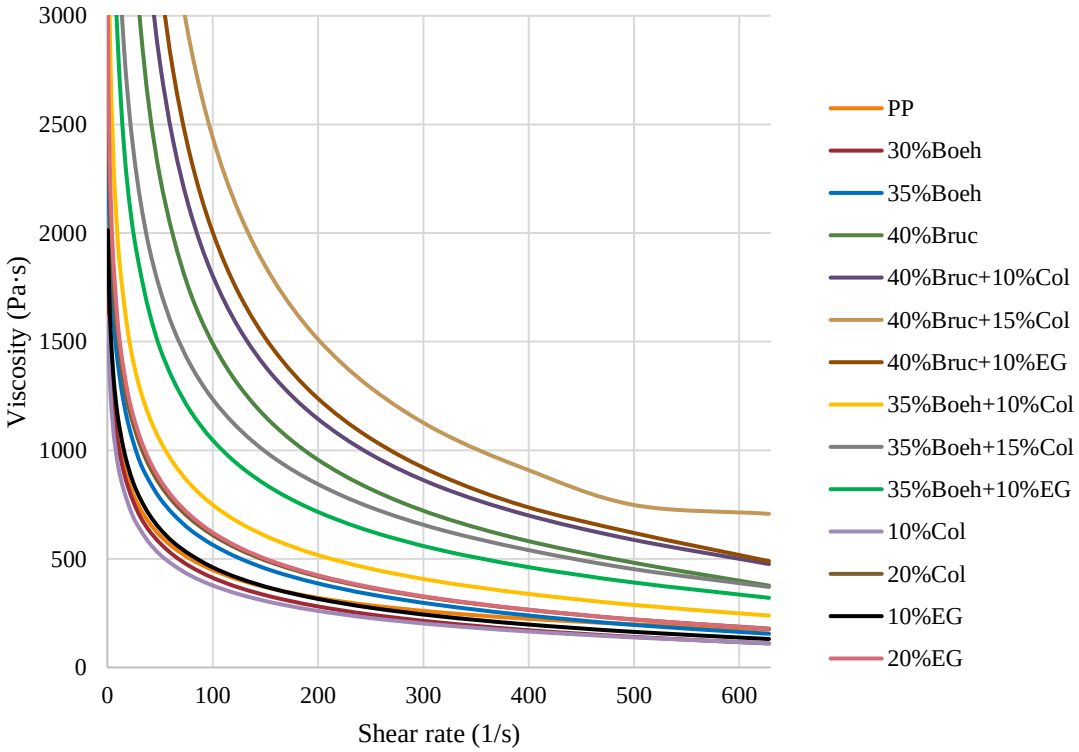

FIGURE 8: VISCOSITY CURVES OF PP SAMPLES OF STAGE 2 AT 190 °C

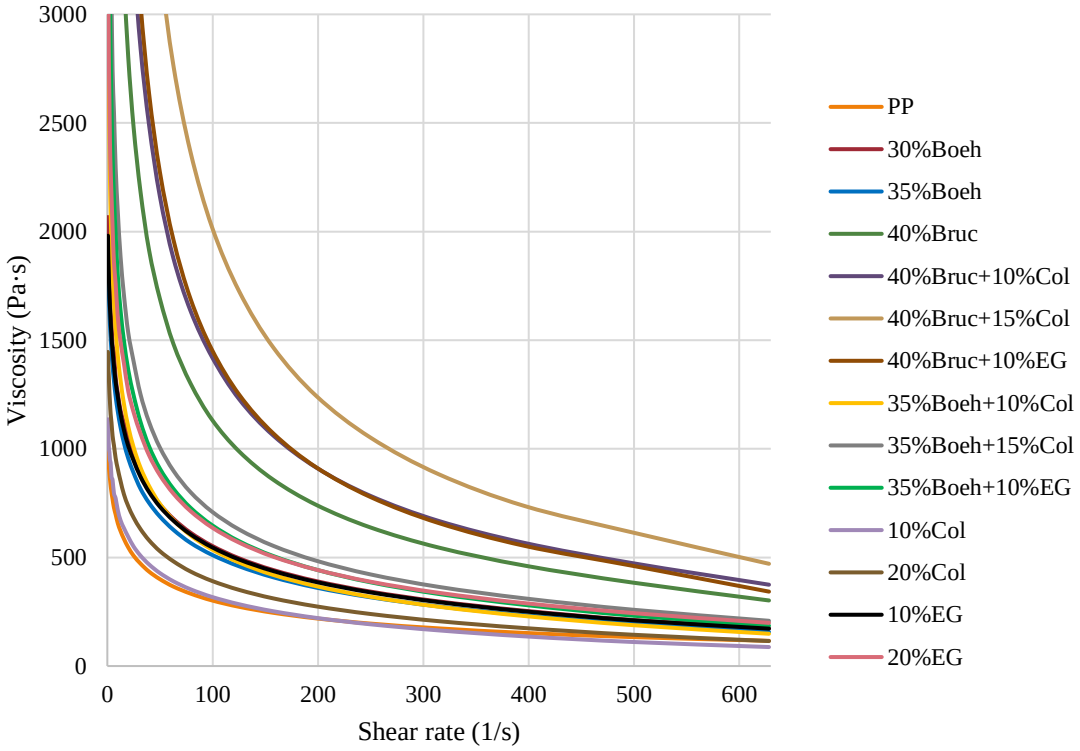

FIGURE 9: VISCOSITY CURVES OF PP SAMPLES OF STAGE 2 AT 210 °C

1.2.3 STAGE 3

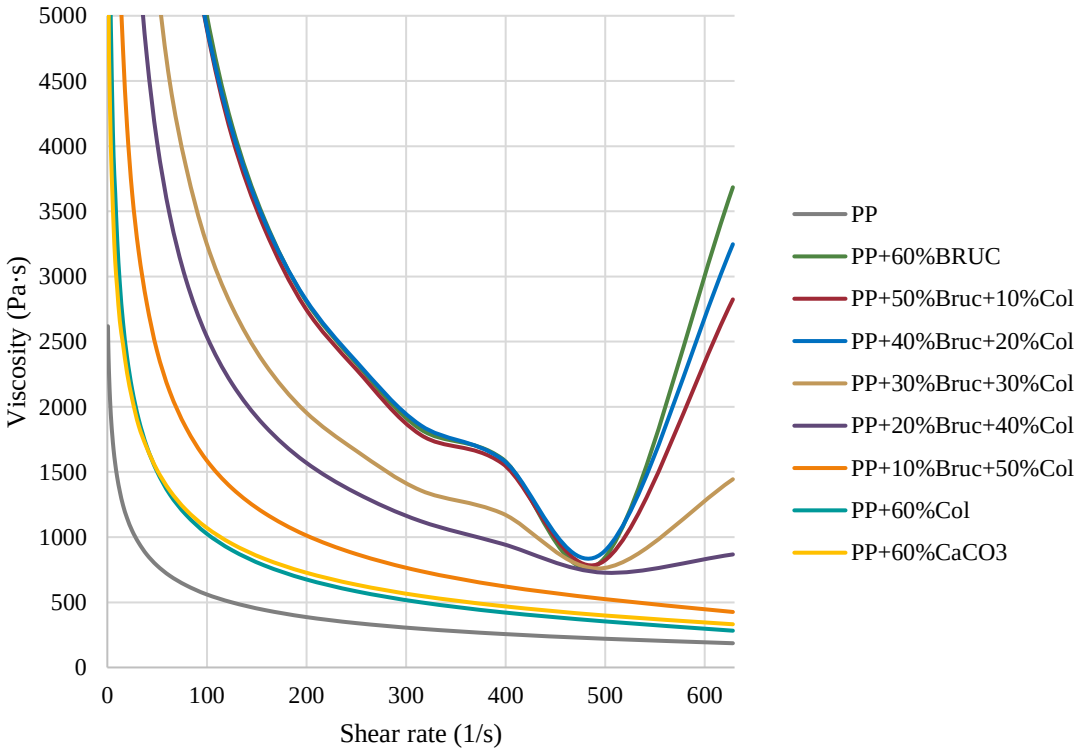

FIGURE 10: VISCOSITY CURVES OF PP SAMPLES OF STAGE 3 AT 170 °C

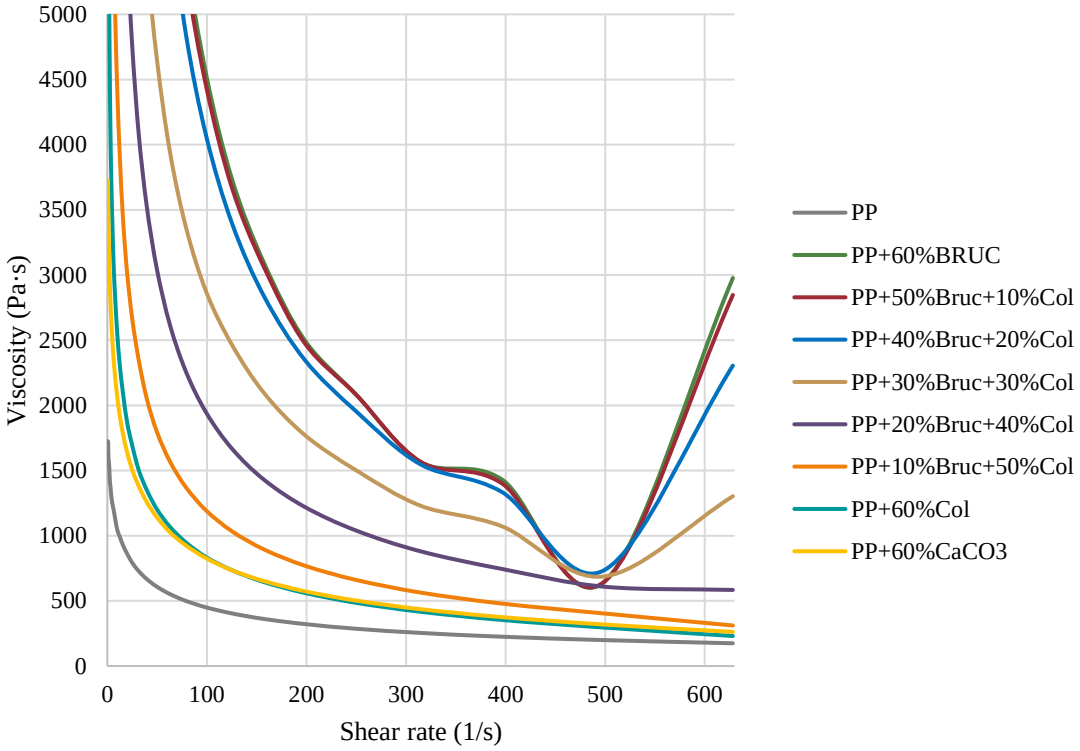

FIGURE 11: VISCOSITY CURVES OF PP SAMPLES OF STAGE 3 AT 190 ℃

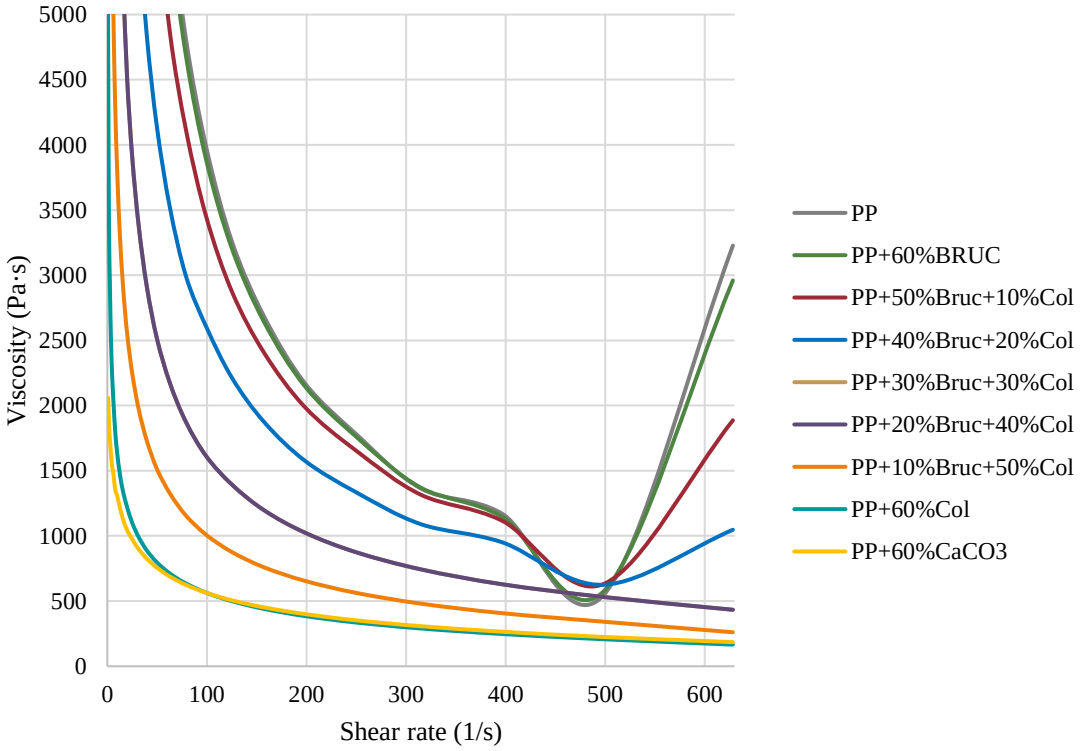

FIGURE 12: VISCOSITY CURVES OF PP SAMPLES OF STAGE 3 AT 210 ℃

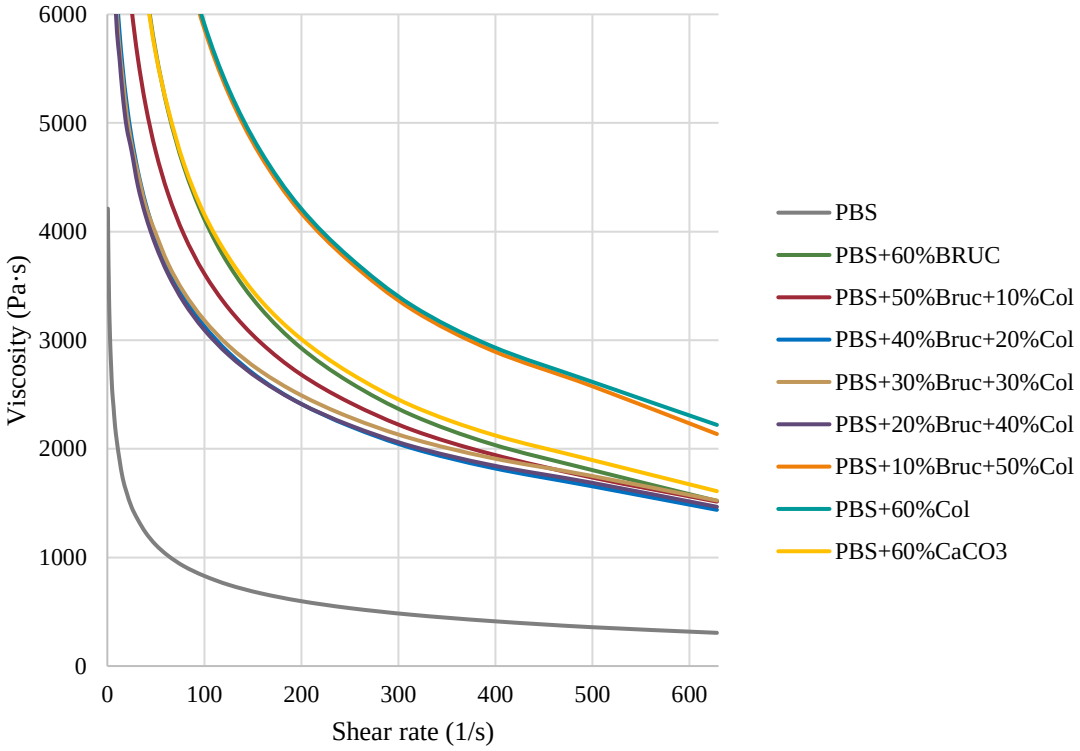

FIGURE 13: VISCOSITY CURVES OF PBS SAMPLES OF STAGE 2 AT 120 ℃

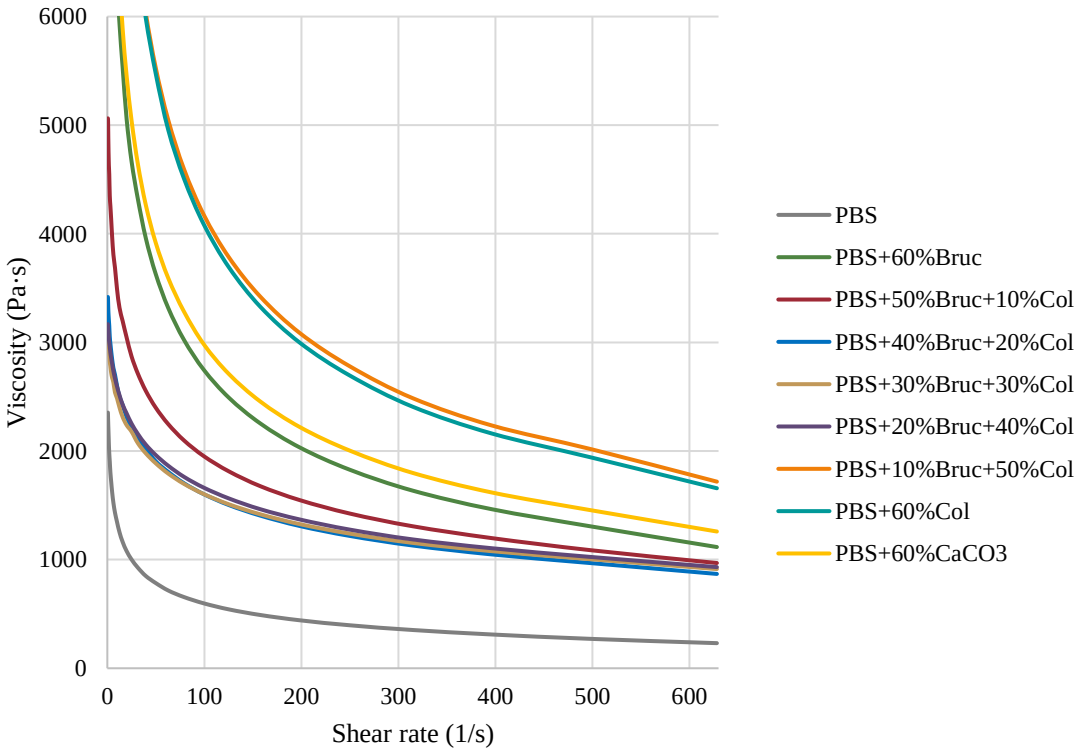

FIGURE 14: VISCOSITY CURVES OF PBS SAMPLES OF STAGE 3 AT 140 ℃

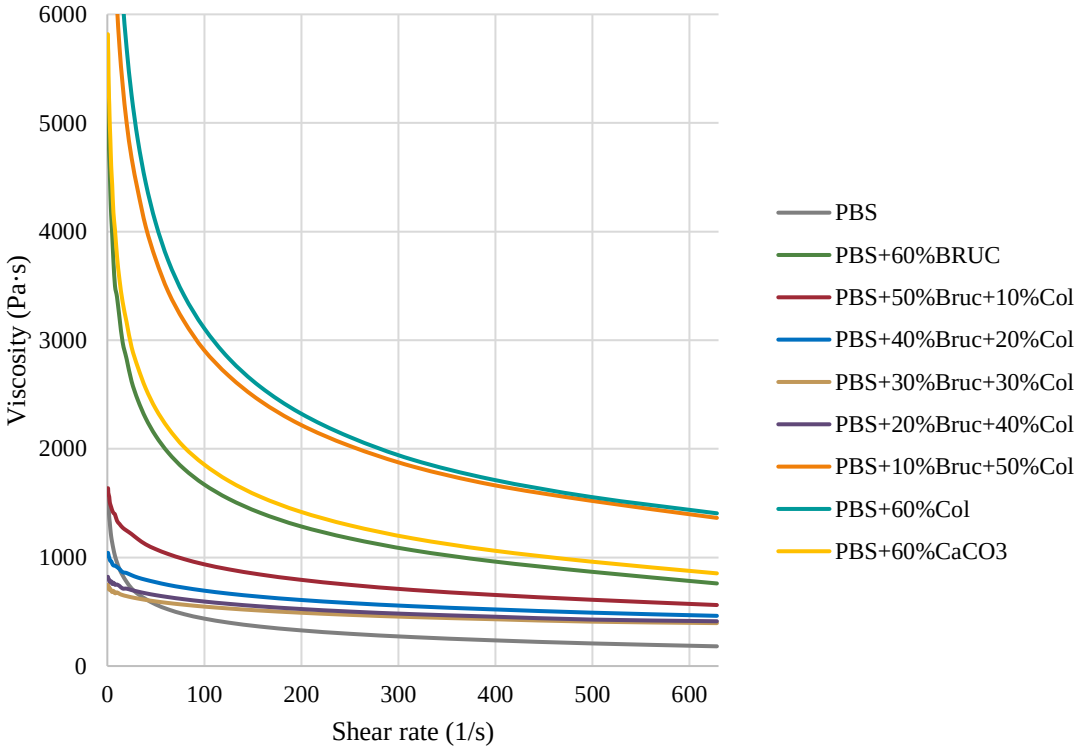

FIGURE 15: VISCOSITY CURVES OF PBS SAMPLES OF STAGE 3 AT 160 ℃

1.3 MECHANICAL TEST

1.3.1 STAGE 1

TABLE 7: MECHANICAL TEST RESULTS OF STAGE 1

Sample		Elastic Modulus (MPa)	SD	Tensile strength (MPa)	SD	Flexural Modulus (MPa)	SD	Impact Resistance (kJ/m^2)	SD
PP1101S		1666.6	62.0	33.55	2.19	1484.5	42.5	28.42	0.89
PP1101S+45%Boehmite		3152.6	82.5	21.13	1.49	2904.8	67.3	21.34	6.27
PP1101S+60%Boehmite		3871.3	324.1	19.90	1.95	4010.5	164.3	6.72	1.09
PP1101S+45%Brucite		3690.0	93.0	24.23	2.92	2905.3	107.6	8.78	1.90
PP1101S+60%Brucite		4433.5	200.5	19.51	2.94	4117.6	67.2	5.32	1.07
PP1101S+10%Lignin		1822.6	52.2	30.11	0.86	1869.5	12.3	26.10	1.06
PP1101S+20%Lignin		1763.1	43.5	25.61	0.41	1665.6	28.0	25.97	5.16
PP1151K		1823.3	114.2	34.67	0.39	1955.1	121.1	38.61	1.29
PP1151K+45%Boehmite		2670.6	219.9	24.37	0.53	2715.9	35.8	36.81	1.24
PP1151K+60%Boehmite		3910.3	222.4	21.49	1.84	3539.9	115.0	13.84	1.97
PP1151K+45%Brucite		3744.7	92.6	24.23	2.92	3161.7	87.0	16.64	2.40
PP1151K+60%Brucite		4426.0	142.9	22.23	1.83	4331.1	128.0	6.93	0.99
PP1151K+10%Lignin		1836.1	48.8	31.50	0.79	1949.5	84.4	30.82	2.47
PP1151K+20%Lignin		1824.0	90.0	23.61	0.56	1729.8	78.7	28.98	1.51
p-value	**Matrix**	0.3486		0.0143		0.2226		0.0000	
	Additive	0.0000		0.0000		0.0000		0.0000	

1.3.2 STAGE 2

TABLE 8: MECHANICAL TEST RESULTS OF STAGE 2

Sample	Elastic Modulus (MPa)	SD	Tensile strength (MPa)	SD	Flexural Modulus (MPa)	SD	Impact Resistance (kJ/m^2)	SD
PP+30%Boeh	2455.9	25.4	27.16	0.19	2651.6	61.8	30.26	3.34
PP+35%Boeh	2697.1	65.8	28.17	0.25	2725.1	25.1	28.26	4.93
PP+35%Boeh+10%Col	3119.0	31.1	24.97	0.31	3675.7	78.6	16.18	2.35
PP+35%Boeh 15%Col	3184.6	38.6	21.86	0.29	3858.0	138.3	13.38	1.33
PP+35%Boeh 10%EG	2778.4	76.0	19.60	0.64	3748.2	155.1	8.92	0.72
PP+40%Bruc	3231.4	71.5	25.05	0.50	2885.9	84.5	14.21	1.86
PP+40%Bruc+10%Col	3547.5	83.7	24.30	0.32	4472.5	125.7	9.69	0.61
PP+40%Bruc+15%Col	4114.4	106.6	24.30	0.25	4851.0	128.4	7.81	0.47
PP+40%Bruc+10%EG	3635.3	41.4	20.94	0.34	4263.4	152.3	6.77	0.45
PP+10%Col	1864.4	42.5	31.37	0.73	2053.6	132.8	30.91	0.96
PP+20%Col	2191.2	52.3	26.60	0.43	2375.6	49.4	30.54	0.68
PP+10%EG	2082.2	67.0	27.30	0.45	2303.0	74.6	22.31	3.82
PP+20%EG	2012.0	22.5	22.87	0.78	2272.5	95.6	12.05	1.32
p-value	0.0000		0.0000		0.0000		0.0000	

1.3.3 STAGE 3

TABLE 9: MECHANICAL TEST RESULTS OF STAGE 3

Sample	Elastic Modulus (MPa)	SD	Tensile strength (MPa)	SD	Flexural Modulus (MPa)	SD	Impact Resistance (kJ/m^2)	SD
PP+60%Bruc	4433.6	200.5	19.51	2.938	4117.6	67.2	5.32	1.07
PP+50%Bruc+10%Col	4715.4	106.7	22.435	0.393	4237.4	146.4	5.91	0.58
PP+40%Bruc+20%Col	4889.5	92.8	22.182	0.558	3583.1	110.5	5.89	0.51
PP+30%Bruc+30%Col	4694.2	172.2	21.754	1.582	4114.0	67.5	5.91	0.27
PP+20%Bruc+40%Col	4512.7	26.2	22.318	0.287	4114.1	128.7	6.24	0.64
PP+10%Bruc+50%Col	4373.4	58.7	21.078	0.283	4263.5	44.1	6.31	1.01
PP+60%Col	4319.5	44.1	20.05	0.306	4129.9	110.5	7.54	1.57
PP+60%$CaCO_3$	3801.1	103.1	19.328	0.086	3699.9	121.9	6.67	0.38
p-value	0.0000		0.0059		0.0000		0.0252	
PBS	653.3	71.8	38.47	0.562	745.4	17.5	16.09	0.56
PBS+60%Bruc	3138.7	51.2	20.838	2.006	3165.1	159.9	9.51	1.22
PBS+50%Bruc+10%Col	3220.9	48.0	21.966	2.114	3320.7	138.4	9.09	1.35
PBS+40%Bruc+20%Col	3107.3	73.3	21.11	0.843	3192.4	65.9	8.53	0.82
PBS+30%Bruc+30%Col	3511.5	125.3	22.728	1.402	3055.6	107.9	8.61	0.41
PBS+20%Bruc+40%Col	3374.4	42.2	20.873	0.846	2797.9	146.3	8.30	0.84
PBS+10%Bruc+50%Col	2898.6	144.9	18.74	0.733	2656.5	49.1	9.90	0.74
PBS+60%Col	3010.3	61.4	17.87	0.488	2632.3	98.8	9.31	0.55
PBS+60%$CaCO_3$	2532.4	47.6	20.616	0.29	2058.9	129.6	11.48	0.31
p-value	0.0000		0.0000		0.0000		0.0794	

1.4 UL94

1.4.1 STAGE 1

TABLE 10: UL94 TEST RESULTS OF STAGE 1

		Horizontal test 94HB				Vertical test 94V			
Sample		**Propagation time (s)**	**SD**	**Propagation speed (mm/min)**	**SD**	**Flame time (s)**	**SD**	**Propagation speed (mm/min)**	**SD**
PP1101S		101.9	6.8	46.00	1.89	136.3	13.9	90.56	6.41
PP1101S+45%Boehmite		133.8	9.2	34.27	2.35	139.8	27.0	73.94	3.04
PP1101S+60%Boehmite		145.5	1.9	31.44	0.42	158.4	31.3	69.94	2.89
PP1101S+45%Brucite		221.2	27.5	20.92	2.72	149.9	52.1	71.34	3.77
PP1101S+60%Brucite		0.0	0.0	0.00	0.00	219.1	34.3	46.63	6.34
PP1101S+10%Lignin		100.9	5.6	45.40	2.54	132.8	5.6	138.84	5.44
PP1101S+20%Lignin		120.7	3.6	37.88	1.15	79.4	39.0	170.20	7.04
PP1151K		102.6	6.2	44.66	2.73	148.4	10.9	84.75	6.86
PP1151K+45%Boehmite		124.4	2.3	36.77	0.66	146.4	22.3	74.17	2.91
PP1151K+60%Boehmite		139.2	3.7	32.85	0.86	189.0	7.3	65.21	1.86
PP1151K+45%Brucite		266.6	2.0	17.15	0.13	202.2	22.8	67.45	4.83
PP1151K+60%Brucite		0.0	0.0	0.00	0.00	198.0	53.7	49.36	4.63
PP1151K+10%Lignin		103.9	4.8	44.04	1.71	145.8	3.4	115.29	10.35
PP1151K+20%Lignin		108.1	5.1	42.37	2.06	99.4	28.5	142.96	9.01
p-value	**Matrix**	0.8264		0.4550		0.0287		0.0000	
	Additive	0.0000		0.0000		0.0000		0.0000	

1.4.2 STAGE 2

TABLE 11: UL94 TEST RESULTS OF STAGE 2

	Horizontal test 94HB				Vertical test 94V			
Sample	**Propagation time (s)**	**SD**	**Propagation speed (mm/min)**	**SD**	**Flame time (s)**	**SD**	**Propagation speed (mm/min)**	**SD**
PP+30%Boeh	110.4	2.3	41.43	0.88	165.2	4.6	90.00	6.51
PP+35%Boeh	110.9	6.0	41.31	2.15	152.7	16.4	82.21	2.79
PP+35%Boeh+10%Col	111.2	5.4	41.17	1.96	107.8	35.7	99.33	6.90
PP+35%Boeh 15%Col	84.8	60.2	33.98	1.89	109.0	31.4	93.68	7.07
PP+35%Boeh 10%EG	112.7	18.1	35.37	1.50	152.7	6.5	66.81	5.62
PP+40%Bruc	138.7	2.5	32.42	1.18	190.6	22.0	84.41	4.18
PP+40%Bruc+10%Col	138.7	11.0	33.10	2.52	141.3	16.1	70.24	4.49
PP+40%Bruc+15%Col	156.2	13.1	29.41	2.55	183.3	11.1	64.44	1.57
PP+40%Bruc+10%EG	80.3	139.1	6.33	10.96	153.0	55.1	57.01	7.53
PP+10%Col	88.4	2.8	51.73	1.59	161.3	19.6	109.50	6.63
PP+20%Col	85.6	0.3	53.40	0.20	121.4	15.2	115.32	5.48
PP+10%EG	106.9	2.1	42.79	0.82	165.8	7.4	80.42	3.83
PP+20%EG	130.1	9.7	35.28	2.60	103.3	18.7	72.79	5.88
p-value	0.0000		0.0000		0.0000		0.0000	

1.4.3 STAGE 3

TABLE 12: UL94 TEST RESULTS OF STAGE 3

	Horizontal test 94HB				Vertical test 94V			
Sample	**Propagation time (s)**	**SD**	**Propagation speed (mm/min)**	**SD**	**Flame time (s)**	**SD**	**Propagation speed (mm/min)**	**SD**
PP+60%Bruc	18.9	32.7	3.34	5.78	155.2	87.7	46.00	26.24
PP+50%Bruc+10%Col	0.0	0.0	0.00	0	140.8	119.0	42.89	39.21
PP+40%Bruc+20%Col	51.9	89.8	1.01	1.76	90.3	103.9	37.86	34.95
PP+30%Bruc+30%Col	0.0	0.0	0.00	0	189.8	86.2	59.79	1.75
PP+20%Bruc+40%Col	141.7	2.2	32.28	0.51	159.9	46.4	65.35	2.01
PP+10%Bruc+50%Col	133.1	7.0	34.41	1.79	109.3	29.8	83.12	5.22
PP+60%Col	112.8	7.6	40.64	2.63	87.4	21.5	119.24	4.21
PP+60%$CaCO_3$	91.1	3.9	50.27	2.16	131.2	7.1	109.40	4.04
p-value	0.0000		0.0000		0.3348		0.0000	
PBS	24.5	23.3	14.41	13.13	20.3	6.21	6.93	4.26
PBS+60%Bruc	10.6	18.3	8.13	14.09	20.0	14.6	11.83	9.54
PBS+50%Bruc+10%Col	0.0	0.0	0.00	0.00	15.8	8.5	6.54	4.28
PBS+40%Bruc+20%Col	0.0	0.0	0.00	0.00	7.0	5.1	4.24	5.92
PBS+30%Bruc+30%Col	0.0	0.0	0.00	0.00	0.5	0.8	0.00	0.00
PBS+20%Bruc+40%Col	0.0	0.0	0.00	0.00	0.5	0.9	0.00	0.00
PBS+10%Bruc+50%Col	0.0	0.0	0.00	0.00	0.4	0.6	0.00	0.00
PBS+60%Col	55.4	95.9	9.17	15.89	27.8	11.1	6.83	4.47
PBS+60%$CaCO_3$	108.6	29.7	37.91	2.83	94.6	68.1	36.08	18.81
p-value	0.4808		0.5631		0.0000		0.0000	

2. ANNEX OF CHAPTER 6

2.1 DSC

TABLE 13: DSC RESULTS OF MELTING CURVE FOR PP AND PBS COMPOSITES

Sample		$T_{onset,m}$ (℃)	$T_{end,m}$ (℃)	Range (℃)	X_1 (%)	X_2 (%)	X_3 (%)	ΔH_m (J/g)	T_m (℃)	w_c (%)
PP/LN-NT		154.99	169.76	14.77	35.43	42.68	24.63	77.4762	163.24	43.87
PP/LN-T		155.20	170.06	14.86	42.54	48.38	15.02	77.8655	163.59	45.67
PP+40-20/LN-NT		155.57	168.19	12.62	45.07	40.31	15.79	36.3455	163.90	48.29
PP+40-20/LN-T		153.85	167.82	13.97	44.03	37.10	16.57	40.1473	164.03	54.20
PP+30-30/LN-NT		155.42	168.68	13.26	38.66	38.03	16.57	38.1833	164.52	50.79
PP+30-30/LN-T		153.55	168.48	14.93	43.96	42.91	17.25	35.7295	162.90	48.50
PP+60CC/LN-NT		155.53	168.26	12.73	40.14	35.37	19.41	34.6528	162.57	45.95
PP+60CC/LN-T		155.58	168.79	13.21	37.37	35.99	22.91	37.557	163.18	50.70
p-value	**Matrix**	0.6082	0.0262	0.1079	0.6062	0.2411	0.0788	0.0006	0.5485	0.2585
	Treatment	0.2322	0.7775	0.0928	0.1753	0.4715	0.7622	0.4693	0.8102	0.2585
PBS/LN-NT		107.73	120.6	12.87	23.69	44.13	30.43	57.1938	115.43	31.88
PBS/LN-T		106.16	119.72	13.56	18.26	48.11	31.74	55.8564	114.59	31.85
PBS+20-40/LN-NT		107.36	115.20	7.84	1.75	70.88	23.28	22.0400	112.71	29.97
PBS+20-40/LN-T		108.43	117.91	9.48	12.83	55.18	28.27	24.5307	115.02	34.12
PBS+10-50/LN-NT		106.93	116.9	9.97	17.14	57.15	22.47	21.9526	114.55	29.81
PBS+10-50/LN-T		107.28	115.64	8.36	11.17	59.16	26.61	25.1228	112.55	34.87
PBS+60CC/LN-NT		105.99	116.65	10.66	13.00	58.69	25.24	25.7412	113.69	34.63
PBS+60CC/LN-T		103.54	115.45	11.91	0.87	71.96	96.49	28.0257	112.68	38.30
PBS/LN-NT		107.73	120.6	12.87	23.69	44.13	30.43	57.1938	115.43	31.88
p-value	**Matrix**	0.2196	0.1380	0.0582	0.3222	0.2913	0.4947	0.0004	0.6060	0.1486
	Treatment	0.4853	0.8800	0.5469	0.5755	0.8924	0.3149	0.2019	0.7079	0.0642

TABLE 14: DSC RESULTS OF COOLING CURVE FOR PP AND PBS COMPOSITES

Sample		$T_{onset,c}$ (℃)	ΔH_c (J/g)	T_c (℃)	$T_{onset,c}$-T_c
PP/LN-NT		121.45	76.9255	116.19	5.26
PP/LN-T		121.38	78.0077	116.18	5.20
PP+40-20/LN-NT		126.34	35.6213	122.25	4.09
PP+40-20/LN-T		131.90	39.7076	127.74	4.16
PP+30-30/LN-NT		127.51	38.0869	123.15	4.36
PP+30-30/LN-T		123.35	36.2556	119.12	4.23
PP+60CC/LN-NT		123.19	34.6475	117.90	5.29
PP+60CC/LN-T		124.36	37.4411	117.95	6.41
p-value	**Matrix**	0.2247	0.0004	0.1450	0.0641
	Treatment	0.7752	0.3168	0.8601	0.4562
PBS/LN-NT		88.82	57.9572	83.53	5.29
PBS/LN-T		87.81	56.6601	82.65	5.16
PBS+20-40/LN-NT		87.56	22.9632	83.01	4.55
PBS+20-40/LN-T		89.50	24.894	84.87	4.63
PBS+10-50/LN-NT		87.69	22.0898	82.33	5.36
PBS+10-50/LN-T		85.51	24.9589	80.32	5.19
PBS+60CC/LN-NT		86.59	26.2171	80.87	5.72
PBS+60CC/LN-T		84.49	27.6060	78.87	5.62
PBS/LN-NT		88.82	57.9572	83.53	5.29
p-value	**Matrix**	0.2673	0.0003	0.1432	0.0031
	Treatment	0.4487	0.2648	0.4671	0.2433

2.2 MECHANICAL TESTS

TABLE 15: MECHANICAL TEST RESULTS OF PP AND PBS COMPOSITES

Sample		Elastic Modulus (MPa)	SD	Tensile strength (MPa)	SD	Flexural Modulus (MPa)	SD	Impact Resistance (kJ/m^2)	SD
PP/LN-NT		1073.2	55.2	47.91	0.80	3169.2	56.3	15.48	0.77
PP/LN-T		1098.6	120.3	38.54	2.44	2948.5	70.4	8.51	1.12
PP+40-20/LN-NT		1562.8	19.0	20.58	2.041	4885.9	105.0	6.60	0.42
PP+40-20/LN-T		1615.2	40.2	17.38	0.26	3964.8	107.2	4.37	0.92
PP+30-30/LN-NT		1588.2	25.3	20.82	1.604	4645.6	129.7	6.55	0.39
PP+30-30/LN-T		1548.9	39.5	20.04	0.64	4808.0	442.0	5.77	0.82
PP+60CC/LN-NT		1272.0	49.6	32.54	1.579	4116.0	336.9	11.28	0.78
PP+60CC/LN-T		1273.5	107.876	24.24	1.822	4031.7	184.1	6.85	0.58
p-value	**Matrix**	0.0000		0.0000		0.0000		0.0000	
	Treatment	0.6385		0.0000		0.0096		0.0000	
PBS/LN-NT		765.7	21.5	48.57	1.854	2321.3	46.6	18.44	1.45
PBS/LN-T		868.7	10.4	40.93	1.439	2238.3	55.3	9.92	1.83
PBS+20-40/LN-NT		1269.2	75.2	20.23	1.019	3641.2	176.0	9.51	0.75
PBS+20-40/LN-T		1311.0	51.0	14.52	0.751	3446.9	207.0	6.19	0.54
PBS+10-50/LN-NT		1339.4	21.5	22.36	1.297	3507.2	139.7	12.66	1.48
PBS+10-50/LN-T		1244.0	57.3	16.38	0.646	3026.1	115.6	7.20	0.43
PBS+60CC/LN-NT		1067.3	15.3	27.00	1.473	2650.7	342.6	17.86	1.29
PBS+60CC/LN-T		973.1	40.4	19.45	2.531	2119.2	165.7	10.50	1.69
PBS/LN-NT		765.7	21.5	48.57	1.854	2321.3	46.6	18.44	1.45
p-value	**Matrix**	0.0000		0.0000		0.0000		0.0000	
	Treatment	0.5677		0.0000		0.0000		0.0000	

2.3 UL94

TABLE 16: UL94 RESULTS OF PP AND PBS COMPOSITES

		Horizontal test 94HB				Vertical test 94V			
Sample		**Propagation time (s)**	**SD**	**Propagation speed (mm/min)**	**SD**	**Flame time (s)**	**SD**	**Propagation speed (mm/min)**	**SD**
PP/LN-NT		216.2	6.1	21.16	0.59	123.1	36.8	108.52	12.1
PP/LN-T		241.4	5.4	18.95	0.42	146.4	47.3	104.30	4.29
PP+40-20/LN-NT		0.0	0.0	0.00	0.00	266.3	58.6	51.18	5.68
PP+40-20/LN-T		0.0	0.0	0.00	0.00	16.6	4.2	0.00	0.00
PP+30-30/LN-NT		0.0	0.0	0.00	0.00	205.0	163.4	33.63	20.08
PP+30-30/LN-T		0.0	0.0	0.00	0.00	21.7	22.2	0.00	0.00
PP+60CC/LN-NT		209.5	12.7	21.88	1.38	127.0	13.8	87.57	3.68
PP+60CC/LN-T		231.7	10.7	19.76	0.90	131.9	6.8	84.22	4.21
p-value	**Matrix**	0.0000		0.0000		0.0000		0.0000	
	Treatment	0.6385		0.0000		0.0096		0.0000	
PBS/LN-NT		158.6	12.2	28.94	2.15	119.2	24.4	99.84	5.73
PBS/LN-T		287.0	45.4	16.22	2.75	94.8	6.7	98.35	4.76
PBS+20-40/LN-NT		0.0	0.0	0.00	0.00	1.8	1.1	0.00	0.00
PBS+20-40/LN-T		0.0	0.0	0.00	0.00	0.5	0.1	0.00	0.00
PBS+10-50/LN-NT		0.0	0.0	0.00	0.00	3.0	1.8	0.00	0.00
PBS+10-50/LN-T		0.0	0.0	0.00	0.00	1.0	0.4	000	000
PBS+60CC/LN-NT		0.0	0.0	0.00	0.00	84.1	5.8	82.76	5.93
PBS+60CC/LN-T		0.0	0.0	0.00	0.00	103.4	6.6	72.41	6.00
PBS/LN-NT		158.6	12.2	28.94	2.15	119.2	24.35	99.84	5.73
p-value	**Matrix**	0.0000		0.0000		0.0000		0.0000	
	Treatment	0.5677		0.0000		0.0000		0.0000	

3. INDEX OF TABLES AND FIGURES